

# High Energy Physics

High Energy Physics Research  
Accelerator Department

CBA

**DISCLAIMER**

DR # 0263-1

This report was prepared as an account of work sponsored by an agency of the United States Government. Neither the United States Government nor any agency thereof, nor any of their employees, makes any warranty, express or implied, or assumes any legal liability or responsibility for the accuracy, completeness, or usefulness of any information, apparatus, product, or process disclosed, or represents that its use would not infringe privately owned rights. Reference herein to any specific commercial product, process, or service by trade name, trademark, manufacturer, or otherwise does not necessarily constitute or imply its endorsement, recommendation, or favoring by the United States Government or any agency thereof. The views and opinions of authors expressed herein do not necessarily state or reflect those of the United States Government or any agency thereof.

BNL 51700  
UC-2 and 13  
General, Miscellaneous, and Progress Reports  
(Nuclear and Nonnuclear) — TIC-4500

BNL--51700

DE84 015153

# BROOKHAVEN HIGHLIGHTS

January '82 — March '83

- High Energy Physics
- Physics and Chemistry
- Life Sciences
- Applied Energy Science
- Support Activities
- General and Administrative

Editors: J.B. Horner Kuper and Mary C. Rustad

## BROOKHAVEN NATIONAL LABORATORY

Upton, Long Island, New York 11973

Operated By Associated Universities, Inc.  
Under Contract No. DE-AC02-76CH00016 with the

United States Department of Energy

**MASTER**

# Contents

INTRODUCTION .....	v
HIGH ENERGY PHYSICS .....	1
Accelerator and High Energy Physics Programs .....	3
High Energy Physics Research .....	5
Accelerator Department and CBA Project .....	14
The AGS .....	14
Planning and Support of the Experimental Program .....	19
The CBA Project .....	24
PHYSICS AND CHEMISTRY .....	33
Physics Department .....	35
Nuclear Physics .....	36
Plans for Future Research in the Tandem Group .....	36
Hypernuclear Physics at AGS .....	39
The High Flux Beam Reactor .....	44
Nuclear Theory .....	47
Solid State Physics .....	48
Neutron Scattering Studies .....	48
Solid State Theory .....	50
Particle-Solid Interactions .....	50
Surface Studies .....	51
Atomic and Applied Physics .....	52
National Synchrotron Light Source .....	58
Chemistry Department .....	65
LIFE SCIENCES .....	73
Medical Department .....	75
Biology Department .....	93
APPLIED ENERGY SCIENCE .....	107
Department of Energy and Environment .....	109
Energy Sciences .....	109
Environmental Sciences .....	114
Energy Technology .....	118
National Center for Analysis of Energy Systems .....	120
Department of Nuclear Energy .....	127
Nuclear Safety .....	127
Nuclear Waste Management .....	134
Nuclear Material Safeguards .....	136
National Nuclear Data Center .....	136
Advanced Reactor Systems .....	137
SUPPORT ACTIVITIES .....	141
Applied Mathematics Department .....	143
Instrumentation Division .....	149
Reactor Division .....	158
Safety and Environmental Protection Division .....	160
GENERAL AND ADMINISTRATIVE .....	165

---

# Introduction

Brookhaven National Laboratory is operated by Associated Universities, Inc. (AUI) under a contract with the United States Department of Energy (DOE). The Laboratory conducts a broad range of basic and applied research programs in the physical and life sciences. It occupies a 21-km<sup>2</sup> (5265 acre) tract of land at Upton, NY, approximately at the geographic center of Long Island, about 100 kilometers east of New York City.

AUI was formed in 1946 by a group of nine universities for the purpose of establishing and managing Brookhaven National Laboratory and other research centers. This action represented a new approach to the management of fundamental research with the support of the Federal government, especially for large-scale scientific enterprises of importance to the academic community.

From 1947 to 1975 the Laboratory was supported by the U.S. Atomic Energy Commission. In 1975 the Atomic Energy Commission was abolished, and most of its research programs were taken over by the Energy Research and Development Administration, which in 1977 was incorporated into the newly created Department of Energy. The U.S. Nuclear Regulatory Commission, which was formed in 1975 to take over the regulatory functions of the AEC, supports a continuing program of studies at Brookhaven on the safety of nuclear power reactors.

The primary objectives of the Laboratory are:

- To seek new scientific knowledge, with emphasis on programs that require large-scale research tools such as particle accelerators, nuclear reactors, and special laboratories that are beyond the scope of individual educational institutions.
- To encourage use of its facilities by scientists from universities, research institutions, and industry.
- To assist the Department of Energy (DOE) in the performance of tasks that utilize the Laboratory's unique facilities and organization or the special talents of its staff.
- To serve as an important auxiliary in the training of scientists and engineers, and other-

wise to assist in the dissemination of scientific and technical knowledge.

To fulfill the first and second of these objectives, the Laboratory has designed and built a series of large research devices. The first generation of these, the Cosmotron and the Brookhaven Graphite Research Reactor, have already completed long and useful programs of research and have been replaced by newer machines. Today the Alternating Gradient Synchrotron (AGS) accelerates protons to energies up to 30 GeV and continues as one of the nation's primary devices for high energy physics research. The High Flux Beam Reactor provides intense beams of neutrons for fundamental experiments in nuclear and solid state physics, chemistry, and biology. The Medical Research Reactor serves for activation analyses and for medical dosimetry studies. The Tandem Van de Graaff installation provides beams of many varieties of ions at energies up to several hundred MeV for fundamental research in nuclear physics. Several smaller accelerators are also employed for solid state physics and nuclear research. Two cyclotrons and the linac injector to the AGS produce many special isotopes, primarily for medical research and treatment. A scanning transmission electron microscope provides extremely high resolution for investigation of biological molecules and subcellular structures. A pulmonary toxicology facility allows the study of animals exposed to atmospheres of hazardous substances.

The newest user-oriented research facility is the National Synchrotron Light Source which is essentially two facilities; one providing intense beams of vacuum ultraviolet (VUV) light, and the other beams of x rays, both for experiments in physics, chemistry, the life sciences, and technology. A very diverse and successful program of experiments has been under way on the VUV ring for a year. The x-ray ring is expected to provide similar capabilities to its users during the coming year.

In furtherance of its role of providing major research machines, the Laboratory is planning a very large heavy-ion colliding beam accelerator which will be capable of accelerating ions as

heavy as uranium to energies approaching 100 GeV per nucleon. The machine will allow deeper studies into the nature of matter and the fundamental forces which hold it together.

At each of these facilities a corps of Brookhaven scientists and engineers performs research and oversees the maintenance and upgrading of the facility. Scientists from universities, other laboratories, and industry also use the facilities, sometimes in collaboration, and often independently. At many of the facilities the visitors outnumber the Brookhaven users substantially. At the AGS, for example, about 80% of the research is done by visitors.

The third of the Laboratory's primary objectives is met by a variety of programs in energy technology, applied sciences, and in various kinds of technical support to the Department of Energy and Nuclear Regulatory Commission. Included are programs to gain insight into the action of catalysts in the production of synfuels; to study power reactor safety problems (for the NRC); to develop a new method for the flash hydrolysis of coal; and to develop better electrochemical systems for energy conversion and storage. Technical support to the DOE is provided by a variety of national and regional studies on energy systems, their characteristics, and their impacts on health; the Technical Support Office for Safeguards, which analyzes systems for preventing the diversion of fissionable materials to unauthorized uses; and the National Nuclear Data Center which assembles and disseminates data on the properties of atomic nuclei.

It should also be emphasized that the Laboratory's programs in nuclear, atomic, and solid state sciences, in chemistry, and in applied mathematics are designed to help create a technology base for the entire energy program of the DOE. These and the various applied programs

build on the strengths and unique facilities of the Laboratory, utilizing its special character, particularly its devotion to frontier science, its close coupling to the academic community, and its experience in working with industry. The contributions are vigorous, broad, and effective.

The Laboratory's objective of training is accomplished primarily through the provision of research opportunities for students from colleges and universities. The Laboratory is not a degree-granting institution, but helps such institutions through its research facilities. From its inception Brookhaven has had an active postdoctoral program with a total of over 1000 young scientists participating for periods of one to three years. Also, students and faculty come to the Laboratory throughout the year, particularly in the summer, not only to use the unique devices but as participants in all of the Laboratory's research programs. In addition, numerous conferences in sciences and technology are sponsored by Brookhaven. Developments of technological significance made at the Laboratory continue to be passed on to industry for commercialization, and an increasing effort is being made to this end.

In the hope of making things easier for readers who wish to know more about particular items, staff lists with indication of individuals' particular interests have been appended. The comments of readers would be most welcome.

Finally, this publication is the work of many people, but I would especially like to acknowledge the efforts of Dr. J.B. Horner Kuper, Mr. Kenneth Ryan, and Mrs. Mary Rustad.



Nicholas P. Samios  
Director

# Accelerator and High Energy Physics Programs

## General Introduction

The frontier of knowledge which most occupies the elementary particle physicist is the world of the very small; as matter is broken down into more and more fundamental constituents, shorter and shorter distance scales are probed. By the uncertainty principle of quantum mechanics, such studies necessarily entail work with particles of high momenta or energies. Thus the synonymy between elementary particle and high energy physics appears.

The need for large and powerful accelerators to study elementary particles has resulted in large user groups performing experiments at such major national laboratories as Brookhaven, the Fermi National Accelerator Laboratory, and the Stanford Linear Accelerator Center. Indeed, the high energy physics program is the largest single item in the Brookhaven Laboratory budget.

At present, the high energy experimental program at Brookhaven centers around the Alternating Gradient Synchrotron (AGS), which accelerates protons to an energy of 30 billion electron volts (GeV). Beams of these protons, or secondary particles produced by them, are used as projectiles to explore subnuclear matter. By studying the way in which the projectile particles interact with target particles inside an atomic nucleus, much can be learned about the constituents of subnuclear matter and about the forces which govern their interactions. At present it appears that the neutrons and protons that make up atomic nuclei are themselves formed of more fundamental entities called quarks, which are bound together by gluons, special particles which transmit the strong force. Many other particles produced in high energy scattering experiments are also believed to be composed of various combinations of quarks held together by gluons. All together

there are perhaps half a dozen varieties of quarks, and a similar number of leptons (an equally fundamental class of particles of which a familiar example is the electron). This modest number of quarks and leptons plus their antiparticles and a few force-carrying particles such as the gluon are thought to explain all of the rich variety of matter. This model of the physical world has had outstanding success, but many questions and puzzles remain. Not all the predicted particles have yet been observed and not all the observed ones are fully understood.

One of the puzzles relating to particle dynamics is the apparent impossibility of isolating a single quark. After a high energy collision, all quarks and antiquarks involved manage to cluster together into the known bound states. Much recent elementary particle physics research has sought to understand the nature of the interquark forces which give rise to this confinement phenomenon while leaving the quarks relatively weakly interacting when near each other.

It is the aim of the Brookhaven High Energy Physics program to investigate these most fundamental questions while providing a center where scientists from other institutions can use the most powerful research tools available for this purpose.

Proposals for experiments using the AGS must be submitted to the High Energy Advisory Committee which is composed of highly qualified physicists representative of the entire user community. This committee advises the Deputy Director for High Energy Physics, who must approve all experiments scheduled on the AGS. About 80% of the research is carried out by visiting scientists from universities, from other national laboratories, and occasionally from abroad.

The Accelerator Department operates the AGS and its experimental areas, providing the beams of protons, antiprotons, kaons, pions, and neutrinos needed for experiments. Department personnel assist the experimenters in setting up their apparatus and provide many services essential to carrying out experiments. Large facilities, such as the Multiparticle Spectrometer and the On-Line Data Facility, are constructed, operated, and maintained by the Department. Some of the Department physicists also participate in research.

The Physics Department is staffed with both experimentalists and theorists. The experimentalists are mainly engaged in research at the AGS, but a fraction of their work is carried out at other accelerators. The theorists provide the

stimulus of exciting new ideas in particle physics and devote much of their time to a study of results from experiments using the AGS and other high energy accelerators in the U.S. and Europe.

The High Energy Discussion Group (HEDG) is an organization brought into being by the community of university and national laboratory users of AGS "to provide an organized channel for the interchange of information between those who utilize BNL high energy facilities for their research and the Laboratory administration." HEDG holds one general meeting at BNL every spring. Much of the work of the users group is coordinated by the HEDG Executive Committee which meets three times a year.

# High Energy Physics Research

## INTRODUCTION

High Energy Physics is the major research activity at Brookhaven National Laboratory. Most of the experimental research is carried out at the Alternating Gradient Synchrotron (AGS) by members of the Physics Department (listed on p. 56) and the Accelerator Department in collaboration with many university groups. The AGS accelerates protons up to energies of 30 GeV. The primary proton beam can be used directly or to produce secondary beams of other particles, such as neutrinos, mesons, antiprotons, etc. These particle beams are the main resources for experimentalists who have used them to perform six to ten experiments each year for the last 22 years. Some of these experiments led to discoveries that had a profound impact in this field. Over the last eight years (since the discovery of the  $J/\psi$  particle at the AGS and SLAC), a consensus has emerged on a standard model for describing the fundamental interactions of nature: quantum chromodynamics (QCD) for the strong interactions and the Weinberg-Salam theory to describe the weak and electromagnetic forces as manifestations of a unified field theory.

Despite its venerable age, the AGS continues to support a very vigorous and diversified program; experiments being carried out now or in the next few years still have the potential of altering the standard model in a significant way. The AGS provides the most intense  $\nu_\mu$ ,  $\bar{\nu}_\mu$  (muon neutrino, antineutrino) beams available anywhere in the energy range 1 to 10 GeV, which are ideally suited for the study of the  $\nu_\mu(\bar{\nu}_\mu)e$  and  $\nu_\mu(\bar{\nu}_\mu)p$  elastic scattering and for the search for neutrino oscillations — the change of  $\nu_\mu$  into another type of neutrino such as  $\nu_e$  (electron neutrino) or  $\nu_\tau$  ( $\tau$  neutrino). The observation of oscillations would imply that neutrinos have mass, an observation with profound implications for cosmology, since in that case most of the mass of the universe would be in the form of neutrinos. The study of  $\nu_\mu e^-$  and  $\bar{\nu}_\mu e^-$  scattering is a very sensitive check of the Weinberg-Salam unified theory.

The most intense K-meson beams are provided by the AGS in the same energy range. These beams are used for the study of rare K-meson decays, a low energy probe of the structure of interactions at much higher energies. The phenomenon of charge-parity (CP) violation, or, equivalently, time-reversal (T) violation (discovered in  $K^0$  decays at the AGS in 1964), which implies that matter and antimatter are not symmetric, is still poorly understood. The only way physicists have found to study it is with K decays. Also, sensitive searches of K decays forbidden by the standard model are very powerful tests of the model; observations of such decays would necessarily lead to modifications or expansions of the model in a very fundamental way.

Intense beams of  $\pi$ , K, and  $\bar{p}$  particles are also used to study hadron spectroscopy, a field to which experiments at the AGS have made significant contributions in the past (among them the discovery of the  $\Omega^-$  and  $\Lambda_c^+$  baryons and the  $J/\psi$  meson). The standard model explains practically all observed hadrons as made of a quark and antiquark ( $q\bar{q}$  mesons) or three quarks ( $qqq$  baryons). It also requires the existence of glueballs (states with no quarks) and does not forbid the possibility of more complex states such as six quarks (dibaryons) or two quarks and two antiquarks ( $qq\bar{q}\bar{q}$  mesons). The existence of glueballs is fundamentally related by QCD to the permanent confinement of quarks inside hadrons; in other words, the fact that no free quarks are observed in nature implies the existence of massive states with no quarks. It is difficult to distinguish glueballs from neutral  $q\bar{q}$  states, and only detailed studies of hadronic states and their decay properties can eventually show whether glueballs are required to explain the observed spectrum.

In addition to experiments at the AGS, members of the Physics Department also collaborate on experiments at FNAL and CERN. In the former, photographs of neutrino interactions in the FNAL 15-ft bubble chamber are scanned and measured using the facilities for



bubble chamber film existing at BNL. The main objective of these experiments has been to study  $\nu_{\mu}e^{-}$  scattering and charm-particle production. At the ISR at CERN a number of physicists from the Physics Department are part of the Axial Field Spectrometer collaboration (R807), one of the largest and most ambitious experiments ever mounted at that facility. The highest center-of-mass energy at the ISR is ideally suited for the study of quark-quark scattering, a very basic process in QCD.

Not all high energy experiments require the use of accelerators or colliding beams; in fact, a test of our understanding of physics at energies beyond those accessible by any conceivable accelerator involves the search for proton decay. Attempts to unify the strong interactions with electroweak interactions (grand unified theories, or GUTs) predict that the lifetime of protons is finite, albeit very long compared to the age of the universe (since its formation, less than 10 kg of the earth may have decayed). In a collaborative search for such improbable events, physicists from BNL, the University of Michigan,

and the University of California at Irvine have built a large tank containing 8000 tons of water inside an Ohio salt mine 600 m underground. This is the largest facility of its kind and the only one at present sufficiently massive to rule out the simplest grand unified theory if no proton decay is observed.

The Physics Department is also home to a very active high energy physics theory group that helps formulate or investigate the consequences of existing models of the fundamental interactions. Grand unified theories have been studied in an effort to refine predictions of proton decay, numerical calculations with lattice gauge theories (a method pioneered at BNL) have been done to predict glueball masses, and a Monte Carlo program has been developed to describe as realistically as possible the types of events to be expected in present and future hadron colliders; these are but a partial list of the contributions of the theory group.

In addition to the above endeavors, many experimentalists and theorists have been working together over the past year generating ideas

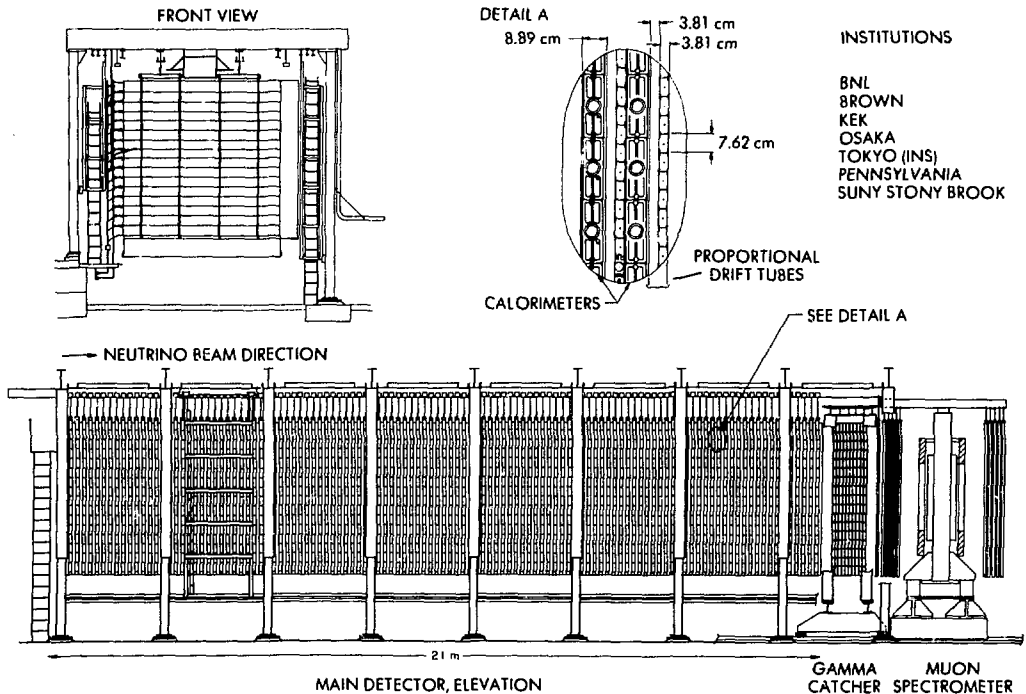


Figure 1. a) The BNL neutrino detector: 100 tons of liquid scintillator calorimeter and proportional drift tubes.

for experiments at the planned Colliding Beam Accelerator (CBA).

The most interesting results of the research carried out during the past year are discussed in the following sections.

### NEUTRINO EXPERIMENTS

Experiments with neutrino beams have been among the main staples of the AGS since it began operation; the first experiment at BNL in 1962 demonstrated that the muon neutrino,  $\nu_\mu$ , is different from the electron neutrino,  $\nu_e$ . As neutrinos have very small cross sections, a great deal of effort has gone into making the beams as intense as possible and the experiments as massive as can be afforded.

For many years one of the major facilities for neutrino experiments was the BNL 7-ft bubble chamber which was decommissioned in 1980.

Data from that chamber are still being analyzed in collaboration with Tohoku University, Japan. A new 100-ton detector has now been operating for almost two years. It consists of 118 modules of scintillator and proportional drift tubes which form both the target material and the detector for the secondary products of a neutrino interaction. The detector needs to be this massive, as one of its major goals is to measure  $\nu_\mu e - \nu_\mu e$  scattering. This is one of the cleanest reactions for testing the Weinberg-Salam theory, but it has an extremely small cross section:  $10^{-42}$  cm<sup>2</sup>, 16 orders of magnitude below that of strong interactions. The detector is shown schematically in Fig. 1a. In an international collaboration (E734), a group of Japanese and American physicists (BNL-Brown-KEK-Osaka-Stony Brook-Tokyo) has been taking data and getting one neutrino interaction per AGS pulse on the average. The detector is optimized for the de-

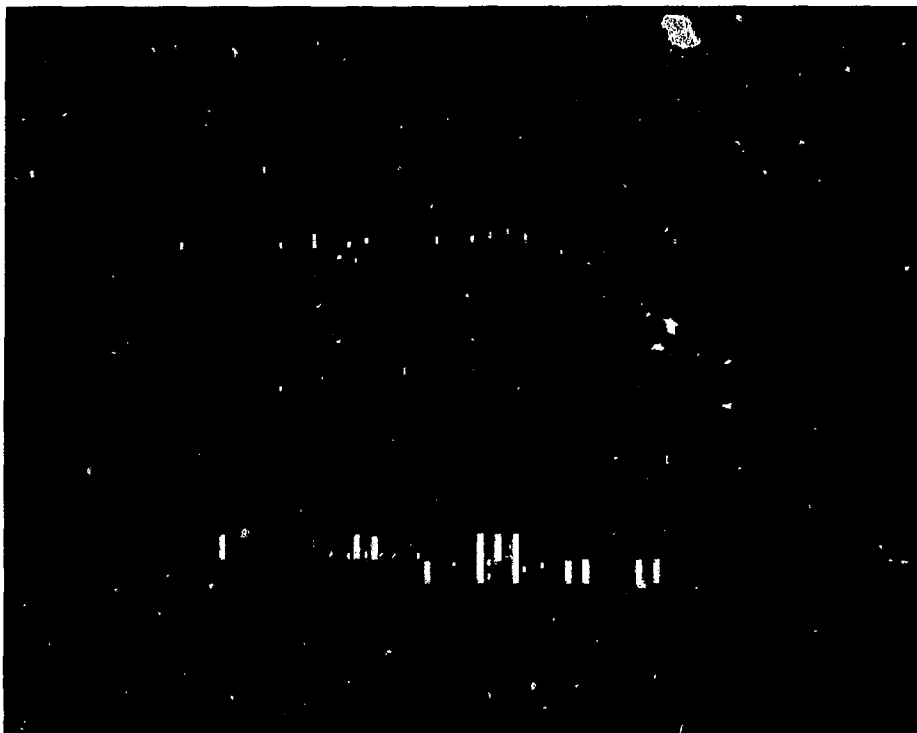


Figure 1. b) A  $\nu_\mu e^- \rightarrow \nu_\mu e^-$  event in the detector. The color in each cell gives the amount of energy deposited, dark blue is the lowest detectable (<0.5 minimum ionizing) and red the highest grade (>4.5 minimum ionizing).

tection of the elastic scattering reactions  $\nu_\mu e^- \rightarrow \nu_\mu e^-$  and  $\nu_\mu p \rightarrow \nu_\mu p$ . The first reaction is characterized by a single outgoing electron in the forward direction. Figure 1b shows what such an event looks like in the detector, a very characteristic electromagnetic shower in the forward direction. The color of each cell in the picture is related to the energy deposition, and it is straightforward to observe the fluctuations in energy typical of electromagnetic showers. Such showers can also be produced by high energy photons, but the beginning of the shower would show twice as much energy since a photon converts to an electron-positron pair. The event separation from the photon background is very clean, as can be seen in Fig. 2. The peak at the origin is due to the  $\nu_\mu e^-$  reaction; the events at wider angles are from background processes. The signal-to-background ratio of 5 to 1 is about 5 to 10 times better than that achieved in higher energy experiments elsewhere.

The same apparatus has been used in a five-week run (E775) to search for  $\nu_\mu \rightarrow \nu_e$  oscillations using the existing BNL narrow-band beam. This short experiment is a test run for a more ambitious program to search for  $\nu_\mu$  oscillations with a more intense lower energy narrow-band beam ( $E_\nu \approx 1$  GeV) being built now. Even with

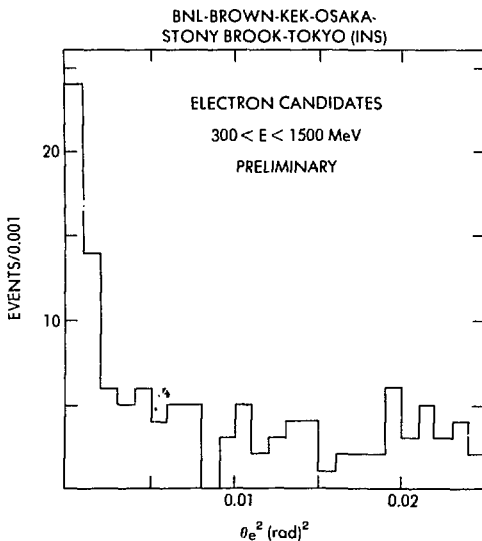


Figure 2. Angular deviation of electron candidate events from incoming neutrino beam direction. The peak near  $\theta_e^2 = 0$  is due to  $\nu_\mu e^- \rightarrow \nu_\mu e^-$  events.

this short run it is expected that E775 will be more sensitive to mixing angles than previous experiments. The signal for  $\nu_\mu \rightarrow \nu_e$  oscillations would be the observation of electrons with the same energy as  $\mu^-$  produced by  $\nu_\mu$ . It is also possible to look for  $\nu_\mu \rightarrow \nu_\tau$  oscillations; the signal would be an apparent attenuation of the  $\nu_\mu$  beam as it goes through the detector. A more sensitive method is to use two detectors some distance apart, and there are plans to do this in a future experiment.

The scanning and measuring facilities for bubble chamber film are still being used for neutrino experiments in the FNAL 15-ft bubble chamber. The emphasis of those experiments has been on  $\nu_\mu e^- \rightarrow \nu_\mu e^-$  scattering, charm production, and dilepton production. Among the most interesting observations from those experiments is that, while events into opposite-sign dileptons ( $\mu^- e^+$ ) have the characteristics expected from charm production, the equal-sign dileptons (about 11  $\mu^- e^-$  events) cannot be explained by associated charm production; the number of events is too large and no strange particles seem to be produced with them. The mechanism responsible for these events is not understood at present.

## WEAK DECAYS

So far the only examples of a violation of time-reversal invariance (T) are  $K^0$  decays. In Exp. 735, a Yale-BNL collaborating group has looked for a violation of T in the decay  $K^+ \rightarrow \pi^0 \mu^+ \nu_\mu$ . If this decay is T invariant the spin of the  $\mu^+$  must lie in the plane of the decay, so the experiment searched for a component of the  $\mu^+$  polarization perpendicular to the decay plane. This was accomplished by stopping the  $\mu^+$  in an aluminum polarimeter and observing its decay to an  $e^+ + \nu_e + \bar{\nu}_\mu$ . The  $e^+$  goes predominantly in the direction of the spin of the  $\mu^+$ . After sampling 33 million such decays (the world sample of such decays before this experiment was two million), the  $\mu^+$  polarization in the forbidden direction was found to be  $0.0018 \pm 0.0036$ , consistent with zero. This limit places strict constraints on theories which attempt to explain T violation by the exchange of Higgs scalars; depending on what order exchange gives rise to T violation, these theories are of two classes: milliweak or superweak.

The same group is ready to take data in an experiment (E749) designed to measure any difference in the ratio of charged-to-neutral two-pion decays for K-short and K-long meson decays. One unique feature of this experiment is that both  $K_s^0$  and  $K_L^0$  decays (and both decay modes) are measured in the same apparatus so that systematic differences in efficiencies are eliminated. Superweak T-violation models predict no measurable difference in this ratio, unlike milliweak models. The sensitivity of the experiment is expected to be sufficiently high to observe for the first time effects predicted by milliweak theories.

In another high-sensitivity experiment (E777), BNL is collaborating with the University of Washington and Yale University in get-

ting ready to search for the rare decay mode  $K^+ \rightarrow \pi^+ \mu^+ e^-$ . This mode is forbidden by the standard model as it violates lepton number conservation. However, it is possible in extended technicolor models. An attempt will be made to measure this branching ratio with a sensitivity better than  $10^{-12}$ , about two orders of magnitude below the present limit.

The first results from the Irvine/Michigan/BNL (IMB) proton lifetime experiment have been reported. The IMB detector is a chamber surrounded by 2000 photomultipliers and filled with 8000 tons of water ( $10^{33}$  protons). It is located 600 m underground in an Ohio salt mine to shield it from cosmic rays. An example of what an event looks like in that detector is shown in Fig. 3. The signal for a proton decay is



Figure 3. Computer graphics of Cherenkov light produced by a stopping muon, as seen in its direction of motion. One can see the ring of light. The number of crossing lines at each phototube is proportional to the amount of light seen by the phototube. The color indicates time of arrival of the signals at the phototubes, red is earliest time and blue latest.

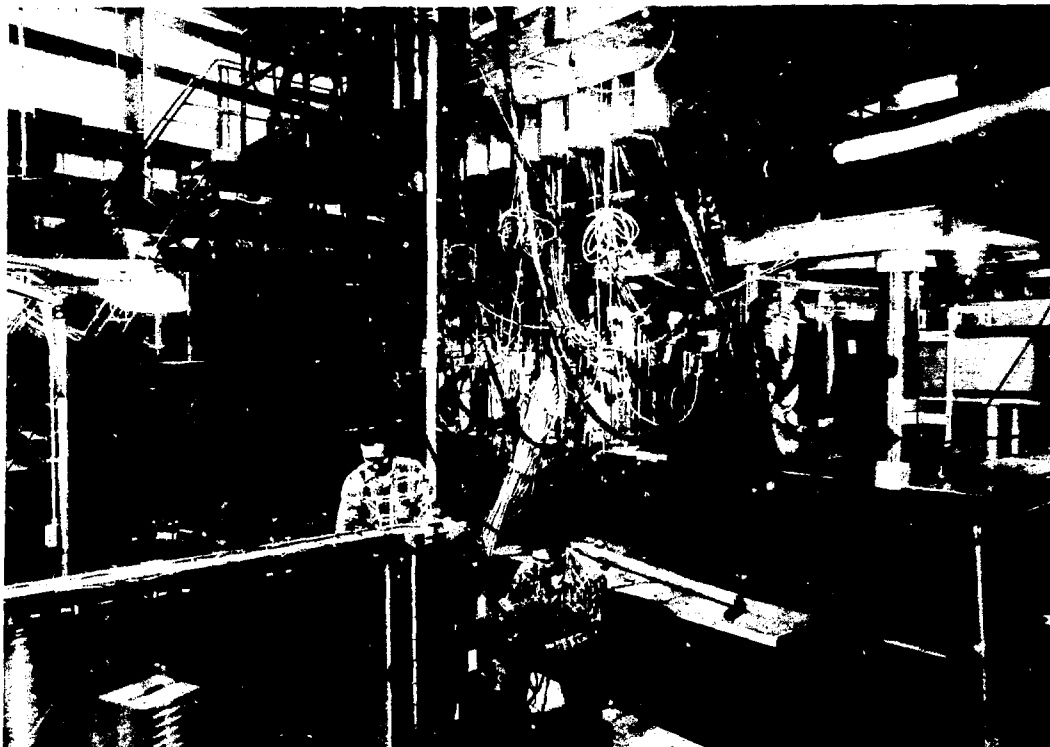


Figure 4. The MPS magnet and a drift chamber module being readied for insertion.

the Cherenkov light produced by relativistic electrons. In 80 days of continuous data taking no examples of the decay  $p \rightarrow e^+ \pi^0$  have been found, corresponding to a lower limit of  $6.5 \times 10^{31}$  years as the partial lifetime to this decay mode. The minimal SU(5) model (the simplest GUT model proposed) predicts a lifetime of  $2 \times 10^{29 \pm 1.7}$  years for the proton and  $e^+ \pi^0$  as its largest decay mode ( $\sim 45\%$ ). The present limit is sufficiently stringent to rule out that model. Further data taking should push this limit beyond  $10^{32}$  years and eventually (in two to three years) approach the ultimate limit of  $10^{33}$  years. This upper limit is dictated by the background from cosmic neutrino interactions. Other GUT models becoming popular these days are supersymmetric theories, so called because they combine fermions and bosons into superfamilies. Their popularity is not due to any positive evidence but to their potential (not yet fulfilled) of unifying gravity with the other interactions.

Supersymmetric models predict that the largest proton decay modes will be of type  $K\mu$  or  $K\nu$ . These modes are much more difficult to detect, but it is expected that the IMB experiment will be able either to observe them or to put stringent limits on them.

### STRONG INTERACTIONS

During 1982, all the spark chambers in the Multiparticle Spectrometer were replaced by a high-data-rate high-resolution drift chamber system. This new system (MPS II), shown in Fig. 4, was quickly brought into operation and 1200 events of the reaction  $\pi^- p \rightarrow \phi \phi n$  were accumulated in a three-week run (E747) with a 22-GeV/c  $\pi^-$  beam; this is eight times more than were accumulated during a longer run with MPS I. From the data in MPS I, it was clear that this may be an interesting channel, as the

production cross section was surprisingly large. A partial-wave analysis of the new data shows that it could be described by two interfering resonances with quantum numbers  $I = 0$ ,  $J^{PC} = 2^{++}$ , one with mass  $2160 \pm 5$  MeV and width  $310 \pm 70$  MeV and the other with mass  $2320 \pm 40$  MeV and width  $220 \pm 70$  MeV. Although the cross section for the reaction is small ( $\sim 20$  nb), it is much too large to be easily explained by ordinary  $q\bar{q}$  states decaying to  $\phi\phi$ , as such a decay mode is expected to be strongly suppressed for  $q\bar{q}$  states produced by  $\pi$  beams. The most likely explanation in the context of QCD is that one or both of those states are glueballs or they are strongly mixed with glueball states. For glueballs the decay to a channel like  $\phi\phi$  is as likely as any other (if they are sufficiently massive). At present, more data are being taken and the number of events is expected to increase by a factor of 4 to 5, which should make it possible to tighten the errors and look for additional states.

Three more experiments are scheduled to take data on the MPS II during the coming year, two concerned with glueballs and another studying radiative decays of hyperons.

While MPS II is now operating smoothly, data from the old MPS I are still being analyzed, with interesting results. An experiment studying the reaction  $\pi^- p \rightarrow K_s K_s n$  (E705) with high statistics has produced evidence for two  $I = 0$ ,  $J^{PC} = 0^{++}$  states, one at  $M = 1240 \pm 30$  MeV and width  $\Gamma = 140 \pm 30$  MeV, referred to as  $g_s$  (1240), and another at  $M = 1770$  MeV, called the  $S^{*1}$  (1770). This makes more  $0^{++}$  states in that energy region than can be accommodated by a  $q\bar{q}$  nonet, as the  $g_s$  (1240) does not seem to be the same state as the  $\epsilon$  (1300) observed to decay to  $\pi\pi$ . The most natural way to explain the observed  $0^{++}$  states is to assume that a  $q\bar{q}$  nonet is strongly mixed with a glueball state to produce ten observable states.

In addition to  $q\bar{q}$  (ordinary meson),  $qqq$  (baryons), and glueballs, QCD also allows the possibility of more complex states such as  $qqq\bar{q}$  and six quark states (so-called exotics), although what the characteristics of such states will be is not well understood. It could be that they exist for too fleeting a moment to be ever detected. It is generally acknowledged that above baryon-antibaryon thresholds the  $qqq\bar{q}$  states will preferentially decay to final states containing a baryon-antibaryon pair. Two MPS

I experiments (E682 and E673) looked for these states in reactions expected to produce them, such as  $\pi^- p \rightarrow \bar{p}p\pi^+$  + anything or  $p\Lambda\pi^+$  + anything (a  $qqq\bar{q}$  exchange process) or  $\bar{p}p \rightarrow \bar{p}p\pi^0$  (a baryon exchange process). Both experiments put very low limits ( $\sim 10$  nb) on the cross sections for producing  $qqq\bar{q}$  states with relatively narrow width ( $\leq 30$  MeV) and masses in the range 1.9 to 2.5 GeV. If  $qqq\bar{q}$  states have widths comparable to those of the  $q\bar{q}$  states, they would also have been observed if their cross sections are at the 100-nb level. From these experiments one can conclude that if  $qqq\bar{q}$  states exist at all they will be extremely difficult to observe.

Predictions concerning resonant states with QCD are difficult to make, although a method which seems to offer promise is the Bag model developed at MIT. Among its most striking predictions is the existence of a six-quark state (H) which would decay to  $\Lambda\Lambda$  except that it lies below threshold and thus is expected to decay only weakly. This state has been searched for at the AGS in the reaction  $pp \rightarrow K^+ K^+ + H$  without success so far. In a previous experiment the limit on the production cross section was set at 30 nb. Data are now being taken in a new experiment (E722), which is expected to find the H if its cross section is bigger than 1 nb.

Another set of experiments at the AGS is concerned with the dynamics of quark scattering inside hadrons. Experiment 755, which ran for two weeks in June 1982 and is expected to take most of its data by next summer, studies only two-body final states from  $\pi^- p$  interactions at  $90^\circ$  in the center-of-mass system. These processes are powerful tools for testing quark scattering models, but their cross sections drop so quickly with energy that these studies are not feasible at energies much higher than those available at the AGS. In another experiment concerned with dynamics, E748, proton-proton elastic scattering is being studied with a polarized target. This experiment is really a preparation for future experiments when the polarized proton beams become available at the AGS. At  $90^\circ$  in the center-of-mass system, very large spin effects were observed at the Argonne National Laboratory Accelerator ZGS before it was closed down. This phenomenon is not now understood and experiments with the polarized proton beam would show whether it persists at higher energies.

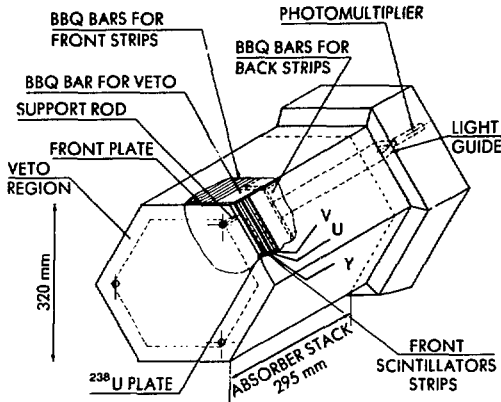


Figure 5. Small-angle electromagnetic calorimeter for the Axial Field Spectrometer at the ISR.

Physicists from BNL have also been very active in experiments at the CERN ISR, a good training ground for future experiments at CBA. The Axial Field Spectrometer Collaboration (R807) is the most ambitious experiment, in complexity and cost, ever mounted at the ISR. Among its novel instruments are hadronic and electromagnetic calorimeters built with scintillator and  $^{238}\text{U}$  plates (provided by the U.S. government). At BNL a small special-purpose electromagnetic calorimeter with  $^{238}\text{U}$  plates was built specifically to look for single  $\gamma$ ,  $\pi^0$ , and  $\eta$  production at small angles (Fig. 5). The main motivation was the discovery of significant single  $\gamma$  production at  $90^\circ$  by a previous experiment (R806), also involving large BNL participation. This important discovery was the first indication of Compton scattering of quarks and gluons and bremsstrahlung by quarks. These processes should also produce single  $\gamma$ 's at smaller angles, and various models based on QCD make different predictions on the expected cross section. The results from new measurements at  $\theta = 11^\circ$  show substantial single  $\gamma$  production although much less than that expected by models predicting large contributions from bremsstrahlung of quarks at small angles. Another important result from R807 last year has been the first clear demonstration of the existence of jets at the ISR and, in particular, a demonstration of how jets become more and more apparent as the center-of-mass energy increases.

## PARTICLE THEORY

The theory group's work has a very wide range, from numerical lattice calculations to fundamental interactions including grand unification schemes. Considerable effort has gone into studying the relevance of these ideas to future high energy machines.

Numerical computations with lattice gauge theories have been done to estimate the masses of pure gauge states (glueballs) as well as the spectrum of  $q\bar{q}$  states. Among the important results of these computations are a demonstration of the recovery of rotational invariance in the continuum limit and a reduction of large  $N$  lattice gauge theory (the twisted Eguchi model).

In addition to lattice studies, continuum non-Abelian gauge fields were investigated, and connections to other nonlinear systems, such as soliton equations and general relativity, have been found. Solutions of the Dirac particle in the presence of 't Hooft-Golmouie-Prasad-Sommerfeld monopole have been found. These promise to clarify the possibility of proton-decay catalysis by monopoles.

In the Weinberg-Salam electroweak theory, radiative corrections were analyzed and the complete  $O(\alpha)$  corrections to atomic parity violation and  $\nu_\mu e$  scattering were computed. These calculations are important for interpreting the present neutrino experiment.

In the studies of GUTs, predictions of the supersymmetric SU(5) model were refined; in particular, the effects of intermediate-mass Higgs scalars on the predictions for  $\sin^2\theta_W$  (Weinberg angle) and the proton lifetime. It was demonstrated that supersymmetric theories do allow an observable lifetime consistent with the present observed value of  $\sin^2\theta_W$ . It was also shown that the spontaneous breakdown of global baryon-lepton symmetry leads to possibly detectable neutron-antineutron and hydrogen-antihydrogen oscillations, with time scales related to the neutrino mass.

The phenomenology of quark mixing angles and CP violations in weak interactions has been studied in great detail, as has the production and decay properties of Higgs mesons, supersymmetric particles, and "bottom" and "top" particles, keeping in mind the new opportunities opened up by the CBA project. The Monte Carlo program ISAJET which simulates jet production in hadronic reactions has been

used extensively to simulate the physics for CBA, including the production of supersymmetric hadrons, study of rare b-quark decays, and measurement of the  $W^\pm + \gamma$  cross section. The program is also quite useful for analyzing many of the current experiments at CERN and FNAL.

### PHYSICS AT CBA

During the past year working groups of theorists and experimentalists from the Physics Department, with some active participation from physicists in various universities, have been doing detailed studies on the feasibility of performing various experiments at CBA that exploit its unique features.

The physics potential of a pp collider at  $\sqrt{s} = 800$  GeV was found to be extremely rich. Some of the important discoveries are expected to occur at the CERN  $\bar{p}p$  collider ( $\sqrt{s} = 540$  GeV), such as the  $W^\pm$  and  $Z^0$  bosons and the top quark (if its mass is below 70 GeV). However, many other fundamental measurements require the high luminosity of CBA: precision measurement of the  $W^\pm - Z^0$  mass difference (with a precision  $\sim 0.26$  GeV); measurement of the reaction  $pp \rightarrow W^\pm + \gamma + X$ , which measures the magnetic moment of the W and tests the non-Abelian coupling of the gauge theory;  $W^+W^-$  pair production which probes the  $W^+W^-Z^0$  cou-

pling characteristic of non-Abelian gauge theory; and searches for Higgs particles, etc. CBA will provide the highest sensitivity to any new phenomena up to masses of 300 GeV and is well matched to the mass scale set by the  $W^\pm$  and  $Z^0$ . The ability to measure all the above important processes was studied in great detail using the Monte Carlo program ISAJET. Methods were found which promise to be very sensitive to supersymmetric particles such as gluinos, scalar quarks, and winos (supersymmetric partner to the W). In the latter case, the possibility of polarized protons in CBA may provide a very important handle as they would be produced in parity-violating processes. Another particle worth searching for is the  $\eta_T$ , predicted by technicolor models to lie in the range 200 to 300 GeV.

CBA is of course ideal for studying rare processes. At  $L = 10^{33} \text{ cm}^{-2} \text{ sec}^{-1}$  it should produce about  $5 W$ 's  $\text{sec}^{-1}$ ,  $10^4$  B mesons  $\text{sec}^{-1}$ ,  $10^3$   $\tau$  leptons  $\text{sec}^{-1}$ , etc. As an example of what is possible, the use of Si micro-vertex detectors with a small interaction region was investigated and shown to be very promising. It would allow the measurement of the branching ratio of the rare process  $B^\pm \rightarrow K^\pm e^+ e^-$  with a sensitivity of  $10^{-5}$  or better. The difficulties of doing experiments at very high rates were studied in detail and it was determined that experiments at luminosities of  $10^{33} \text{ cm}^{-2} \text{ sec}^{-1}$  are feasible but require careful planning.



# Accelerator Department and CBA Project

## INTRODUCTION

The Accelerator Department is responsible for the operation of the major high energy facilities at Brookhaven, principally the Alternating Gradient Synchrotron (AGS) and the CBA construction project. Other work within the Department includes the development of advanced accelerator technology for nonaccelerator applications.

In the AGS, protons are accelerated to 28.4 GeV/c, then extracted and steered to five metal

targets where they interact and produce secondary particles. Beams of secondary particles are focused and transported by systems of magnets to areas where they are used to perform experiments. The Department oversees the scheduling of these experiments and provides services to non-BNL user groups, e.g., help with setting up heavy apparatus, provision of electronic instrumentation, cryogenic targets, and the use of special facilities such as the Multiparticle Spectrometer (MPS).

## The AGS

The acceleration cycle begins with the formation of negative hydrogen ions by electron pickup from a cathode whose work function has been reduced by adsorption of cesium vapor. The negative hydrogen ions are then accelerated down the column of a Cockcroft-Walton preinjector from which they emerge with a kinetic energy of 750 keV. The beam is then transported into the 200-MeV linear accelerator (Linac) where it is accelerated and injected into the AGS. The negative ions are stripped of their electrons by a thin foil at injection.

The AGS is a proton synchrotron of the alternating gradient type. The basic elements of a synchrotron are the ring of magnets which guide the protons around a nearly circular path while applying restoring forces to protons deviating from the central orbit, and the radio-frequency (rf) cavities which provide the energy to accelerate the protons. In the AGS, the transverse slope (gradient) of the magnetic field that a particle in the beam experiences reverses 120 times in one revolution around the machine (hence, "alternating gradient"). This reversing process causes strong focusing, which confines the beam cross section to a relatively small region, thus allowing a much smaller evacuated

beam pipe to contain the beam, and smaller magnet gaps to contain the beam pipe, than is possible without the strong focusing. The rf cavities, located at ten positions around the ring, increase the energy of the protons with every pass until, after about two hundred thousand passes and 0.5 sec of time, it has risen to 28.4 GeV. In the AGS, the radio frequency is chosen to be 12 times the revolution frequency, which results in the circulating protons being divided into 12 tight bunches during most of the accelerating cycle. Once full energy is reached, the protons are ejected from the main ring and sent down beam lines to target stations where they can be used for experiments. Then the cycle begins anew.

There are two extraction modes at the AGS. In the slowly extracted beam (SEB) mode, the circulating beam is first debunched and then slowly extracted over many turns. This is accomplished by causing the beam size to slowly increase by exciting resonances in the orbit and gradually "shaving" off some of the beam particles with an electrostatic septum. The extracted proton beam is then split further and directed to external beam lines by a series of septa and magnets which make up the highly efficient

SEB "switchyard." The entire circulating beam is extracted in this manner over about 1 sec. This relatively long time allows experimenters to take data smoothly without overloading their detectors. The total machine cycle requires about 2.5 sec.

While a particular experiment may not be able to use all the protons available from the AGS, the extracted beam can be split into four beams and, hence, serve as many as eight experiments and a test beam simultaneously. Thus, it is usually desirable to accelerate as many protons as possible. The standard available intensity is now greater than  $0.9 \times 10^{13}$  protons per pulse, and a peak intensity of more than  $1.25 \times 10^{13}$  has been achieved.

For experiments that are not rate-limited and, in particular, experiments using a neutrino beam generated by the proton beam, it may be desirable to receive the full beam with its rf time structure intact over a short period. In the fast-extracted beam (FEB) mode, the proton beam is not debunched and is fully extracted in a single turn. In this case, the beam pulse is delivered within  $3 \mu\text{sec}$ . For this mode, the repetition rate is higher than for SEB, with one pulse delivered every 1.6 sec.

Figures 1 and 2 give the accumulated total protons accelerated and the total hours available for doing high energy physics (HEP) experiments over the past several years. As Fig. 1 illustrates,  $4 \times 10^{19}$  protons were accelerated in FY 1982 during 23 weeks of running time. The operating efficiency, defined as the ratio of (HEP hours) to (HEP hours + unscheduled downtime), was 69%. This parameter has remained nearly constant over the past few years despite tightening budgets. During an average week of scheduled running time, 122 hours were available for HEP. Average intensity per pulse was  $0.76 \times 10^{13}$ , 14% higher than in FY 1981. Total protons delivered increased by 29%.

While the AGS is busy accelerating protons to 28.4 GeV, its injector, the 200-MeV Linac, is able to continue cycling, delivering protons to two other facilities, the Brookhaven Linear Isotope Producer (BLIP) and the Chemistry Linac Irradiation Facility (CLIF). The total 200-MeV proton charge delivered to the BLIP in FY 1982 was 0.19 ampere-hour, 10% more than in FY 1981.

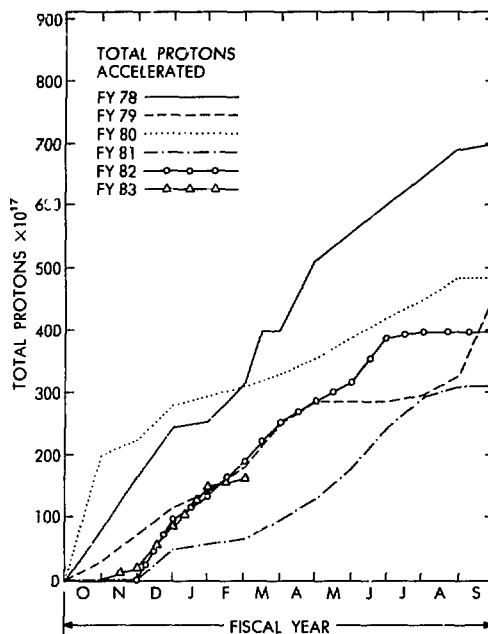


Figure 1. The accumulated total number of protons accelerated each fiscal year since FY 1978.

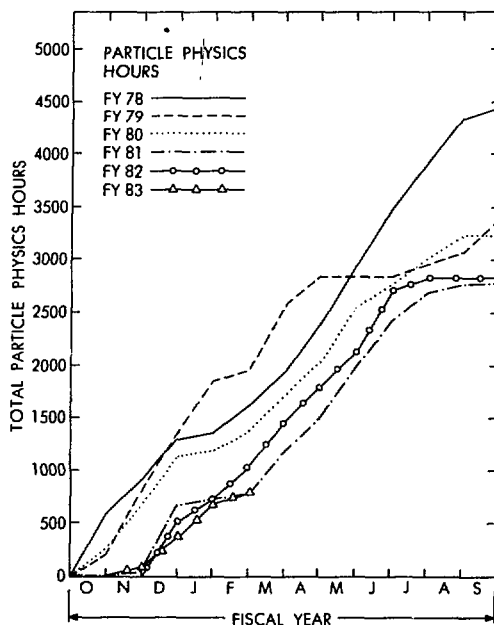


Figure 2. The total hours available for high energy physics experiments since FY 1978.

## IMPROVEMENTS TO THE AGS

During the summer shutdown of 1982, several changes of greater than usual scope and significance were accomplished. The most important of these was the changeover to  $H^-$  charge exchange injection at the AGS (Fig. 3). This new injection scheme has reduced beam losses and provided higher reliability of the injection systems. Indeed, new intensity records have already been set shortly after restarting the machine with a peak intensity of  $12.5 \times 10^{12}$  protons per pulse and a one-shift (8 hour) average of  $11.32 \times 10^{12}$  per pulse.

By injecting negative hydrogen ions into the AGS and stripping the electrons away by passing the beam through a thin carbon foil inside the ring, a source of protons is created whose position in phase space within the machine acceptance can be held fixed throughout the injection pulse. All the protons can be "overlaid" into the same phase space rather than "stacked" into adjacent phase-space areas as required with the previous  $H^+$  (proton) injection.

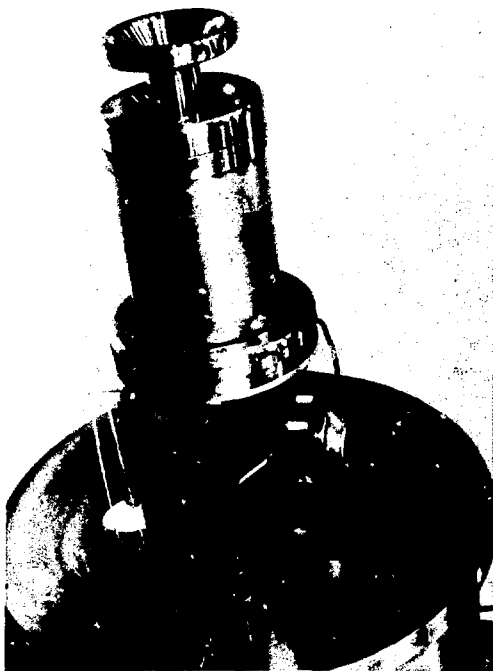


Figure 3. The new  $H^-$  source.

This approach provides greatly increased flexibility in filling the AGS. As a result, the present intensity limitations may be pushed back, or at least better understood. In addition, the radiation levels in the injection region have been greatly decreased. Previously, 70% of the injected beam was lost during injection. With  $H^-$  injection, these losses have dropped to about 10%. The beam current handled by the Linac is thereby reduced, improving reliability and increasing the lifetime of Linac components.

With the intrinsically greater simplicity and reliability of the injection system, other factors limiting the beam intensity will come into focus and proper measures can be planned to remedy them in the future. In FY 1983, the radio-frequency acceleration system has become the subject of detailed scrutiny to explore how it limits the intensity of the beam, during capture after injection and during acceleration.

### Polarized Proton Acceleration

The most extensive program of modification now under way in the AGS Division is the effort to accelerate polarized protons. The spins of the protons accelerated in the AGS are randomly oriented. During the late 1970s, some extremely surprising experimental results were produced at the ZGS, a 12-GeV proton accelerator at Argonne National Laboratory, using polarized protons, i.e., protons whose spins were preferentially aligned in a single direction. With the objective of studying polarized proton interactions at the higher energies available at the AGS, a collaborative effort has been mounted by BNL and groups from the University of Michigan, Argonne, Yale University, and Rice University. Essentially every step in the accelerating process poses challenging problems.

The polarized ion source has achieved  $0.5 \mu A$  of beam on the test stand, and, with an upgraded cesium gun which is under construction, it is expected to deliver several microamperes, as required by the program, in the near future.

Acceleration from source to Linac will take advantage of recent advances in low beta accelerators, using an RFQ, an rf cavity with vanes shaped to produce focusing and accelerating forces on the protons, rather than a Cockcroft-Walton preaccelerator.

In order to maintain the polarization of the protons through the acceleration cycle, a number

of schemes must be employed to avoid a series of 50 imperfection and 8 intrinsic depolarizing resonances. The worst of these are the intrinsic resonances which are caused by the same strong focusing magnetic fields that allow the AGS to accelerate its beams. The effects of these resonances can be suppressed by moving through the resonance condition rapidly, which can be accomplished by suddenly changing the quadrupole field that particles in the beam experience.

Four of the 12 pulsed quadrupole magnets to be used for polarized proton acceleration were installed in the AGS and another 8 are expected to be installed in 1983. These magnets will permit a rapid variation of the vertical "tune" of the ring to maintain proton polarization while crossing the 8 intrinsic depolarizing resonances during the acceleration cycle.

An engineering prototype pulsed quadrupole power supply is being tested and plans are being made for the manufacture of 6 of the required 12 quadrupole modulators in FY 1983. With 6 power supplies, polarized protons can be accelerated to about 20 GeV which will permit the start-up of the polarized proton program after the end of FY 1983. Six more power supplies to be assembled later will permit extension of the energy to 26 GeV. Beam diagnostic equipment in the Linac and the AGS will be adapted for the low polarized proton intensity. Polarimeters will be installed in the LEBT (at 20-keV energy), in the Linac-AGS transport line (200-MeV energy), in the AGS vacuum chamber (up to 26 GeV), and in the external beam line near the D target (top energy). These polarimeters will permit determination of the polarization of the beam as a function of energy throughout the acceleration and spill cycle.

### Instrumentation

With a view toward the commissioning of the new H<sup>-</sup> injection system, the development of a polarized proton beam capability, and the future needs of the CBA injection system, new beam diagnostic instrumentation was developed and tested in the AGS in FY 1982. The Internal Profile Monitor, a device using the induced residual gas ionization to obtain a profile of the beam distribution in the AGS, was installed and tested successfully. This diagnostic tool permits a quantitative study of the AGS beam size as a function of time in the acceleration cycle. The

capabilities of the extracted beam profile monitors in the FEB line were expanded and a systematic measurement of the extracted beam emittance has been obtained with new devices, multiwire secondary emission monitors. Both the internal profile monitor and the external beam profile monitors are extremely valuable for conventional operation. They will be essential for polarized proton operation, where vertical beam size affects the strength of depolarizing resonances, and for CBA injection, where beam emittance affects the final luminosity.

It is expected that in FY 1983 an automatic betatron tune measuring system will be developed for the AGS. In conjunction with the new beam profile monitor, it will then be possible to test various tune operating points in the AGS as a function of time with a view to minimizing transverse beam dilution. In polarized beam operation, the tune is carefully programmed throughout the acceleration cycle, and a convenient tune measurement system is vital to the success of that program.

### Other Improvements

A major event during the summer shutdown was the repair of the Siemens motor and generator rotors in a General Electric service shop in New Jersey. These components had developed weaknesses in the coil windings and the repair work was both timely and successful. At the same time, the Westinghouse motor generator set, which had served the AGS prior to the conversion in 1970, was recommissioned with a rewound stator. At the start of FY 1983, the Siemens set was back in operation, and the Westinghouse set (with about half the duty-cycle capability of the Siemens) was in fully operational standby status.

Replacement of a number of badly corroded vacuum chamber bellows in the AGS was also accomplished during the shutdown. Still more of them will need to be replaced in FY 1983. The ring vacuum system was upgraded with a gauge system, and the monitoring of the ion pumps was changed to allow better localization of areas with high leak rates.

A fast kicker magnet has been installed and beam has been extracted to serve the D line with a single bunch of beam, simultaneously with the extraction of the remaining 11 bunches to the neutrino experiments in the north area

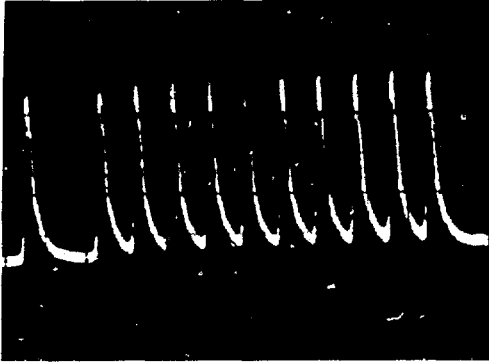


Figure 4. The proton beam bunches extracted in the FEB line following the extraction of the second bunch in the SEE.

(FEB). The kicker magnet is a duplicate of the one serving the FEB, but the excitation pulse is very short (400 nsec). This is necessary in order to cleanly extract the single bunch for Exp. 745, a test of quantum electrodynamics in muonic helium, while not disturbing the remaining 11 bunches which are destined for fast extraction to the neutrino area. Figure 4 shows the 11 remaining bunches in the AGS following extraction of the second bunch.

In the rf system, shunting switches were installed across the accelerating gaps. These switches are activated during the flattop while a slow spill is being delivered to the external beams. This is done to suppress the undesirable high-frequency modulation which adversely affects the duty cycle of the spill. For many experiments the absence of spill modulation improves the data-taking capability.

### NEUTRAL BEAM DEVELOPMENT

The objective of the program is the development of high energy steady state neutral beams for future fusion devices, for heating experiments in tokamaks and mirror machines, for current drive in tokamaks, and for on-line plasma diagnostics. The BNL Neutral Beam Development Group currently has concentrated its efforts on developing high-density negative deuterium sources and plasma neutralizers, the latter as an alternative to laser neutralizers. The ion sources are based on the direct extraction of negative ions from a plasma surface sys-

tem, either without or with plasma injection from an independent hollow cathode discharge; hollow cathode arcs also serve as the plasma source for the neutralizer.

During the past year, ion studies have been concentrated on the system with hollow cathode discharges, where plasma generation and negative ion production are separated and can be independently controlled. A true steady state operation (several days) of the plasma generator and the converter electrode has been achieved; more than 0.2 A of  $H^-$  ions has been extracted over several hours, with peak values of 0.5 A. Plasma uniformity and gas efficiency have been greatly improved by changing the electrode shape. A new source module has been fabricated to produce a flat sheet of plasma in front of the converter; it should yield a ribbon  $H^-$  beam with a line current density of 6 A/m, with a gas efficiency better by a factor 3 than any existing source. The geometry of the source has been chosen to match the LBL accelerator.

Plasma neutralizers for negative ions have been studied further and a 1-m-long system is in fabrication. It will be used to determine neutralization efficiencies of hydrogen and other negative ions, in cooperation with the BNL Physics Department.

### FUTURE PLANS

A preliminary design study for an accumulator ring between the Linac and the AGS was completed in early 1983. The accumulator ring is envisioned as part of a two-pronged approach to increasing the polarized proton beam intensity above the limit of about  $10^{10}$  protons per pulse provided by the presently conceived ion source. After commissioning of the present ion source and the initial polarized proton physics program, long-term research and development will be directed at improving the intensity of polarized ion sources by two or more orders of magnitude. The accumulator will provide more than an order of magnitude above whatever is achieved with the ion sources. Moreover, its magnet lattice will be designed to permit, in a subsequent expansion phase, the acceleration of protons to about 1-GeV kinetic energy prior to injection into the AGS. This will make it possible to raise the space-charge limit on the AGS intensity.

# Planning and Support of the Experimental Program

The Experimental Planning and Support (EP&S) Division is responsible for the operation of the AGS experimental research program. This responsibility includes the development and execution of both long- and short-range schedules as outlined by the Director. The EP&S staff carries out the planning and construction of particle beams; installation and servicing of large experimental equipment such as spectrometer magnets, hydrogen targets, and large particle detectors; maintenance and operation of beam separators and cryogenic devices; installation and maintenance of electrical power and cooling water systems; maintenance of a large pool of electronics equipment for experiments (HEEP); safety review of experimental setups; design of new beams and experimental facilities; and development of new detectors and electronics, all as required to support the research activities of guest and resident scientist users. Operational crews are maintained on

a 24-hour, 7-day-per-week basis to operate, service, and provide safety surveillance of the experimental areas and equipment. The EP&S Division also is responsible for the operation of the On Line Data Facility (OLDF).

Twelve experiments were run and three were completed in FY 1982 during the 12 weeks of the counter program and the 11 weeks of the neutrino program. Seventeen experiments are expected to run in FY 1983 during the 14 weeks of the counter program and the 7 weeks of the neutrino program. The experimental area layout is illustrated in Fig. 5, and the characteristics of the beams used to support the program are given in Table I. Table II describes both the completed FY 1982 program and the anticipated FY 1983 program.

The major EP&S projects can be classified into two categories: experimental area operations and support; research and development projects.

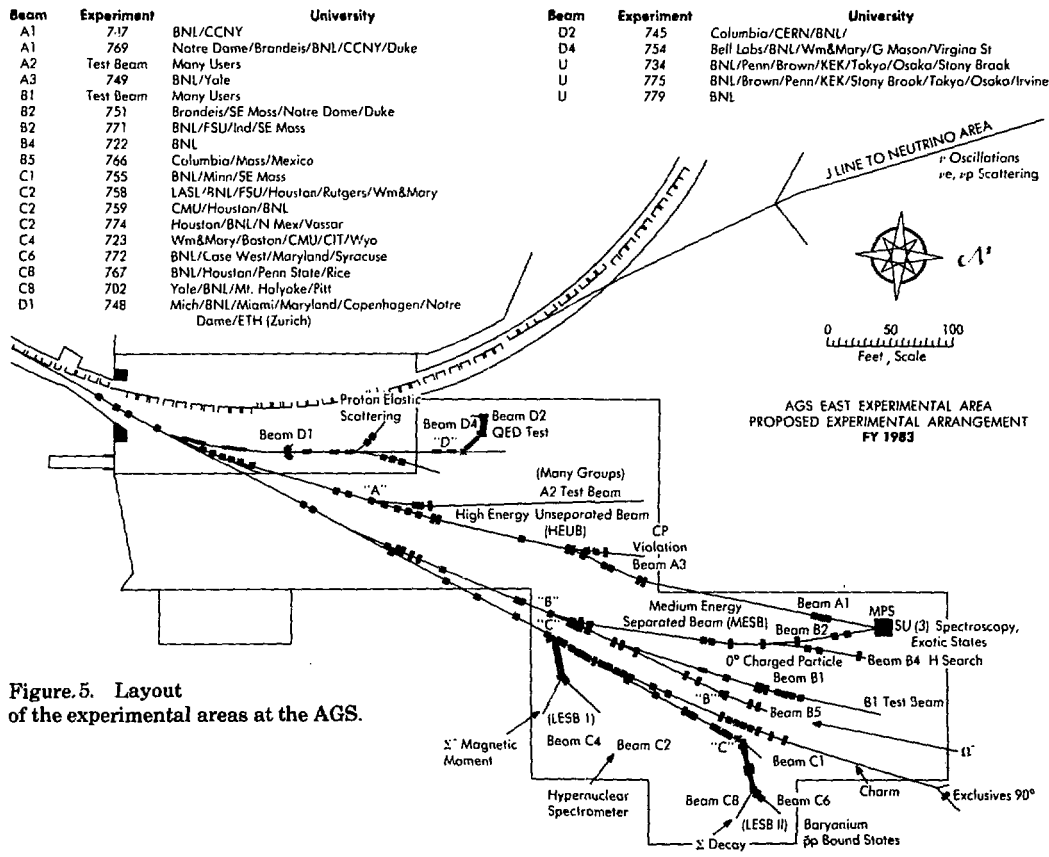


Figure 5. Layout of the experimental areas at the AGS.

Table I  
BNL Beams Operational  
January 1983

Separated Beams for General Use			Flux in thousands/ $10^{12}$ protons on target										
Beam	GeV/c	$\pm \frac{\Delta p}{p}$ (%)	Prod. Angle	$\Omega$ (msr)	$K^+$	$K^-$	$p$	$\bar{p}$	$\pi^+$	$\pi^-$	@ GeV/c	Purity	Remarks
B4	1.5-6(K) 1.5-9( $\bar{p}$ )	3	3°	0.3	270	120	$2 \times 10^4$	100	$4 \times 10^4$	$3 \times 10^4$	4	$\pi^+/K^- \sim 3$ $\pi^-/\bar{p} \sim 2$ $\pi^+/K^- \sim 10$	Usually $2 \times 10^{12}$ ppp; L = 81 m
C2,C4	<1.1	2	10.5°	2.6	40	12	$2 \times 10^4$	2	$8 \times 10^4$	$8 \times 10^4$	0.75	$\pi^+/K^- \sim 10$	Usually $2 \times 10^{12}$ ppp; L = 15 m
C6,C8	<0.8	2.5	5°	15.0	200	60	$1.4 \times 10^5$	14	$6 \times 10^5$	$6 \times 10^5$	0.7	$\pi^+/K^- \sim 20$	Usually $2 \times 10^{12}$ ppp; L = 15 m
Separated Beams for Fixed Facilities													
B2	(Same characteristics as B4)											MPS	
Unseparated Charged Beams for General Use													
B1	5-24	3	0°	0.3	2500	700	$1.5 \times 10^5$	200	$\pi^+$	$\pi^-$	10		Usually $2 \times 10^{12}$ ppp; L = 75 m
C1	5-24	5	0°	0.0	900	400	$3 \times 10^4$	30	$1 \times 10^4$	$3 \times 10^4$	13	$\mu^+/\pi^+ = .03$	Usually $2 \times 10^{12}$ ppp; L = 61 m
Unseparated Charged Beams for Fixed Facilities													
A1	5-24	1.6	0°	0.2						1000	22		MPS; L = 130 m; $10^{12}$ ppp; 25-cm Be target
Neutral Beams for General Use													
A3	1-28		0°	0.0035				2000	$10^6$		1-28		< $10^{12}$ ppp; alternates with A1; L = 8 m; design intensity
Muon Channel													
B5	1-28		0°	0.01					$3 \times 10^5$		1-28		$10^{10}$ ppp typical; L = 2.6 m; design intensity
Muon Channel													
D2, D4	1-0.3( $\pi$ ) 0.05- 0.15( $\mu$ )	9( $\pi$ )	55°( $\pi$ )	50( $\pi$ )		2000					0.10		Flux in $100 \text{ cm}^2$ with $\Delta p/p = \pm 2\%$ ; design intensity
Neutral Beam for General Use													
U							$10^7/\text{m}^2$	$7 \times 10^6/\text{m}^2$				$9 \times 10^{12}$ ppp typical	Fast spill, flux av over 0.7-m radius, peaks at 1.5 GeV/c

\*A3 has been converted to a neutral beam for FY 1982.

Table II  
Utilization of Beam Lines

Beam	Exp. No.	Institutions Description of Experiment	
A1	747	BNL/CCNY Study of $\phi$ production from $\pi^- p$ reactions, including $\pi^- p \rightarrow \phi p n$ , with a search for resonances in the $\phi\phi$ system (glueballs).	To be completed in FY 1983.
A1	769	Notre Dame/Brandeis/BNL/CCNY/Duke A search for glueballs and other meson states. Study the reactions $\pi^- p \rightarrow n K_S^0 K_S^0 \eta^0$ and $\pi^- p \rightarrow n K_S^0 K_S^0 \pi^0$ at 21 GeV/c with a lead glass hodoscope in the MPS.	To begin FY 1984.
A3	749	Yale/BNL Test milliweak CP-violation models by accurately measuring difference in the ratio of charged to neutral two-pion decays for $K_S$ and $K_L$ meson decays.	To be completed in FY 1983.

Table II (Continued)  
Utilization of Beam Lines

Beam	Exp. No.	Institutions Description of Experiment	
B2	771	BNL/FSU/Ind/SE Mass Study of E meson characteristics in $\pi p$ , $K^- p$ , and $\bar{p}p$ interactions in the MPS. The possible glueball and strangeonium components will be distinguished by the production reaction.	To be completed in FY 1983.
B2	751	Brandeis/SE Mass/Notre Dame/Duke Measurement of the radiative hyperon decays $\Xi^0 \rightarrow p\gamma$ , $\Xi^0 \rightarrow \Lambda\gamma$ , and $\Omega^- \rightarrow \Xi\gamma$ in the MPS with a lead glass hodoscope.	To begin FY 1983.
B4	722	BNL A second-generation search for exotic six-quark states in the reaction $p + p \rightarrow K^+ + K^+ + X$ . Exotic states would be observed as missing mass peaks recoiling against the two $K^+$ 's.	To be completed in FY 1983.
B5	766	Columbia/Mass/Mexico Study of $\Omega^-$ production from $np \rightarrow \Omega^- X$ resonances.	Continuing into FY 1983
C1	726	NYU/BNL Search for charm in hadronic interactions near threshold. The reactions: $\pi^- p \rightarrow D^{*-} B_c^+ \quad (B_c^+ = \Lambda_c^+, \Sigma_c^+, \dots)$ $\quad \quad \quad \downarrow \bar{D}^0 \pi^-$ $\quad \quad \quad \quad \quad \downarrow K^+ \pi^-$	To be completed in FY 1983.
		will be studied. The final two decay particles will be analyzed in a large-aperture spectrometer, with sensitivity estimated to be better than 20 nb.	
C1	755	BNL/Minn/SE Mass Study of hard quark-quark scattering in two-body exclusive reactions at $90^\circ$ in the center of mass. $\pi^- p \rightarrow p\pi^-, p\rho^-, p\Lambda^2, \pi^+\Delta^-, K^+\Sigma^-, K^+Y^*, \Delta K^0$ .	To be completed in FY 1983
C2	758	LANL/BNL/FSU/Houston/Rutgers/Vassar/Wm&Mary The ( $\pi^+ K^+$ ) reactions as a new tool for the study of hypernuclear structure. The reaction $\pi^+ + n \rightarrow K^+ + \Lambda$ will be used to produce hypernuclei at higher momentum transfers than is possible with the often used $K^- + n \rightarrow \pi^- + \Lambda$ process. This should make heavier nuclei and higher spin states more accessible.	To be completed in FY 1983.
C2	759	CMU/Houston/BNL A study of the weak decay modes of the hypernucleus ${}^{12}_{\Lambda}C$ .	To be completed in FY 1983.
C2	760	MIT/BNL/Torino/Houston/NYU/Vassar/Peking Spin dependence of the Lambda Nucleon interaction determined by observation of hypernuclear $\gamma$ rays. The hypernuclei to be studied are ${}^7_{\Lambda}Li$ , ${}^9_{\Lambda}Be$ , and ${}^{16}_{\Lambda}O$ .	Completed FY 1983.
C2	774	Houston/BNL/N. Mex/Vassar Search for $\Sigma^-$ hypernuclear levels in ${}^4He$	
C4	723	Wm&Mary/BU/CMU/Caltech/Wyo Precision measurement of the $\Sigma$ magnetic moment by the exotic atoms technique, using a stopping $K^-$ beam: $K^- p \rightarrow \Sigma^- \pi^+$ , with the $\Sigma^-$ captured in a high Z material. Observation of a monoenergetic $\pi^+$ tags the presence of the $\Sigma^-$ , and the $\mu_{\Sigma^-}$ is obtained by measurement of the hyperfine splitting in the transition x ray.	To be completed in FY 1983.



Table II (Continued)  
Utilization of Beam Lines

Beam	Exp. No.	Institutions Description of Experiment	
C6	762	BNL/Mich State/Syracuse/Temple Search for narrow structures in the $\bar{p}p$ annihilation cross section from 1900 to 1960 MeV, with 2.5-MeV resolution.	Completed FY 1982.
C6	772	BNL/Syracuse/Case Western/Maryland Search for $\bar{p}n$ bound and resonant states, in particular, the reported effects at 1795 and 1987 MeV. The reaction $\bar{p}d \rightarrow p + \bar{p}n$ is studied with a recoil proton spectrometer.	To be completed in FY 1983.
C8	702	Yale/BNL/Mt. Holyoke/Pitt Measurement of the asymmetry in the decays of polarized hyperons produced from a polarized target. Measurement of the $\Sigma^+$ decay parameters in $\Sigma^+ \rightarrow n\pi^+$ decays and $\Sigma^+$ in $\Sigma^+ \rightarrow p\pi^0$ .	To be completed in FY 1983.
C8	767	BNL/Houston/Penn State/Rice Development of a low energy antineutron source and measurement of $\bar{n}p$ annihilation cross section near NN threshold. The construction of an antineutron beam will permit the study of the $\bar{N}N$ interaction at very low energies where $dE/dx$ limits the usefulness of $\bar{p}$ beams. $\bar{n}$ 's will be produced by 500 MeV/c in the charge-exchange reaction $\bar{p}p \rightarrow \bar{n}n$ .	To begin FY 1983.
D1	748	BNL/Mich/Miami/Copenhagen/Maryland/Notre Dame/ETH (Zurich) Measurement of the analyzing power in proton-proton elastic scattering as a function of $s$ and $p_T^2$ using a polarized proton target at several proton beam energies up to 28 GeV.	To be completed in FY 1983.
D2	745	Columbia/CERN/BNL A precise measurement of the $3d \rightarrow 2p$ transition in muonic helium as a test of quantum electrodynamics. A high-power $CO_2$ laser is employed to induce the transition following a muon stopping in helium gas. The emitted 9.75-keV x ray is detected with a solid state device.	To begin FY 1983.
D4	754	Bell Labs/BNL/G. Mason/Virginia State/Wm&Mary Study of positive muon depolarization in doped aluminum. The measurements are intended to discriminate among various models of $\mu^+$ motion in metals. These results are needed for future use of the $\mu^+$ spin rotation technique in more complex condensed matter systems.	To begin FY 1983
U	775	BNL/Brown/Penn/KEK/Osaka/Stony Brook/Tokyo (INS)/UC Irvine Search for neutrino oscillations via $\nu_\mu \rightarrow \nu_e$ transitions, using a narrow-band $\nu_\mu$ beam and the E734 detector.	To begin FY 1983.
U	734	BNL/Brown/Penn/KEK/Osaka/Stony Brook/Tokyo (INS) Measurement of elastic scattering of neutrinos from electrons and protons. These are weak neutral current processes. The outgoing electron or proton in the reactions $\nu e \rightarrow \nu e$ $\nu p \rightarrow \nu p$ is identified by its characteristic behavior in a large aluminum-scintillator-proportional wire counter detector.	Completed FY 1983.
U	779	BNL Nuclear spectroscopy and nuclear reaction studies. 28-GeV/c protons will irradiate thin targets, producing new or little-studied neutron-rich nuclides below thorium.	To begin FY 1983.

## EXPERIMENTAL AREA OPERATIONS AND SUPPORT

Highlights of the program in FY 1982 include 11 weeks of running in the North Area for the  $\nu$ -e elastic scattering group, E734 (BNL/Penn/Brown/Osaka/Stony Brook/KEK/Tokyo). They acquired 80  $\nu$ e events ( $E_e > 200$  MeV), 3000  $\nu$ p elastic events ( $Q^2 > 0.04$  GeV<sup>2</sup>), and 20  $\nu$ e elastic scatters ( $E_e > 200$  MeV). In the East Area A1 line, E747 (BNL/CCNY) found evidence for composite gluon systems (glueballs). Using the improved MPS, they observed resonances in the  $\phi\phi$  system by detecting the decays of the two  $\phi$ 's into  $K^+K^-$  pairs. In the C1 line, E726 (NYU/BNL) completed a search for hadronic charm production. In LESB I, E760 (MIT/BNL/Torino/Houston/NYU/Vassar/Peking) completed a study of the spin dependence of the lambda-nucleus interaction by observing hypernuclear gamma rays. Also in this beam, E723 (Wm&Mary/BU/CMU/Caltech/Wyo) measured the magnetic moment of the  $\Sigma^-$  hyperon. They studied the hyperfine splitting in exotic atoms produced by stopping  $K^-$ . Their results will complement those obtained at higher energies which measure the spin precession directly. In the LESB II, E762 (BNL/Mich State/Syracuse/Temple) completed a search for narrow structures in the  $\bar{p}p$  system between 1900 and 1960 MeV, and E702 (Yale/BNL/Mt. Holyoke/Pitt) continued their study of the asymmetry in the decays of polarized  $\Sigma^\pm$  hyperons produced by  $K^-$  incident on a polarized proton target. The first experiment in the D1 line, E748 (BNL/Mich/ANL/Miami/Copenhagen), was begun. It is a study of the analyzing power of pp elastic scattering, using a polarized target, and is a precursor to the development of this area for use with polarized protons.

The stopping muon beam D2 was installed and commissioned early in FY 1983. Experiment 745 (Columbia/CERN), a test of quantum electrodynamics in muonic helium, will have a test run in FY 1983, as will E754 (Bell Labs/BNL/Wm&Mary/G. Mason/Virginia State), the muon spin rotation experiment.

A new test beam was under construction in the B1 area early in FY 1983. It will provide particles up to 20 GeV/c for several groups which will test detectors in FY 1983.

Installation of quadrupole magnets in Beam C1 behind Exp. 726 greatly improved the beam

optics for Exp. 755 (BNL/Minn/SE Mass) (Fig. 6) which is in tandem with the apparatus of E726 which was completed in FY 1982.

A 5-in.-gap electrostatic beam separator was built and installed in the LESB II, replacing the 6-in.-gap separator whose performance had greatly deteriorated in FY 1982 running. A marked improvement in performance and reliability resulted. A 2-in.-gap separator doublet was installed in the MESB, providing greatly improved beam purity for E722 (BNL), a search for six-quark exotics, and Exp. 771 (BNL/FSU/SE Mass/Ind), a search for gluonium states. The hypernuclear spectrometer underwent a major upgrade early in FY 1983, providing nearly an order of magnitude increase in particle flux for E758 (LANL/BNL/FSU/Houston/Rutgers/Vassar/Wm&Mary) and E759 (CMU/Houston/BNL). A new narrow-band neutrino horn was designed for the long base line neutrino oscillation experiment, E776 (Columbia/III/Johns Hopkins/NRL), which is under construction in the North Area. A high-



Figure 6. Experiment 755 (BNL/Minn/SE Mass) under construction.

intensity beam was designed for Exp. 777 (Yale/BNL/Wash), a rare kaon-decay experiment which will test technicolor theories.

## RESEARCH AND DEVELOPMENT

Development work was concentrated in multiwire secondary emission chambers which were used for emittance measurements in the extracted beam to the neutrino area and in further development of FASTBUS in collaboration with Exp. 749 (Yale/BNL).

## ADVANCED TECHNOLOGY APPLICATIONS DIVISION

During the past year the 1000-MVA superconducting power transmission cable Test

Facility has been operated for three running periods, each of about two weeks' duration. The system performance has been measured with simultaneous voltage and current excitation up to the rated levels of 80 kV and 4100 A, corresponding to 138 kV, 1000 MVA on a three-phase basis. In addition, the cables have been energized up to the 30-minute emergency rating of 6000 A.

A first full-wall trial cable was constructed of the fully synthetic tape insulation developed by Brookhaven. Tests of oil compatibility, oil impregnation, and high-voltage performance have been carried out.

A 300-ft-long cable will be made in May 1983, for installation in the outdoor Test Facility. Methods of terminating the cable are under investigation. The cable is rated for 230-kV service.

## The CBA Project

---

The Colliding Beam Accelerator (CBA) project which was designed to accelerate protons at energies up to 400 GeV was canceled late in 1983. Cessation of the construction project was predicated upon the belief of the high energy physics community that every effort must be made to design and build, in the United States, a superconducting super collider (SSC) with proton energies in excess of 2 TeV (2000 GeV). This decision was made after it was apparent that Brookhaven could finish the construction of the CBA on time and on budget. Although we believe that such a decision was not in the best interest of high energy physics, we have joined the efforts to plan for the SSC and we expect to play a leading role in magnet design for the new machine. In addition, there is a strong move to take advantage of the construction already completed and the expertise on hand to build a heavy-ion colliding beam accelerator which will again make Brookhaven a unique center for an important area of physics.

Although what follows was aimed at the CBA, most of it will also apply to the proposed heavy-ion accelerator.

## SUPERCONDUCTING MAGNETS

As reported in the previous HIGHLIGHTS, 1981 was devoted to implementing the modified two-layer superconducting magnet design devised by R.B. Palmer, i.e., a design based on a cabled conductor similar to that used at Fermilab, wound in a two-layer coil prestressed by a laminated split iron yoke. The magnet is shown schematically in Fig. 7. In light of the fine performance of the initial short and full-length model dipoles tested during the summer and autumn of 1981, this magnet design was formally adopted in December of that year.

The spring of 1982 saw additional prototype dipoles constructed and tested at an accelerated pace, with the Magnet Division's initial goal of testing six full-length dipoles by March successfully achieved on time. All dipoles, when tested in liquid helium at a bath temperature of  $\sim 4.5$  K, reached a quench "plateau" of approximately 55 kG with very modest "training," independent of ramp rates well in excess of the maximum CBA ramp rate of 8 A/sec. This rate corresponds to 8 minutes' current rise time from the CBA magnet injection current of 264 A (3.9 kG)

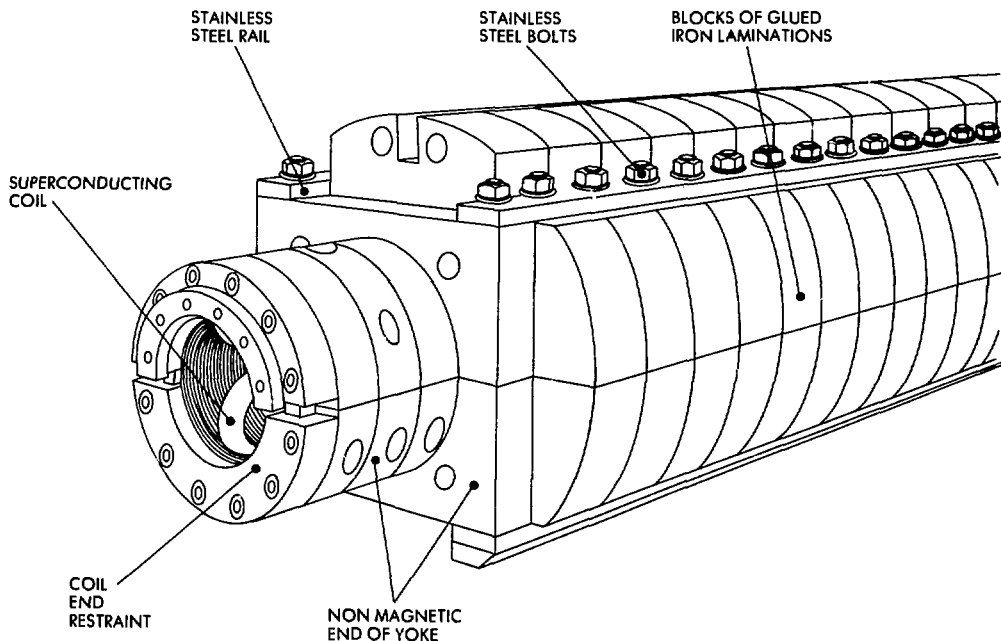


Figure 7. Schematic of superconducting dipole magnet end configuration.

to the operating current of 3770 A (52.8 kG) at 400-GeV proton energy. When tested at temperatures near 3.8 K (the maximum CBA design operating temperature), the magnets reached fields of  $\sim 58$  kG, and  $\sim 60$  kG in the 3 K temperature region, the lowest temperature attainable in these magnet tests.

The first prototype quadrupole magnet was tested as well; it also exceeded design operating specifications by a substantial margin with little training. Other R&D efforts during the spring of 1982 concentrated on the following areas. 1) Magnet construction details and assembly procedures necessary to ensure that the magnets would satisfy the stringent CBA tolerances on field quality were studied. This program centered initially on the construction of a series of dedicated short ( $\sim 2$  m long) dipoles. An important component of the program was the fabrication of a high pressure molding fixture for achieving dimensional uniformity of assembled magnet coils. 2) Quench protection studies were initiated to ensure that the magnets are able to safely absorb their own stored energy (1 MJ in the case of a dipole at full field) during a quench

without damage or deterioration in performance. 3) Various alternative superconducting "trim coil" designs were studied; these are located within the main dipole or quadrupole coils, intended to correct for iron saturation and superconductor magnetization effects and to aid in steering the proton beams in the accelerator. 4) Finally, construction of a short demonstration dipole of the so-called 2-in-1 design was initiated. Such a magnet would contain a pair of dipole (or quadrupole) coils, belonging to adjacent proton rings, side-by-side in a common iron yoke, and was devised to achieve significant cost savings by halving the required number of magnet yokes and cryostats.

By the end of the summer of 1982, fairly exhaustive quench protection studies on full-length dipoles (including the first dipole tested horizontally in the forced-flow supercritical helium cooling mode intended for the CBA) had verified that the magnets appear to have an adequate margin of safety from quenching under "worst case" quench conditions visualized in the accelerator. Even so, it was considered prudent to incorporate a quench protection system;

therefore, a "passive double diode" protection scheme was devised and adopted for subsequent deployment in all magnets. Its function is to divert current from the quenching half coil in a magnet, thereby effectively bypassing the energy in the other magnets around it. A trim coil design was adopted, wound in two layers from a 7-strand superconducting cable, prestressed by high-strength Kevlar filamentary wrap. Having been first tested in several short dipoles, a full-length version of the trim coils was tested with satisfactory results in mid-summer. Finally, the 2-in-1 dipole, DCM-1, had also been tested in several stages by the end of the summer, providing proof-in-principle of this interesting and alternative magnet approach.

During the remainder of 1982, further regular (i.e., 1-in-1) prototype dipoles and quadrupoles were tested in liquid as well as in supercritical helium. One dipole reached a record field level of 62.2 kG in liquid at  $\sim 3.4$  K. The field quality program culminated with the first long dipole, explicitly constructed with this as an objective, successfully tested. Moreover, the autumn of 1982 marked an important new milestone, namely, the start of installation of prototype magnets in the CBA tunnel. The first member of the Full Cell, comprising six dipoles and two quadrupoles, was transported to Sextant 5 of the tunnel on October 8—two weeks short of the anniversary of the testing of the first full-length dipole. By the end of December, five dipoles and one quadrupole had been installed and were in the process of being interconnected. The Full Cell would provide an important systems test, including cryogenics, vacuum, and electrical systems, needed for operating a string of magnets in the CBA tunnel environment. Equally important, it would test magnet installation procedures.

On December 21, P. Reardon, the CBA Project Head, announced a major decision on the question of adopting the 2-in-1 magnet design, noted earlier, for the CBA. It had been decided that, although this magnet design appears feasible and offers a promising approach for future accelerators, it would not be adopted for the present effort. The 1-in-1 magnet had met the specifications for a proton-proton Colliding Beam Accelerator and would be retained as the basic superconducting magnet for the CBA. While one full-length 2-in-1 demonstration dipole

was in the assembly stage at that time, it would be completed and tested on a low-priority basis. Thus, as the year ended the Magnet Division was poised to concentrate its efforts on the 1-in-1 magnet.

The first quarter of 1983 saw the attainment of several very important milestones in the CBA superconducting magnet program, well ahead of schedule. The most dramatic event was the initial powering of the Full Cell (Fig. 8) to the operating field of 52.8 kG on February 25, with the final two magnets installed and all remaining interconnections having been completed without delay the previous month. The net time required to cool down the cell was three days. Following a series of cryogenic and electrical measurements, a long-term test commenced, in which it was intended to cycle the string of magnets to full field a number of times representing a significant fraction of those expected over the CBA lifetime. At the end of March the magnets had been cycled approximately 100 times at the maximum CBA operating ramp rate. In addition, the cell had operated at full field in the dc mode for a total of approximately 40 hours.

The second milestone, reached in mid-February, was the testing of the eighth successive dipole to meet field quality specifications, thus achieving a major goal of the R&D plan established the previous year—namely, the demonstration of field quality in eight out of ten "identical" dipoles constructed to the stringent CBA design specifications by the end of the first quarter of 1983. Furthermore, by that date the tooling necessary for magnet production was on hand.

## CONVENTIONAL CONSTRUCTION

October 28, 1978, marked the official groundbreaking for the conventional construction phase of the project, and actual site clearing took place in January 1979. The entire main magnet enclosure, including earth shielding, required approximately 28 months and was completed in August 1981. As originally planned there were to be four experimental halls and two open areas where experiments could be installed in temporary structures. The first effort was the construction of the Wide Angle Hall at the 6 o'clock location; it was completed in April 1981.

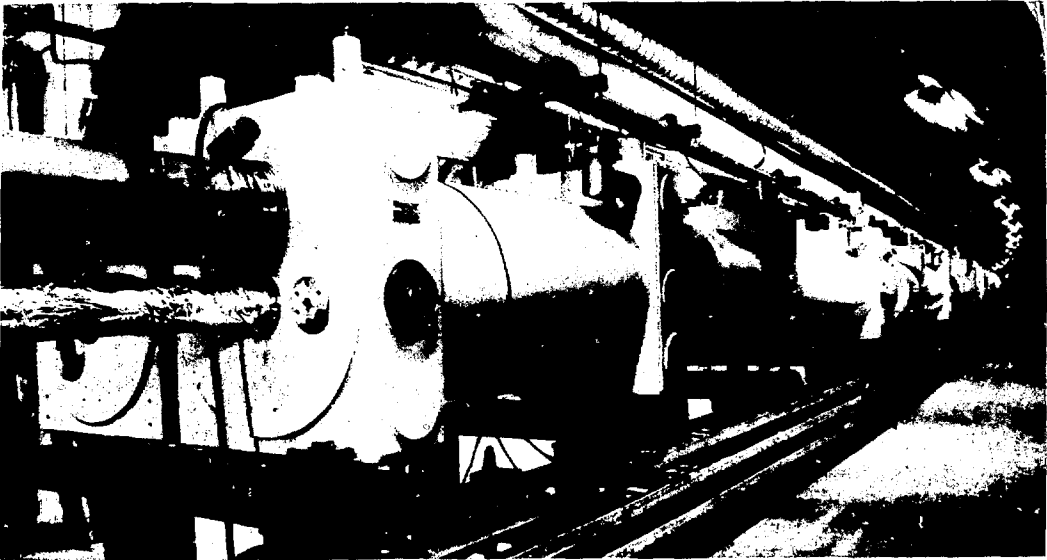


Figure 8. The first string of CBA magnets being prepared for testing in the tunnel.

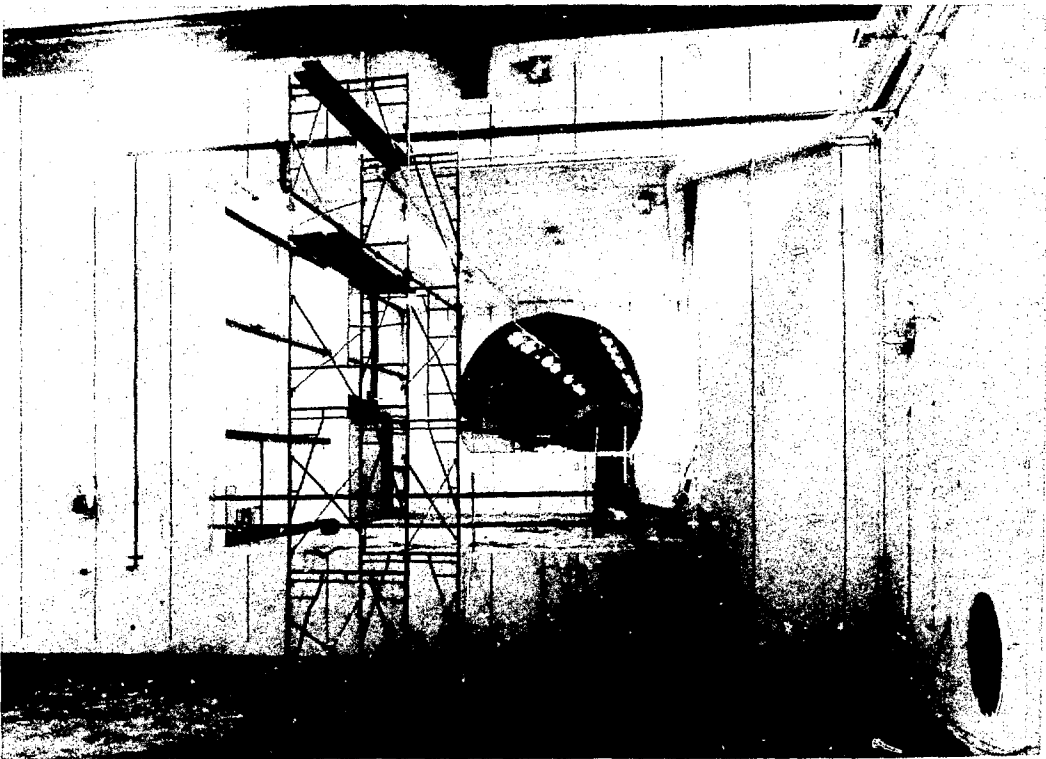


Figure 9. The interior of the Major Facility Hall.

It is sized to house large-aperture spectrometers for identification and analysis of particles of high transverse momentum. The open area at 4 o'clock followed and was completed two months later. The Major Facility Hall at 8 o'clock, the largest of the halls built to date and designed to accommodate a large class of major general purpose detectors, was completed in May 1982. It is shown in Fig. 9. The fourth experimental area, the Narrow Angle Hall (2 o'clock), designed to house a typical single-particle spectrometer capable of particle identification at very high energies, was completed in the autumn of 1982. By that time the injection beam tunnels from the AGS to the CBA magnet enclosure were also completed.

The Service Building Complex was designed and constructed under two separate contracts. Phase I included the Cryogenic Wing and the Compressor structure; these were completed in August 1981 and are depicted in Fig. 10. Phase II covered the four-story main building, to house control and computer rooms, office space, shops and laboratories, and the Rf/Power Supply Wing. Work on this building got under way in July 1981, and completion is scheduled for the autumn of 1983. At the time of writing, with site

work and installation of utilities also in progress, approximately 75% of the physical plant is complete or under contract. Major elements of the uncompleted portion are the experimental areas at 10 and 12 o'clock, which have been deferred until more construction funds are available. Area 10 is currently envisioned as an open area similar to the existing one at 4 o'clock, and for Area 12 an extra-large experimental hall is contemplated.

### Rf Systems

Two rf systems are required to accumulate and accelerate the design current of 8 A in the CBA. A 6-m stacking cavity was fabricated and successfully tested. Tests of a model accelerating cavity, which is shown in Fig. 11, were successful. The design of both the stacking and accelerating systems is complete and many components are under construction or on order.

### Vacuum

The design parameters of the ring vacuum and the magnet insulating vacuum were achieved earlier a) in tests on 45 m of beam tube in which pressures  $<10^{-11}$  Torr were routinely obtained and maintained for several months

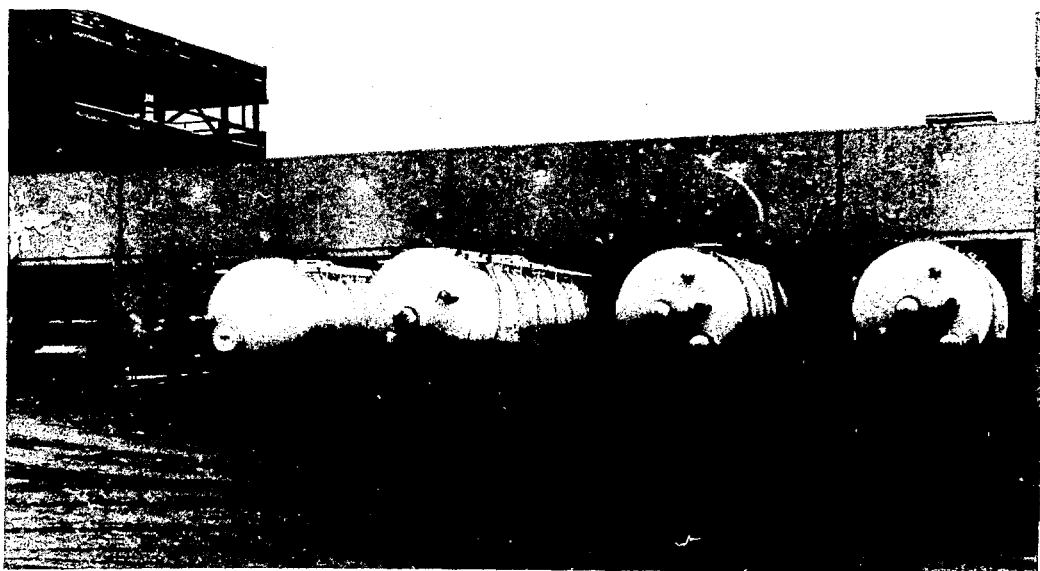


Figure 10. The CBA refrigeration building with cold boxes in the foreground; the service building is under construction behind and to the left.

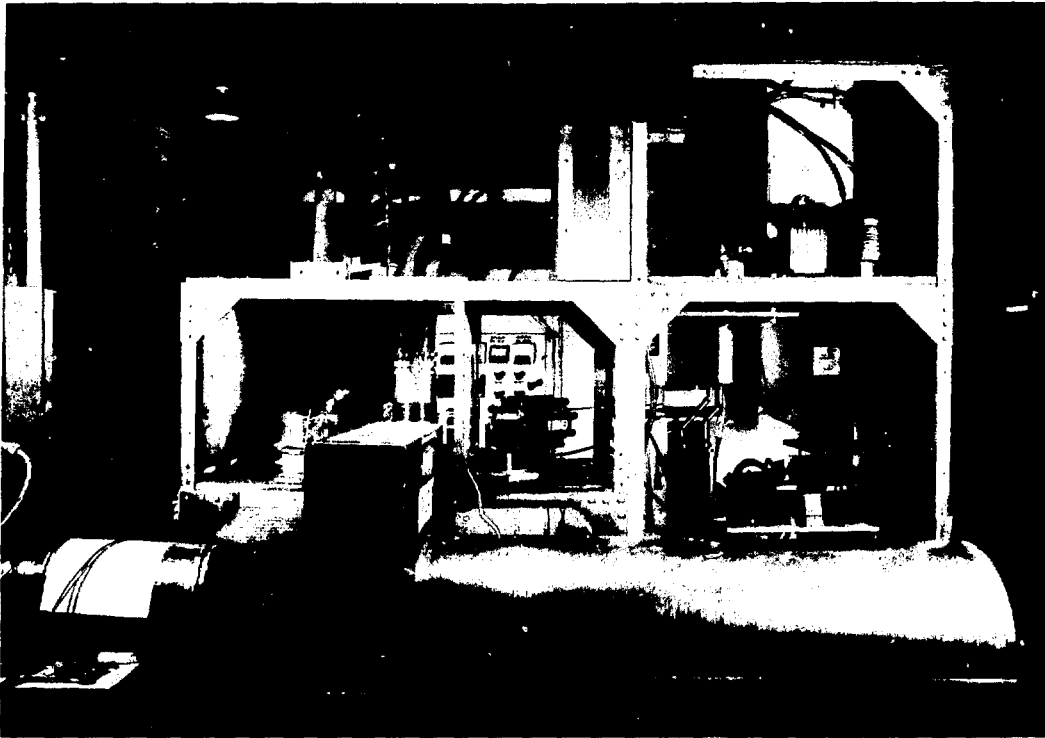


Figure 11. A model of the ferrite loaded accelerating cavity and IB driver, which was successfully tested with more than 12 kV across the cavity gap.

with a single titanium sublimation pump, and b) in the pumpout and leak check of a half cell containing three dipoles and a quadrupole and associated vacuum components which reached  $10^{-7}$  Torr. The recent cooldown and test of the eight full-cell magnets in the CBA tunnel reconfirmed the adequacy of the vacuum system design. Cooldown was started after two days of pumping when the pressure dropped into the low  $10^{-4}$  Torr range. The ultrahigh-vacuum sys-

tems again reached  $10^{-11}$  Torr without difficulty and the insulating vacuum again exceeded specifications. The heat load from the bore tube to the magnets was found to be less than 1.3 W per dipole, well below the allowed 2 W.

#### **Injection, Cryogenics, and Controls**

Basic design is complete in these areas, with components on order or under construction.



**ACCELERATOR DEPARTMENT**

**J. R. Sanford**, Chairman  
**D.I. Lowenstein**, Deputy Chairman  
**D.H. White**, Deputy Chairman  
**J.E. Becker**, Administrator

**AGS DIVISION**

**H.W.J. Foelsche**, Head

<b>L. Ahrens</b> Accelerator Physics, Low Field Corrections, Instability and Rf Pickup Electrodes, Polarized Protons, Physics Research	<b>A. Kponou</b> Polarized Proton Ion Source
<b>J. Alessi</b> H <sup>-</sup> Ion Source Development, Polarized Proton Ion Source	<b>Y.Y. Lee</b> Polarized Protons, Accumulator/Booster
<b>D. Barton</b> Chief AGS Operations, H <sup>-</sup> Injection, Physics Research	<b>A.W. Maschke</b> Cluster Ion Fusion Project, MEQALAC Development, Physics Research
<b>D.A. Davis</b> Electrical Engineering, Power Distribution	<b>R. McKenzie-Wilson</b> Mechanical Engineering, Neutral Beams, RFQ
<b>H.W.J. Foelsche</b> AGS and CBA Transfer, Accelerator Physics Research	<b>M. Month</b> Accelerator Theory
<b>G. Gammel</b> Low Beta Acceleration, Physics Research, MEQALAC Development	<b>K. Prelec</b> Neutral Beams Development, Physics Research
<b>J.W. Glenn</b> AGS Operations, Accelerator Physics	<b>Th. Sluyters</b> Neutral Beams, Polarized Proton Ion Source
<b>J.J. Grisoli</b> Deputy Division Head	<b>L.W. Smith</b> Accumulator/Booster, Physics Research
<b>A. Herscovitch</b> H <sup>-</sup> Ion Source Development, Physics Research	<b>H. Weisberg</b> Accelerator Physics, Slow Extraction and Switchyard System
	<b>W. Weng</b> Accelerator Physics, Fast Extraction

**EXPERIMENTAL PLANNING AND SUPPORT DIVISION**

**D.I. Lowenstein**, Head

<b>H.N. Brown</b> Beam Design, Experimental Area Liaison, Polarized Proton LEPT Design, Particle Physics Research	<b>B. DeVito</b> Mechanical Engineering, Polarized Proton Beam Transport
<b>G.M. Bunce</b> Deputy Division Head, Beam Design, Experimental Area Liaison, Particle Physics Research	<b>D. Lazarus</b> Beam Design, Experimental Area Liaison, Radiation and Industrial Safety, Particle Physics Research
<b>A.S. Carroll</b> Beam Design, Experimental Area Liaison, Particle Physics Research	<b>D.I. Lowenstein</b> Deputy Chairman, Division Head, Control Systems, Particle Physics Research
<b>I-H. Chiang</b> Detectors, Electronics, Experimental Area Liaison, Particle Physics Research	<b>Y. Makdisi</b> Experimental Area Liaison, Particle Physics Research, Acceleration of Polarized Protons, Polarized Proton LEPT Design
<b>G.T. Danby</b> Superconducting Magnet Development, Acceleration of Polarized Protons, Particle Physics Research	<b>S.P. Yamin</b> Beam Design, Detectors, Experimental Area Liaison, Particle Physics Research

**ATA DIVISION**  
**E.B. Forsyth, Head**

**E.B. Forsyth**  
 ATA Division Head, Electrical Engineering  
**K.F. Minati**  
 Mechanical Engineering of Laboratory Equipment  
 and Terminations

**A.C. Muller (DEE)**  
 Development of Polymeric Insulation for Both  
 Superconducting and Room-Temperature Cables

**CBA PROJECT**

**P.J. Reardon, Project Head**  
**E.P. Rohrer, Deputy Project Head**  
**H. Hahn, Technical Staff**

**MAGNET SYSTEMS DIVISION**

This Division is responsible for the design, construction, and installation of all superconducting magnets.

**R.B. Palmer, Head**  
**R.P. Shutt, Sr. Associate**  
**C.L. Goodzeit, Associate**  
**W.G. Walker, Assistant**

M. Anerella	M. Garber	W. Lenz	M. Shapiro
F. Atkinson	D. Gardner	R. LeRoy	J. Skaritka
G. Bagley	A. Ghosh	G. Mayman	A. Stevens
S. Baker	D. Gough	W. McGahern	C. Sylvester
A. Bertsche	A. Greene	G. Morgan	P. Thompson
E. Bleser	W. Gubler	R. Oram	D. Tuttle
V. Buchanan	J. Herrera	S. Plate	P. Wanderer
J.G. Cottingham	R. Hogue	I. Polk	T. Wild
J. Cullen	S. Kahn	L. Repeta	E. Willen
P. Dahl	E.R. Kelly	K. Robins	M. Woodle
Y. Elisman	J. Keohane	R. Rosenka	
R. Fernow	H. Kirk	W. Sampson	
G. Ganetis	K. Koehler	W. Schneider	

**ACCELERATOR PHYSICS AND CONTROLS DIVISION**

This Division is responsible for the development of the accelerator physics concepts, and the design and construction of control systems and power supplies.

**M.Q. Barton, Head**

M. Cornacchia	R. Edwards	S. Kennell	B. Pope
E. Courant	R. Frankel	G. Parzen	J. Wang
G.F. Dell	K. Jellett	J. Poole*	R. Warkentein

**INJECTION/EJECTION SYSTEMS DIVISION**

This Division is responsible for the design and construction of the injection system from the AGS to CBA, and for the design and construction of the beam ejection systems.

**H.W.J. Foelsche, Head**

J. Claus	P. Montemurro	R. Thern	W. Weng
E. Jablonski	R. Nawrocky	J. Tuozzolo	P. Zuhoski
J. Keane	E. Rodgers		

\* On Leave.

### CRYOGENICS SYSTEMS DIVISION

This Division is responsible for the design and installation of the helium refrigeration system required for the superconducting magnets.

**R.I. Louttit, Head**  
**D.P. Brown, Deputy**

Y. Farah

A. Schlafke

J. Sondericker

K. Wu

### VACUUM/RF AND BEAM INSTRUMENTATION SYSTEMS DIVISION

This Division is responsible for the design and construction of all vacuum systems, rf stacking and acceleration systems, and beam instrumentation.

**H.J. Halama, Head**

T. Chou  
 C. Foerster  
 S. Giordano

K. Hillman  
 H. Hseuh

M. Plotkin  
 M. Puglisi

E. Raka  
 P. Stattel

### ADMINISTRATION DIVISION

This Division is responsible for all administrative activities associated with budgets, contracts, management systems, quality assurance, conventional construction, safety, and experimental facilities.

**J.R. Sanford, Head**  
**J. Spiro, Deputy**

J. Becker  
 E. Dale  
 E. Dexter  
 J. Feldman

V. Gutierrez  
 J. King  
 H. McChesney

P. Mohn  
 M. Schaeffer  
 M. Shear

F. Thornhill  
 L. Turf  
 D.H. White

# Physics Department

## INTRODUCTION

The Physics Department carries out fundamental research in elementary particle (or high energy), nuclear, solid state, and atomic physics. In each discipline, the experimental program is based in large part on Brookhaven's major facilities. These research facilities provide unique capabilities not only to the BNL staff but also to the national scientific community.

Because research in high energy physics is performed by members of the BNL Physics Department, university users, and members of the Accelerator Department, frequently in teams representing more than one group, it seemed best to report that work in a separate section.

The low and medium energy nuclear physics programs carried out by members of the BNL Physics Department and many university community users address questions of the fundamental nature of the structure and interaction of nuclei and nucleons. Beams from the Tandem Van de Graaff Facility, the High Flux Beam Reactor, and the AGS are used in a variety of experiments to study new phenomena. Heavy-ion beams are used for diverse investigations of the reaction mechanisms of heavy ions and the forces between them, the production and decay of nuclei in states of very high angular momentum, the existence and production of nuclei far from stability, and nuclear electromagnetic properties such as  $\gamma$ -transition rates and static moments. Reactor neutrons are used to perform detailed studies of the structure and dynamics of nuclei utilizing the  $(n, \gamma)$  reaction, as well as for studies of resonance parameters and neutron cross sections of interest to applied fields. The AGS nuclear physics program is concerned presently with the spectroscopy of hypernuclei

— nuclei which contain a  $\Lambda$  or a  $\Sigma$  hyperon. The Nuclear Theory group has a close interaction with the experimental groups, as well as a wide-ranging program in many exciting topics in nuclear theory. The Laboratory thus provides an opportunity for a very broad program of fundamental nuclear physics. In addition, the Tandem Van de Graaff is used for investigations of the atomic physics of highly excited and stripped atoms.

Considerable redirection of the Nuclear Physics Program is in progress to capitalize on the unique opportunities for new nuclear physics utilizing both the National Synchrotron Light Source to produce very high quality high energy (200–400 MeV) photon beams and the AGS to accelerate heavy ions to relativistic energies. Both new initiatives are described in detail below.

The solid state research effort is concerned with the cohesive forces that bind atoms together to form the various phases of condensed matter. The facilities such as the High Flux Beam Reactor and the National Synchrotron Light Source provide unique probes for studying the properties of solids on the atomic scale. Particular emphasis is placed on the studies of materials exhibiting phase transformations where a delicate balance of the interatomic forces exists such that a slight change in the external environment (such as temperature or pressure) can produce a significant modification of the atomic arrangement. These studies provide a means of testing the various theories of phase transformations and lead, in many cases, to the prediction of interesting new types of solid structures. Other studies try to unravel the properties of "real" solids, i.e., solids in which the symmetrical arrangement of atoms is disturbed by impurities and crystallographic de-

fects. The resulting changes in the interatomic forces and properties are not always predictable and the experimental results provide a phenomenological understanding of imperfect solids. A further region of growing interest is the study of surfaces. One intriguing problem arising in this field is how the interatomic forces and their arrangement vary when atoms are bound on one side only. Frequently, a different atomic species can be attached to a surface and a new type of atomic arrangement is obtained.

The atomic physics program studies atomic structure and the lifetimes of exciting states of highly ionized atoms. Research in applied physics is concerned with measurement of the quantity and location of stable isotopes for a wide variety of problems in solid state physics, biology, medicine, marine science, and other fields. Both of these programs make use of the Brookhaven Van de Graaff accelerator facilities and will also utilize the National Synchrotron Light Source.

## Nuclear Physics

---

This section is organized in a somewhat unorthodox way. The reports from Hypernuclear Physics, the High Flux Beam Reactor, and Nuclear Theory follow the established pattern of reviewing the past year's accomplishments. However, the Tandem Physics report is a preview rather than a review. And just as the review format does not imply that one does not plan for the future, the fact that a preview is presented does not mean that little was accomplished during the year. We simply thought it might be exciting for the reader to hear something about future plans.

### PLANS FOR FUTURE RESEARCH IN THE TANDEM GROUP

The Tandem Laboratory has had a fine year of heavy-ion and atomic physics research, and the accelerators have performed consistently at potentials over 16 million volts. Alongside its research efforts, the Group has devoted time to looking into new areas of physics that could provide opportunities for future research which would build on the talents and experience of the Laboratory staff. Two such areas have been defined and proposals were made to the DOE for the construction of two novel physics facilities, one providing a monochromatic photon beam of unique intensity at energies approaching 1 GeV, and one providing heavy nuclei up to energies of 15 GeV per nucleon, e.g., 600 GeV for  $^{40}\text{Ca}$  and 1.62 TeV for  $^{129}\text{I}$ . Both facilities would open up exciting new areas of nuclear research, and we are presenting the main ideas of these two proposals in this year's HIGHLIGHTS. The DOE, at

the time of writing, has funded the photon beam line.

### Heavy Ions in the AGS

One of the most remarkable discoveries in recent years is that of quark confinement. All fundamental forces known decrease in strength with increasing distance between the interacting objects. Not so for quarks. When three quarks making up a neutron or a proton are close together, they do not interact, whereas the attractive forces strengthen as the quarks move away from one another. This suggests that the quarks are confined within the nucleon, or, in particle physics jargon, they are confined within their "bag." Since the energy of the three quarks of a nucleon is finite, it is clear that the quarks can be pulled from one another under the right circumstances. As free quarks have not been encountered, deconfinement will have to be forced upon the quarks in some violent collision arranged either by physicists in a laboratory or by nature in the earliest second of the Big Bang. We have chosen to pursue the first possibility.

The experimental goal is to bring together, very close, many nucleons so that the quarks no longer can discern which bag they belong to, but start moving as many quarks in one large bag. If this can be arranged, one has forced a fundamental change upon nature. Confinement of three quarks in a bag is normally thought to come about by the action from the medium (also called vacuum) in which quarks move. For electromagnetic waves the vacuum is passive; the waves pass through it with minimal disturbance. The photons are not confined but travel

with the speed of light. The quark vacuum is active; it sets up bags and is thus highly structured. The transition to deconfined quarks means a transition from the normal active quark (or color) vacuum to a passive vacuum — indeed, a fundamental change in nature's order.

How can we bring this about in the laboratory? We shall attempt to collide samples containing many nucleons, i.e., heavy nuclei, with so much energy that the density during the collision is large enough to push many nucleons tight together, to a density estimated at 3 to 10 times that of normal nuclei. From knowing how much energy a nucleon can deposit in a nucleus during a collision, one can estimate that bombarding energies of at least 10 GeV per nucleon are needed for the projectile and, of course, it would be desirable to use as heavy a projectile as possible on as heavy a target as possible.

To achieve this, the Tandem Accelerators will be combined with the AGS. The heavy ions leaving the Tandems at about 8 MeV per nucleon will be transported 558 m through the hill behind the Tandem Laboratory and injected into the AGS (Fig. 1). After acceleration there, energies of 15 GeV per nucleon can be reached, and the experimental areas and, to a large extent, the equipment of the AGS can be used to study quark deconfinement. In fact, the Tandems have already been run in the modes required to produce beams acceptable to the AGS, and the low magnetic fields necessary in the AGS for the beginning of the acceleration

cycle have been produced and measured. All that is lacking is a 558-m beam line which will cost about 7 million dollars.

The program for Tandem injection into the AGS is limited to relatively light ions, say up to mass 40. Above mass 40 an energy boost above the Tandem capability is needed for successful AGS injection. A cyclotron, using iron already at hand, has been planned for this second phase. Nuclei up to mass 130 and, after some modification of the AGS vacuum, up to mass 235 can be accelerated. The additional cost for this phase is about 12 million dollars. The time scale for the first phase is 1½ years and perhaps 3 years for the second phase.

A truly unique perspective appears beyond this phase. The construction of a Relativistic Heavy-Ion Colliding Beam facility, using the AGS as injector, will be proposed. This facility, as presently envisioned, would achieve energies of order 50 GeV per nucleon in each beam. A totally new regime of physics, intended to evidence a "quark-gluon plasma," will become accessible.

The plans sketched above were developed in a collaboration between nuclear, particle, and accelerator physicists at BNL.

### Photonuclear Physics With Laser Plus Electron Gamma Source

Excited states of the nucleon, which appear as baryon resonances in high energy collisions, have been studied for many years at accelera-

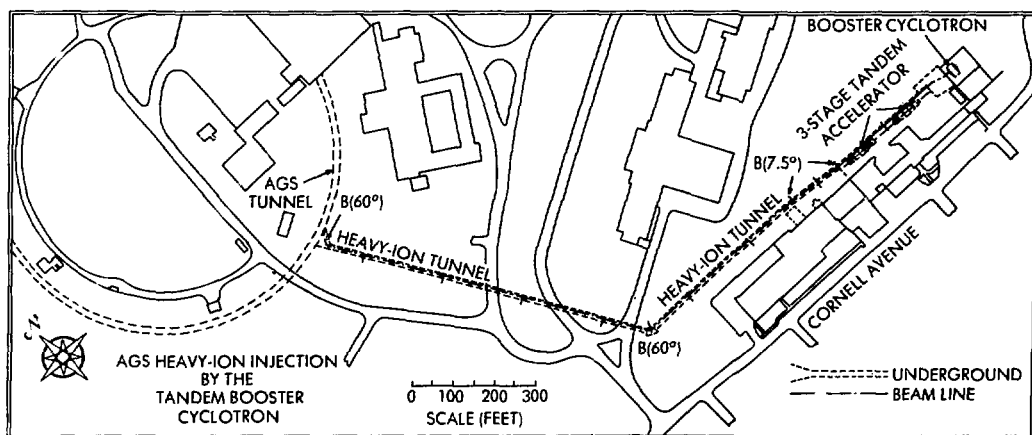


Figure 1. Layout of the proposed heavy-ion beam transport line from the Tandem accelerators to the AGS.

tors such as the AGS at Brookhaven. When the energy transferred to a nucleus becomes very large (greater than about 200 MeV), the excitation of one of the constituent nucleons into such a resonance [ $\Delta(1232)$ ,  $P_{11}(1470)$ , ...] becomes very probable. However, the nuclear medium is a new laboratory for these excited baryons, quite different from the comparatively simple environment of elementary particle physics. New degrees of freedom and constraint are provided by the Fermi motion of the nucleons, by the operation of the Pauli exclusion principle within the nucleus, and by interactions with other nuclear constituents. The study of nuclei at these high excitation energies is currently of great interest. Recent low energy-transfer experiments [(p,n) to Gamow-Teller states] have indirectly hinted at the existence of an unusual structure in the high excitation-energy spectrum of nuclei — a Giant Delta resonance, made up of a coherent superposition of nucleon-hole and  $\Delta(1232)$  particle states. Other unusual phenomena such as enhancements in the virtual pion field within the nucleus (pion condensation) and the formation of 6-quark dibaryon substructures are anticipated in this excitation energy range.

The cleanest probe to use in investigating these phenomena is the photon. However, medium energy photonuclear physics has long suffered from a lack of intense low-background  $\gamma$  rays that have high resolution and are variable in energy. Furthermore, polarized  $\gamma$  rays, which are potentially even more versatile, have never been available with hundreds of MeV of energy.

Within the next year we hope to begin the construction of a facility that will provide intense beams of monochromatic and polarized photons with energies in the range of several hundreds of MeV. These  $\gamma$  rays will be produced by Compton backscattering laser light from the electrons circulating in the 2.5- to 3.0-GeV x-ray storage ring of the National Synchrotron Light Source (NSLS) at Brookhaven. In the backscattering process a laser photon and an electron approach each other head on. In the frame of reference in which the electron is initially at rest the photon, which has been boosted up in energy to an x ray by the Lorentz transformation, Compton scatters from the stationary electrons. Those x rays that scatter into backward

angles are then boosted up to  $\gamma$ -ray energies by the transformation back to the laboratory frame. For  $180^\circ$  scattering, the final energy achieved is approximately  $4\gamma^2$ , where  $\gamma mc^2$  is the initial electron energy. Thus when 3-eV laser light is sent against 2.5-GeV electrons, 300-MeV  $\gamma$  rays come back. Because of the small spin-flip amplitude in backward Compton scattering, the  $\gamma$ -ray beam retains most of the polarization of the incident laser light, and both linear and circular polarizations are easily achievable.

This technique has been used to produce relatively low fluxes ( $500 \text{ s}^{-1}$ ) of photons in the 1- to 20-GeV range (at SLAC), and with a slightly increased intensity ( $5 \times 10^4 \text{ s}^{-1}$ ) in the energy range below 75 MeV (at Frascati). The excellent emittance, phase space, and high current of the NSLS x-ray storage ring will, for the first time, allow the production of the intensities needed for photonuclear research (over  $2 \times 10^7$  photons per second). Since the highest energy  $\gamma$  rays are traveling at  $0^\circ$  relative to the electron direction, quasi-monochromatic beams of  $\sim 10\%$  resolution have been obtained at SLAC and Frascati by collimating to small angles. However, at the NSLS the electrons that give up energy to produce high energy  $\gamma$  rays will be stripped away from the primary beam and momentum analyzed. Every  $\gamma$  ray reaching the nuclear target will thus be "tagged," with its energy determined to high precision (2–3 MeV).

The initial goals of the program are to produce a 175- to 300-MeV tagged photon beam, using an argon-ion laser operating in the UV at 3511 Å. Although the experimental area available in the existing NSLS building is sufficient for initial tests, it will be far too restrictive for the magnetic spectrometers and similar equipment necessary to detect the reaction products of medium energy  $\gamma$  rays. An extension to the existing building is planned to provide target areas for the projected physics program. A preliminary design of this extension, together with the layout of the laser and electron interaction region, is shown in Fig. 2.

When the x-ray ring achieves 3.0-GeV operation, the facility will provide up to 420-MeV photons. Significant increases in  $\gamma$ -ray energy above this level can be achieved only with shorter wavelength lasers. Since a high duty-cycle laser must be used to maintain the high  $\gamma$ -ray flux, the only source is a Free Electron Laser

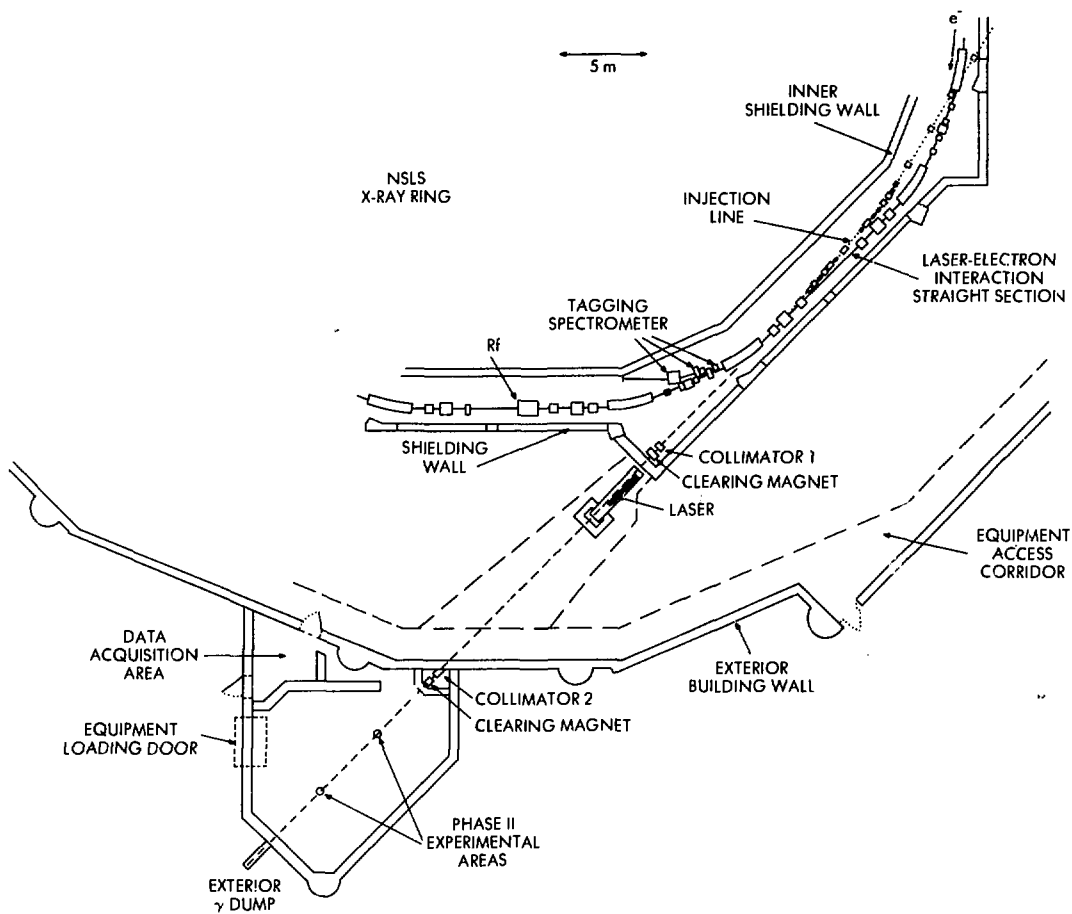


Figure 2. Layout at the high energy gamma source at the NSLS.

(FEL). The construction of an FEL is nearing completion on the VUV ring at the NSLS. In a later stage of the project, we plan to take the FEL light produced at the VUV ring, transport it to the x-ray ring, and there backscatter it to produce up to 700-MeV  $\gamma$  rays. This possibility is unique to the NSLS at Brookhaven because of the proximity of the two storage rings and because both rings can be run from the same rf oscillator and thus be synchronized.

We expect the beams produced by the new facility to chart a new and stimulating course for medium energy nuclear physics in the coming years.

## HYPERNUCLEAR PHYSICS AT THE AGS

An essential aspect in the study of nuclear physics is the understanding of nuclear forces. Ordinary nuclei are composed of neutrons and protons. These particles, however, are members of a larger class of particles called baryons. The baryon octet is made up of  $\Lambda$ ,  $\Sigma$ , and  $\Xi$  (cascade) hyperons, as well as neutrons and protons. A fundamental study of nuclear forces must include the forces between all hyperons.

Baryons differ from one another in their quark composition. The hyperons, such as the



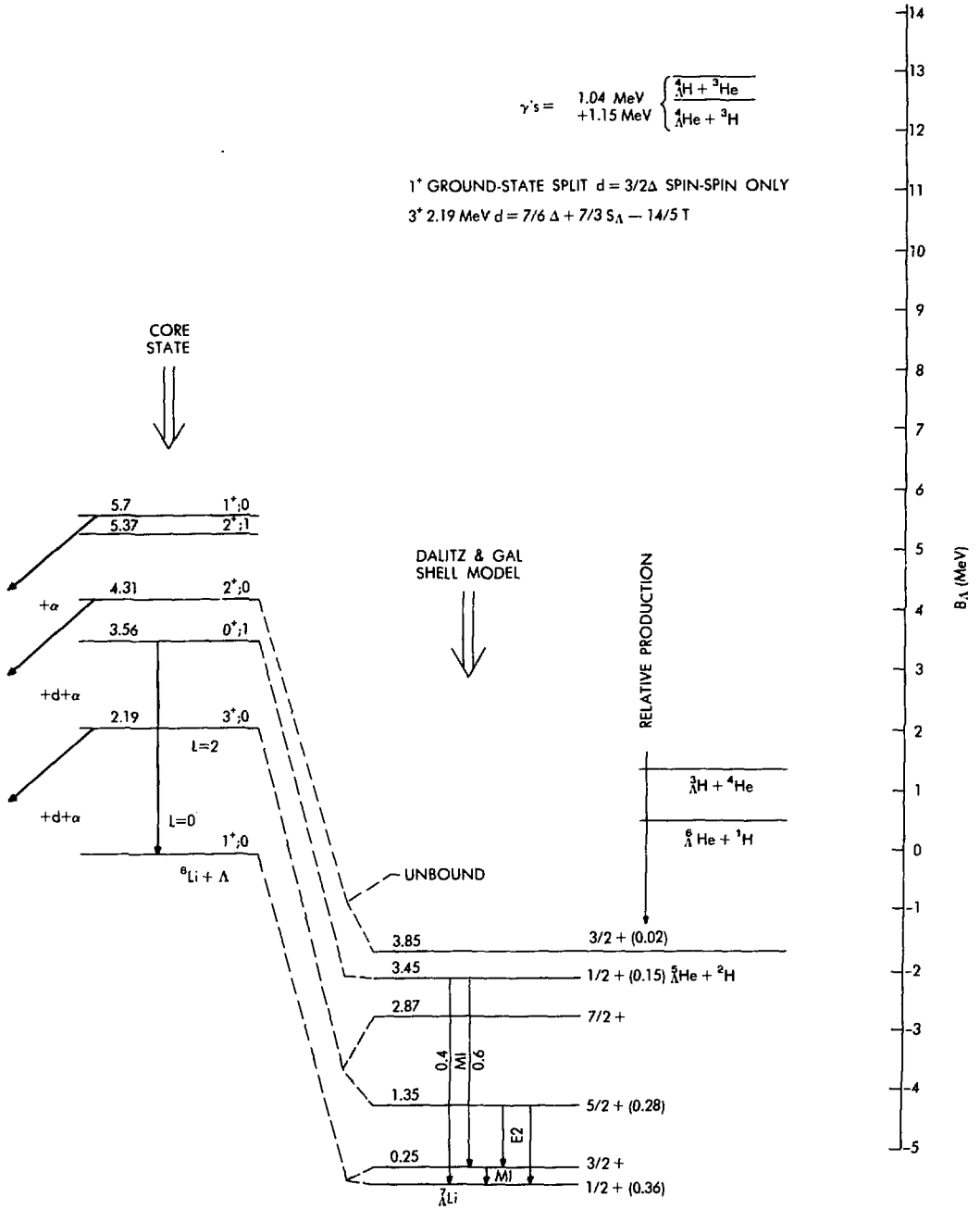


Figure 3. Theoretically expected level scheme for the hypernucleus  ${}^7_{\Lambda}\text{Li}$  compared to the level scheme for the nucleus  ${}^6\text{Li}$ .

with high resolution (~1 cm). The speed and increased sensitivity of this scanner greatly reduce the radiation dose given to the subjects. The  $^{11}\text{C}$ -labeled analog of glucose,  $^{11}\text{C}$ -2-deoxyglucose ( $^{11}\text{C}$ -DG), is being used frequently in PETT VI studies. Because of the short half-life of  $^{11}\text{C}$  (20 minutes), a subject can serve as his own control. Thus studies can be carried out on the same day to follow the effects of drug intervention in a patient, or to study the regional changes in glucose metabolism in subjects responding to various types of stimuli or motor activation as illustrated in Fig. 6.  $^{18}\text{F}$ -fluorodeoxyglucose ( $^{18}\text{F}$ FDG) prepared by a new high-yield synthesis is being used routinely in PETT studies as a probe for the quantitative measurement of regional glucose metabolism in various psychiatric and neurological dysfunctions, such as schizophrenia, Alzheimer's disease, endogenous depression, aphasia, and brain tumors.

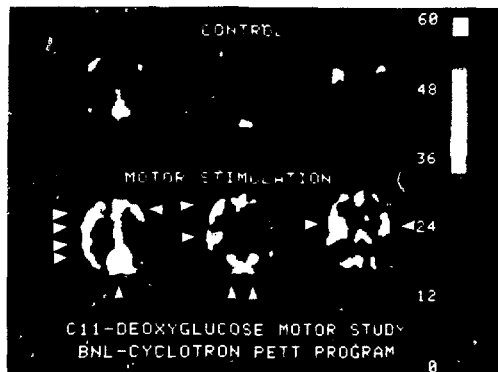


Figure 6. PETT VI motor study with  $^{11}\text{C}$ -2-deoxyglucose. This experiment was designed to study regions of the brain that are activated in using the right hand. Top row: resting subject (eyes open, ears plugged). Bottom row: during movement of right hand.

## CHEMISTRY DEPARTMENT

A.P. Wolf, Chairman

R.E. Weston, Deputy Chairman

M.D. Newton, Assistant Department Chairman

N.B. Munhofen, Department Administrator

### Analysis:

G. Harbottle, E.V. Sayre, R.W. Stoenner, E.F. Norton

### Chemical Physics:

R.J. Beuhler, L. Friedman, J.R. Grover, A.P. Irsa, J. Preses, R.E. Weston, M. White

### Electronic and Structural Studies of Solids and Surfaces:

E. Abola, R. Carr, L.M. Corliss, J.M. Hastings, T.F. Koetzle, W. Kunmann, A. Kvik, R.K. McMullan, J.P. McTague, T.K. Sham, R. Thomas

### Hot Atom Chemistry and Radiotracer Research:

C. Arnett, D.R. Christman, D. Edwards, R. Ferrieri, J.S. Fowler, W.B. Jones, R. Lambrecht, J. Logan, C.S. Redvanly, C.-Y. Shiue, B. Wieland, A.P. Wolf

### Mathematics and Computing:

H.J. Bernstein

### Solar Neutrino Research:

B.T. Cleveland, R. Davis, G. Friedlander, L.P. Remsberg, J.K. Rowley

### Nuclear Spectroscopy and Reactions:

Y.Y. Chu, J.B. Cumming, P.E. Haustein, S. Katcoff

### Studies of Radiation-Produced Species:

B.H.J. Bielski, R.A. Holroyd, H.A. Schwarz

### Theoretical Chemistry:

S. Ehrenson, J.T. Muckerman, M.D. Newton

### Thermal and Photochemical Reaction Mechanisms in Solution:

M.A. Andrews, B. Brunshwig, C. Creutz, T.L. Netzel, S. Seltzer, N. Sutin

# Physics and Chemistry

Nuclear Physics

Solid State Physics

Atomic and Applied Physics

National Synchrotron Light Source

Chemistry Department

$\Lambda$ , contain one or more "strange" quarks in their composition. The presence of these strange quarks has a profound influence on the meson exchange forces between baryons. It is the primary goal of the intermediate energy program to gain information on these forces by a study of the energy levels of hypernuclei. From such studies the effective interaction between baryons in nuclei can be derived and ultimately related to the two-body hadronic forces.

Experiments with hypernuclei are carried out at the low energy separated beam at the AGS by using the  $(K^-, \pi^-)$  reaction to produce hypernuclei. Earlier experiments, described in previous HIGHLIGHTS, have demonstrated that the spin-dependent one- and two-body interactions of the  $\Lambda$  hyperon are very weak. The weakness manifests itself in the fact that the spin-dependent splitting of hypernuclear levels is very small. To study the small spacing of such levels requires resolution not obtainable with present-day magnetic spectrometers. Because of the precision that can be attained with measurements of the electromagnetic transitions between levels, the BNL Intermediate Energy Group has recently carried out a search for such transitions.

The  $(K^-, \pi^-)$  reaction is used to prepare hypernuclei with excitations appropriate to the emission of  $\gamma$  rays. The  $\gamma$  ray can be isolated from competing background radiation by requiring a coincidence with the  $(K^-, \pi^-)$  reaction. Targets of  ${}^7\text{Li}$ ,  ${}^9\text{Be}$ , and  ${}^{16}\text{O}$  were examined with an improved version of the spectrometer used in previous studies, and an array of  $10.2 \times 12.7$ -cm and  $20.3 \times 15.7$ -cm NaI detectors was used to detect the  $\gamma$  radiation. In spite of the small cross section, typically  $50 \mu\text{b}/\text{sr}$  for the formation of these states, success was achieved in detecting the transition. A flux of  $10^5$  kaons/sec on target was produced by the improved spectrometer, and a total of  $10^{10}$  kaons on target were produced for each of the three samples.

Figure 3 shows an expected level scheme for the hypernucleus  ${}^7_\Lambda\text{Li}$ , compared to the corresponding level scheme for the nucleus  ${}^6\text{Li}$ . The scheme is derived from a theoretical study of p-shell hypernuclei undertaken a few years ago by R. Dalitz and A. Gal. In the weak-coupling approximation, the level scheme for  ${}^7_\Lambda\text{Li}$  can be understood in terms of a  $\Lambda$  particle coupled to

excited states of  ${}^6\text{Li}$ ; the  $\Lambda$  is produced by conversion of one of the neutrons in the  ${}^7\text{Li}$  target. Each pair of hypernuclear levels shown is attributed by associating the  $\Lambda$  with each of the parent  ${}^6\text{Li}$  levels in one of two alternate spin orientations of the  $\Lambda$ . The energy of the observed transitions is thus dependent on the size of the  $\Lambda$ -nucleus spin-dependent interaction. For example, the  ${}^6\text{Li}$  ground state can be visualized as an  $\alpha$  particle and a deuteron in a relative S, or  $l=0$ , orbit. The hypernuclear doublet splitting in this case is indicative of a spin-spin interaction strength. For the  $3^+$  first excited state of  ${}^6\text{Li}$ , the  $\alpha$  and deuteron are in relative D, or  $l=2$ , orbits; the splitting in this case contains contributions from both a spin-spin interaction and a spin-orbit interaction.

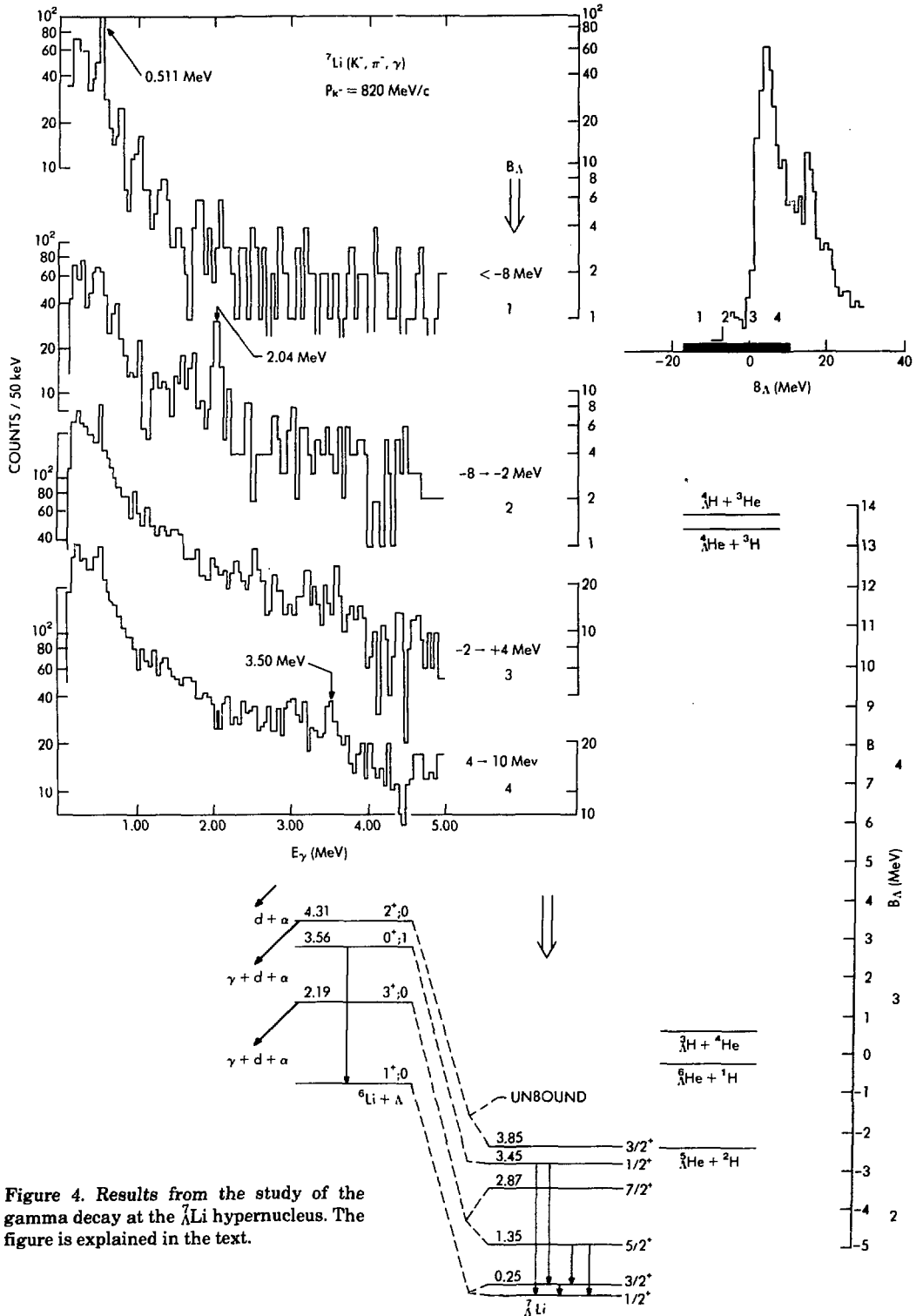
The results of the experiment are shown schematically in Figs. 4 and 5. Shown on these figures are  $\gamma$ -ray spectra obtained for various selections, or "cuts," on the excitation energy spectrum of the  ${}^7_\Lambda\text{Li}$  hypernucleus. The cut labeled 2 corresponds to the excitation region containing bound states of the  $\Lambda$  system. In that cut one sees a pronounced peak corresponding to the transition between the  $5/2^+$  member of the doublet and the hypernuclear bound state.

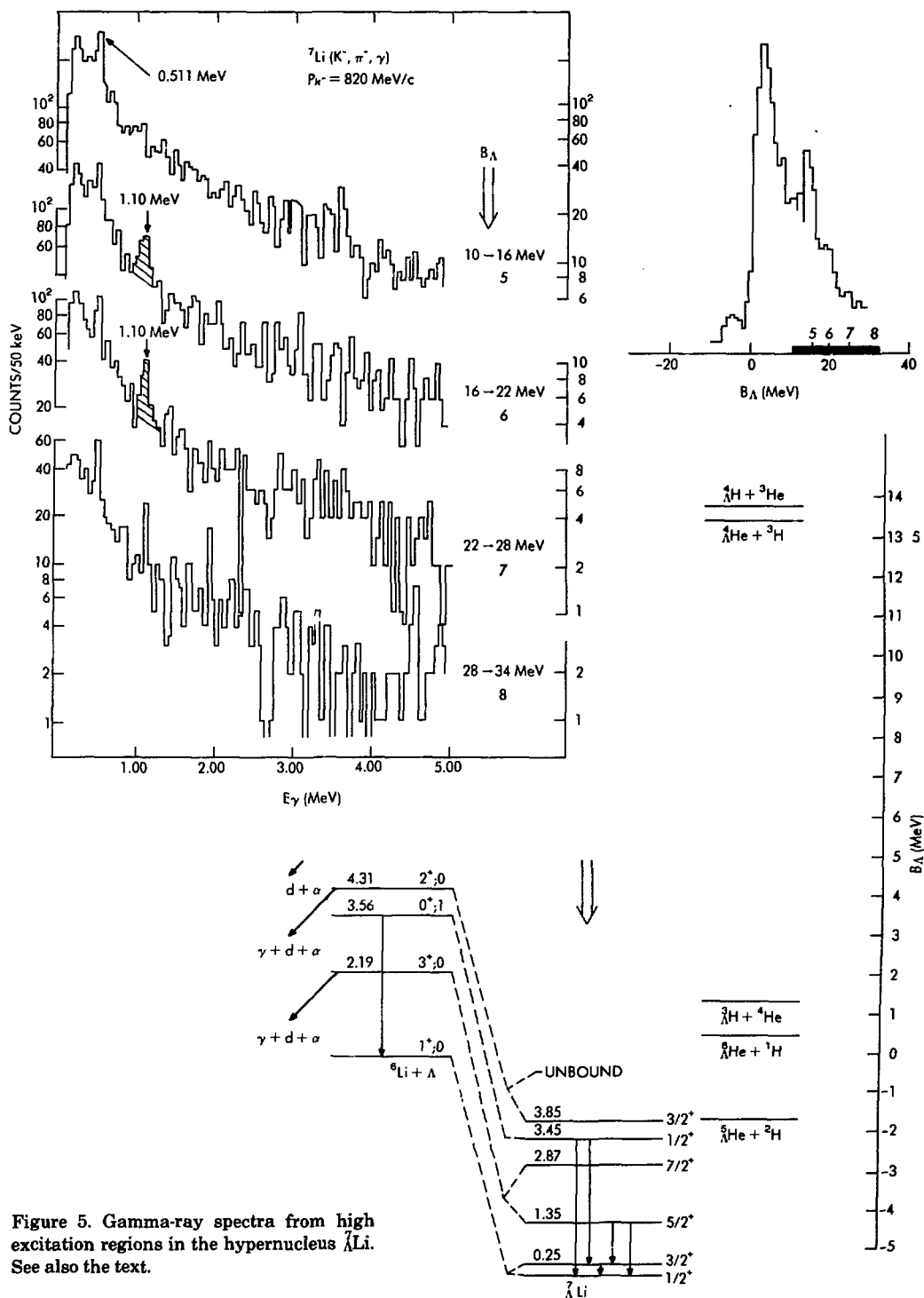
In cut 4, a region above the  $\Lambda$  separation energy is selected, and the recoiling system is in this case an excited state of the ordinary nucleus  ${}^6\text{Li}$ . In that spectrum appears clear evidence of the radiative decay of the  $3.56\text{-MeV } 0^+, T=1$  level of  ${}^6\text{Li}$ . The appearance of the nuclear  $\gamma$  ray serves to confirm our interpretation.

In Fig. 5 appear spectra derived from higher regions of  ${}^7_\Lambda\text{Li}$  excitation. In cuts 6 and 7 of this figure, we examine regions where the breakup of the hypernuclear system into fragments containing  ${}^4_\Lambda\text{H}$  and  ${}^4_\Lambda\text{He}$  occurs. The  $1.1\text{-MeV}$  peaks seen in these two spectra are attributable to the M1 spin-flip transitions in the mass-4 system.

Similarly, for  ${}^9_\Lambda\text{Be}$ , a  $\gamma$  transition near  $3.05\text{ MeV}$  was observed. This transition is attributed to the decay of the  $3/2^+, 5/2^+$   $\Lambda$  multiplet built on the corresponding  $2.94\text{-MeV } 2^+$  state of  ${}^8\text{Be}$ .

In all these cases, a hypernuclear  $\gamma$  ray was observed to occur within about  $100\text{ keV}$  of the corresponding transition energy of the corresponding nuclear core state. This observation strongly suggests that all spin-dependent  $\Lambda$





multiplet splittings in the p shell are quite small, being on the order of 100 keV or less.

### THE HIGH FLUX BEAM REACTOR

The High Flux Beam Reactor at Brookhaven is a unique facility in this country which provides a variety of neutron beams for use in nuclear physics experiments. At BNL, the reactor neutrons are used in two characteristic ways, to initiate the  $(n, \gamma)$  reaction and to produce neutron-rich nuclei by inducing fission in uranium.

#### a) $(n, \gamma)$ Reaction

In the  $(n, \gamma)$  reaction, an incident neutron is absorbed by a target nucleus, producing another nucleus at a high excitation energy. This nucleus then deexcites to low-lying states by the emission of  $\gamma$  rays, either directly by so-called primary transitions or via a statistical cascade. The overriding characteristic of this process which renders it a completely unique and essential tool is its *nonselectivity*. This is most dramatically apparent when using the so-called ARC technique (Average Resonance Capture) whereby, under appropriate conditions, one may enjoy an *a priori guarantee* of directly populating all final states in certain spin and excitation energy ranges. As a consequence, one can test nuclear models in a comprehensive way not heretofore possible. For example, it becomes trivial to test for a one-to-one correspondence between predicted and observed levels, and thereby either confirm or disprove a model, or to find evidence for extra degrees of freedom not included in it.

#### b) TRISTAN

The reactor neutrons are exploited in a second way by utilizing the process of thermal-neutron-induced fission of uranium. This process yields a spectrum of fission product nuclei centered on masses  $A \approx 80$ -150. These neutron-rich fission products lie far from the valley of stability. They thereby give access to entirely new realms of nuclear species where new phenomena can be expected, since unique combinations of neutron and proton orbits produce interactions and couplings not observable elsewhere. The implementation of this program is carried out with the on-line mass separator TRISTAN which has recently gone into full operation as a national user facility at the HFBR.

### Role of Finite Boson Number in the IBA

In the last few years a new nuclear model, the Interacting Boson Approximation (IBA) model, has been proposed and has generated enormous interest and discussion. The model attempts to incorporate the major features of collective states by treating the neutrons and protons outside closed shells in terms of pairs called bosons and by introducing a simple set of interactions between these bosons. In any IBA calculation, an ever-present element is the recognition and treatment of the finite number,  $N$ , of these bosons. However, it has not been clear up to now whether this is merely a complication of little importance or a key ingredient in generating the characteristic IBA predictions. Studies at BNL this year have sought to address this central question.

In geometric models of deformed nuclei the level spectra consist of a series of rotational bands built on intrinsic collective excitations. The lowest of these are the so-called  $\gamma$  and  $\beta$  vibrations, which are characterized by a quantum number  $K$ , equal to 2 and 0, respectively, which describes the orientation of the nuclear angular momentum relative to the nuclear symmetry axis. Superficially similar excitations appear in the IBA as well, although, as emphasized in previous HIGHLIGHTS, they are substantially different from the geometrical excitations. The present study centered on the decay of the  $\gamma$ -band states to states of the lowest, or ground ( $g$ ), rotational band. In the simplest picture these transitions will depend on the spins of the initial and final states but, nevertheless, all such transitions can be viewed as essentially involving the destruction of a  $\gamma$ -vibrational quantum. If one considers *ratios* of the transition intensities, therefore, this common aspect cancels out, leaving only an easily calculated set of relations (Alaga rules) among the transition strengths. For years it has been known that there are substantial deviations from these simple rules which have traditionally been interpreted in terms of very weak  $\Delta K = 2$  mixing of  $\gamma$  and  $g$  bands. The mixing has been parameterized in terms of a quantity,  $Z_\gamma$ . The present study began by extracting an extensive set of  $Z_\gamma$  values from the data on deformed rare-earth nuclei and by plotting these not against mass but against the boson number. The results,

shown in Fig. 6, are seen to display a remarkably simple and regular systematics. They have minima at mid-shell and rise uniformly toward the edges of the deformed region.

The next step consisted of recasting the usual IBA formalism so that calculations can be performed as a function of only a single parameter, denoted  $\chi$ , which occurs in the boson quadrupole operator. It then turns out that for most deformed nuclei the  $\chi$  values lie in a very narrow band. Since the IBA calculations of  $Z_\gamma$  agree very well with the empirical ones and since the only parameter,  $\chi$ , is nearly constant, the reproduction of the cup-shaped  $Z_\gamma$  systematics cannot arise from parameter variations but rather occurs primarily because of the *changing boson number*. The implication is that the IBA, although ostensibly a macroscopic phenomenological model, automatically incorporates microscopic effects by virtue of its inherent dependence on the number of bosons.

When a detailed analysis is made of the origin of the  $N$  dependence, a further and particularly interesting point emerges. It does not arise, as expected, primarily from weak  $\Delta K = 2$   $\gamma$ - $g$  mixing but, crudely speaking, from very strong (nearly  $N$  independent)  $\Delta K = 0$  mixing of the  $\beta$  and  $g$  bands, coupled with weak  $\Delta K = 2$  mixing of  $\beta$  and  $\gamma$  bands which carries a  $1/N^2$  dependence. This combination of mixing leads, in effect, to crucial contributions to  $\gamma \rightarrow g$  transi-

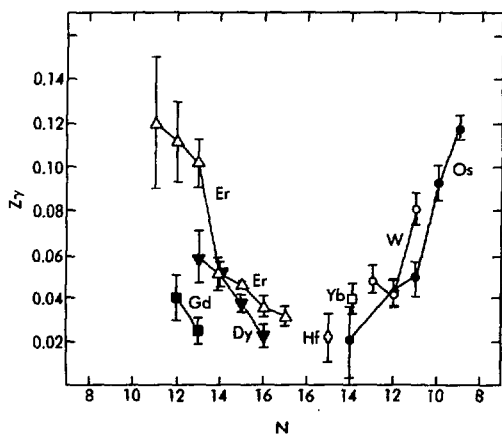


Figure 6. Systematics of the parameter  $Z_\gamma$ , which describes the deviations of  $\gamma \rightarrow g$  transitions from the Alaga rules, plotted against boson number.

tions from  $\gamma \rightarrow \beta$  amplitudes. Allowed  $\gamma \rightarrow \beta$  transitions are a unique prediction of the IBA, essentially different from that obtained with geometric models, which have now been observed empirically. It is remarkable that these same amplitudes are now seen to play such a crucial role in  $\gamma \rightarrow g$  transitions.

### Search for Multi-j Supersymmetries in Nuclei

Ever since the IBA was first applied to even-mass nuclei, with its natural inclusion of limiting symmetries, it has been of considerable interest to determine if analogous symmetries could be developed to encompass both odd and even nuclei and whether such "supersymmetries" would be manifest empirically. Such a supersymmetry envisions an odd particle (fermion) coupled to an even core which itself exhibits one of the three IBA symmetries. The best established of the latter is the so-called  $O(6)$  limit, which is found empirically in the even Pt nuclei. The first supersymmetry to be deduced theoretically corresponded to a fermion in a  $j = 3/2$  orbit coupled to an  $O(6)$  core. Unfortunately, this is a rather unrealistic situation since, in the shell model, an isolated  $3/2$  orbit never occurs. Although some tests of this single-j supersymmetry were made in the odd-proton Ir and Au nuclei, the results were, not surprisingly, inconclusive. To remedy this situation, a multi-j supersymmetry was subsequently proposed by Balentekin, Bars, and Iachello involving an  $O(6)$  core coupled to a fermion that can occupy any of the  $j = 1/2, 3/2, \text{ or } 5/2$  orbits. This is now precisely what one expects for negative parity states in the odd Pt isotopes. Therefore, a series of  $(n, \gamma)$  experiments utilizing the ARC technique were performed at BNL in order to disclose the complete set of  $1/2^-$  and  $3/2^-$  levels (along with some  $5/2^-$ ,  $7/2^-$  levels) in  $^{195,197,199}\text{Pt}$  and to compare these with the supersymmetry.

The results show, first, that contrary to previous perceptions, these three nuclei are very similar empirically: each has the same number of low-lying  $1/2^-$ ,  $3/2^-$  states and there is a smoothly evolving energy systematics. In Fig. 7 the results for  $^{195}\text{Pt}$  are compared with the supersymmetry. It is evident, up to the energy indicated, that there is an exact 1:1 correspondence between the model and the data, provid-



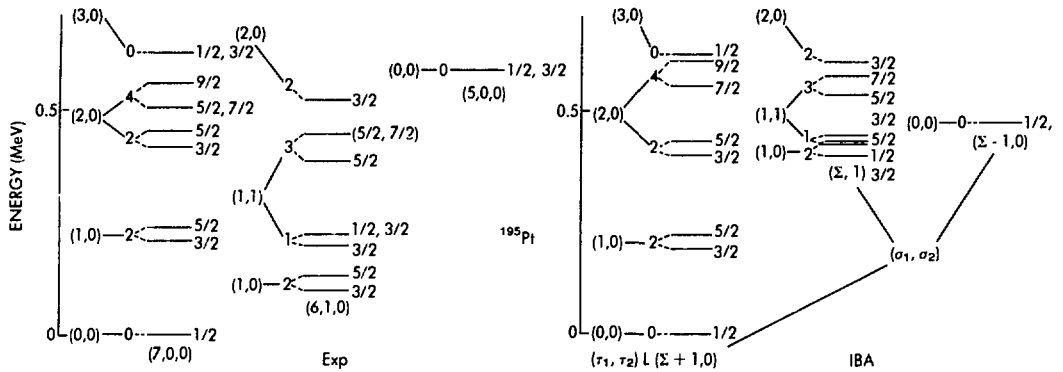


Figure 7. Comparison of the low-lying levels of  $^{195}\text{Pt}$  with the predictions of the  $O(6) \times j = 1/2, 3/2, 5/2$  supersymmetry. The levels of the predicted scheme are labeled by a set of quantum numbers that distinguish different families and interrelations of states. At higher energies than shown, the number of predicted levels greatly exceeds those found experimentally.

ing substantial initial support for the basic supersymmetry scheme. One particularly interesting feature is the recurrence of level couplets (e.g.,  $3/2, 5/2$  pairs) throughout the level scheme. These are a characteristic feature of the supersymmetry arising automatically from its inherent group structure. The data also exhibit a significant discrepancy with the model. The states of the second principal family of states [denoted by the quantum numbers  $(\Sigma, 1)$ ] empirically occur below the first excited couplet of the first family. In the supersymmetry scheme this cannot occur. While it was first thought that this last result implied a degree of symmetry breaking, recent theoretical work now indicates that an alternative formulation of the group theory can yield a related supersymmetry that reflects the empirical structure. Clearly this is an entirely new field of study that is only beginning. The present results are the first exciting steps in the testing and understanding of advanced group theoretic approaches that hold the promise of unifying our understanding of odd- and even-mass nuclei.

### g Factors in Transitional Nuclei

In recent years there has been growing evidence that the proton number  $Z = 64$  corresponds to a major break or gap in the sequence of shell-model orbits, somewhat smaller than, but of the same type as, those at  $Z = 28$  or  $82$ . This has led (see last year's HIGHLIGHTS) to a

reexamination of the reasons for the onset of deformation near mass 150 and to the suggestion that the *proton*  $Z = 64$  shell gap is active for *neutron* numbers at or just above  $N = 82$  but rapidly dissipates when the neutron number reaches 90. This in turn has implications for IBA calculations in this region, since the number of bosons is directly related to the number of valence nucleons. Interestingly, it turns out that calculated magnetic moments in the IBA are nearly parameter independent but highly sensitive to boson number and therefore provide an empirical tool for assessing the changes in  $N$ . Again, because of their parameter-independence, they relate not only to the IBA, but give a rather direct sense of the underlying shell structure in a nearly model-independent way.

In order to utilize these ideas,  $g$  factors for the  $2_1^+$  states in  $^{144}\text{Ba}$  and  $^{146}\text{Ba}$  were measured at TRISTAN, using the perturbed angular correlation technique. The experiments were successful and the results, along with those for neighboring nuclei, are shown in Fig. 8. The abscissa is a ratio of two matrix elements calculated in the IBA, while the ordinate is the experimental magnetic moment deduced from the  $g$  factor divided by one of those calculated matrix elements. In the IBA such a plot should be a straight line and, if it agrees with the data, the latter should lie on this line. In the upper plot, which corresponds to the assumption that there is *no*  $Z = 64$  shell gap, there is a clear disagree-

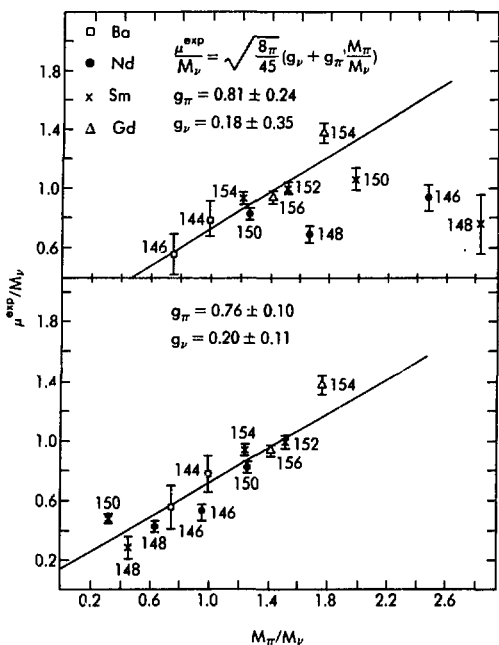


Figure 8. Experimental magnetic moments for  $2^+$  states divided by a calculated matrix element plotted against a ratio of calculated matrix elements. The solid lines are the IBA predictions. (Top) No shell closure is assumed at  $Z = 64$ . (Bottom) The (somewhat exaggerated) assumption is made that there is a  $Z = 64$  closure for neutron numbers  $N \leq 88$  but that the gap is dissipated for  $N \geq 90$ .

ment, evident for the nuclei closest to  $Z = 64$ , namely, Sm ( $Z = 62$ ) and Nd ( $Z = 60$ ), and more pronounced for  $N = 86$  than  $N = 88$ . In the lower plot, which is based on the same data but incorporates the idea of a  $Z = 64$  shell gap, the data very closely approximate a straight line for  $N \leq 88$ , thus confirming both the conclusions that the IBA can correctly account for these measurements, in a nearly parameter-free way, and that the  $Z = 64$  concept is relevant, at least for global integrated properties of the lower-lying levels, for neutron numbers  $N \leq 88$ .

## NUCLEAR THEORY

Nuclear Theory at BNL has evolved over the course of several years into a discipline treating not only the important structure of a nucleus in

terms of its nucleon constituents, but also the structure of the nucleons themselves in terms of their confined constituents, the quarks. The research topics considered vary from short-lived molecular states of two complex nuclei to the possible breakdown in baryon number conservation anticipated in the transmutation of neutrons into antineutrons. Other investigations involve the hydrodynamic collapse of massive stars expected to be the antecedents of Type II Supernovae, the nuclear structure aspects of weak interactions, the continuing search for solar neutrinos, and reactions initiated by strangeness-carrying particles. Some of these subjects, which have yielded interesting results in the past year, are described below.

Studies of the quark structure of baryons have focused on three important problems. The recently proposed Grand Unified Theories, which place electromagnetic, weak, and strong interactions on an equal footing, have suggested that the important quantum number (the baryon number) is not conserved. The time period for decay of the baryon into leptons is, of course, extremely long. Some versions of these theories yield, as a consequence of the very weak communication between quarks and leptons, a spontaneous conversion of neutrons into antineutrons. Since this conversion can take place inside finite nuclei, one may observe the pion radiation resulting from the annihilation of the antineutron on a nearby nucleon. Theorists at BNL and the University of Jerusalem have investigated the relation between the annihilation lifetime  $T$  of the nucleus and the oscillation or conversion time  $\tau_{nn}$  for a neutron in free space. Using the best limits on  $T$  from present negative results in nucleon decay experiments, they find  $\tau_{nn} > 6 \times 10^7$  sec, a more stringent limit than that obtained from reactor neutrons.

A second problem of crucial importance to the MIT bag theory of hadron structure concerns the possible existence and production of six-quark systems confined in a single bag. The most likely such object is the H baryon, equivalent to two strange  $\Lambda$ 's bound deeply in the bag. The  $(K^-, K^+)$  reaction has been identified as most promising for possible formation of the H, with measurable cross sections predicted for the process  ${}^3\text{He}(K^-, K^+ n)\text{H}$ . An experimental search for

this exotic particle, predicated on these calculations, is in preparation.

Finally, again in collaboration with theorists at Saclay, a field theoretic description of the MIT bag is being pursued. Following early work by M. Creutz and more recent work by T. D. Lee, a model is being developed which yields hadrons as soliton solutions of classical field equations. This model has been rendered chirally invariant by the introduction of not only a scalar confining field but also a companion isovector, the pseudoscalar meson. The resulting theory contains monopole-like topological solitons which resemble the little bag solutions of M. Rho and G. E. Brown.

In a recent structure calculation involving electromagnetic and weak processes in nuclei, the use of realistic radial forms for the single nucleon wave functions has been demonstrated to be crucial. This is, of course, especially true when some of the nucleons involved in the specific processes examined move in weakly bound orbits. A particularly striking example is the decay of the  $1/2^-$  320-keV first excited state of  $^{11}\text{Be}$ , which deexcites to the  $1/2^+$  ground state by a very strong electric dipole transition. A calculation using the nonrealistic oscillator wave functions gives rise to a rate too small by a factor 30. Large effects are also found in first forbidden beta transitions involving no change in angular momentum, i.e.,  $J^+ \rightarrow J^-$  transitions. Matrix elements for light nuclei involving the  $2s$   $1/2$  orbit, an orbit with a node, show the greatest

sensitivity. Again, because of inherent cancellations between interfering matrix elements in  $2s \rightarrow 1p$  transitions, order-of-magnitude effects are seen. Pinning down these effects has important consequences for parity mixing in nuclei, and for the extraction of the structure of the fundamental parity-nonconserving currents.

The backward angle phenomenon observed in the quasi-elastic scattering of light heavy-ion systems, such as oxygen on silicon, is often presented as evidence for nuclear molecular behavior. The oscillating angular distributions of the products and the resonant-like peaks in the backward excitation function are the signatures of this phenomenon. No fundamental explanation for this behavior has yet been presented. Two results obtained recently, however, point towards such an explanation. A phenomenological optical theory predicted the existence of a precipitous drop in the  $180^\circ$  differential cross section at some prominent low energy minima in the excitation function, and this drop has been observed experimentally in a collaboration with experimentalists at Saclay, France. Moreover, a coupled-channel calculation at these low energies has uncovered a heretofore ignored physical mechanism and subsequently has yielded an excellent description of the entire range of observations. States whose excitation energies leave them at an effective scattering energy near the Coulomb barrier have been shown to play a profound role in a channel-coupling model of the process.

## Solid State Physics

---

### INTRODUCTION

The solid state program is concerned with understanding the physical, electronic, and magnetic properties of both surfaces and bulk matter. Photons, neutrons, protons, electrons, and positrons are used to explore the influence of temperature, pressure, magnetic fields, and defects on the microscopic properties of solids and liquids.

There are two major facilities at Brookhaven for solid state research: the High Flux Beam Reactor, which provides intense beams of low energy neutrons for structural and dynamical

studies, and the National Synchrotron Light Source, which serves as an intense source of tunable infrared, ultraviolet, and x radiation for use in electronic and structural investigations. Also available are intense positron beams and facilities to produce defects in solids by irradiation.

### NEUTRON SCATTERING STUDIES

Thermal neutrons have wavelengths and energies comparable to the atomic spacings and excitation energies characteristic of condensed matter. They are thus excellent probes of the

static and dynamic properties of solids and liquids. In addition, neutrons have magnetic moments which interact with atomic magnetic moments. Hence they can also be used to probe magnetic structures and excitations. The following are examples of the types of investigations currently being made with neutrons at the High Flux Beam Reactor.

### Fractional Staging in Intercalated Graphite

One of the more unusual properties of graphite is that other atoms and molecules can be readily introduced into its structure. When so incorporated, a staged-lattice is often formed, i.e., a lattice with a periodic sequence of intercalate and host layers. [For example, in stage-2 potassium-intercalated graphite there are two layers of carbon (C) atoms for every potassium (K) layer, the repeating unit being ...CKC...] Staging is thought to be a manifestation of long-range elastic interactions between layers. Calculations based on this view predict nonintegral as well as integral staging, although only integral staging has thus far been observed. But in a recently completed neutron scattering study of stage-1 potassium graphite under pressure, evidence of nonintegral staging has finally been obtained (Fig. 1). When this material was compressed, a stage-3/2 (...CKCK...) lattice was found to form. Then, at still higher pressures, this stage-3/2 phase was converted to stage 2. Both transitions were accompanied by in-plane densification of the potassium layers. The observation of nonintegral staging lends strong support to the current theoretical view that relatively simple elastic interactions are involved and removes the rationale for invoking a complicated screening of interlayer repulsions.

### Magnetic Ordering in $\text{TmRh}_4\text{B}_4$

Although magnetic ordering was long thought to be incompatible with superconductivity, it is now known that this is not always the case. Among systems which exhibit both superconducting and magnetically ordered phases is a group of rare-earth rhodium borides that provide dramatic evidence of how remarkably delicate is the balance between magnetic and superconducting states.

Erbium rhodium boride is found to be a re-entrant superconductor, i.e., its superconductiv-

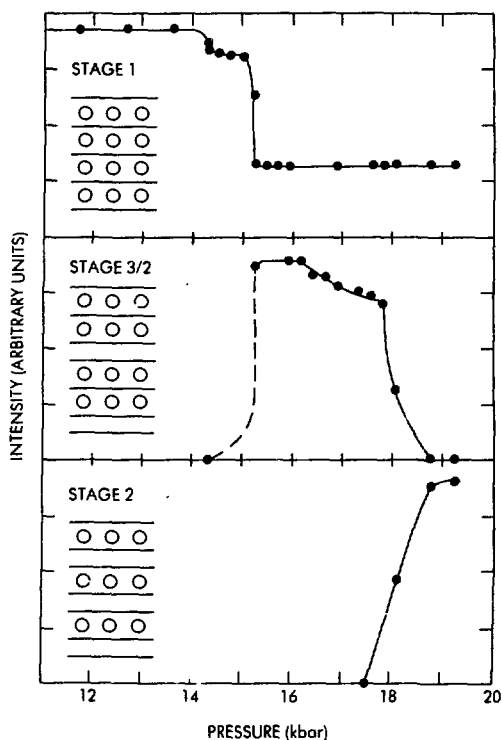


Figure 1. Diffracted neutron intensities versus pressure for stage-1 potassium-graphite. The disappearance of stage 3/2 at 19 kilobars leaves stage 1 unaffected but coincides with the emergence of stage 2.

ity is destroyed by ferromagnetic ordering. A recent neutron diffraction study of thulium rhodium boride ( $\text{TmRh}_4\text{B}_4$ ) shows this material to be quite different in its behavior. The superconducting transition in  $\text{TmRh}_4\text{B}_4$  occurs at a temperature of 9.8 K. At 0.7 K it is observed to form a magnetically ordered phase which coexists with the superconducting phase. This phase is not ferromagnetic. Instead, a modulated antiferromagnetic structure appears with the modulation along (101) directions, the rare-earth spins aligning along (010) directions. Applying a magnetic field induces a ferromagnetic moment, but the electrical resistivity remains zero, suggesting that the system divides into superconducting and ferromagnetic domains.

### Ethylene Overlayers on Graphite

Weakly adsorbed overlayer films are often found to behave like idealized two-dimensional

solids and liquids and thus offer interesting insights into how "dimensionality" affects the properties of matter. Among such overlayer systems is one, ethylene ( $C_2H_4$ )-on-graphite, that exhibits highly unusual behavior. At the lowest temperatures, only a single layer of ethylene forms on graphite basal planes. When more material is added, three-dimensional solid ethylene is observed to form. Above a temperature of about 80 K, however, a second adsorbed layer appears, and, near 100 K, a third layer, in each case with a corresponding reduction in the amount of three-dimensional solid. Investigation of deuterated ethylene ( $C_2D_4$ ) monolayers on graphite with neutrons shows evidence of two low temperature two-dimensional solid phases: (i) a low-density triangular-lattice phase in which the molecules are presumed to have their C-C axes parallel to the film plane, and (ii) a high-density triangular-lattice phase assumed to be associated with a reorientation of the C-C axes of the molecules perpendicular to the film plane. Both solid phases are incommensurate with the underlying graphite substrate. At 80 K (where the second adsorbed layer forms), the first layer is observed to undergo a structural transition from the high-density solid phase to one of intermediate density, the two-layer adsorbed system being thus composed of two solid layers of nearly the same density. Formation of three adsorbed layers appears to be associated with a solid-to-fluid phase transition. An almost exact balance between adatom-adatom and adatom-substrate interactions is believed to underlie this curious tradeoff between two- and three-dimensional ordering.

### SOLID STATE THEORY

Experimental solid state research at Brookhaven has an important impact on the development of related areas of condensed matter theory. Work in the Theory Group, therefore, tends to be closely coordinated with the ongoing experimental programs. Major emphasis is given to (i) interpreting experimental data in the light of existing theoretical models, (ii) extending and revising these models as new information becomes available, and (iii) suggesting new directions for experimental exploration. Topics covered in recent years include phase transitions, organic superconductors,

alloys, surface properties of metals and insulators, photoionization, hydride kinetics, and crack propagation in crystal lattices.

### Electronic Structure of Metallic Overlayers

Recent experimental studies of few-atomic-layer palladium films on niobium surfaces made at Brookhaven show that palladium [in three dimensions, a face-centered-cubic (fcc) solid] forms a commensurate overlayer on niobium even though niobium is body-centered cubic (bcc) in structure. Furthermore, the presence of the film is found to drastically alter the rate of hydrogen uptake into the niobium lattice, the rate being very sensitive to the thickness of the overlayer film.

Calculations of the electronic structure (energy bands) of monatomic palladium films and palladium-niobium composites provide a natural framework within which to view these experiments. First, the energy bands of isolated bcc and fcc palladium monolayers were calculated. The results indicated that the electronic properties of the palladium were little altered by the change in structure and suggested that surface geometry *per se* did not explain the differences in behavior. Also, the calculated energy bands were in very good agreement with those observed experimentally using angle-resolved photoemission. Second, the energy bands of a five-atomic-layer niobium film with palladium overlayers were calculated. These calculations showed that the palladium electronic states in the composite were filled in a way similar to the d-bands of a noble metal, a situation resembling that found in niobium-palladium alloys. The effects of palladium overlayers on hydrogen uptake in niobium are thus seen to result from hybridization and charge transfer between niobium and palladium atoms rather than from the altered palladium structure. Indeed, if an isolated bcc palladium layer could be investigated experimentally, its interaction with hydrogen would not be expected to be very different from that in bulk fcc palladium metal.

### PARTICLE-SOLID INTERACTIONS

Particle-solid interaction physics entails the use of high and low energy particles such as positrons, electrons, and heavy ions to study

lattice defects, vibrational motions, and related properties of solids. The following example illustrates an important new application of such techniques to surface overlayer characterization.

### Positron Emission as a Probe of Surface Vibrations

A precise understanding of how molecules behave on surfaces is basic to surface-related technology. An interesting new approach to this very difficult problem is currently under development at Brookhaven. It involves the use of positrons (the positively charged analog of the electron) to probe the vibrational motions of surface atoms and overlayers. What is done is to inject positrons of well-defined energies into surfaces and analyze their energy spectrum on re-emission. This approach offers certain advantages over the more commonly employed electron-energy-loss spectroscopy, the most important being that positron spectroscopy has the potential to provide better resolution than equivalent measurements made with electrons.

The first experimental studies were of the vibrational motions of carbon monoxide (CO) molecules on nickel (Ni) surfaces. Figure 2 shows the positron loss spectrum observed with a  $2 \times 2$  commensurate CO overlayer on room

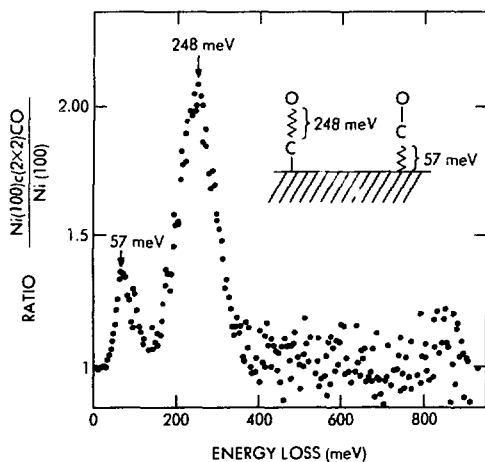


Figure 2. Positron-energy-loss spectrum from a  $2 \times 2$  carbon monoxide monolayer on nickel (100) surfaces at room temperature. The spectrum has been normalized to that from clean nickel.

temperature Ni (100) surfaces. Energy loss peaks at 57 and 248 meV, corresponding respectively to Ni-C and C-O stretching vibrations, are clearly evident. The energies agree well with those observed in earlier electron-energy-loss investigations.

It is anticipated that positron-energy-loss spectroscopy will apply equally well to the study of more complex molecules such as hydrocarbons on metal surfaces and will be of particular value in monitoring catalytically induced molecular disassociations and recombinations.

## SURFACE STUDIES

This program focuses on the electronic properties of surface atoms and atoms in thin overlayer films. Along with a well-equipped laboratory for surface spectroscopy, the group also operates a recently completed VUV photoemission facility at the NSLS.

### Carbon Overlayers and Methanation Catalysis

Surface carbon is known to play an important role in methanation catalysis. Investigation shows that the activity of the catalyst is strongly dependent on the structural form of the carbon overlayer, highly graphitic layers being much less effective than their carbidic counterparts. It has been suggested that dangling carbon bonds in the carbidic form are responsible for its enhanced activity. Current studies of the graphitic-to-carbidic structural transition in few-atomic-layer carbon films on niobium made at the Synchrotron Light Source support this view. Auger, photoemission, and near-edge absorption measurements show features that are consistent with a substantial decrease in carbon-carbon bonding as the carbon overlayers transform from graphitic to carbidic structure and the spacing between carbon atoms increases. Moreover, features due to  $p_z$  atomic orbitals (which form the  $\pi$  part of the C=C bond in graphite) become more prominent in the carbidic near-edge spectra indicating that these orbitals may indeed be important in enhancing carbidic catalytic activity.

### Hydrogen in Thin Niobium Films

Hydrogen uptake in metals is not only of basic scientific interest but is also of potential

practical importance for gas storage in hydrogen-powered motor vehicles. Not surprisingly, the utility of metal gas storage systems depends crucially on how much gas can be retained within a given volume of the host lattice. Recent studies of thin niobium films (100 to 300 Å thick) show them to have a substantially greater capacity for hydrogen storage than bulk niobium metal. The films are deposited on glass substrates with a palladium overlayer 100 Å thick to protect them from airborne contaminants (palladium is extremely permeable to hydrogen). Gas uptake is monitored both by

measuring the expansion of the niobium lattice with x-ray diffraction and by observing the change in electrical resistance during the charging process. It is found that hydrogen solubility increases dramatically with decreasing niobium film thickness; for example, in a film 400 Å thick the hydrogen concentration can be as much as 130 at.%, while 3 at.% is more typical of the bulk metal. Multilayers of niobium and palladium show the same striking effect. Thus, layered composites containing perhaps several micrometers of niobium in total may be good candidates for vehicular hydrogen storage.

## Atomic and Applied Physics

---

The determination of the elemental and isotopic composition of matter is a longstanding and fundamental scientific problem. Although it may be thought that ordinary chemical methods and more exotic techniques such as mass spectroscopy, neutron activation analysis, or inductively coupled plasma emission spectroscopy could be used to completely solve such problems, this is not actually the case. Recently, ion and synchrotron radiation photon beams have proved to be extremely useful additions to the analyst's arsenal of techniques, with several uniquely valuable features.

The applications and uses of ion beam analysis span many fields of science; for example, materials sciences and semiconductor, medical, and archaeological areas have benefited. In the future the comprehensive facilities at Brookhaven comprising particle beams at the Van de Graaff facilities, photon beams at the NSLS, and neutron beams from the HFBR and the Medical Reactor will serve to place Brookhaven in the forefront of the rapidly progressing field of nuclear analytical techniques.

In the past year several experiments were carried out with beams from the Brookhaven 3.5-MV Research Van de Graaff Accelerator which serve to illustrate the usefulness of ion beam analysis. The Research Van de Graaff provides copious beams of p, d, t,  $^3\text{He}$ ,  $^4\text{He}$ , and some heavier elements up to Xe with precisely defined energies. These beams can be used for analytical measurements with techniques such as

proton-induced x-ray emission (PIXE), Rutherford backscattering (RBS), nuclear reaction analysis, resonance depth profiling, microbeams, and others to determine composition of materials and the spatial and depth distribution of each element. The analysis with the ion beam is, in many cases, nondestructive. Samples require little preparation, with small quantities needed, and analyses can often be performed at atmospheric pressure or in wet environments. Sensitivities for trace element determinations in thick samples exceed those for the electron microprobe by several orders of magnitude. In the experiment presented here as an example, proton inelastic scattering is used to produce gamma rays which uniquely identify the elements Al and Si. The work was stimulated by a project in catalysis, but the method is applicable to many other fields.

Zeolites are an important type of catalyst, and many active experimental programs are in progress to determine their properties. In this work it is important to know the relative concentrations of silicon and aluminum to determine the number and strength of proton sites, the hydrophilic character of the zeolite, the thermal and chemical stability of the zeolite framework, and, if ion-exchanged with metal ions, the cation distribution and coordination. Taken together, these factors determine the molecular selectivity and chemical activity of the zeolite.

In practice, accurate values for the Al and Si content of catalysts have been difficult to obtain

with the standard chemical techniques available today. Therefore, in collaboration with G. D. Stucky's group at du Pont, an investigation was undertaken to ascertain the value of nuclear methods for this type of analysis.

A convenient solution is to use proton inelastic scattering to identify the silicon and aluminum. Inelastic scattering produces 844- and 1014-keV gamma rays from Al and a 1779-keV gamma ray from Si, gamma rays that are suitable for use as tags for the presence of Al and Si. The probability for producing these gamma rays is shown in Fig. 1. From the excitation curve it can be seen that the use of protons with an energy of 3.2 MeV gives almost the best sensitivity within the range of the accelerator, combined with little change in sensitivity with respect to the bombarding energy. A typical spectrum obtained in the bombardment of a zeolite catalyst is shown in Fig. 2 where the gamma rays from Al and Si are clearly visible. This type of spectrum can be obtained in 15 minutes with a Ge(Li) gamma-ray detector with an efficiency of 12% relative to

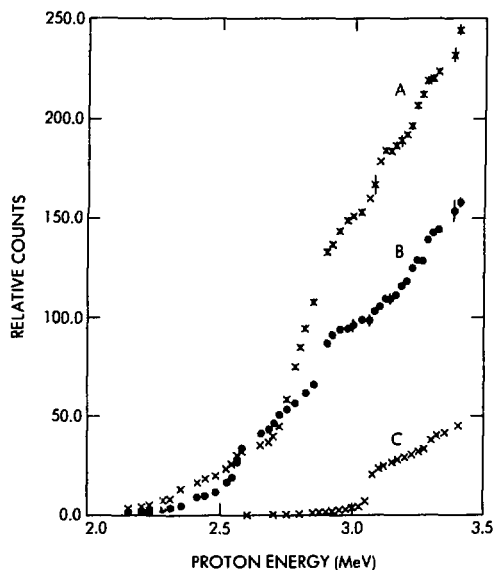


Figure 1. Relative cross sections for production of gamma rays induced by the (p,p') reaction in aluminum and silicon as a function of the incident proton energy. Curves A(x) and B(•) refer to the aluminum 1014- and 844-keV gamma rays, respectively. Curve C shows the yield of the 1779-keV silicon gamma ray.

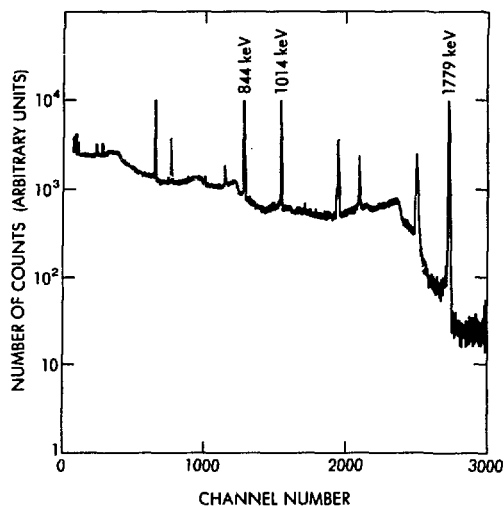


Figure 2. Typical gamma-ray spectrum produced by bombardment of a zeolite sample with 3.4-MeV protons. The gamma rays from aluminum and silicon are shown at 844 and 1014 keV for Al and at 1779 keV for silicon.

a  $7.6 \times 7.6$ -cm Na I(Tl) scintillation detector and a beam current of 4 nA.

The conversion of the measured gamma-ray yields to find absolute values for concentrations and for Si/Al ratios was accomplished by comparison with Standard Reference Materials from the National Bureau of Standards. If necessary this could also be done on an absolute basis by measuring the detector efficiency as a function of energy and by integrating the production cross section over the range of the proton.

A comparison of the nuclear inelastic scattering results with the average value obtained in a "round-robin" study is shown in Table I. The average value given includes determinations from laboratories using atomic absorption, x-ray fluorescence, inductively coupled plasma emission, neutron activation analysis, and chemical methods. It can be seen that our results agree very well with the average value. Indeed, deviations from the averages for the present work are less than for all other methods. This should help to improve the accuracy of the other methods and also the experimental capabilities available to zeolite researchers.



Table I  
Determination of Al and Si Content of Zeolite  
Samples by Proton Inelastic Scattering

Sample	Si/Al <sup>a</sup>	Si/Al <sup>b</sup>	(Si/Al) Nuclear (Si/Al) Average
E-30711-78-1	1.00 ± 0.03	1.01 ± 0.04	0.99
2	4.76 ± 0.18	4.58 ± 0.11	1.04
3	3.56 ± 0.16	3.48 ± 0.08	1.02
4	3.00 ± 0.21	2.91 ± 0.11	1.03
5	5.10 ± 0.26	5.08 ± 0.16	1.00
6	4.81 ± 0.39	4.92 ± 0.17	0.98
7	3.71 ± 0.21	3.76 ± 0.19	0.99
8	11.0 ± 0.2	11.0 ± 0.19	1.00
9	22.9 ± 0.2	20.7 ± 2.8	1.11
10	35.0 ± 2.3	36.4 ± 1.2	0.96
12	2.97 ± 0.16	3.02 ± 0.08	0.98

<sup>a</sup> Determined by proton inelastic scattering.

<sup>b</sup> Average of determinations using atomic absorption, x-ray fluorescence, inductively coupled plasma emission, neutron activation analysis, and chemical methods.

This specific example demonstrates the efficacy of ion beam analysis for accurate determination of light element concentrations in different types of zeolite materials and shows that the capability is essential and necessary in any large multipurpose research laboratory such as Brookhaven. The description of the total number of applications of ion beam analysis with beams from the 3.5-MV Van de Graaff extends far beyond the scope of this brief summary.

In atomic physics, interesting new experiments on molecular orbital x rays, precision energy measurements of high energy x rays, resonant transfer of electrons (RTE) to highly charged ions, and design of new experiments for the NSLS were in progress during the year. The experiment on RTE is discussed because of the resemblance of the process to dielectronic recombination.

In dielectronic recombination, an ion captures an electron from the continuum into a doubly excited state formed by the simultaneous excitation of a bound electron. A photon can then be emitted as the atom decays into a stable final electron configuration. This process, first identified forty years ago, has since been recognized as playing an important role in determin-

ing the rate of energy loss in a dilute high temperature plasma. It is a process that should be understood experimentally because of its significance in both astrophysical and tokamak-type laboratory plasmas. As a result, the laboratory study of dielectronic recombination has recently been of considerable interest to the atomic physics community.

During the past year several groups reported the successful observation of dielectronic recombination for the first time in experiments using beams of *slow ions merged* with high-current electron beams. Such experiments are difficult, and it is useful to consider alternative approaches.

One possibility is to replace the diffuse electron beam by a gas target. In this case electrons that are captured come from a bound state of the target atom with a definite velocity distribution relative to the incident ion. Transfer of the electrons to the moving ion should be a resonant process, with a maximum at the ion velocity corresponding to the velocity of an electron with the energy of an Auger electron emitted in the inverse process minus the bound state binding energy. The resonance width reflects the velocity distribution of the target electrons.

A multi-institutional group composed of scientists from Western Michigan University, the New University of Ulster, the University of North Carolina, and Brookhaven undertook this experiment using  $S^{13+}$  beams produced by the Brookhaven Double MP-Tandem Facility. Charge-state purification of the incident beam and analysis of the charge-state distribution after the interaction region were accomplished by the use of electrostatic analysis. A low-pressure differentially pumped gas target was used to ensure that the experiment was done under well-defined single collision conditions. Ions undergoing single-electron capture ( $q - 1$ ) and loss ( $q + 1$ ) were detected with surface barrier detectors. The main beam ( $q$ ) was detected in a Faraday cup. A Si(Li) x-ray detector was used to detect K x rays emitted in the interaction in coincidence with the capture and loss events. The results of the experiment are displayed in Fig. 3.

It can be seen that there is a resonant-like peak in the single-electron capture ( $q - 1$ ) cross section, and this is attributed to the resonant transfer of electrons (RTE) as discussed above. The shape and magnitude of the observed cross sections can be reasonably well accounted for by use of theoretical dielectronic recombination cross sections and the momentum distributions of the target electrons.

This first RTE experiment will require additional experimental work to verify the systematics of the observed resonance energy and width, and provide a more accurate comparison of the magnitude of the cross section with the results of theory. A comparison of this type of experiment with the results of a crossed beam experiment on the same ion is important to demonstrate clearly the equivalence of the two processes. Another type of experiment that is possible at Brookhaven is the use of a plasma target as a source of free electrons. In this case the resonance width would be very narrow, but a peak should be seen at a particular ion velocity. Since electron densities in a plasma can be orders of magnitude higher than in an electron beam, this could turn out to be a particularly clean and easy way of making precision dielectronic recombination measurements.

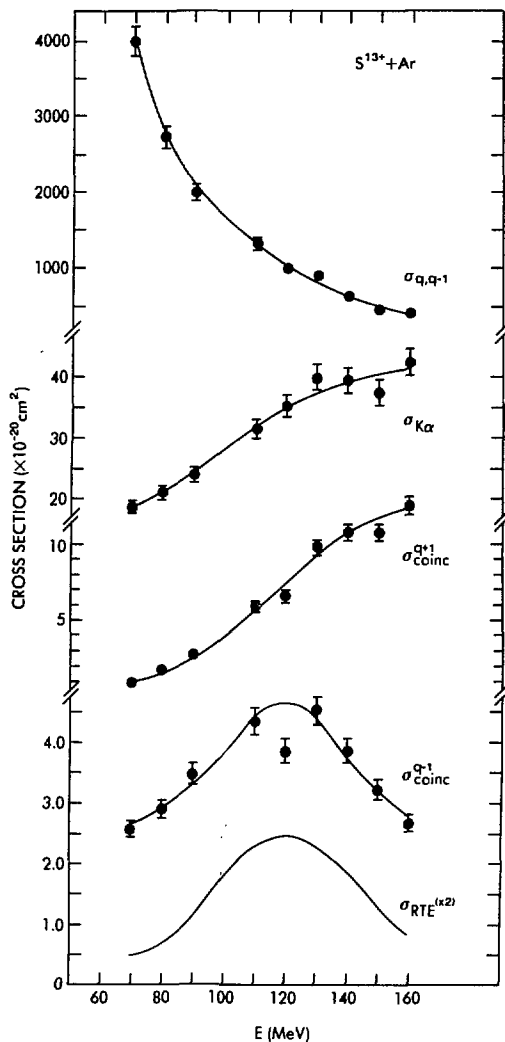


Figure 3. Projectile cross sections for 70- to 160-MeV  $S^{13+} + Ar$  collisions.  $\sigma_{\text{coinc}}^{q-1}$  is the cross section for projectile K x-ray emission associated with single-electron capture;  $\sigma_{\text{coinc}}^{q+1}$  is the cross section for projectile K x rays associated with single-electron loss; and  $\sigma_{K\alpha}$  is the cross section for single sulfur  $K_{\alpha}$  x-ray emission. The solid lines are resonance theory fits to the data. The curve labeled  $\sigma_{\text{RTE}}^{(K2)}$  is a theoretical calculation of the resonant part of  $\sigma_{\text{coinc}}^{q-1}$ .  $\sigma_{q,q-1}$  is the total electron capture cross section. In this latter case, the curve is drawn to guide the eye.

## PHYSICS DEPARTMENT

### Scientific and Professional Staff

**Arthur Schwarzschild, Chairman**  
**T. Laurence Trueman, Deputy Chairman**  
**Victor J. Emery, Associate Chairman**

### High Energy Physics Groups

#### Electronic Detector

**T.F. Kycia, Group Leader**

R.A. Johnson	L.S. Littenberg
K.K. Li	R.C. Strand

#### Electronic Detector

**L.B. Leipuner, Group Leader**

R.C. Larsen  
W.M. Morse

#### Spectrometer\*

**S.J. Lindenbaum, Group Leader**

**K.J. Foley, Deputy Group Leader**

W.H. Dieffenbach	A. Etkin	R.S. Longacre	T.W. Morris	V. Polychronakos
S.E. Eiseman	D.L. Jacobs	W.A. Love	E.D. Platner	A.C. Saulys

### Omega

**Howard A. Gordon, Group Leader**

S.H. Aronson	B.G. Gibbard	D.C. Rahm	M.J. Tannenbaum
N.J. Baker	T.W. Ludlam	P. Rehak	S. Terada
S.U. Chung	M. Montag	M. Sakitt	D.P. Weygand
P.L. Connolly	M.J. Murtagh	I. Stumer	M. Winik
T.E. Erickson	S. Protopopescu	M. Tanaka	C.L. Woody

### Theory

**Ling-Lie Chau, Group Leader**

E.D. Courant	I.J. Muzinich	C. Rebbi
M.J. Creutz	M.C. Ogilvie	G. Senjanovic
W.Y. Keung	M. Okawa	R.M. Sternheimer
W.J. Marciano	F.E. Paige	M.D. Tran

### Physics Personnel Assigned to CBA Magnet R&D

**R.B. Palmer, Head, Magnet Systems Division**

J.T. Koehler  
R.P. Shutt

### Nuclear Physics Groups

#### Tandem Van de Graaff Research

**E.K. Warburton, Group Leader**

D.E. Alburger	O. Hansen	M. Rafailovich
P.D. Bond	O.C. Kistner	A.M. Sandorfi
C. Chasman	M. LeVine	A.W. Sunyar
E. der Mateosian	J.W. Olness	H.E. Wegner

\*S. Ozaki on leave.

**Tandem Van de Graaff Operations****P. Thieberger, Group Leader**

R.C. Lee	E.A. McBreen	T.G. Robinson	C.E. Thorn
M.A. Manni	Michael McKeown	R.A. Scheetz	

**Neutron Nuclear Measurements****R.F. Casten, Group Leader**

R.L. Gill	D.D. Warner
-----------	-------------

**Medium Energy****R.E. Chrien, Group Leader**

S.M. Bart	E.A. Meier	P.H. Pile
V. Manzella	E. May	

**Theory****S. Kahana, Group Leader**

A.T. Aerts	A.J. Baltz	D.J. Millener	J. Weneser
E.H. Auerbach	C.B. Dover	M.E. Sainio	

**Solid State Physics Groups****Surface Studies****M. Strongin, Group Leader**

W.U. Eberhardt	F.E. Loeb	D.A. Wesner
P. Johnson	S.L. Weng	

**Neutron Scattering****G. Shirane, Group Leader**

J.D. Axe	A. Kevey	A.H. Nintzel	S.M. Shapiro
D.P. Belanger	F.T. Langdon	L. Passell	O. Steinsvoll
C. Cantera	C.F. Majkrzak	J. Plonski	J. Wicksted
B.H. Grier	K. Motoya	S.K. Satija	H. Yoshizawa

**Low Energy Particle Investigations of Solids****K.G. Lynn, Group Leader**

D.E. Cox	P.W. Levy	P. Schnitzenbaumer
J. J. Hurst	A.R. Moodenbaugh	P.J. Schultz

**X-ray Scattering****D.E. Moncton, Group Leader**

K.L. D'Amico	A.P. Meade	K.M. Mohanty	S.L. Ulc
M.C. Kaplan	A.H. Moudden	E.D. Sperry	

**Theory****V.J. Emery, Group Leader**

J.W. Davenport	W. Finger	R.E. Watson	A.M. Zangwill
G.J. Dienes	Marilyn H. McKeown	M.T.A. Weinert	

**Atomic and Applied Physics****Atomic Physics & Nuclear Microscopy Group****K.W. Jones, Group Leader**

A.L. Hanson	B.M. Johnson	M. Meron
-------------	--------------	----------

# National Synchrotron Light Source

On November 22, 1982, the National Synchrotron Light Source (NSLS) was officially dedicated, marking the transition of the NSLS from a construction project to an operating synchrotron radiation research facility for basic and applied studies in biology, chemistry, physics, material science, engineering, and medicine. At the dedication ceremony (Fig. 1), the Presidential Science Advisor, George A. Keyworth, II, stressed that the NSLS, which has received enthusiastic support from federal, academic, and industrial scientists, clearly meets the cri-

teria of excellence and relevance. At the close of the ceremony, BNL Director Nicholas Samios announced that, because of the diversity of its program, the Light Source Division would become a BNL Department.

The NSLS entered a preliminary operational phase in the summer of 1982 as the first synchrotron radiation was let out of several ports on the 750-MeV vacuum ultraviolet (VUV) storage ring. Since that time, experimental chambers and monochromators on ten UV beam lines have been commissioned and are produc-

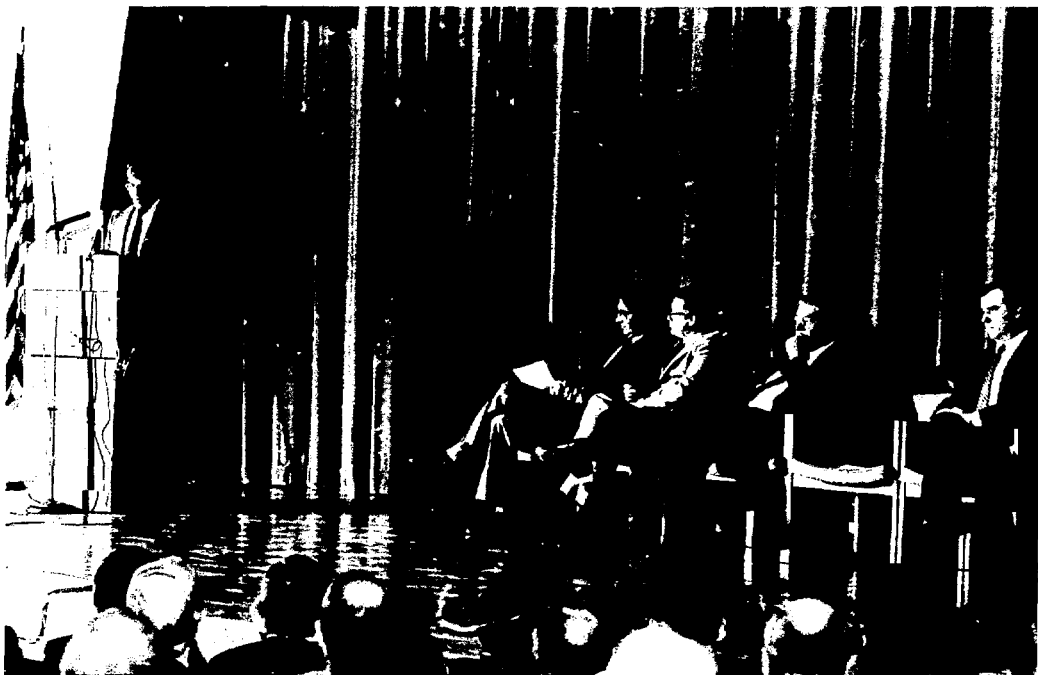


Figure 1. NSLS dedication ceremony, November 1982. Keynote speaker, Presidential Science Advisor George A. Keyworth, II. Seated (from left) Nicholas Samios, John McTague, Donald Stevens (DOE), and Representative William Carney.

ing the facility's first experimental results (Fig. 2). Eventually, when all the x-ray and UV beam lines are fully developed, it will be possible to run as many as 90 experiments simultaneously.

The first step towards the commissioning of x-ray beam lines was taken in December as x rays streamed out of Port X13 into an experimental hutch. During the autumn of 1983, x rays will be used by experimenters as they align their beam line optical components and begin to take preliminary data.

In this issue of the Brookhaven HIGHLIGHTS, the first experimental data obtained on NSLS beam lines operated by Brookhaven's Physics, Chemistry, and Biology departments will be reported separately in each department's section. It is important to note that most members of the NSLS Participating Research Teams (PRT's), as well as general users, will come from outside industrial, academic, and government laboratories. Results from two such user groups, the Bell Labs Photoemission PRT and the IBM Lithography PRT, are highlighted below.

## ACCELERATOR/STORAGE RING PROGRESS

Much progress has been made towards reaching full operational status, not only of the VUV ring but also of the x-ray ring. Both beam intensity and beam lifetime on the VUV ring improved gradually to a level where peak currents of 215 mA have been achieved, with a high intensity beam life time of approximately one hour and a low intensity beam lifetime of about two hours. This permitted an operational mode wherein beam injection took place periodically every four hours.

Work on beam parameters in the VUV ring has been concentrated not only on improving beam intensity and lifetime, but also on improving "brightness" at higher circulating beam currents. At low beam current, the measured beam quality is in agreement with the beam emittances calculated for a "zero current" basic VUV lattice. For higher beam currents, the measured beam sizes indicate significant trans-



Figure 2. VUV storage ring and experimental beam lines.

verse phase-space growth. This is currently thought to be directly associated with the presence of longitudinal (via the lattice dispersive component) beam instabilities, and the incoherent beam tune spread, associated with partial bunch neutralization as a result of synchrotron radiation desorbed ion trapping. Damping antennae were incorporated in the VUV rf cavity during the January 1983 VUV shutdown period. Improvements with regard to the longitudinal coupled bunch instabilities have been significant. The lowest longitudinal mode instability threshold has been increased by a factor of about 4. Presently, at a beam current level of nominally 80 mA, the beam bunches exhibit at most small-amplitude "dipole" oscillations with a maximum longitudinal jitter  $\pm 0.2$  nsec (for a bunch spacing of about 19 nsec), whereas the corresponding behavior prior to the implementation of the rf cavity improvements showed longitudinal beam bunch jitter of  $\pm 0.8$  nsec. Also, there has been no evidence of sudden beam blowup as was frequently observed before the cavity improvements.

Other measures to improve the beam brightness in the VUV ring will be taken in the future. These include the installation of a longitudinal feedback system, a harmonic rf cavity, and the use of either a three- or a one-bunch mode of operation (as opposed to a nine-bunch mode) to reduce beam instabilities and ion trapping in the electron beam well.

To enhance the photon spectrum near the 20-Å region, specifically for the microscopy and the lithography lines, the VUV ring energy was increased to 750 MeV, well above its design value. Eventually, it is planned to operate the VUV ring at 800 MeV.

The undulator for the free-electron laser experiment was also installed during the January shutdown. As expected, no perturbing effect has been measured on the beam during normal operations. Measurement of the undulator radiation in the visible part of the spectrum has been carried out and radiation gain measurements, as a result of electron beam-external laser interaction in the presence of the undulator field, will be made during 1983.

In September a major step forward was taken in the commissioning of the x-ray ring. At that time, long-surviving beam was attained, paired

with rf capture and multiple charging of the x-ray ring. Although limited circulating beam had been obtained on a number of previous occasions, the competing pressures for full operational status of the VUV ring prevented a complete follow through earlier. Subsequent periodic x-ray ring studies led to improvements of the beam closed orbit and to modest increases in beam intensity such that, by early November, beam acceleration studies could be carried out. Acceleration to 2-GeV electron beam energy was achieved by mid-November, with a beam current of 1 to 2 mA, and an observed 2-GeV beam lifetime of 20 minutes. This was followed by the observation of the first photons in an external beam hutch (X13) just before Christmas.

Work continued on the development and construction of special radiation sources. As indicated above, the undulator for the free-electron laser experiment was installed in the VUV ring. In addition to serving the specific objectives of the FEL experiment, this undulator will also provide a highly collimated photon beam (at 750-MeV electron energy) in the 10- to 100-eV photon energy region. The 60-kG superconducting wiggler for the x-ray ring was completed and will be installed in the x-ray ring in 1983.

As part of the overall scheme for facility expansion (NSLS Construction Phase II), full utilization of essentially all x-ray and VUV long straight sections for special radiation sources is planned. Design work has begun on two such sources, a permanent magnet hybrid wiggler and a high energy undulator. The final parameters of these and other special sources will depend on their relevance to the scientific needs of the NSLS user community.

## VUV BEAM LINES — FIRST EXPERIMENTAL RESULTS

During 1982, operations began on a total of ten beam lines on the UV ring. The first experimental results obtained on the Bell Labs photoemission line (U4), the IBM lithography line (U6), the NSLS facility photoemission line (U14), and the facility x-ray microscopy/holography line (U15) are given below. Experiments performed on the U9A time-resolved fluorescence line (BNL Chemistry), the U9B circular dichro-

ism line (BNL Biology), and the U11 gas phase spectroscopy line (BNL Chemistry) are reported in the Biology and Chemistry sections.

#### U4A — Bell Labs

##### Photoemission Beam Line

This beam line utilizes a plane grating monochromator (PGM) to provide photons in the 20- to 1600-Å region for high-resolution photoemission studies. In the summer of 1982, the first UV photons were used to align the PGM and experimental chambers. Photoelectron energy spectra have been taken in the vicinity of the carbon K-edge ( $\hbar\omega \approx 285$  eV) for CO molecules adsorbed on the (111) surface of metallic palladium (Fig. 3). Study of the spectra in this near-edge region permits a determination of the orientation of the CO molecules and the detailed nature of the chemisorptive bond. These data have been used to argue that features in the spectra on passing through the carbon K-edge can be understood in terms of Auger transitions. In the past, these features had been attributed to a "giant enhancement" effect at the photon energy corresponding to transitions from the C 1s core level into the bound  $2\pi^*$  state of the CO molecule.

#### U6 — IBM X-ray

##### Lithography Beam Line

Beam line U6 has been designed to uniformly illuminate an area of at least  $2.5 \times 2.5$  cm with soft x rays in order to replicate submicron features from a mask into resist on a silicon wafer. The goal of the project is to develop a technology that may have commercial application in the manufacture of integrated circuits. X rays from conventional sources have already been shown to give good results, but long exposure times are necessary because of the weak nature of these sources. The much greater intensity of a storage ring source should allow much greater throughput with simple resist processing, which may lead to a greatly expanded use of synchrotron radiation in this country with electron storage rings becoming an integral part of semiconductor factories.

The exposures take place in helium. A thin beryllium window is used to separate the exposure chamber from the ultrahigh vacuum upstream. The window and the helium column, coupled with the spectrum of synchrotron radiation and the properties of the mask, limit the

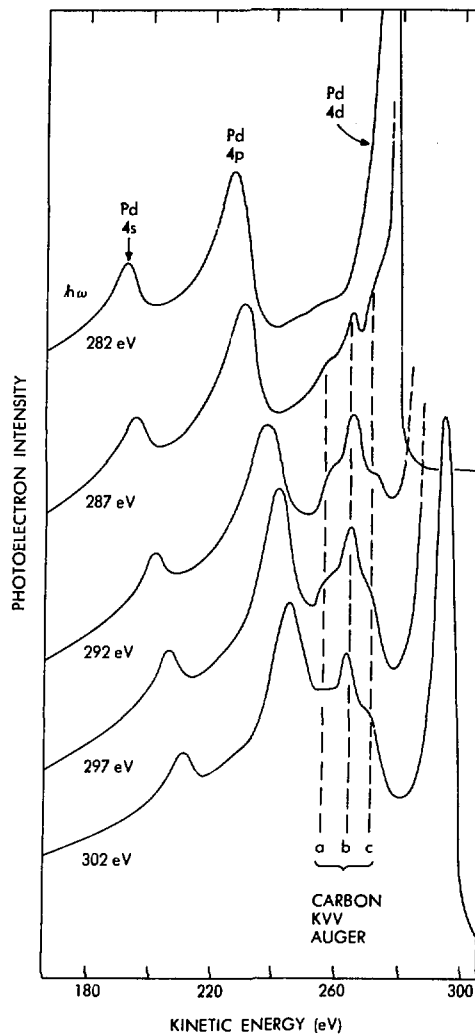


Figure 3. Photoelectron energy spectra taken in the vicinity of the carbon K-edge ( $\hbar\omega \approx 285$  eV) for CO molecules adsorbed on the (111) surface of metallic palladium. These data were taken on the Bell Labs Photoemission Beam Line U4 on the VUV storage ring.

lithographically useful spectrum to between 8 and 12 Å. The first exposures have been very promising. Exposures have been made in a variety of resists, and features as small as  $0.25 \mu\text{m}$  have been replicated with high aspect ratios (Fig. 4).



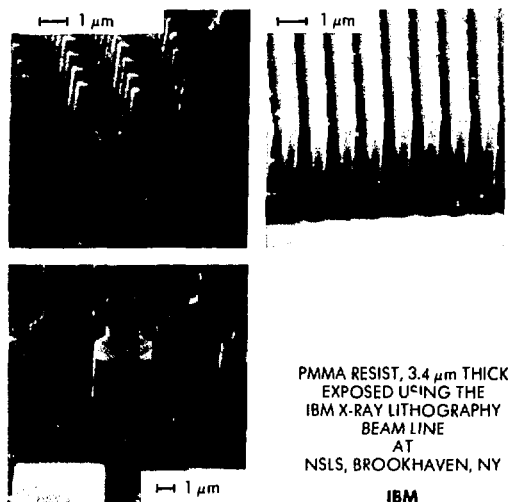


Figure 4. High aspect ratio replication of submicron features from an IBM mask into PMMA photoresist using synchrotron radiation. The exposures were performed on the IBM Lithography Beam Line U6 on the VUV storage ring.

#### U14 — NSLS Photoemission Beam Line

The surface science chamber on this line has been fully commissioned with both the angle integrating cylindrical mirror analyzer and the angle (momentum) resolving hemispherical analyzer working. The liquid nitrogen-cooled sample manipulator, which also incorporates heating to 600°C, was used in conjunction with low energy electron diffraction, Auger analysis, and argon ion sputtering to study a variety of systems on Pd(111). It was possible to observe the

surface magnetic moment of an overlayer of Fe on Pd(111) by studying the exchange split Fe 3s level. Other resonances on the Fe core levels are now being studied. This work has been done in collaboration with groups from Leicester, England, Stevens Institute, and the University of Pennsylvania.

#### U15 — NSLS Toroidal Grating Monochromator/X-ray Microscope and Holography Beam Line

On port U15 of the VUV storage ring, a research team from the State University of New York at Stony Brook, in collaboration with the NSLS, is constructing a soft x-ray scanning microscope that may provide the first pictures of the internal structure of *living* cells in aqueous solutions while imparting a minimal radiation dose. Previously, electron microscopes have been employed to study cells. However, both the vacuum environment and the high radiation dose from the electrons prohibit the study of living cells, and destroy the cell's internal structure. With spatial resolutions expected on the submicron level and with the ability to locate the position of specific elements within the cell, this instrument could open up entirely new areas of biological research.

The NSLS-designed toroidal grating monochromator on this beam line has been aligned and tested and a zone plate produced at IBM has been installed to focus the synchrotron radiation to provide spatial resolution on the submicron level.

This beam line will also be used in the future for experiments on x-ray holography, soft x-ray diffraction, contact microscopy, and absorption spectroscopy experiments.

## NATIONAL SYNCHROTRON LIGHT SOURCE

**J. McTague, Chairman**

**A. van Steenberg, Deputy Chairman**

<b>User Liaison</b>	<b>Administration</b>	<b>Safety</b>	<b>Phase II Construction</b>	<b>Department Office</b>
R. Klaffky	W. Foyt, Head G. Grigg	K. Batchelor C. Flood, Liaison	J. Godel, Project Head	S. White-DePace

### Accelerator/Storage Ring Section

K. Batchelor, Head

#### Electrical Engineering

J. Sheehan, Group Leader  
R. Olsen  
O. Singh  
M. Thomas

#### Computer Systems

B. Culwick, Group Leader  
J. Smith  
H. Langenbach  
S. Ramamoorthy

#### Machine Operations

N. Fewell, Group Leader

#### Controls and Diagnostic Group

D. Klein, Supervisor

#### Beam Diagnostics

J. Bittner

### Engineering Section

H. Hsieh, Head

#### Mechanical Engineering

H. Hsieh, Group Leader  
R. Hawrylak  
P. Mortazavi  
M. Schleifer

#### Design Drafting

W. Jordan, Supervisor  
C. Neuls

#### Vacuum and Engineering Support

J. Schuchman, Group Leader  
T. Lehecka, Supervisor

### Research Section

C. Pellegrini, Head  
W. Thomlinson, Deputy Head

R. Blumberg  
E. Bozoki

Z. Galayda  
J. Hastings

M. Howells  
R. Klaffky

S. Krinsky  
A. Luccio

D. Moncton  
G. Williams

**Beam Line Operations Section**

W. Thomlinson, Head  
R. Klaffky, G. Williams

**Beam Line  
Support**

M. Iarocci  
N. Lucas  
G. Watson

**Experimental Area  
Operations**

G. Hummer  
G. Schwender

**Safety  
Operations**

T. Dickinson

**Experimental Technical  
Support**

V. Rancaniello, Supervisor

**Beam Line R&D Section**

D. Moncton, Head  
J. Hastings, M. Howells

**Instrument Development**

T. Oversluizen, Group Leader  
M. Kelly Supervisor

## Chemistry Department

The discipline of chemistry addresses the properties of matter on an atomic or molecular level and is thus a very broad one. Research activities in the Chemistry Department, reflecting this breadth, encompass a wide spectrum of topics — from theoretical studies of intramolecular motion to the preparation of radio-labeled metabolites used for *in vivo* studies of the human brain. Many of the studies draw on the Laboratory's great instrumental resources. Neutron diffraction studies of the nuclear and electronic structures of solids exploit the High Flux Beam Reactor. The structure of the nucleus is probed via heavy-ion beams prepared in the Tandem van de Graaff. Lasers are used in a wide number of applications — from microsecond studies of the disposition of vibrational energy in small gaseous molecules to picosecond studies of electron transfer processes in large molecules which are photosynthesis models. The National Synchrotron Light Source (NSLS), which made its debut in 1982 as a research tool, greatly extended the energy range of radiation which can be used to probe molecular behavior. Chemistry Department members have been engaged in creating beam lines for use in x-ray structural studies (using both diffraction and absorption techniques) and for ultraviolet/vacuum ultraviolet photophysical experiments, and the first scientific results are beginning to emerge from Chemistry Department — NSLS experiments. These efforts, as do a number of the other activities to be described, involve extensive collaboration with other BNL departments, and with scientists from university and industrial laboratories, as well as among colleagues within the Chemistry Department itself. The intellectual resources available to Department members thus match the technological

strengths of the Laboratory and create a unique research environment.

### EXPERIMENTS AT THE NSLS

The VUV ring at the National Synchrotron Light Source began emitting light in early spring 1982. During the several weeks following that event, Chemistry Department staff members were engaged in the optical alignment and final installation of three Chemistry beam lines on this ring. Since then, it has been possible to devote attention to experiments, and some of the results obtained are described below. Although these initial experiments were performed by BNL staff members for the most part, several off-site collaborators have already carried out experiments, and a large number are expected to become active users as synchrotron operation becomes more routine. The larger x-ray ring is being commissioned at the time this is being written (March 1983), and major components of the Chemistry beam line dedicated to crystallography are already installed. Completion and alignment will proceed when the necessary x-ray intensity is achieved. Here, also, a large number of outside users are already interested in doing x-ray diffraction experiments on this beam line.

### Photoionization of Gaseous Molecular Clusters

With the completion of the Chemistry-NSLS U-11 beam line at the VUV storage ring, new studies of gas-phase intermolecular interactions and photoionization dynamics have begun. Molecular clusters formed by high-pressure jet expansions are ionized by the intense tunable VUV radiation (30 to 300 nm) available from this beam line, and the resulting ion products

are mass analyzed. From comparisons of the ionization thresholds and fragmentation onsets of the clusters and constituent atoms or molecules, it is possible to determine the strength of the intermolecular bonding and the energetics of highly specific ion-molecule reactions. As the mechanisms of many common chemical reactions proceed via transition states that involve molecular complexes, such studies of intermolecular bonding are of fundamental importance. Initial experiments studied the simplest molecular clusters, i.e., the dimers and higher clusters of the rare gases, and results obtained with argon are shown in Fig. 1. New highly excited Rydberg states involving the excitation of an inner-valence electron were identified for the first time and extrapolations of their series led to estimates of the long-range forces for the corresponding electronically excited dimer and trimer ions.

#### Photoionization in Solution

Synchrotron radiation from the NSLS is being used to investigate the mechanism of photoionization of molecules in solution. Many organic solutes photoionize in the 150- to 200-nm region of the spectrum, and synchrotron radiation is an ideal light source at these wavelengths because of its continuous spectrum. For anthracene as solute, the photoconductivity threshold is at 6.14 eV in liquid 2,2,4-trimethylpentane, considerably below the gas-phase ionization potential of 7.47 eV. Measurements in various nonpolar solvents show that the threshold is sensitive to the conduction band level ( $V_0$ ) of the solvent; the conductivity threshold for anthracene decreases as  $V_0$  decreases. In general, for ionization in solution the threshold ( $E_{th}$ ) is given by  $E_{th} = I.P. + V_0 + P^+$ , where I.P. is the gas-phase ionization potential and  $P^+$  is the polarization energy of the positive ion in the solvent and is of the order of  $-1.0$  eV. The anthracene results verify the above equation. Similar results are observed for 1,2-benzanthracene, azulene, perylene, triphenylamine, and diazabicyclooctane in solution.

At threshold, the photocurrent is very small but increases as the photon energy increases, and for aromatic hydrocarbons like anthracene several relative maxima or peaks are observed in the photoconductivity spectra. As shown in Fig. 2, maxima for anthracene in 2,2,4-trimethyl-

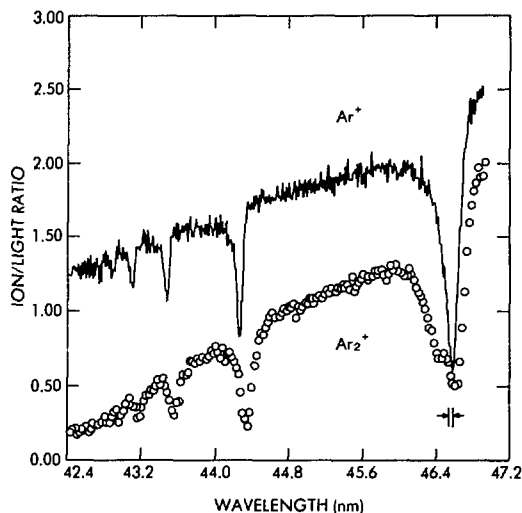


Figure 1. Comparison of the photoionization cross-section versus wavelength curves for atomic Ar and the van der Waals dimer  $Ar_2$  in the region of the  $3s - np$  ( $n = 4, 5, 6, \dots$ ) Rydberg-state excitation.

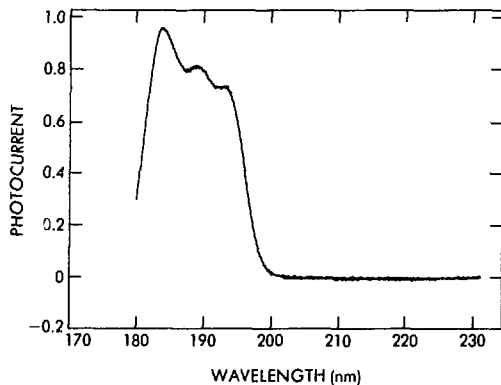


Figure 2. Photoconductivity as a function of wavelength for anthracene in 2,2,4-trimethylpentane solvent. The maxima at 183–193 nm indicate the involvement of Rydberg states in the photoionization process.

pentane are observed at 193, 189, and 183 nm. Such maxima are observed only in solvents which exhibit high excess electron mobility and occur at approximately the same wavelengths where electronically excited Rydberg states are observed in the gas phase: in the case of gaseous anthracene, Rydberg states are observed at 193,

190, and 185 nm. Vibrational spacings between some of the maxima are the same (0.17 eV) as the vibrational spacing of Rydberg states in the vapor. Thus our results provide the first evidence from conductivity studies that the mechanism of solution photoionization involves Rydberg states. Such states are "partially ionized" because the electron that is excited is in a large orbit away from the core of the molecule. These states rapidly collapse to an ion pair. Studies of other aromatic solutes indicate that the involvement of Rydberg states is a general phenomenon and that the mechanism of ionization is similar in other molecules.

### THEORETICAL CHEMISTRY

In recent years the availability of infrared lasers has made possible experimental studies of vibrational-state-specific chemistry. Thus, in a number of molecules, it has been possible to inject energy into a particular vibration in a moderately complex molecule. While the details of the nuclear motion in the resulting vibrationally excited polyatomic molecules are best described by quantum mechanics, considerable insight into the nature of the molecular vibrational states is provided by classical and semiclassical techniques. Our approach entails intensive use of computers for the numerical solution of the ordinary differential equations defining the classical trajectories and of computer graphics for the representation and analysis of the computed results.

In treating the localization of vibrational energy in a molecule having symmetrically equivalent X—H bonds (X is any heavy atom), the properties of "normal" and "local" quasiperiodic classical trajectories are compared. Normal trajectories are those for which the time-averaged amplitudes in all the X—H stretching vibrations are equivalent, while local trajectories exhibit a permanent imbalance in the amplitudes of the various X—H stretching vibrations. If a local mode state can be prepared by laser excitation, the energy deposited in the molecule will reside primarily in the single X—H bond. A semiclassical normal eigentrajectory corresponds to a quantum-mechanical eigenstate of the molecule. However, a local mode state corresponds to a nonstationary quantum state resulting from the superposition of nearly degenerate

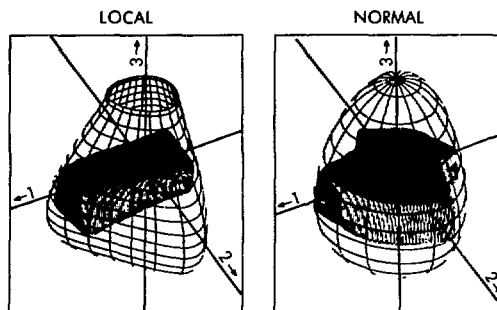


Figure 3. The coordinate space envelopes of local and normal mode classical trajectories for the nonrotating  $\text{H}_2\text{O}$  molecule. The origin of the coordinate system corresponds to the equilibrium geometry of the molecule. The coordinates 1, 2, and 3 refer to displacements of one O—H bond, the other O—H bond, and the H—O—H bond angle, respectively. A grid of lines rotated  $\pm 45^\circ$  from the direction of view has been placed on the envelope of the trajectory to define its three-dimensional character. The outer grid lies on the three-dimensional potential energy contour corresponding to the total energy.

erate stationary states and can be quite long lived if the quantum states are very nearly degenerate.

The localization of energy in a local mode state is illustrated in Fig. 3 which contrasts three-dimensional representations of the coordinate space envelopes of local and normal mode trajectories in a realistic model of the nonrotating water ( $\text{H}_2\text{O}$ ) molecule. It is clear that in the local mode trajectory one O—H bond is more highly excited than either the other O—H bond or the H—O—H bending vibration. Hence, the excited O—H bond should be much more reactive than the other, and more reactive than either O—H bond in a normal mode with a similar energy. By contrast, in the normal mode trajectory the two O—H bonds have equivalent amplitudes; the excitation energy is not localized in a specific bond.

### GASEOUS ION CHEMISTRY

One aspect of our studies of gaseous ion chemistry involves ion-molecule reactions in very low temperature ion sources and in the free-jet expansion of gases from these low temperature ion sources. Upon expansion of weakly ionized

plasmas of helium with small concentrations of either argon or nitrogen, singly charged cluster ions are produced with molecular weights ranging up to several tens of thousands. These high molecular weight cluster ions are produced from gases cooled to liquid nitrogen temperature (78 K) prior to free-jet expansion. An unusual feature of the mass spectra of the argon or nitrogen cluster ions produced under these experimental conditions is illustrated by the data shown for argon in Fig. 4. The mass distribution obtained is not smooth, but instead features high relative abundances of ions with 142, 302, and 553 argon atoms. These fall close to the Mackay "magic numbers" 147, 309, and 561 which are predicted for the packing of spheres (Ar atoms) in closed-shell icosahedra. By contrast, in polyatomic systems (water, isopropanol, or isooctane) at room temperature no evidence for magic number structures is found; in these, cluster growth appears to occur through addition of one neutral molecule at a time. An understanding of processes in very low temperature plasma ion sources is necessary for the

development of hydrogen cluster ion sources which may be of value in basic studies related to controlled thermonuclear reactions.

## MECHANISMS OF REACTIONS IN SOLUTION

### Olefin Epoxidation

More than half the chemicals needed in industry are produced by the oxidation of hydrocarbons. Such reactions are plagued by inefficiencies due to low selectivities, which are generally the results of radical-chain reactions or complete combustion. Our research is conducted with the goal of understanding the role that transition metal complexes can play in the homogeneous catalysis of hydrocarbon oxidations. A new approach to alkene epoxidation has been demonstrated; it is based on symmetrical oxygen cleavage by metal-nitrosyl complexes to give metal-nitro complexes which subsequently undergo O-atom transfer reactions to alkenes (Scheme I). A detailed mechanistic understanding of this reaction has been ob-

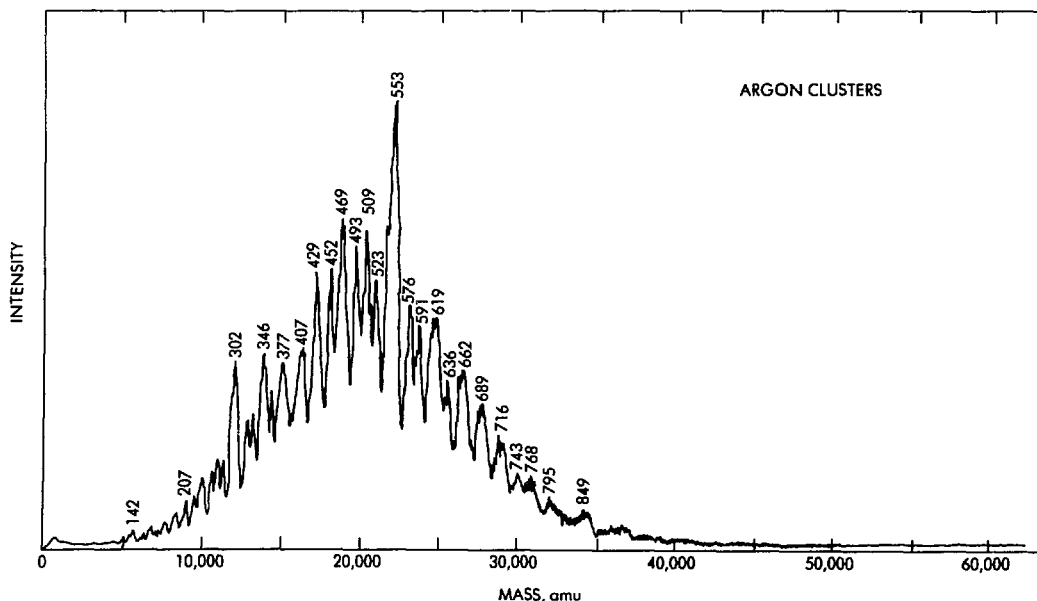
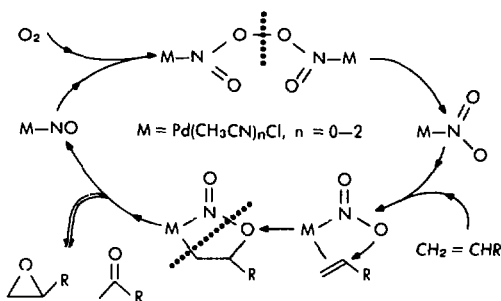


Figure 4. Mass spectrum of argon cluster ions obtained from approximately 2% argon-helium mixture expanded from an initial pressure of one atmosphere and initial temperature of 77 K. The numbers above the peaks indicate the approximate numbers of atoms per cluster ion. Peaks containing 142, 302, and 553 argon atoms fall very close to Mackay "magic numbers" for closed-shell spheres 147, 309, and 561.

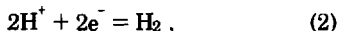
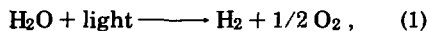
tained through the observation of reaction intermediates and analysis of the varying product distributions as a function of alkene. A particularly significant accomplishment this year was the x-ray crystallographic characterization of a typical heterometalalocyclopentane intermediate (the species in the lower left center of Scheme I) conducted in collaboration with the Structural group in Chemistry. Species of this type have been widely proposed in a variety of metal-catalyzed oxidations but have rarely been characterized. The knowledge gained from these studies provides a guide to the design of more efficient and selective catalysts.



Scheme I.

### Water Oxidation

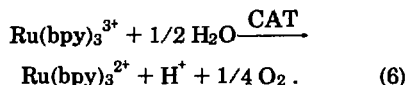
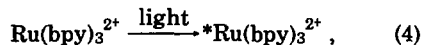
For several years, the use of metal complexes to mediate storage of light energy [Eq. (1), photoinduced decomposition of water] has been a subject of vigorous research in this Department. Our approach has centered on using excited states of metal complexes to generate extremely reactive reductants and oxidants to bring about water reduction [Eq. (2)] and oxidation [Eq. (3)], respectively.



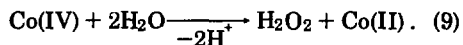
Last year a detailed sequence of photoinduced reactions culminating in  $\text{H}_2$  formation was reported here. Recently, substantial progress with the complementary process,  $\text{O}_2$  formation, has been achieved and is now described.

The strongly oxidizing complex  $\text{Ru}(\text{bpy})_3^{3+}$  (bpy = 2,2'-bipyridine) may be generated

through visible-light irradiation of  $\text{Ru}(\text{bpy})_3^{2+}$  in the presence of an electron acceptor (A). In the presence of a catalyst (CAT),  $\text{Ru}(\text{bpy})_3^{3+}$  oxidizes water so that the photooxidation of water is brought about:



A wide variety of suspended metal oxides catalyze reaction (6), but few homogeneous catalysts are known. We have studied the mechanism of the reaction in the presence of the homogeneous catalyst aquocobalt(II). At pH 7, 25°C, the rate of product formation is proportional to  $[\text{Ru(III)}]^2[\text{Co(II)}]/[\text{Ru(II)}]$ , where Ru(III) and Ru(II) denote the  $\text{Ru}(\text{bpy})_3^{3+}$  complexes. This rate law indicates that Co(II) is oxidized to Co(IV) in a sequence of one-electron transfers [Eqs. (7) and (8)].



The Co(IV) complex then reacts with water [Eq. (9)], undergoing a two-electron change to produce  $\text{H}_2\text{O}_2$  (which is subsequently oxidized to  $\text{O}_2$ ) and regenerate the Co(II) catalyst. In this fashion two oxidizing equivalents from the one-electron oxidant  $\text{Ru}(\text{bpy})_3^{3+}$  are assembled on a single site [Co(IV)], and water oxidation is facilitated because formation of the high energy one-electron oxidation product OH radical is circumvented. Experiments directed to learning how Co(IV) assembles the O—O bond are now under way.

### NUCLEAR REACTIONS

When a high energy projectile such as a 2100-MeV/nucleon  $^{12}\text{C}$  ion interacts with a target, the duration of the collision is so short that there can be little flow of energy into those regions of the target nucleus not directly involved in the initial collision. While the interaction region may be abraded during such an encounter, a major portion of the nucleus may remain rela-



tively undisturbed. Experimental studies of heavy-ion interactions with copper indicate that about 70% of all interactions give a product which can be identified as the remnant of the undisturbed "spectator" region. Momentum transferred in such target fragmentation reactions is low and can be related by a simple peripheral interaction model to the corresponding excitation energy transferred in the initial step of the reaction.

Such a simple participant-spectator picture is expected to break down as the projectile velocity decreases and the interaction time becomes sufficiently long to permit extensive mass and energy flow out from the contact region. To examine how and where such changes evolve, BNL studies of the interactions of high energy  $^{12}\text{C}$  ions have been extended down to 84 and 22 MeV/nucleon (using the CERN synchrocyclotron and the LBL 88-in. cyclotron, respectively). The new results are presented in Fig. 5. The observed mean forward range, FW, of a product is plotted as a function of mass loss,  $\Delta A$ , from the target. Included for comparison are existing data for 400- and 2100-MeV/nucleon  $^{12}\text{C}$  ions which show the typical monotonic dependence of FW on  $\Delta A$  predicted by the simple model mentioned above.

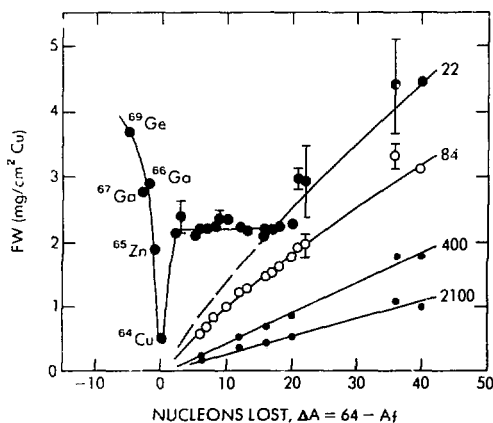


Figure 5. Dependence of mean ranges measured in the forward direction (FW) on the number of nucleons ( $\Delta A$ ) which were removed from the target to form the observed product. New data for the interaction of 22- and 84-MeV/nucleon  $^{12}\text{C}$  ions with copper are compared with earlier results at 400 and 2100 MeV/nucleon as indicated.

The pattern of data at 84 MeV/nucleon is not qualitatively different from that observed at higher energies, although quantitative analysis suggests the ranges are somewhat greater than the model predictions. However, there are obvious changes as the energy is decreased further to 22 MeV/nucleon. Particularly striking is the left-hand branch of the curve extending from  $^{64}\text{Cu}$  to  $^{69}\text{Ge}$ . Such mass transfer from the projectile to the target is not observed at the higher energies. Another distinctive feature is the region of constant FW values extending over a range of  $\approx 20$  mass numbers below the target. When the observed data are transformed to give momentum transfers, it is found that essentially full momentum transfer is associated with  $^{69}\text{Ge}$  and the light products with  $\Delta A \approx 40$ . The flat region corresponds to the transfer of approximately two thirds of the projectile's momentum. The low value for  $^{64}\text{Cu}$  is probably due to the fact that it can be formed by a single-neutron transfer reaction which is known to proceed with small momentum transfer. Although these experiments measure only mean quantities, the new results at 22 MeV/nucleon clearly show many of the features of low energy reactions: mass and momentum transfers indicative of strongly damped processes of the type involved in deep inelastic collisions and compound nucleus formation.

## RADIOTRACERS, CYCLOTRON, AND PETT RESEARCH

Production of short-lived cyclotron-produced positron-emitting radionuclides ( $^{11}\text{C}$ ,  $^{13}\text{N}$ ,  $^{15}\text{O}$ , and  $^{18}\text{F}$ ) which can be incorporated into molecules of biological, biochemical, and medical interest has been facilitated by the recent acquisition of a small medical cyclotron. The small cyclotron, a two-particle machine capable of accelerating 10-MeV deuterons and 17-MeV protons, will serve as the source of large quantities of positron-emitting radionuclides. In addition, the PETT VI scanner, a state-of-the-art brain-imaging device, became operational in midyear 1982 (PETT: Positron Emission Transaxial Tomograph). Modeled after a design originating at Washington University, St. Louis, PETT VI has four rings of cesium fluoride detectors allowing the simultaneous imaging of seven "slices" of the human brain in a short scan time

# Medical Department

## INTRODUCTION

The Medical Research Center contains three major divisions: the Hospital, the Research Laboratories, and the Occupational Medicine Clinic which serves Brookhaven National Laboratory. Basic science in biology, chemistry, and physics is directed toward application of research findings to clinical medicine. The Hospital of the Medical Research Center, which is devoted entirely to research patients, supports clinical studies in areas which include pulmonary diseases; neuropsychiatric disorders; hematological diseases (e.g., chronic lymphocytic leukemia); cardiopulmonary disorders; hepatobiliary dysfunction; cancer of various types, including malignant ocular melanoma; toxicological problems of many kinds; bone and mineral metabolism; and dietary and nutritional disorders. Research efforts are also made to improve therapeutic measures for disease: brain tumor therapy through boron capture of epithermal neutrons, and proton beam irradiation; extracorporeal irradiation of blood in leukemia; iron chelator efficacy in thalassemia; and nonsurgical treatment of ocular melanoma. Early diagnoses and studies of the mechanism of disease are approached through medical applications of nuclear technology, including such nuclear medicine techniques as positron emission tomography.

The Department's success in achieving these various scientific goals is due to (1) the excellent cadre of skilled scientists in the Department and the Laboratory; (2) the freedom and ease with which one may work with scientists in other departments; (3) the high quality of laboratory service divisions responsible for prototype

fabrication, design, and instrument maintenance; and (4) the unique facilities and instrumentation available in the Medical Department and the Laboratory.

The Research Hospital of the Medical Research Center, although reduced in operation from 44 beds (in the mid-60s) to 11 beds today, is still equipped and staffed to carry out the projects outlined above. This facility, though not unique in itself, is unusual, by virtue of its association with a research laboratory and major facilities and devices, such as particle accelerators, reactors, and other complex diagnostic tools.

The Medical Department as part of Brookhaven National Laboratory is a national resource for research and training and may be called upon by the Department of Energy (DOE) to solve specific problems affecting national health and welfare. Maintenance of the excellence of this institution is thus essential to its capability to respond to such requests, as it has responded to recent mission changes as the Department of Energy evolved from ERDA and the AEC. Core scientific capability has been maintained, although at a lower level because of DOE budget limitations.

Relatively new efforts in the Department center on toxicology, pulmonary physiology, and pathology related to pollutants derived from energy production; cytogenetic and genetic studies at the request of DOE and EPA; and clinical and animal studies of health effects related to fossil fuel technologies at the request of DOE, EPA, and NIH.

The following report gives some idea of the work being done. Additional information may be obtained from publications of the Department.

## RETINYL ACETATE INHIBITION OF RAT BREAST CANCER

The purpose of this study is to determine to what degree retinyl acetate (vitamin A acetate) can arrest, delay, or reverse the development of mammary cancer in an established model system, the female Sprague-Dawley rat. More specifically, our three main goals are to determine if: (1) retinyl acetate can inhibit x-ray-induced or chemically induced mammary cancer, (2) the retinyl acetate inhibition of mammary cancer, induced by x rays or a chemical carcinogen, will continue for the entire life of the animal, and (3) retinyl acetate can inhibit spontaneously occurring mammary cancers.

In the current study, 55-day-old female Sprague-Dawley rats were given either whole-body external irradiation (200 R of 250-kVp x rays) or a chemical carcinogen, dimethylbenz-(a)anthracene (3.3 mg/100 g body weight) in a sesame oil solution placed in the stomach. Seven days later, half the rats receiving one of the carcinogens and half the appropriate control rats began receiving standard rat chow supplemented with retinyl acetate at 0.45 mmoles (=435,000 I.U.) per kg diet. Blood samples and breast biopsies are taken periodically for studies on the mechanisms by which the retinoids inhibit mammary cancers.

At this time, 650 days after the carcinogen treatments, retinyl acetate added to the diet of x-irradiated rats has produced a 52% reduction in the number of rats with a mammary cancer and a 73% reduction in the total number of mammary adenocarcinomas produced compared to irradiated rats fed the standard diet. Similarly, retinyl acetate added to the diet of the chemical-carcinogen-treated rats produced a 26% reduction in the number of rats with a mammary cancer and a 38% reduction in the total number of mammary adenocarcinomas produced compared to chemical-carcinogen-treated rats fed the standard diet. Thus far, too few spontaneous mammary adenocarcinomas have appeared in the noncarcinogen-treated rats to evaluate the effect of retinyl acetate on these tumors. The animals fed the supplemental diet had a mean body weight 15% lower than rats fed the standard diet. This may indicate some retinyl acetate toxicity, but it does not appear to be significant at this time.

Before retinoids (vitamin A derivatives) could possibly be used for the practical chemoprevention of human breast cancer, more information is needed about their inhibitory action on animal breast cancer and about their toxicity. Data from this experiment should provide information about the mechanisms by which retinyl acetate inhibits mammary cancer, the long-term toxicity of retinyl acetate, and the ability of retinyl acetate to inhibit breast cancer for the entire life-span of the rat.

## PULMONARY PROGRAM

The goal of the pulmonary program is to develop integrated research through which health effects of energy-related air pollutants can be assessed in small animals, large animals, and man. Such a program requires a multidisciplinary approach, using expertise of engineers, physicians, toxicologists, biochemists, pharmacologists, and pathologists. We are interested in knowing if and how air pollutants cause disease and how to diagnose and treat the disease before the changes become irreversible. This program is unique because, within the same department, human clinical research is augmented by pulmonary studies using both large and small animals.

Since the ultimate goal is to assess health effects in man, it was desirable to develop the technology to assess in animals the same kinds of end points we can measure in man. Thus, we have developed a highly sophisticated system to measure pulmonary function in rats, and are currently developing such a system for use with sheep. In association with the Nuclear Medicine Division, we are using radioisotopes to assess pulmonary ventilation/perfusion mismatches as well. Hematologic variables and urinary and serum chemical constituents are other end points which can be assessed in large and small animals and in man.

The research described below has several specific objectives: (1) to improve the technology of inhalation exposures; (2) to develop techniques for assessing subtle morphologic and physiologic changes in the respiratory tract of man (noninvasive techniques) and laboratory animals; (3) to determine whether or not there is a relationship between hypertension and air pollution; (4) to identify factors such as stress,

exercise, existing disease, etc. which may modify toxicity; (5) to understand organismal and cellular mechanisms which control respiratory function and pulmonary host defenses, and whether exposure to energy-related air pollutants might alter those mechanisms; (6) to understand why humans already compromised with such diseases as chronic lymphocytic leukemia or chronic obstructive lung disease are at a greater risk when exposed to air pollutants than healthy individuals; (7) and finally, using all the techniques at our disposal, to assess changes occurring in occupationally exposed groups and to attempt to correlate these changes with exposure.

### Small Animal Studies

The inhalation toxicology facility, which has been in operation since January 1980, allows performance of well-controlled reproducible experiments using large numbers of rodents, often with minimal technical intervention. A system developed here at Brookhaven is used to monitor and control the environment both in the chambers and in the facility. The system monitors exposure chamber and chamber room

temperature, humidity, static pressure, and a number of variables in the air conditioning system. In addition, the system has an automated weighing station and allows for complete data management. This system facilitates performance of inhalation studies in conformance with Good Laboratory Practice Regulations. Since the facility was occupied, a number of compounds have been studied, including ozone, acrolein, benzene, cadmium chloride, carbon monoxide, chlorine, and silica. Studies are under way with methyl bromide and a series of metal and metal oxide aerosols.

In a study of the subchronic impact of exposure to chlorine on functional, structural, and compositional aspects of the lung, rats were exposed to either 0.0, 0.5, 1.5, or 5.0 ppm chlorine for three months. While both males and females showed a marked depression of growth rate (Fig. 1), particularly after exposure to 5.0 ppm, no statistically significant biochemical or functional changes were noted, except for an increase in the collagen content of the lungs of animals exposed to either 1.5 or 5.0 ppm of chlorine. Histopathological evaluation of the lungs of rats exposed to chlorine also showed very few changes which could be attributed to chlorine

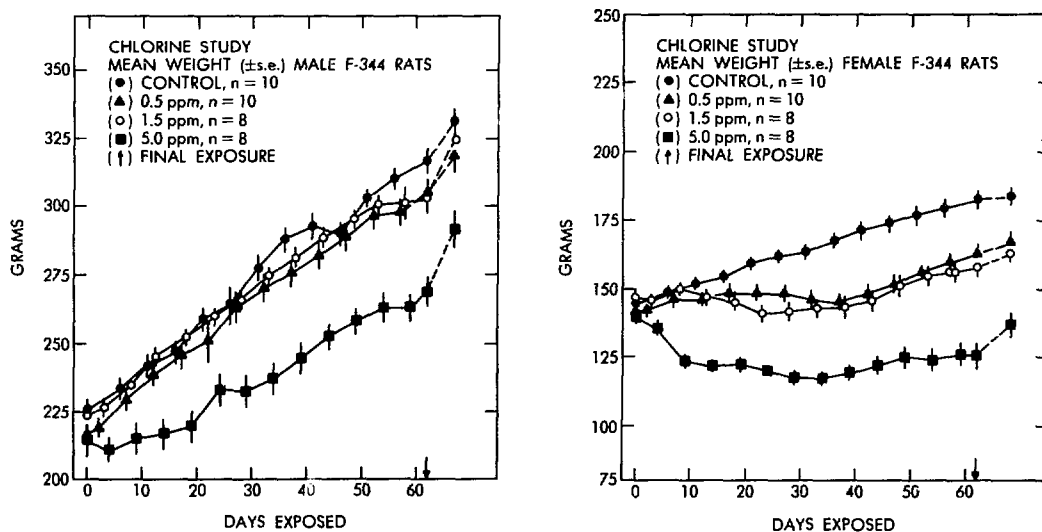


Figure 1. Weights of control and chlorine-exposed male and female Fischer-344 rats with increasing time of exposure. Exposures were for 6 hours per day, 5 days per week, for 62 days. The dashed line between the last two data points for each group indicates the weight gain during a 6-day period after exposures were terminated. See text for details.

exposure. These results suggest that the rats were able to adapt to chlorine despite the continuing exposure. However, had we looked earlier, other changes might have been apparent.

One area of specific interest involves assessment of factors which might modify toxicity. Such factors might include preexisting disease, stress, environmental conditions, exercise, or diet. Studies assessing the acute toxicity of carbon monoxide after a 1-h exposure have been reported. We have recently investigated the influence of restraint on this toxicity. Carbon monoxide was observed to be more toxic to rats restrained in tubes and exposed via the nose than to rats allowed to range over the bottom of an inhalation chamber. These results were of particular interest since many laboratories are considering the use of nose exposures when studying highly toxic particles.

Hypothesizing that the stress resulting from restraint might be the cause of this enhanced toxicity, we conditioned rats to nose exposure tubes for two months. The animals then were subjected to a series of 1-h exposures and the previous results were confirmed: carbon monoxide was still more toxic to restrained rats than to unrestrained rats when the exposures were one hour in duration. However, since carbon monoxide and carboxyhemoglobin levels are not in equilibrium after only one hour, we repeated this experiment, lengthening the exposure to six hours. In this case, there was no difference in the toxicity of carbon monoxide, which suggests that restraint does not alter toxicity if exposures are for six hours.

We have also investigated the effects of exposure to benzene on a number of biological systems. In one series of studies, we demonstrated that a single 4-h exposure to as little as 25 ppm of benzene was sufficient to double the incidence of sister chromatid exchange, a phenomenon observed in chromosomes, implying a possible genetic change. In other studies, it has been shown that exposure to benzene reduces the number of stem cells in bone marrow and that the number is depressed as long as 16 weeks after 16 weeks of exposure to 300 ppm benzene. It was also observed that 10 exposures (6 h/day, 5 days/week) to as little as 25 ppm benzene depresses the lymphocyte count. These studies are extremely significant in view of the fact that the current threshold limit value (TLV)

for benzene exposure is 10 ppm. We are seeing changes resulting from exposure to 25 ppm, in one case after a single 4-h exposure and in another case after 10 exposures.

### Large Animal Studies

One of the objectives of the large animal pulmonary program is to study the mechanisms which may be involved in increased susceptibility of certain human populations, such as children and individuals with emphysema, to inhaled pollutants. For this purpose we are developing models of emphysema and also investigating the development of pulmonary host defenses in lambs. Pulmonary emphysema in sheep (in collaboration with Dr. Janoff, Department of Pathology, SUNY at Stony Brook) is induced by intrabronchial instillation of porcine pancreatic elastase.

Following the intrabronchial instillation of elastase, the early inflammatory response is evaluated by  $^{67}\text{Ga}$  citrate pulmonary scans. The degree of pulmonary elastin degradation is determined by measuring desmosine in the urine of sheep treated with elastase. Desmosine, a cross-linking amino acid unique to mammalian elastin, is measured by a radioimmunoassay. Serial pulmonary function tests, before and after elastase instillation, employ radionuclide imaging techniques. Regional lung perfusion, ventilation, and lung volume are determined utilizing  $^{99\text{m}}\text{Tc}$  MAA (macroaggregated albumin),  $^{81\text{m}}\text{Kr}$ , and  $^{127}\text{Xe}$ , respectively. At 4 weeks after elastase instillations, lungs are fixed *in situ* and sections are prepared for morphological evaluation of alveolar septation. For this purpose, mean linear intercepts of enzyme-treated and control lungs are obtained.

The uptake of  $^{67}\text{Ga}$  citrate is confined to the induced lesion and is correlated positively ( $r = 0.8$ ,  $p < 0.01$ ) with the dose of the instilled elastase (range 800 to 8000 units). Most of the elevation in the urinary desmosine excretion occurred in the first 48 hours after elastase administration. This increase in desmosine excretion was positively correlated with enzyme dose ( $r = 0.748$ ,  $p < 0.01$ ), decrease in regional lung perfusion ( $r = 0.77$ ,  $p < 0.01$ ), and increase in mean linear intercepts ( $r = 0.61$ ,  $p < 0.05$ ). These results demonstrate that desmosine excretion and regional lung perfusion impairment represent reliable, sensitive, and nondestructive

tive means of assessing elastase-induced pulmonary emphysema. The pathological lesions are very similar to those seen in human subjects with panacinar emphysema.

These results obtained from the sheep model have opened up new possibilities for studying the pathogenesis of emphysema from the formation of acute inflammatory lesion to alveolar departmenting in a fashion not previously available. Experiments are being designed to evaluate pulmonary injury produced by chronic oxidant gas exposure, alone and in combination with endobronchial elastase. It is expected that these new studies will permit quantitative assessment of inhaled-oxidant-induced impairment as well as possible interactions between oxidant and proteolytically mediated lung injury.

The susceptibility of newborn infants to a variety of infections, particularly respiratory infections, is well known, and it is not unreasonable to suspect that they may comprise a population highly susceptible to the harmful effects of inhaled pollutants. A study has thus been initiated to define the neonatal development and maturation of pulmonary host defense mechanisms which may be adversely affected by pollutant exposure.

Coping with inhaled microorganisms, as well as other pollutants, during early life is largely dependent upon resident phagocytic cells found in the pulmonary air spaces. Important functions of these cells include: ingestion (phagocytosis) and killing of microorganisms, clearance of particulate materials, elaboration of factors which attract blood leukocytes for the expansion of the local inflammatory response, cellular cytotoxicity, and antigen metabolism and immune regulation. Using techniques of bronchoalveolar lavage and *in vitro* assays, changes in pulmonary host defense as a function of age are currently being studied in neonatal lambs. The results indicate that cell populations in the lung air spaces undergo dramatic changes during the first few days of life. These changes are associated with measurable deficiencies in functions which may be critical for effective protection against lung infections. The results suggest that the increased susceptibility of newborns is associated with a cell population which is in direct contact with inhaled pollutants. Since these cells are already functioning

suboptimally, added insults from the environment may be particularly devastating. We are now developing, in collaboration with the Department of Pediatrics, SUNY, Stony Brook, protocols to investigate the effects of gaseous pollutants on the maturation of pulmonary host defense in neonatal lambs.

### Clinical Studies

The clinical studies, conducted in healthy individuals and in patients with a variety of pulmonary disorders, are performed in the Medical Research Hospital. Our hospital contains some of the most modern technology available for evaluating human respiratory function, including state-of-the-art and new nuclear medicine techniques to measure radioactive tracers in inspired gases and in pulmonary blood. These techniques provide a highly sensitive and accurate measurement of early injury to small airways and terminal lung units.

The probable transition back to coal as a major source of energy in the next few decades raises questions concerning potential health problems. Adverse health effects are associated not only with the mining of coal, but also with the atmospheric pollution due to processing and burning the coal. Therefore, it is important to design clinical studies which identify and define early signs of injury (when therapy is most effective) and to identify specific susceptible populations. Animal models of human respiratory disease are being developed to permit intensive mechanistic studies and experimental forms of therapy.

A major goal of the clinical program has been to measure changes occurring in miners exposed to coal dust and to correlate these findings with the degree of exposure. A comprehensive study, in collaboration with Marshall University and the Appalachian Pulmonary Laboratory in West Virginia, is continuing. To date, we have quantified respiratory function in two groups of retired coal miners: (1) 26 lifelong nonsmokers, and (2) 30 cigarette-per-day smokers. Despite normal chest films in some patients, our more sensitive techniques have shown pulmonary impairment in the peripheral lung units of all miners, including abnormal ventilation and gas exchange, and obstructed small airway flow. In contrast, conventional spirometric measurements were within normal limits for

the nonsmokers, while a majority of the smokers showed large-airway obstruction.

These studies are continuing with special emphasis on improving the lung air and blood flow measurements. The lung is a unique organ with respect to its size and shape and the effect of functional changes occurring at the alveolar level. Measurement artifacts are produced by lung motion resulting from expansion and contraction during respiration. Studies are therefore being carried out with the dual camera single photon emission system (UNICON) to enhance measurement sensitivity by correcting the gamma camera images for motion, as well as tissue attenuation. Both air and blood flow are being measured in patients using  $^{81m}\text{Kr}$  and  $^{99m}\text{Tc}$  MMA, respectively, and the data are being gated with the lung volume during the breathing cycle.

Transmission studies, using an uncollimated scintillation camera and a 10-mCi  $^{99m}\text{Tc}$  point source, are being carried out to measure changes in amplitude and the shift in the phase angle of patients' lungs during quiet breathing cycles. This is a particularly interesting imaging modality because of the extremely low dose to the patient. Preliminary evaluation of lung transmission studies on healthy volunteers and coal miners has shown that the computed amplitude and phase images highlight areas of decreased airflow in the lung. A comparison of the transmission and  $^{81m}\text{Kr}/^{127}\text{Xe}$  images will facilitate our understanding of the diagnostic value of the transmission images and the distribution of lung volume and airflow.

A collaborative effort to improve pulmonary diagnostics is under way with the Pulmonary Branch of the National Heart, Lung, and Blood Institute at the National Institutes of Health in Washington, DC. To increase the scope of the studies, the miners go to the NIH after studies at BNL for measurements of the lung  $^{67}\text{Ga}$  index and for analysis of alveolar macrophages and other cells from bronchoalveolar lavage. The NIH group has achieved success in classifying and treating interstitial lung diseases, such as sarcoidosis and idiopathic pulmonary fibrosis, and it is believed that lung disease in coal miners may fall into the same disease category. Imaging with  $^{67}\text{Ga}$  is widely used as a noninvasive method to assess the extent and location of inflammatory lesions. The type and distribu-

tion of the different cell populations in the lavage fluid is an indicator of the nature and activity of the disease process.

## MEDICAL APPLICATIONS OF NUCLEAR TECHNOLOGY

The objective of this program is to improve current nuclear techniques and to develop new ones for the analysis and solution of medical problems, particularly those associated with environmental pollution. Measurement facilities developed, to date, include a unique whole-body counter (WBC); a total-body neutron activation facility (TBNA); a partial-body, (prompt gamma) neutron activation facility (PGNA); nuclear resonance scattering techniques for in vivo measurement of metals; an absorptiometric technique for measuring bone density; and an in vivo x-ray fluorescence technique for bone Pb. These new techniques provide data in numerous clinical studies not previously amenable to investigation. The development and perfection of these techniques provide unusual applications of radiation and radioisotopes to the early diagnosis and evaluation of therapy in human disease.

The PGNA technique has been developed and calibrated for the in vivo measurement of cadmium and mercury. Prompt gamma neutron activation, x-ray fluorescence, and nuclear resonance scattering techniques are being investigated for in vivo measurement of other elements: silicon, beryllium, and lead. Cardinal to all toxicological studies of cadmium and other metal pollutants is an accurate and sensitive noninvasive technique for measuring organ burdens. A variation of the prompt gamma neutron activation technique for measuring total-body nitrogen has been developed to study interrelationships among cancer, nutrition, and body composition.

### PROMPT GAMMA NEUTRON ACTIVATION ANALYSIS (PGNA)

#### Cadmium

The primary objective of this study was to develop dose-response relationships of cadmium in human beings. In vivo measurements of kidney and liver cadmium, urine and blood cadmium, and urinary levels of  $\beta_2$ -microglobulin

and total protein were obtained in 82 industrially exposed workers and 30 control subjects. The values of 200  $\mu\text{g/g}$  creatinine for urinary  $\beta_2$ -microglobulin and 250 mg/g creatinine for urinary total protein were used to define the upper limit for normal kidney function. Forty-one of the cadmium workers (18 active, 23 retired) were classified as having abnormal kidney function; all control subjects had normal kidney function. Most workers with cadmium levels above 70 ppm in the liver were judged to have some evidence of kidney abnormalities. The dose-response relationship for liver cadmium for the actively employed workers could be described by a linear logistic regression model.

The relationship between kidney and liver cadmium data for the subjects with normal kidney function was combined with the logistic equation for the liver, and a predicted response curve was obtained for the kidney. The logistic models predict a 50% probability of having kidney dysfunction at 38.4 mg Cd for the kidney and 42.3 ppm Cd for the liver, respectively.

Biological indicators of body burden of cadmium were evaluated in the above industrially exposed workers. The cadmium content in the left kidney (KCd) and concentration in the liver (LCd) were measured in vivo in the 51 adult male workers actively employed at the cadmium plant and in 10 age-matched controls. Cadmium levels in blood (BCd), urine (UCd), and hair (HCd) were also obtained for each subject. Grouped on the basis of urinary excretion of  $\beta_2$ -microglobulin, albumin, and total protein, 33 workers had normal renal function and 18 had renal dysfunction. All biological indices of cadmium exposure in the industrial workers were statistically elevated, on a group basis, when compared with the controls. Examination of the interrelationships among KCd, LCd, BCd, UCd, and HCd leads to the following conclusions: (a) KCd decreases in the workers with renal dysfunction, whereas LCd continues to increase, (b) UCd and BCd are moderately correlated with body burden on a group basis in workers with normal renal function, and (c) HCd had the largest variability of the biological indices. The results of this investigation demonstrate that the indirect indices of exposure (BCd, UCd, HCd) are not sufficiently quantitative for predicting the body burden of an indi-

vidual worker. The wide variability observed in BCd, UCd, and HCd values seems to reflect recent changes in exposure conditions and not body burden.

### Nitrogen Body Composition and Dietary Intake in Neoplastic Diseases

In the present study, the effects of combined nutritional support (parenteral, enteral, and oral) were measured in cancer patients unable to maintain normal alimentation. The changes in body composition in cancer patients were quantified by measurement of total-body levels of nitrogen, potassium, water, and fat. The protein-caloric intake of the patients was also evaluated by dietary survey. In addition, standard anthropometric and biochemical measurements for nutritional assessment were obtained for comparison.

The dietary evaluation, based on the four-day recalls, indicated that the dietary supplementation for all four groups was more than adequate to meet their energy requirements. Almost all the patients gained weight on combined nutritional support regimens. The change in the body weight was equal to the sum of the changes in body protein, total-body water, and total-body fat. The findings from the anthropometric nutrition indices (arm muscle circumference and triceps skinfold) were consistent with the results of the body composition study.

Information on the nature of the tissue gained was obtained by comparison with the ratios of protein/water/lean body mass for normal tissue. The mean gain of protein in these patients was quite small (0.3–0.6 kg). The main change in body weight appeared to be due to gains in body water and body fat. The total-body nitrogen-to-potassium ratio (TBN/TBK) served to define the extent of tissue anabolism following hyperalimentation. The ratio dropped in the cancer patients following hyperalimentation toward the value of the normal controls. The body compartment techniques described have already demonstrated their usefulness in determining the effects of hyperalimentation on cancer patients.

### Indices of Body-Cell Mass: Nitrogen vs Potassium

In vivo neutron activation has provided investigators with a powerful tool for research



on body composition. TBN, TBK, and total-body water (TBW) were measured in 133 normal subjects. TBN, measured by neutron activation, is a measure of total-body protein, an index of body-cell mass. TBK, also measured by a nuclear reaction, is an index of body-cell mass as well as lean-body mass. The mass and protein contents of two compartments, muscle and nonmuscle lean tissue, were determined from the combined TBN-TBK data by compartmental analysis. In the present study, nitrogen was separated into the actively metabolizing body-cell mass component and the slowly metabolizing structural component. The TBK, which is 95% intracellular, was found to be more closely related to the actively metabolizing nitrogen than to TBN. The relationship of body-cell mass, a concept originally proposed by Moore, to lean-body mass is shown through the relationship of TBN and TBK. The clinical significance of this study is that TBK is the more sensitive and reliable indicator of changes in body-cell mass. Maximum information on body composition, however, is obtained by the measurement of both TBK and TBN.

## NUCLEAR RESONANCE SCATTERING

A technique for the measurement of body iron utilizing nuclear resonant scattering of gamma rays has been developed and validated. From this prototype study, a full-scale facility was developed for clinical application. Photons (847 keV) emitted from a gaseous  $^{56}\text{MnCl}_2$  source (prepared in the BNL High Flux Beam Reactor) are scattered resonantly from  $^{56}\text{Fe}$  present in the liver and heart. The spatial uniformity of activation, the sensitivity of the detection system, and the limits of detection have been investigated. Measurements were made on a liver, heart phantom, and 26 patients. The resonance scattering technique permits detection of normal levels of Fe in the liver with a radiation dose of 2 rem. A research grant was obtained from NIH for support of this research and its clinical application (thalassemia).

## DELAYED GAMMA NEUTRON ACTIVATION ANALYSIS

### Physical Therapy

Studies of the effects of physical therapy on the skeletal mass of older human subjects are in

progress with the original support of an NIH Aging Institute grant and currently with the support of a renewed grant for three more years. These studies include measurement of the normal changes in skeletal mass with age. The measurement of total-body calcium levels in 135 normal subjects, 20 to 90 years of age, was completed.

### Combination Therapy for Osteoporosis

A 24-month randomized parallel study of the treatment of postmenopausal osteoporosis with calcitonin alone vs calcitonin alternating with growth hormone (combined treatment) was conducted. Each group received 1000 mg daily of oral calcium supplements. The rate of change in total-body calcium for the combined and calcitonin groups was +1.68% and +1.33% per year, respectively ( $P < 0.05$ ), a difference that is not statistically significant. Further, the total-body calcium level did not increase after 12 to 18 months of treatment. There was a significant difference in the rates of change of bone mineral content (BMC) between the two groups, with a loss of BMC in the combined treatment group ( $F = 4.80$ ,  $P < 0.05$ ). Calcitonin treatment is effective in producing an increment in bone mass. The addition of growth hormone to this regimen appears to have a deleterious effect on cortical bone mass.

### Changes in Bone Mass With Age

Eighty white women, mean age 52 years, within 1 to 6 years postmenopausal, were studied to examine the relationship of various factors to bone mass. Forty-four of the women had annual measurements of bone mass, so that the rate of bone loss could be determined. Bone mass was measured by total-body neutron activation analysis and photon absorptiometry of the distal radius [total-body calcium (TBCa) and bone mineral content (BMC), respectively].

Breast feeding and pregnancy were noted to be associated with higher bone mass; subjects with lower BMC and/or TBCa tended to have higher serum alkaline phosphatase, lower testosterone, and more years since the cessation of menses. The rate of bone loss from the radius was greater in those with higher Parathormone (PTH) levels; those with reduced dietary intake of calcium and lower 25(OH) vitamin D levels had a greater rate of loss of TBCa.

### Total-body Phosphorus in Postmenopausal Women

Total-body phosphorus (TBP) and TBCa were measured by neutron activation analysis and whole-body counting in 82 white women who were 1 to 6 years postmenopausal. Mean TBP was  $395 \text{ g} \pm 6.3$  (SE). There was no evidence for subgroups of patients with either higher or lower TBP. The TBP was significantly related to TBCa, as well as to the bone mineral content of the distal radius.

Positive associations were found between TBP and urinary phosphate excretion as well as serum  $1,25(\text{OH})_2$  vitamin D levels ( $r = 0.30$ ,  $p = 0.017$ ,  $n = 48$ ). Serum phosphate was related to  $1,25(\text{OH})_2$  vitamin D levels and to the number of years since menopause.

### Whole-body Turnover of $^{85}\text{Sr}$ in Paget's Disease

The whole-body retention of  $^{85}\text{Sr}$  has been measured over a period of 150 days in 12 patients with Paget's disease, 7 of whom were treated with calcitonin, starting 60 days after the  $^{85}\text{Sr}$  administration. Retentions were compared with those in a group of 8 control subjects. In addition, profile scanning identified the regional distribution over parts of the body. On average, the Paget's patients retained more  $^{85}\text{Sr}$  over a longer period than did the controls. There was no appreciable effect of calcitonin treatment.

## NEW NUCLEAR TECHNIQUES

### In Vivo Measurement of Lead by X-ray Fluorescence

A post mortem study was conducted to assess the feasibility of measuring bone lead concentrations noninvasively in vivo. Characteristic L x rays were induced with an external source of  $^{125}\text{I}$  in the superficial tibial cortex of the intact legs of five adults who had no history of occupational exposure to lead. Tibial lead concentrations in the same bones subsequently determined by flameless atomic absorption spectroscopy varied from 15 to  $35 \mu\text{g Pb/g wet weight}$ . These values are within the modern normal range. The linear correlation coefficient ( $r$ ) between the x-ray fluorescence and lead concentration was 0.92 (Fig. 2).



Figure 2. X-ray fluorescence system to measure lead in the human tibia. The source attached to the detection system is positioned above the patient's leg.

A study has been initiated to measure lead in the tibia of children living in an inner city environment. This study is in collaboration with Dr. Rosen of Einstein Medical School/Montefiore Hospital, New York.

### Application of XRF to In Vivo Measurement of Strontium in Human Bone

X-ray fluorescence spectroscopy was utilized for the measurement. In the present study either  $^{125}\text{I}$  (Te x rays) or  $^{109}\text{Cd}$  (Ag x rays) was used to stimulate 14.1-keV Sr K x rays. The emitted x rays were detected by a Si(Li) detector and processed by standard nuclear spectroscopy electronics.

The preliminary results demonstrate the feasibility of measuring normal levels of Sr in the human body in vivo. Although the method is limited to superficial bones, the intensity of the measured Sr signal is satisfactory. The present setup is also used to measure lead in the bone in vivo. The chief limitation of the method is the attenuation of the signal due to overlying tissue. It is important, therefore, particularly for epidemiological studies, that the measured Sr signal be normalized per unit of overlying tissue thickness. In the present study, the thickness of the overlying tissue in cadaver legs has been determined directly by excision of the tissue. In vivo, the overlying tissue thickness can be determined ultrasonically within an accuracy

of 0.3 mm with the use of a 7-MHz ultrasound transducer.  $^{125}\text{I}$  and  $^{109}\text{Cd}$  were found to be equally effective sources for the Sr excitation.

### In Vivo Measurement of Lithium in the Brain

A method for in vivo measurement of lithium levels in the human brain is being developed. In this technique, the brain is irradiated with neutrons and  $^6\text{Li}$  present in the brain interacts with neutrons by the  $^6\text{Li}(n,\alpha)^3\text{T}$  reaction, resulting in energetic recoiling tritium atoms. Since the tritium in the form of HT is quite inert and its solubility in body tissues and fluids is small, the gas is readily exhaled. The tritiated hydrogen exhaled is isolated from other gases in the breath and counted in a low-background proportional counter.

In the future, it is planned to perform animal studies on the exhalation rate of tritium and establish conversion constants and calibration procedures using phantoms.

### Silicon Measurement in a Lung Phantom by Neutron Inelastic Scattering

A study was made to assess the feasibility of determining the silicon level in human lungs in vivo by measuring the gamma rays arising from the neutron inelastic scattering reaction  $^{28}\text{Si}(n,n'\gamma)^{28}\text{Si}$ . Neutron energies in the range 5 to 8 MeV represent the best compromise between the conflicting requirements of high energy for utilization of higher cross sections and low energy to minimize the dose to the subject.

The sensitivity of measurement was enhanced by pulsing the neutron beam and counting only during the period of bombardment. This effectively reduced the background counts emanating from thermal neutron reactions in the phantom and from the fast neutron reactions  $^{31}\text{P}(n,\alpha)^{28}\text{Al}$ .

In measurements with an anthropomorphic phantom, no interference peaks from other prompt inelastic scattering reactions were observed. With one Ge(Li) detector of 19% relative efficiency, a detection limit of 0.6 g of silicon per 10 mSv was obtained. On this basis, it is estimated that six Ge(Li) detectors (25% efficiency each) would be capable of measuring 0.15 g silicon in the lungs, the average level found in non-occupationally exposed adults.

## TARGETING OF STABLE AND RADIOACTIVE ISOTOPES TO TUMORS FOR RADIOTHERAPY

With conventional radiotherapy, it is difficult to achieve adequate dose to the target tissue, while at the same time sparing nontarget normal tissues. Although the use of charged-particle external beams offers some improvement, optimal advantage in terms of control of target dose and selective applications of high-LET radiation at the target sites may be achievable by the targeting of selected radioactive or nonradioactive elements to the tissues of interest.

In principle, it would be desirable to target radioactive nuclei directly to the tumor, as in  $^{131}\text{I}$  therapy of thyroid cancer. In practice, systemic application of radionuclides is generally precluded by uptake in rapidly proliferating normal cell pools such as gut and bone marrow.

An apparent solution to this problem is the molecule thiouracil (TU). Our studies with TU demonstrated such unique uptake in growing melanoma that it became obvious this biomolecule was an ideal candidate for diagnosis and/or therapy via systemic application of radiolabeled TU. Concentration in melanotic melanoma is robust, and is 50 to 200 times higher than that measured in other tissues. Preliminary studies, in which "therapeutic" amounts of  $^{35}\text{S}$ -labeled TU were administered to BALB/c mice carrying Harding-Passey melanoma, have indicated an approximate two-week suppression of tumor growth (Fig. 3). It is apparent from Fig. 3 that  $^{35}\text{S}$ -TU should find clinical application in the treatment of primary and, perhaps most important, metastatic melanoma.

The problem of uptake of radiolabeled substances in competing normal cell pools can be circumvented by targeting of stable nuclei which can subsequently be activated by appropriate external beams. This technique can be implemented with either Photon Activation Therapy (PAT) or Neutron Capture Therapy (NCT).

As an example of PAT, stable  $^{127}\text{I}$  is incorporated into DNA via substitution of iodinated deoxyuridine ( $^{127}\text{I}$ dUrd) for thymidine (Tyd). Low energy photons (32 to 50 keV) can then be used to stimulate radiation sensitization as well as direct damage from Auger cascades. Theoretically,

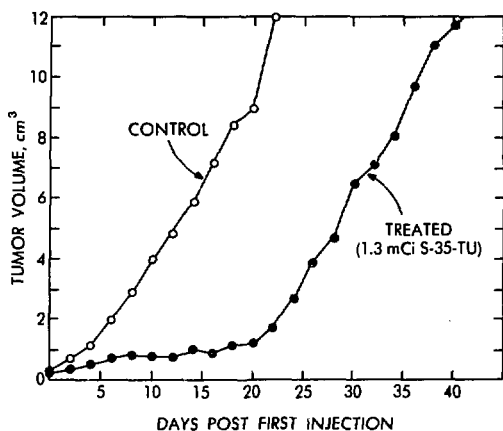


Figure 3. Growth of Harding-Passey subcutaneous melanotic melanoma in BALB/c mice. Treated mice received one i.p. injection every 6 hours for 24 hours, for a total  $^{35}\text{S}$ -thiouracil dose of 1.3 mCi ( $\sim 18$  rad/h to tumor). Each point is the average of four mice.

cal analysis has shown that at 5% replacement (IdUrd for Tyd), therapeutic gain should vary from 2.2 to 17 depending on dose-rate. Therapeutic gains for 5, 25, and 50% replacement are shown in Fig. 4. Studies with murine carcinomas have indicated approximately 20% replacement in vivo.  $^{145}\text{Sm}$  sources (40- to 45-keV x rays) are being used to evaluate the contribution from Auger cascades. These studies will be aided by the availability of monoenergetic photons from the NSLS with energies just above and below the iodine K absorption edge (33.2 keV). It is anticipated that improved brain tumor therapy will be obtained with implanted  $^{145}\text{Sm}$  sources in conjunction with long-term infusions of  $^{127}\text{IdUrd}$ .

The NCT approach utilizes stable  $^{10}\text{B}$ , which interacts with thermal neutrons, to produce high-LET particles via the  $^{10}\text{B}(n,\alpha)^7\text{Li}$  reaction. A variety of classes of compounds for which boronated analogs have been described in the literature show selective uptake in tumors. These classes include phenothiazines, thiouracil, porphyrins, nucleosides, amino acids, antibodies, and steroids. In order to be useful for NCT, the boronated compounds must deposit 10 to 30  $\mu\text{g}$  of  $^{10}\text{B}$  per gram of tumor, with adequate clearance from the blood and surrounding tissue. These parameters are being evaluated for the above classes of compounds using cell

culture and small animal test systems, with samples synthesized here or obtained through collaboration with groups outside BNL.  $^{10}\text{B}$  analysis in tissue samples is being carried out by prompt  $\gamma$  analysis using pencil-thin beams of thermal neutrons available at the HFRR. Special emphasis is being placed on the synthesis and biological properties of boronated monoclonal antibodies, as this class of compounds has been shown to accumulate selectively in sufficient concentrations with a long tumor half-life and with good blood and tissue clearance. Monoclonal antibodies can be boronated directly or by way of bridging intermediate carriers to therapeutically significant levels.

In addition to the development and evaluation of the above "3rd generation" compounds showing selective binding to tumor cells, studies are under way on a "2nd generation" boron hydride cage-compound which shows some tumor affinity, and is currently being used clinically in Japan.

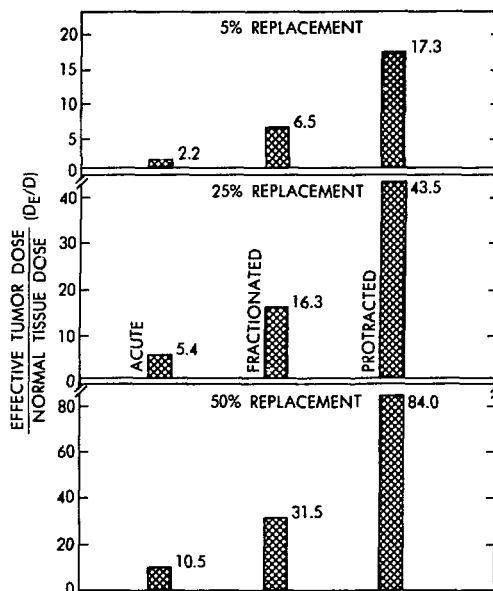


Figure 4. The dose enhancement (DE) is the ratio of effective tumor dose to normal tissue dose D. Replacement of Tyd by IdUrd is assumed to be in tumor only. Fractionated irradiation assumes 30 fractions over six weeks. Protracted irradiation assumes "permanent" sources implanted for ten months.

## THERAPY OF BRAIN TUMORS

Soon after neutrons were discovered in the early 1930s, it was realized that they might be useful in treating malignant tumors. For slow neutron radiation therapy a tumor is perfused, via injection into the blood stream, with a substance labeled during its synthesis with a non-radioactive atom having a strong affinity for neutrons. Such an atom is the lighter of the two naturally occurring boron atoms ( $^{10}\text{B}$ ). An incoming slow neutron is thousands of times more likely to react with  $^{10}\text{B}$  than with any atom normally present in human tissues, and the nuclear reaction between a neutron and a  $^{10}\text{B}$  nucleus is very likely to kill one cell in its immediate vicinity. Irradiation of tissues which are not loaded with a highly neutron-reactive atom such as  $^{10}\text{B}$  is relatively harmless. This means that effective slow neutron therapy depends as much on excluding most  $^{10}\text{B}$  from normal cells as on ensuring that tumors contain enough  $^{10}\text{B}$  and that enough neutrons penetrate to the deeper portions of tumors.

The results of the first clinical trials of slow neutron therapy at Brookhaven National Laboratory and at the Massachusetts Institute of Technology in the 1950s were disappointing, but since then, new boron-labeled substances with improved affinity to tumors have been synthesized. One of these substances, sodium mercaptoundecahydrododecaborate ( $\text{Na}_2\text{B}_{12}\text{H}_{11}\text{SH}$ ), first synthesized in the U.S.A. in 1964, has been used since 1968 to treat brain tumors in Japan with success in some patients. The leader of the Japanese boron neutron capture therapy (BNCT) team is Professor H. Hatanaka of Teikyo University, a neurosurgeon who studied techniques of BNCT under Professor William H. Sweet and his colleagues in Boston.

Encouraged by their own experimental studies and by the Japanese clinical trials, researchers at Brookhaven and elsewhere believe that BNCT techniques have been sufficiently improved to warrant consideration of a second clinical trial in the U.S.A. Review of our facilities and expertise and those of our collaborators by a National Cancer Institute committee suggests that, although a full-scale clinical trial of BNCT may be premature, palliative treatment of selected patients with advanced malignant brain tumors might be undertaken. It is hoped

that the quality of our ongoing preclinical studies and the broad scope of Brookhaven's facilities will attract sufficient funds from government and/or private sources to begin such palliative radiation therapy before 1985, and it is hoped that patients in the U.S.A. with brain tumors may eventually be treated by BNCT at an earlier stage of the disease, as some are being treated in Japan at the present time.

Preclinical investigations of BNCT at Brookhaven include the distribution of  $\text{B}_{12}\text{H}_{11}\text{SH}$  in experimental animals, optimization of the neutron energy distribution at the patient port of the Medical Research Reactor, studies on adjunct therapy by heavy water, assay of extremely small quantities of  $^{10}\text{B}$  by counting neutron-induced plastic tracks, studies on the adverse side effects of BNCT on normal brain tissues, as well as synthesis and evaluation of new boron-labeled molecules showing selective binding to tumors.

## TRITIUM TOXICITY

As the electrical energy requirements of the world increase, it becomes more apparent that a growing fraction of the required electrical energy must be generated from nuclear power plants. At the end of 1980, 31 countries had 483 nuclear power plants in operation or under construction. With this proliferation of nuclear power reactors there has developed a worldwide concern about the possible effects on man and the environment from continuous exposure to radioactive reactor effluents. Much of this concern is centered on the tritium (the radioactive isotope of hydrogen) released from fission reactors. Although the amount of tritium released from the present type of fission reactor (and the fuel reprocessing plants associated with them) does not seem to be a hazard, the larger amounts predicted from the fusion-type reactors of the future are the source of some concern.

To investigate this problem, a broad program was begun within the Medical Department at Brookhaven to evaluate some of the possible effects of exposure to tritium. This continuing program involves the long-term observation of mice maintained on water containing tritium. Among the many parameters measured are somatic effects (effects on the animals' body and tissues), biochemistry (the rate at which

tritium is taken into the body, incorporated into various cells, and subsequently eliminated), microdosimetry (measurements of the radiation dose to various body cells from the tritium), reproductive-genetic effects (effects on the animals' offspring), and cytogenetic studies (effects on the chromosomes of animal tissues such as the liver and bone marrow).

Of particular interest are recent studies of the effects on the deoxyribonucleic acid (DNA) measured by the induction of sister chromatid exchanges (SCEs). DNA is the genetic material of all cells, and disruption or changes of the DNA is thought to lead to mutations, changes resulting in cancer or death of the cells. SCEs, which are symmetrical exchanges of DNA double helices between chromatids during replication, may be visualized by specific staining of the chromosomes (Fig. 5).

The induction of SCEs has been studied in the bone marrow cells of mice maintained on tritiated water and compared to those in animals maintained on regular tap water. Changes in the bone marrow are of particular interest since a known result of exposure to ionizing radiation is the induction of leukemia. Although the direct correlation between the induction of SCEs and

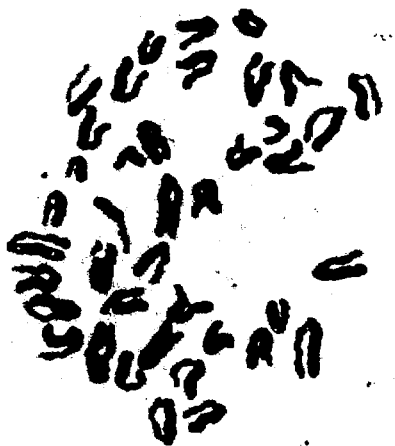


Figure 5. Mouse metaphase chromosomes stained to show sister chromatid differentiation. Six sister chromatid exchanges are visible in this cell. These are at locations where exchanges of darkly and lightly stained material between chromatids can be seen.

the induction of leukemia has not been defined, the measurement of SCEs is of interest and may be taken as evidence of disturbance of the structure of the DNA.

Mice are maintained on tritiated water at concentrations ranging from 3.0 to 30.0  $\mu\text{Ci/ml}$ . The lowest dose investigated is 100 times the recommended maximum permissible concentration for drinking water to be consumed by humans. At intervals ranging from 1 to 280 days, mice are infused with bromodeoxyuridine (BrdUrd) for periods of 24 to 28 hours. This labels the DNA of the bone marrow cells during their growth and division so that the two sister chromatids of each chromosome can be distinguished by staining and thus exchanges between the sister chromatids can be seen. Two hours before the end of the infusion, the mice are given colchicine, a drug which stops their cells during division at such a time that the individual chromosomes are readily visible. The bone marrow is then removed, the cells are stained, and the number of SCEs in animals maintained on the tritiated water and the tap water are counted.

The results of such measurements indicate that the animals drinking tritiated water show evidence of a significantly greater number of SCEs than do those maintained on tap water (Fig. 6). By measuring the number of SCEs as

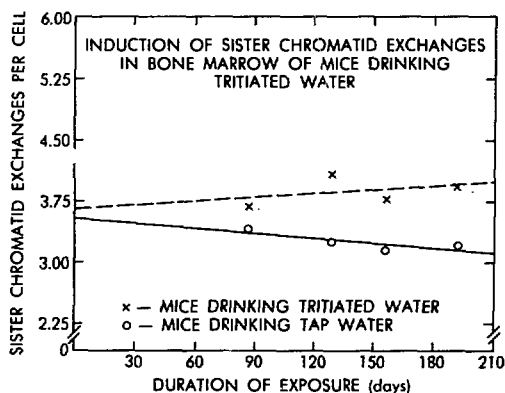


Figure 6. The number of sister chromatid exchanges (SCEs) in mice given tritiated water for various lengths of time compared to the number of SCEs in mice given tap water. A significant increase in the number of SCEs is found in mice fed tritium at all times tested.

compared with the level of tritium exposure, it is possible to construct a dose response curve which will help to predict the possible effect of exposure to tritium at very low levels.

Until these studies, it was possible to measure a significant number of SCEs only in animals exposed to radiation levels significantly above the maximum permissible levels to which humans may be exposed, which in turn is several orders of magnitude greater than that to which humans are expected to be actually exposed from the generation of nuclear power.

Similar studies are being done to determine the induction of SCEs by other environmental pollutants, such as those generated from oil- or coal-fired generating plants. The results of comparisons among these studies will make possible the measurement of the relative environmental and health impacts of generating electricity by various means.

### RADIONUCLIDE AND RADIOPHARMACEUTICAL RESEARCH

This program covers many fundamental aspects of radionuclide and radiopharmaceutical research leading to new and improved diagnostic and therapeutic agents. At present, 80% of all diagnostic nuclear medicine procedures utilize radionuclides developed in this program. We continue to provide research quantities of new radionuclides to many off-site nuclear medicine groups. The Brookhaven Linac Isotope Producer (BLIP), an essential component of this program, was the first facility to utilize the capability of a large linear accelerator for efficient and economical production of difficult-to-make, medically useful radionuclides. In fact a milestone was reached this year as BLIP passed 10 years of operation, with a total fluence of 200-MeV protons in excess of 1.75 million microampere hours (Fig. 7).

A major recent emphasis has been to increase the availability of  $^{123}\text{I}$  to the medical community.  $^{123}\text{I}$ , recognized as the best radioiodine available for use in diagnostic nuclear medicine today, can be used in a wide range of clinical and research applications as the iodide or attached to a suitable radiopharmaceutical. It is produced at BLIP by the  $^{127}\text{I}(p,5n)^{123}\text{Xe} \rightarrow ^{123}\text{I}$  nuclear reaction, which is superior to other widely used reactions because the iodine pro-



Figure 7. Past and present BLIP staff (and Linac representative) celebrate tenth anniversary.

duced has higher radionuclidic purity, thus allowing lower patient dose and better image quality. This year the distribution of this important isotope has been substantially broadened beyond a few research collaborators. It is now supplied to the nuclear medicine community at cost. The distribution of other hard-to-produce radionuclides, including  $^{127}\text{Xe}$ ,  $^{109}\text{Cd}$ , and  $^{68}\text{Ge}$ , continues.

$^{28}\text{Mg}$ , with a half-life of 21 h is the only magnesium isotope suitable for practical use as a tracer. Magnesium is an essential element in human metabolism. For the past 20 years this program has been the country's sole source of  $^{28}\text{Mg}$  for clinical and biomedical research. It was routinely produced by bombarding stable  $^{26}\text{Mg}$  with tritons accelerated in the Physics Department Van de Graaff Generator. Because of the increasing costs of using the Van de Graaff, we evaluated the possibility of producing  $^{28}\text{Mg}$  in the BLIP by spallation reaction on chloride targets. These results were very encouraging. After chemical processing a saturation yield of 2.3  $\mu\text{Ci}/\mu\text{A}$  has been obtained, easily enough to satisfy current needs. The radionu-

clidic purity is excellent and the specific activity is much better than that obtained with the (t,p) reaction.

A new initiative this year was an investigation of the production of  $^{118}\text{Te}$  for the attractive new generator system  $^{118}\text{Te}/^{118}\text{Sb}$ .  $^{118}\text{Te}$  ( $t_{1/2} = 6\text{d}$ ) decays 100% by electron capture with no gamma emission. It is the parent of the 3.5-min positron emitter  $^{118}\text{Sb}$  which may be useful for first-pass angiography and studies of regional blood flow. The availability of short-lived  $^{118}\text{Sb}$  offers significantly lower radiation dose to patients, improved studies with high photon flux, the possibility of repeat studies or rapid sequential studies, and the possibility of multiple radionuclide procedures within a short time.

Additionally,  $^{118}\text{Te}$  represents a bonus in that it can be produced in an antimony target simultaneously with  $^{117\text{m}}\text{Sn}$ . The BLIP production of  $^{117\text{m}}\text{Sn}$  in a carrier-free form is an ongoing project to study the in vivo behavior of tin compounds as well as develop promising diagnostic and possibly therapeutic agents.

The relevant nuclear reaction for tellurium is primarily  $^{121}\text{Sb}(p,4n)^{118}\text{Te}$  with some contribution from the (p,6n) reaction on  $^{123}\text{Sb}$  (42.7% abundant). A preliminary nonoptimal irradiation (1 h) of a 36-g antimony target was attempted at an incident energy of 58 MeV. Although the no-carrier-added chemical separation of both tellurium and tin from a large antimony target is difficult, a workable procedure has been devised. The measured saturation yield was 71 mCi/ $\mu\text{A}$ . Thus curie quantities could easily be produced at BLIP in a several-day bombardment. The only radionuclidic impurity of concern was  $^{119}\text{Sb}$ . However, the amount of  $^{119}\text{Sb}$  eluted with  $^{118}\text{Sb}$  on a generator column can be minimized by taking advantage of the large difference in their half-lives.

Data acquired during the previous three years have demonstrated the potential of  $^{97}\text{Ru}$  for diagnostic nuclear medical applications, particularly for tumor imaging. It was shown that: (i) compared to  $^{67}\text{Ga}$  citrate (the most widely used tumor localizing agent), the uptake of  $^{97}\text{Ru}$ -labeled transferrin ( $^{97}\text{Ru}$ -TF) in tumor tissue in mice is two to three times greater at comparable time periods after injection; (ii) physical properties of  $^{97}\text{Ru}$ , a pure gamma emitter (216 keV, 86%), are superior to those of  $^{67}\text{Ga}$  for imaging, and economic production of clinically useful

quantities of  $^{97}\text{Ru}$  is feasible at the BLIP; and (iii) a great deal can be learned of the various factors responsible for the protein-mediated uptake of metallic radiotracers from appropriate mechanistic studies of the  $^{97}\text{Ru}$ -TF system. In a recent study in collaboration with the Memorial Sloan-Kettering Cancer Research Center, cancerous tissue was clearly visualized in a dog with spontaneous fibrosarcoma using  $^{97}\text{Ru}$ -TF (Fig. 8). In addition, a comparative study of  $^{67}\text{Ga}$ -citrate and  $^{97}\text{Ru}$ -transferrin for the detection of early inflammatory lesions in sheep lungs (produced by intrabronchial instillation

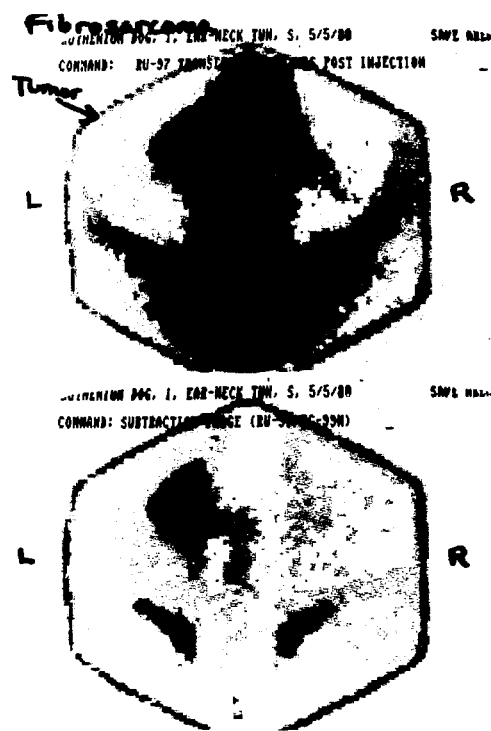


Figure 8. Top:  $^{97}\text{Ru}$ -transferrin images in a dog with fibrosarcoma of the left ear involving lymph glands of the neck and metastases to lungs, 79 hours after intravenous injection. Bottom: Same as above, except that the blood background was computer subtracted, using an injection of  $^{99\text{m}}\text{Tc}$ -labeled human serum albumin (blood pool agent). This procedure made possible the visualization of tumor with greater clarity. This study was carried out in collaboration with the Nuclear Medicine Group at Memorial Sloan-Kettering Cancer Center, New York.



of elastase) demonstrated the superiority of  $^{97}\text{Ru}$ -transferrin when mild lung damage was involved; the uptake was nearly twice that of  $^{67}\text{Ga}$ -citrate. With greater lung damage, no significant difference was noted between the two tracers. This study was carried out in collaboration with the Host Defense Sciences Program.

Continuing studies on the application of  $^{117m}\text{Sn}$ -labeled compounds for the diagnosis and therapy of bone tumors and other bone diseases have shown considerable promise. Stannic chelates of DTPA, MDP, and EHDP (which showed greater bone concentration and higher bone-to-tissue ratios compared to the stannous analogs) were selected to undergo tests for therapeutic usefulness in animal models of osteosarcoma, osteomyelitis, and other disorders with bone involvement. Earlier results in small animals have recently been confirmed in large animals such as dogs. Figure 9 shows bone images in a dog using  $^{117m}\text{Sn}$  (4+) DTPA at 1 and 7 days after injection. Exclusive uptake of

the compound is seen in skeletal tissue with almost no background activity.

Another area of major emphasis involved radiolabeling of monoclonal antibodies for use in diagnosis and therapy of cancer. Monoclonal antibodies are likely to find widespread application for early detection of cancer, for following the response of patients to treatment, and for general cancer therapy. It will be necessary, however, to use highly specific antibody preparations that react selectively with the tumor cell antigens and minimally with normal cells. In collaboration with Columbia University, studies were carried out on the chemistry of labeling and the *in vivo* evaluation in mice of  $^{125}\text{I}$ ,  $^{131}\text{I}$ ,  $^{111}\text{In}$ ,  $^{109}\text{Pd}$ , and  $^{65}\text{Zn}$ -labeled monoclonal antibody to a human high-molecular-weight melanoma-associated antigen. The results showed relatively high uptake of the labeled preparation in tumor tissue and suggest potential diagnostic and therapeutic usefulness of these agents in melanoma patients. Efforts will

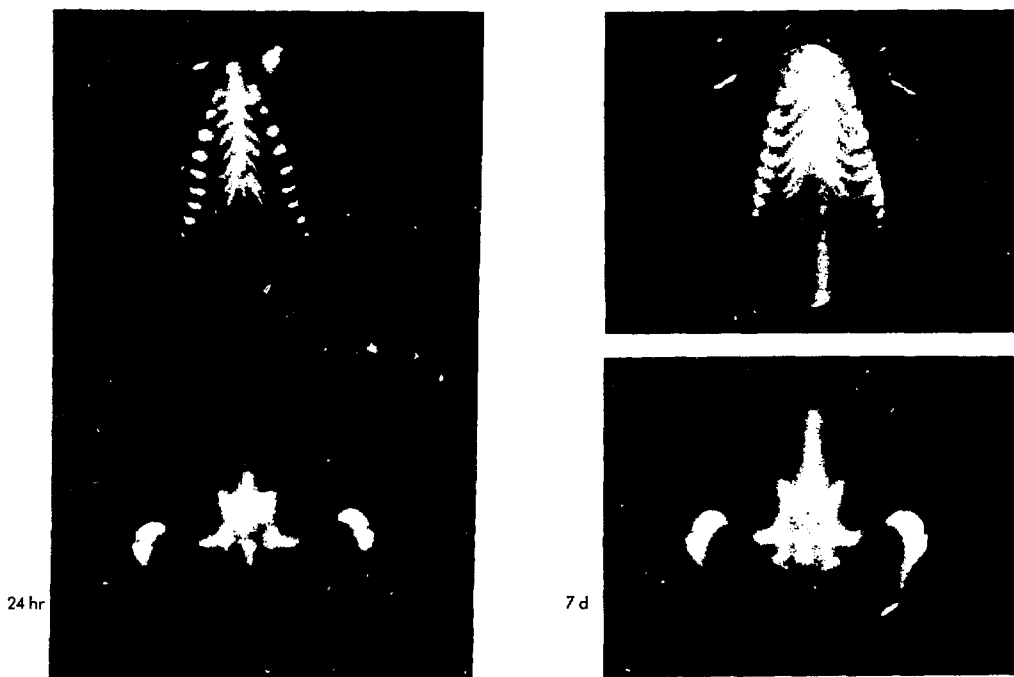


Figure 9. Bone images in dog, obtained 24 h (left) and 7 days (right) after the intravenous injection of about 1 mCi  $^{117m}\text{Sn}$  (4+)-DTPA. Imaging was carried out using an Ohio Nuclear large-field-of-view gamma camera interfaced with a PDP 11/34 computer for quantification. Note the exclusive uptake of radioactivity in skeletal tissue (chest area, top; pelvic area, bottom).

be necessary to further minimize background uptake and renal excretion of the various radiometal-antibody preparations and to label the antibodies with nuclides that possess more favorable nuclear properties, either for imaging or for therapy, e.g.,  $^{97}\text{Ru}$ ,  $^{67}\text{Cu}$ ,  $^{203}\text{Pb}$ ,  $^{69}\text{Zn}$ , etc. These studies are now in progress.

In a collaborative project with the Organ Transplantation Group at Columbia,  $^{109}\text{Pd}$ -labeled lymphocytes underwent further evaluation for generalized lymphoid ablation in animals. These studies will be extended to lymphocytes labeled with other beta emitters that lack an abundance of low energy electrons, e.g.,  $^{69}\text{Zn}$ ,  $^{66}\text{Ni}$ , or  $^{90}\text{Y}$ , etc. A new kit method for selectively labeling red blood cells in whole blood with  $^{99m}\text{Tc}$  was refined and evaluated. The method involves one-vessel operation and no transfers or centrifugation steps, and thus minimizes cell handling and offers greater ease of operation compared to other available techniques. Meanwhile, the previously developed BNL RBC labeling kit is finding increased use and continues to

be distributed at a rate of approximately 1500 per month to various investigators at cost. A recent modification (substitution of a 6 ml saline washing step with 1 ml 4.44% EDTA) has resulted in consistent labeling yields  $\geq 98\%$ .

The available methods for iodinating iodoamphetamine and HIPDM (two pharmacologically active amines, for brain imaging) were optimized for use with BLIP-produced  $^{123}\text{I}$ . These preparations (and others using  $^{125}\text{I}$  and  $^{131}\text{I}$ ) were evaluated in vivo using various animal systems (imaging in dogs, tissue distribution, and autoradiography in mice and rats), jointly with the clinical Nuclear Medicine Program. Tissue distribution remained unaltered after KI pretreatment or when excess amphetamine was administered. No saturation of dopamine receptors was found with up to 0.3 mg amphetamine injected into rats. Results with  $^{123}\text{I}$ -HIPDM were comparable to or slightly better than those with  $^{123}\text{I}$ -iodoamphetamine (brain uptake, brain-to-blood, and brain-to-tissue ratios).

## MEDICAL DEPARTMENT

**D.C. Borg**, Chairman

**R.B. Aronson**, Deputy Chairman

### Environmental Health Sciences Program

**R.T. Drew**, Coordinator

Medical Studies of the People of the Marshall Islands Accidentally Exposed to Fallout — **W.H. Adams, J.A. Harper**.

Inhalation Toxicology and the Physiology, Biochemistry, and Morphology of Human Pulmonary Disease — **R.T. Drew, S.B. Haber, M. Kuschner, D.L. Costa, G. Schidlovsky, R.S. Kutzman, J.D. Glass, M.R. Osheroff, E.A. Popenoe, R.N. Shiotsuka, D.N. Slatkin**.

Interrelationships Among Genetic Factors and Environmental Pollutants in Clinical and Experimental Hypertension — **J. Iwai**.

Inhalation Toxicity of Glass Fibers (TIMA) — **R.T. Drew**.

Respiratory Pathology Training Grant (NIEHS) — **R.T. Drew, R.N. Shiotsuka, J.K. Yermakoff**.  
Inbreeding of Dahl S and R rats (NHLBDI) — **J. Iwai**.

### Medical Applications of Nuclear Technology and Medical Physics

**S.H. Cohn**, Coordinator

Medical Applications of Nuclear Technology — **S.H. Cohn, K.J. Ellis, D. Vartsky, A.N. Vaswani, H.R. Pate, L. Wielopolski, S. Yasumura, I. Zanzi**.

Gerontological Changes in Skeletal Mass (NIA) — **S.H. Cohn**.

Diet, Nutrition and Cancer (NCI) — **S.H. Cohn, A.N. Vaswani, D. Vartsky**.

Computer Applications in Medical Research — **H.R. Pate, J.A.G. Russell**.

In Vivo Measurement of Body Iron by Nuclear Resonance (NIH) — **S.H. Cohn, L. Wielopolski**.

Development of Techniques and Methods of Measurement of Alveolar Clearance of Airborne Particles in Man — **K.J. Ellis, H. Susskind, H.L. Atkins, S.H. Cohn**.

**Nuclear Medicine**  
A.B. Brill, Coordinator

Extension and Improvement of Radiographic and Isotopic Diagnostic Techniques — A.B. Brill, H.L. Atkins, R.G. Fairchild, P. Som, G.W. Bennett, Z.H. Oster, S. Packer, H. Susskind, Y. Yonekura, K. Yamamoto, I.G. Zubal.  
Positron Emission Tomography in Nuclear Medicine Diagnosis — A.B. Brill, H.L. Atkins, G.W. Bennett, Y.J.C. Bizais, R.W. Rowe, W. Brander.

Melanoma Detection (NCI) — S. Packer, H.L. Atkins, R.G. Fairchild.  
Program in Support of Nuclear Medicine (NINCDS) — H.L. Atkins A.B. Brill.  
Boron Epithermal Neutron Capture Therapy — R.G. Fairchild, D.N. Slatkin, D. Gabel.  
Radionuclide Development — P. Richards, S.C. Srivastava, L. Mausner, S. Mirzadeh.

**Genetics and Biochemical Science**  
C.J. Shellabarger, Coordinator

Experimental Chemical-Induced and Radiation-Induced Carcinogenesis — C.J. Shellabarger, S. Holtzman, J.P. Stone.  
Oxidative and Free Radical Mechanisms Involved in the Cytotoxicity and Carcinogenicity/Mutagenicity of Pollutants — D.C. Borg, J.J. Elmore, A. Forman, K.M. Schaich, A.A. Frimer.  
Tryptophan Metabolism — L.V. Hankes.  
Connective Tissue Metabolism — E.A. Popenoe.  
Detection of Environmental Mutagens, Carcinogens, and Teratogens — R.R. Tice.  
Evaluation of Hazards of By-Products from Nuclear and Non-Nuclear Energy Generation — A.L. Carsten, R.D. Benz, S.L. Commerford, D.N. Slatkin.

Human Chromosomal Aberration Production by Energy-Related Agents — M.A. Bender, R. Kale, J. Wieland, J.C. Leonard, R.C. Leonard, S. Gundy, R. Moore.  
Effects of Dose Rate on Rat Mammary Carcinogenesis — C.J. Shellabarger, V.P. Bond, E.P. Cronkite.  
Chemoprevention of Epithelial Cancer by Retinoids — C.J. Shellabarger, J.P. Stone, S. Holtzman.  
NCI Training Grant — C.J. Shellabarger (Medical Department Coordinator).

**Host Defense Sciences Program**  
D.D. Joel, Coordinator

Effects of Energy-Related Pollutants on Respiratory Functions and Pulmonary Defense Mechanisms — A.D. Chanana, D.D. Joel.  
Effects of Chemicals and Radiation on Control of Hemopoiesis — E.P. Cronkite, H. Burlington, S.L. Commerford, D.D. Joel, M.E. Miller.  
Measurement of Cell Death in Animals Chronically Exposed to Toxic Agents — S.L. Commerford.  
Assessment of Exposure-Effects of Relationships of Chemicals Representing Risk Analysis Units to Human Health — M.T. Pavlova, E.P. Cronkite, M.E. Miller.

The Detection of Residual Injury by Pollutants and Rapid Testing for Leukemogenesis — E.P. Cronkite.  
Penetration Through the Gut and Bioeffects of Particulates From Nonnuclear Energy Production — M.E. LeFevre.  
Early and Late Effects of Energy-Related Pollutants on Immunologic Systems — R.D. Stoner.  
Regulatory Mechanisms of Erythropoietin Production (NHLBDI) — M.E. Miller.

**Hospital of the  
Medical Research Center**

K.P. Mohring, Hospital Administrator  
A.D. Chanana, Chief of Staff  
V. Brooks, Supervising Head Nurse

**Occupational Medicine Clinic**

L.D. Sbarra, Head  
K.P. Fatimi                      A.M. LoCastro

**Employee Counseling**

J.F. Katsin

---

# Biology Department

## INTRODUCTION

Highlights are events of paramount interest, and the purpose of this report is to describe some of the major achievements of the Biology Department during 1982. A considerable number of notable advances have been made this year, discoveries that have prompted a rethinking and reassessment of former biological tenets. All of these achievements cannot be described within the space allotted here; for fuller coverage we recommend consultation with the members of the staff of the Biology Department who are listed at the end of this report.

We shall describe our work under four arbitrarily chosen but convenient headings: Biological Structure Determination, Molecular Genetics, DNA Repair, and Plant Sciences. In actual practice, our procedures and approaches to biological problems are such that they call for the integration of the strengths and expertise of our 27 staff members, and encourage cooperation with outside researchers. Last year over 97 researchers from academia and industry came to Brookhaven to use our unique biophysical facilities, and another 61 investigators visited the Department to collaborate on our various biological projects.

In Biology, we have several unparalleled specialized instruments for the study of biological structure. These tools include the National Synchrotron Light Source (NSLS) which supplies high-intensity beams of photons at wavelengths from 0.5 Å to the infrared. Beams in the x-ray region measure small-angle diffraction and x-ray scattering by molecules; a beam line on the ultraviolet ring measures circular dichroism at short wavelengths where the transition from the B to the Z form of DNA is apparent. The High Flux Beam Reactor provides neutrons for studies of the structure of molecules, ribosomes, chromatin, and membranes by diffraction and small-angle scattering. Our Scanning Transmission Electron Microscope can image unstained structures down to resolutions of 2 Å, so that the masses of molecules and viruses can be

determined with precision. Considerable time and effort are devoted to keeping these instruments at the state of the art, and together they form an invaluable national resource available to our own staff members and outside researchers alike.

Knowledge of biological structure without an understanding of function would be a sterile pursuit. A large part of the research effort in the Department therefore is aimed at learning how biological systems work. Central to this aim is the study of DNA, the genetic material of cells. Damage to DNA by physical and chemical agents affects the ability of the cell to reproduce and to use the DNA as a template to make the proper proteins needed for survival. A detailed understanding of these effects requires an intimate knowledge of the sequence of the coding units of DNA and how such coding units control the synthesis of normal or aberrant proteins. Perhaps we are approaching this problem in the best possible way by looking at simple organisms with rather little DNA. Last year there was a major breakthrough when biologists completed the entire sequence of the T7 bacteriophage, 39,936 subunits in all, opening the way to use this information to determine how subtle changes in replication and in protein synthesis might follow from slight changes in the genetic code. Gene cloning is a valuable tool used extensively by members of our Department to investigate genetic mechanisms in bacteria and plants. Both fields of research are highly productive and beneficial. An understanding of the encoded messages of the genomes of bacteria and viruses could lead to the development of new and more effective vaccines. Our basic researches in plant sciences are vital to solving the problems of protecting crops from pests and diseases and increasing agricultural productivity, a worthy endeavor in today's hungry world.

The effects on humans of low doses of radiation and of other energy-derived hazards are long-range problems of universal concern. Exposure to physical and chemical agents in the

environment can cause mutations in cells which might lead to cancer. There are a number of repair mechanisms that cells employ to reverse or remove DNA damage, and these processes lessen the probability of the initiation of cancer by about 10- to 10,000-fold. Several members of our Department are looking closely at DNA repair mechanisms, and very recently they recognized that there were quite large variations in DNA repair capabilities amongst the so-called "normal" population. This line of research is being vigorously followed up, as the outcome of this aspect of the health-effects data will have a significant influence on the evaluation of hazards and current exposure limits recommended by Government agencies.

Julian Huxley pointed out that people living in a revolution often do not recognize it. We have here at Brookhaven National Laboratory a Department which is part and parcel of the current exponential expansion of biology. We hope that our report will convey a satisfactory account of this involvement and excite the interest of those who want to know more about advances in modern biology.

## BIOLOGICAL STRUCTURE DETERMINATION

### Neutron Diffraction

Studies of protein structures by x-ray crystallographic techniques have demonstrated the inherent physical order of proteins and have given insight into their interrelationships, with their architectural, mechanistic, evolutionary, and specificity differences. Three-dimensional structure of proteins is determined largely by the behavior of hydrogen atoms. The general role of hydrogen as a determinant of the structural and functional is well understood, but its role in specific instances is seldom known. Unfortunately, hydrogen atoms are weak x-ray scatterers and therefore cannot be directly located in x-ray Fourier maps.

Neutrons, however, serve as a unique probe for localizing hydrogen atoms and distinguishing between hydrogen and deuterium. This distinction is particularly important in the study of enzymatic sites that include charge relay systems and in studies that probe protein dynamics by hydrogen exchange. Neutron diffraction

studies also provide the ability to distinguish nitrogen from carbon and oxygen and allow correct orientation of groups such as histidine and glutamine. Neutron diffraction studies can be made in the Biology Department because we have the High Flux Beam Reactor and unique related facilities available to our staff and to outside investigators. To date, Benno P. Schoenborn and his associates (in collaboration with outside users) have studied several proteins and their derivatives to elucidate particular functional aspects of the specific protonation of active groups such as histidine and glutamic and aspartic acids. These proteins include carbon monoxide myoglobin, oxy- and met-myoglobin, trypsin, and crambin. Myoglobin forms large crystals (25 mm<sup>3</sup>) and is ideal for neutron studies, producing good diffraction intensities. The group have investigated in detail hydrogen-deuterium exchange in the different forms of myoglobin, and also have preliminary exchange results for trypsin and crambin. There is a continuing effort to develop new counters, shields, and monochromators to improve the efficiency of data collection and the resolution of the spectrometers. The installation of a new plug and shield for the protein station has just been completed, improving the effective flux fivefold.

The crystal structure of the protein crambin, a small hydrophobic plant toxin, is being studied by Martha Teeter (Boston University), and by Anthony A. Kossiakoff and their associates. Neutron diffraction from these crystals extends to very high resolution (1.3 Å) and, therefore, this system presents the rare opportunity to study the structure of a protein at virtually atomic resolution. One ultimate role of the crambin neutron analysis will be to establish the degree of deviation from "ideal" stereochemical geometry that actually exists in a protein molecule, a rather hotly debated issue. The unequivocal location of the hydrogen atoms in crambin as determined by neutron diffraction, together with the high resolution of the data, should provide the accuracy necessary to give pertinent new insights. Neutron data have been collected and analyzed for crambin and the structure is being refined: the current model is of excellent quality, as judged by refinement statistics and the clarity of the resulting Fourier maps. An example of the degree of detail obtain-

able from this analysis is shown in Fig. 1. Our preliminary findings suggest that the protein's bonding geometry is very close to ideal.

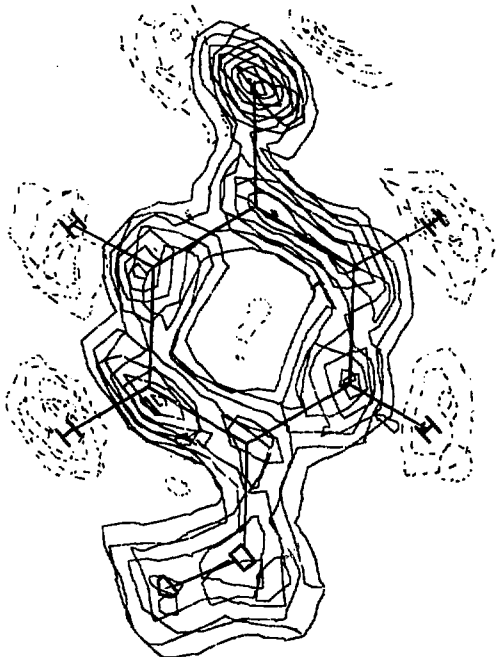


Figure 1. Fourier map of crambin showing the location of the hydrogen atoms on a tyrosine residue including the exchangeable hydroxyl group.

### Synchrotron Ultraviolet Project

The Synchrotron Ultraviolet Project, which is attached to port U9B at the NSLS, was one of the first stations to begin operating when radiation became available to users in the summer of 1982 at the light source. Initial experiments by John C. Sutherland and his group emphasized the vacuum ultraviolet circular dichroism (VUVCD) of DNA. In previous years this group had measured the CD spectrum of poly (dG-dC) · poly (dG-dC) at the ultraviolet radiation synchrotron storage ring at the National Bureau of Standards. These data, combined with their new findings obtained at BNL on poly (dI-dC), a synthetic DNA, indicate that VUVCD at wavelengths of less than 200 nm is a much more accurate indicator of the helical conformation

(i.e., right or left handedness) of double-stranded DNAs than is the CD spectrum of the far ultraviolet (200 to 300 nm) that can be easily studied with conventional spectrometers.

### Scanning Transmission Electron Microscopy

Electron microscopy has been an essential tool in the study of biological systems for the past 30 years. A big step forward was made in 1971 when it was shown that single heavy atoms could be visualized using a new type of electron microscope called the Scanning Transmission Electron Microscope (STEM). In 1972, work began on the installation of a STEM in the Biology Department; the microscope became fully operational in 1977, and our exciting new research facility became available to scientists in the eastern United States. Joseph S. Wall and his group are engaged in structural studies of biological material, employing either quantitative microscopy or heavy-atom staining.

This year the STEM staff have passed a number of significant milestones. They have produced the first pictures of heavy-atom cluster compounds bound to specific sites in biological molecules. They have also demonstrated a new and unexpected structure for dynein, the molecule that serves as the "motor" for cilia and flagella (see Fig. 2). The rapid acceptance of

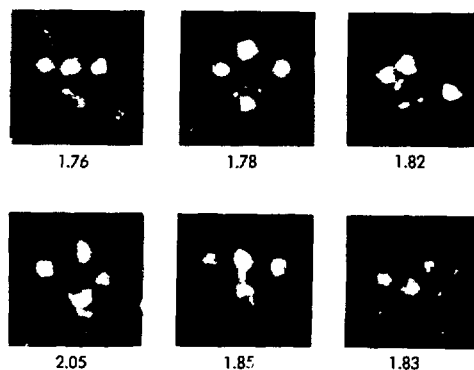


Figure 2. Gallery of dynein molecules (the "motor" from cilia and flagella) showing three balls connected by thin threads to a base assembly. The number below each complex is its mass in megadaltons. Two heads have a mass of 450 kD each and the third has a mass of 550 kD, in good agreement with biochemical studies.

their dynein model by other specialists was due largely to the ability of the STEM to "weigh" single molecules and their subdomains, thus providing a hand-in-glove fit to previous biochemical studies.

Heavy-atom studies use clusters of 11 gold or 12 tungsten atoms as miniature "flags" that can be attached to interesting regions of a molecule in order to spot them in the final image. So far the BNL group have been able to label four different kinds of sites: sugars, two kinds of amino acid side chains, and biotin-binding sites. These reagents are likely to have widespread application both to our own projects and to those of outside users.

Paul V. C. Hough and his group, together with the staff of the STEM facility, Robert Roeder (Rockefeller), and Peter Tegtmeyer and Iris Mastrangelo (both from Stony Brook), are studying the structural components and assembly of DNA-protein complexes that control transcription in eukaryotic cells. The protein TFI<sub>II</sub>A, a transcription factor for RNA polymerase III, is obtained from amphibian oocytes; this protein binds to a specific region within the 5S rRNA gene. Study of this particular gene is of special interest because there is an abrupt switch in its expression during the development of the animal. Another group of proteins from human cells enable accurate and selective *in vitro* transcription by RNA polymerase II, the enzyme that transcribes most other genes. T-antigen, a repressor of transcription, appears to bind to groups of pentanucleotides adjacent to transcription initiation sites. By withholding two ribonucleotide triphosphates, RNA polymerase II initiation complexes are immobilized at promoter regions. One of the several most complex structures observed is shown in 3D projection (Fig. 3). This  $1 \times 10^6$  dalton complex has a characteristic division into a "tau-complex" (~100 kD) on the downstream side and two subregions which can be identified with the large subunits of polymerase II (210 and 140 kD). TFI<sub>II</sub>A appears to bind as tandem monomers, although dimers also bind suggesting that tandem monomers could re-associate with replicating DNA to extend 5S transcriptional control through cell division.

Partially purified T-antigen occurs as different oligomers (mono- to dodecamer). Binding seems to occur first to single pentanucleotides,

and, progressively, to up to seven pentanucleotides in tandem. Assembly of oligomers, after monomer binding to DNA, may be a mechanism of controlling template activity by making particular sites more or less accessible. This work will contribute basic scientific information which will be valuable in understanding mechanisms of carcinogens.

### Protein Chemistry

Marshall Elzinga and his group are studying the chemical nature and structure of contractile proteins, in order to provide a basis for understanding the mechanism of biological force generation in terms of specific interactions among these proteins. Myosin is the crucial protein in the contractile apparatus of muscle, and last year the group essentially completed the amino acid sequencing of the enzymatically active portion of the protein. The energy for muscle contraction comes from the hydrolysis of ATP by myosin, and two regions of the molecule which contribute to the catalytic site have been localized. One unusual feature of myosin is the presence of several methylated amino acids, among which is trimethyllysine, which is found in one of the ATP-binding sites. Movement results from interaction of myosin with another protein called actin, and the region of myosin involved in this interaction has been tentatively located. Our myosin sequence information provides an exact framework upon which to build a precise model showing how myosin carries out its many functions.

The research program of Elliott N. Shaw and his colleagues is aimed at understanding the specificity of proteases and developing small synthetic reagents which can selectively inactivate them. This work has important medical application as it explores the means by which chemists can design therapeutic agents which may counteract the deleterious action of proteases. Of the white blood cells that invade the lungs in large numbers, the polymorphonuclear cells and the macrophages are of major importance with respect to their possible roles in the pathogenesis of the lung. These cells have a high content of hydrolytic enzymes (thiol proteases) that normally function intracellularly to digest foreign material scavenged from the body. However, particulates such as smoke or dust can stimulate these cells to release their

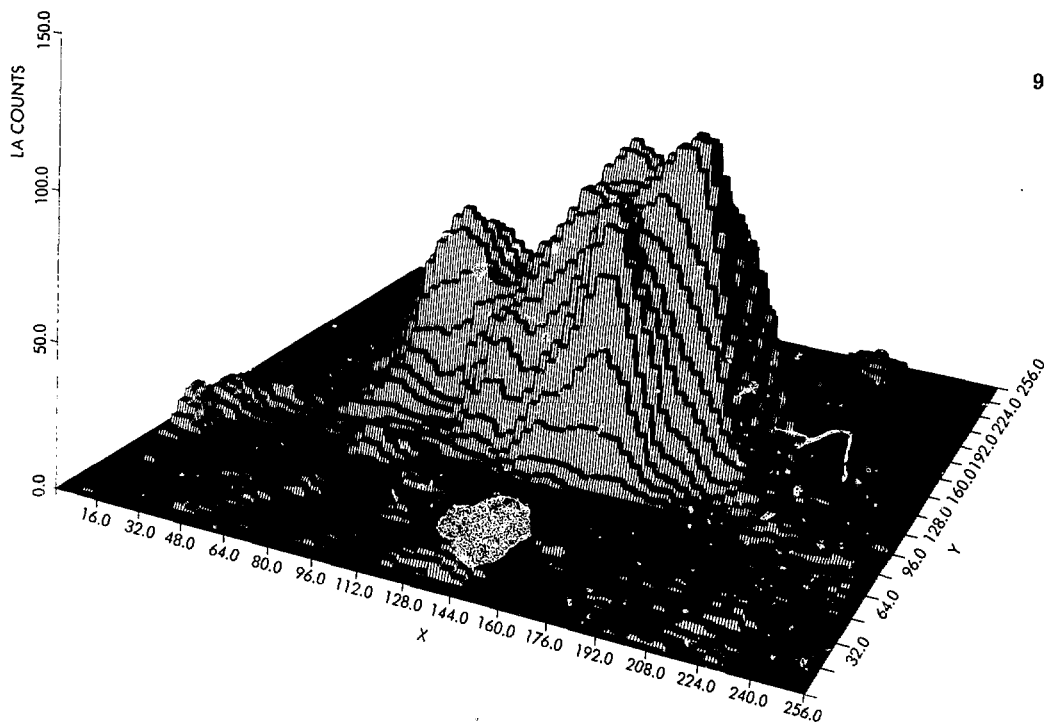


Figure 3. The vertical scale shows the mass distribution for a Pol II initiation complex, as a function of position as given by the axes X and Y. The X and Y scales are in units of 1.25 Å, but, as can be noted by the size of the boxes scattered over the plain, measurements are made only every  $5 \times 5$  Å ( $0.5 \times 0.5$  nm). The vertical scale also gives approximately the vertical height of the molecule on the same scale as X and Y. The initiation complex has assembled on DNA, which can be seen as a low meandering hump entering the complex at the left and leaving at the right. The assembly will move to the left on the DNA and begin synthesizing messenger RNA at a point just off the field shown.

digestive granules (lysosomes) extracellularly where their content of hydrolytic enzymes may attack and degrade connective tissue in the lung.

Cathepsin B and cathepsin L are thiol proteases that coexist in lysosomes and are involved in the intracellular degradation of protein. To determine their relative contributions to this process, the research team has been attempting to develop a specific inhibitor. A group of peptidyl diazomethyl ketones was synthesized with a range of activities against cathepsin B. A representative number of these reagents have now been evaluated as inhibitors of cathepsin L. As expected, some of them are very effective against both proteases. However, the ones with large side chains in the primary specificity site region that prevent them from being effective against cathepsin B nevertheless are active against cathepsin L. The research team had earlier described the inactivation of cathepsin B by reagents that function by disulfide

exchange. New disulfides have been synthesized that are effective in binding to the active center of cathepsin B due to a peptide structure. This binding property was used to develop a new procedure to isolate and purify proteases; it seems likely that the new technique will have wide applications. The protein chemistry of purified cathepsin B has been examined also as a prelude to establishing the site of action of irreversible inhibitors of the enzyme. By labeling the active center thiol with a radioactive peptidyl chloromethyl ketone, the subsequent protein chemistry was made easier, and it was shown that the enzyme was present in a single-chain form and a double-chain form. The amino acid sequence of the smaller chain was investigated in collaboration with Marshall Elzinga's group. It is nearly identical to the sequence of the rat liver enzyme that had been purified by multiple-ion-exchange procedures. Thus, there is no doubt about the nature of the product obtained by this new procedure. The technique



is an advance over earlier methods, both in its simplicity and in its yield of a relatively large amount of material.

During the past year inhibitors have been synthesized for the serine proteases, plasmin and thrombin, which are involved in blood coagulation and clot lysis. Plasmin tends to favor proteolysis at lysyl rather than arginyl residues; therefore, the newly synthesized inhibitors are derivatives of lysyl chloromethyl ketone. Since plasmin does not seem to be as sensitive to amino acid sequence as other trypsin-like proteases, amino acids with large side-chain extensions were introduced that could be topographical probes for potential binding regions near the usual specificity sites.

## MOLECULAR GENETICS

### Bacteria and Viruses

Researchers in Carl W. Anderson's laboratory are studying the interaction of a group of human viruses called adenoviruses with different types of cells. Adenoviruses cause a cold-like disease in humans, although most human colds are caused by other kinds of viruses. However, adenoviruses can be safely used in studies of how viruses work and of the human cells in which they grow. The BNL group are particularly interested in the differences between cells which will and cells which will not allow virus growth, and in changes in viruses that will allow growth in cells that previously did not support such growth. Such studies will identify the viral and cellular functions important to virus growth, and they may point to pathways which can be interrupted by antiviral drugs.

Recently it was found that peripheral human lymphocytes neither support the growth of nor are killed by adenovirus type 2. One reason is that the lymphocytes do not have receptors that are necessary for adenovirus 2 to bind to the cell membrane. It is interesting, however, that several cell lines derived from human lymphocytes do have adenovirus 2 receptors, but most of these cells also are not killed by the virus, nor do they allow the virus to grow. Thus receptors alone are not sufficient for virus-induced cell killing or for the initiation of a virus infection. Adenoviruses seem to require a host cell function for growth, and it may be possible to identify this function and prevent viral infection by finding drugs which inhibit it.

In a second study, these investigators have examined four virus mutants that can grow in African green monkey cells which normally do not permit adenovirus growth. DNA sequence analysis has shown that all four mutants have exactly the same nucleotide change, which strongly suggests that there is only one way that adenovirus can change to acquire this extended growth capacity. The changed nucleotide was found to reside in a viral gene for a DNA-binding protein that is required for virus replication and for the control of the expression of some other viral genes. Why a change of a single amino acid in this protein allows the virus to grow in both human and monkey cells is not yet known. One possibility is that the mutant viral protein is better able to interact with a monkey cell protein necessary for growth.

The objective of the researches carried out by Sanford A. Lacks and his associates is to gain a basic understanding of the underlying mechanisms of the regulation of gene expression and DNA damage and repair. Cells from several species, including mammals, have been observed to take up externally provided DNA and to incorporate it into their own genomes. The bacterial species *Streptococcus pneumoniae*, in which genetic transformation by DNA was first discovered, has an elaborate system for incorporating external DNA. It is an excellent system in which to achieve the understanding which the BNL group seeks.

Insight into the regulation of gene expression was obtained by the cloning of normal and mutant forms of the gene in *S. pneumoniae* that enables the bacteria to grow on the sugar maltose. Determination of the nucleotide sequence along the length of a 3500-base DNA segment revealed for the first time in this species the nature of control signals for transcription and translation of the genetic message. Mutations that disrupted the transcription control signal or altered the composition of its adjacent DNA sequence drastically reduced the formation of the gene product, an enzyme that breaks down maltose to glucose.

Mistakes made in the replication of the DNA can lead to mutations and cell malfunction. Cells of *S. pneumoniae* and other living organisms have the ability to correct DNA strand mismatches that result from such mistakes. Determination of the DNA sequence in a nor-

mal gene and a series of mutants and the analysis by genetic transformation of the frequency of correction have demonstrated a correlation between the frequency of repair and the type of base change corresponding to a particular mutation. The "heteroduplex" repair system recognizes and corrects certain types of base mismatches more readily than others. Those mismatches that are not readily repaired may cause deleterious mutations.

Bacterial cells protect themselves from infection by viruses with restriction enzymes that destroy the DNA of the virus. *S. pneumoniae* cells can produce either of two complementary restriction systems that differ in the methylation of the target sequence in the DNA. In experiments designed to define the genetic basis of restriction enzyme production, DNA-mediated transfer of genes for the formation of these restriction systems was achieved.

Drastic changes in gene expression occur when a mutation, either directly or indirectly, affects a cellular mechanism that regulates gene expression. Viruses such as T7 have a well-characterized program of gene expression and are invaluable for studying regulatory mechanisms. Last year John J. Dunn and his associates determined the entire nucleotide sequence of T7 bacteriophage (39,936 residues), the longest known sequence. Thus equipped, they proceeded with intensive studies dealing with gene expression, especially the factors important in controlling the overall rate and fidelity of translation. In one such study they have shown that nearly 92% of the T7 DNA is utilized as coding sequences for T7 proteins. The junctions between the 50 coding sequences for adjacent genes are close, with the termination triplet for the first protein often overlapping the initiation codon for the next protein. Untranslated regions interspersed with the coding regions are not large and usually contain other genetic signals such as transcription termination signals and promoters. Almost all T7 proteins seem to be synthesized independently, each from its own ribosome-binding and initiation site. A few genes specify pairs of overlapping proteins by initiating synthesis at two separate initiation sites in the same or a different reading frame. At least two genes specify pairs of proteins that result from a shifting of the reading frame during translation.

The most striking example of frameshifting occurs during synthesis of the major capsid protein of T7, specified by gene 10. This protein, p10, separates into two bands during gel electrophoresis; the faster migrating band, p10A, has a molecular weight of 38,000 and is the most abundant T7 protein made in infected cells. The more slowly migrating band, p10B, with a molecular weight of 45,000, is made in far smaller amounts, but it is also present in phage heads. Both forms of p10 are eliminated by single amber mutations in gene 10, which is consistent with their being coded for by the same gene. Experiments have ruled out the possibility that p10B is a precursor of p10A. The gene 10 nucleotide sequence suggests that the smaller version is synthesized by ribosomes that remain in the normal reading frame and that p10B is made by a shift in reading frame during translation of the p10A protein.

A direct consequence of having the entire nucleotide sequence of T7 DNA is that one can clone individual T7 genes and genetic signals with a great degree of precision, since every potential restriction site in the DNA is known. F. William Studier and his group in continued collaboration with John Dunn and his associates have extensively cloned T7 genes and their genetic signals; last year this work reached the stage where all parts of T7 DNA were represented as cloned fragments. They also are constructing complementing plasmids, which have complete T7 genes that can supply T7 proteins during infection. Under appropriate conditions, these plasmids can be made to produce T7 proteins in uninfected cells. The goal is to obtain such a plasmid for each T7 gene. A notable success this year was the cloning of the gene for T7 RNA polymerase, which a number of laboratories have tried unsuccessfully to accomplish. With their detailed experience and the aid of a large collection of T7 mutants, the BNL group devised a strategy that cloned the active gene and placed it under the control of a host promoter.

An especially interesting problem is that of how the T7 DNA escapes degradation by host enzymes upon entry into the cell. The first T7 protein made after infection, the gene 0.3 protein, prevents the DNA restriction system of *E. coli* from degrading T7 DNA. The antirestriction protein, however, is not made until three or

four minutes have elapsed after infection. Research is now aimed at elucidating the factors that prevent restriction but not transcription in the early stages of infection.

### Plants

Daniela Sciaky and her colleagues have continued their studies of crown gall, a neoplastic disease of dicotyledonous plants caused by the bacterium *Agrobacterium tumefaciens* (Fig. 4). Crown gall is especially interesting to biologists as it is a naturally occurring genetic engineering system in which bacteria transfer and express their genes in plants. Virulent forms of the bacteria contain a large tumor-inducing (Ti) plasmid. This year the group has analyzed the sequence arrangement of two different mutational events that have produced tumors of

altered morphology; normally undifferentiated callus is now producing shoots (teratomas) (Fig. 4). One mutational event can now be ascribed to the insertion of an *A. tumefaciens* transposable element in the T-region of the Ti plasmid. The other mutational event appears to be due to a rearrangement of the T-DNA within the transformed plant cell. How this rearrangement has occurred will be the subject of future investigations.

One of the phenomena in plants that may be useful for genetic manipulation is that of controlling elements, which are subunits of genetic material that transpose from one location to another in the chromosome complement and modulate gene activity where they reside. When controlling elements insert into a functional gene, they frequently inactivate the gene or alter its activity, thereby giving rise to a mutant



Figure 4. Graft of *Nicotiana otophora* differentiating octopine tumor on *N. tabacum*. Note the "waffling" texture of the leaves.

phenotype. Benjamin and Frances A. Burr and their group have been studying insertions of such transposable elements at the *Shrunken* (*Sh*) locus in maize which encodes the enzyme sucrose synthetase. Using recombinant DNA methodology they obtained a genomic clone of sucrose synthetase. Subclones constructed from the initial genomic clone were used to define the positions and structures of controlling elements associated with mutations of the gene. Elements called *Ds* (*Dissociation*) were found to be very large (over 20 kilobases in length) with a rather heterogeneous internal structure, an unexpected finding as the elements were genetically derived from the same progenitor. The structural differences might be related to inherent qualities of these elements which promote internal rearrangements during transposition. Two mutants of *Sh* contain *Ds* insertions 5' to the start of transcription but the *Ds* insertions in two other mutations actually map within the transcribed region itself, albeit in an intervening sequence.

Other transposable elements in maize are not as large and can be distinguished from *Ds* by their activity. By virtue of having a clone of the *Sh* gene, the group have begun to isolate other transposable elements that have inserted at this locus. One such element is a "mutator," called *Mu*, that is only 1.4 kilobases in size. Restriction analysis indicates the presence of inverted repeated sequences at the ends that are known to be characteristic of some described transposons. When the *Mu* element is used as a probe, it is found to be repeated a number of times in stocks with mutator activity, but is absent from those without this activity. *Mu* will now be used as a probe to isolate other genes of interest which contain *Mu*-induced mutations.

## DNA REPAIR

Repair of damage to DNA caused by environmental agents is in many instances a continuous process that enables the cell to continue replication, transcription, and division. In the case of the removal of  $O^6$ -methylguanine, a DNA adduct resulting from the exposure of the cell to environmental nitrosamines, the repair process may be inducible. For example, treatment of wild-type strains of *E. coli* with low chronic doses of *N*-methyl-*N'*-nitro-*N*-nitroso-

guanidine (MNNG) results in an adaptive response in which the cells are no longer readily mutagenized by high acute doses. This adaptive response is associated with the production of a high level of methyl-accepting protein. Chronic administration of alkylating agents to rats also indicates that there is an adaptive response in which the repair system is enhanced. Richard B. Setlow and his group found inducible repair in human cultured cells. HeLa cells were treated with single or multiple nontoxic doses of MNNG, and extracts were analyzed at various times afterwards. The acceptor activity after single exposures decreased linearly with dose, indicating that the acceptor protein was used up by reacting stoichiometrically with endogenous  $O^6$ -methylguanine. Multiple exposures resulted in a dose-dependent increase in the amount of acceptor protein up to a cumulative dose of 100 mg per ml, above which the acceptor activity decreased. Under conditions of maximum induction there were approximately threefold more acceptor sites than at the normal constitutive level.

Mammalian cells fall into two groups: proficient ( $Mer^+$ ) or deficient ( $Mer^-$ ) in methyl excision repair in terms of their cytotoxic reactions to agents that form  $O^6$ -alkylguanine and their abilities to reactivate alkylated adenoviruses. Measurements of the abilities of cell extracts to transfer the methyl group from exogenous DNA containing  $O^6$ -methylguanine showed that the constitutive level of acceptor activity, ~100,000 acceptor sites per cell, was independent of the  $Mer$  phenotype. Treatment of cells with 1  $\mu$ M MNNG for 15 min or with 2  $\mu$ M for about 2 min uses up >95% of the constitutive activity. However,  $Mer^+$  cells, which are resistant to MNNG, rapidly resynthesize new acceptor proteins, and the activity returns to the basal level in approximately 90 min. In  $Mer^-$  tumor cells and Chinese hamster cells, which are sensitive to MNNG, there is no detectable resynthesis in 90 min. Treatment of  $Mer^+$  fibroblasts or  $Mer^+$  tumor cells with multiple low doses of MNNG enhances the production of  $O^6$ -methylguanine-accepting protein, but such treatments reduce the activities in  $Mer^-$  tumor cells and in cultured Chinese hamster cells. The adaptive resynthesis of acceptor protein appears to be an important correlate of cell resistance to methylating agents.

Although the cultivation of mammalian cells *in vitro* goes back for more than fifty years, many types are not easy to grow in culture. Human cells are notoriously difficult, and systems for studying human cell transformation have been sought for years. Last year Betsy M. Sutherland and her group made an important step forward when they developed a human cell system for recognition of tumor genes. Human cells are made permeable with polyethylene glycol, and DNA is administered to the cells as a calcium phosphate coprecipitate. After growth, cells are screened for the ability to grow without anchorage; anchorage-independent growth is an excellent marker of tumorigenicity in many mammalian systems. Human cells treated with DNA from lymphoblasts of a patient with acute lymphocytic leukemia acquire the ability to grow in soft agar without anchorage (Fig. 5); DNase or restriction enzyme treatment of the DNA inactivates its transforming ability. Such anchorage-independent colonies can be picked up individually, grown in large aggregates of cells, and characterized. The transformants have high frequencies of anchorage-indepen-

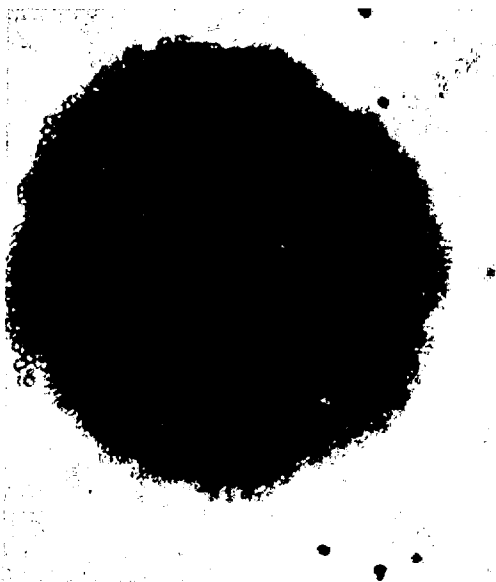


Figure 5. Anchorage-independent colony of human cells transformed by treatment with DNA from a squamous cell carcinoma.

dent growth, and their DNA can transfect naive human cells to anchorage independence.

In collaboration with investigators from Harvard and Stanford, the group continued their studies of damage to DNA caused by ultraviolet light and its repair by photoreactivation. They investigated the substrate requirements of the *E. coli* DNA photoreactivating enzyme and showed that these include the presence in DNA of a *cis-syn* cyclobutyl pyrimidine dimer (two pyrimidines joined by a cyclobutyl ring). The following bonds must be intact: the *N*-glycosyl, and the phosphodiester bonds 5' to the dimer and internal to the dimer. The enzyme is not active on the 6-4 pyrimidine-cytosine adduct (a two-pyrimidine photoproduct not joined by a cyclobutyl bond) nor on a thymine-8-methoxypsoralen adduct (a pyrimidine linked to a non-pyrimidine via a cyclobutyl ring).

Often we wish to look at DNA damage and repair in nonproliferating fresh tissue, where radioactive labeling is impractical. A short while ago, an alkaline agarose gel method for measuring DNA damage and repair in non-radioactive DNA was developed in the Biology Department which would allow accurate determination of the average molecular weights of heterogeneous populations of DNAs. Further refinements have now been added. A new, non-destructive method for making precise measurements of DNA concentrations in very small DNA samples over a wide concentration range allows us to measure DNA damage and repair in biopsy material from human skin.

## PLANT SCIENCES

The conversion of solar energy into chemical energy by plant cells sustains the biomass of the earth. The trapping of photons in photosynthetic membranes is a remarkably efficient means of converting one form of energy into another. ATP and a strong reductant are produced that together are used to fix carbon dioxide or nitrogen, synthesize cell products, or perform osmotic work. Geoffrey Hind and his associates are working within the framework of the DOE program on Biological Energy Conversion and Conservation and are especially interested in processes crucial to adaptation of or improvements in photosynthesis, nitrogen fixation, and photoproduction of hydrogen.

Heme proteins known as cytochromes occur in the energy-transforming membranes of aerobic organisms. Their role in photosynthetic electron transport is poorly understood, yet they are clearly involved in the process of bioconversion. Least amenable to study are the *b*-type cytochromes, which reside in the lipid matrix of the membrane. The group are investigating cytochrome *b*<sub>6</sub> for which they have developed an improved extraction procedure; the resulting cytochrome *b*<sub>6</sub>-*f* complex has been analyzed by low temperature spectroscopy. By careful partial reduction, a cytochrome *b* component with a split absorption band can be detected (left panel of Fig. 6). The remaining half of the cytochrome *b*<sub>6</sub> possesses a single absorption band and is thus a distinct species. These components have been designated cytochromes *b*<sub>H</sub> and *b*<sub>L</sub>, respectively, and are present with cytochrome *f* in a 1:1:1 ratio in the membrane complex. Flash spectroscopic analysis of the turnover of cytochromes *b*<sub>6</sub> and *f* in intact photosynthetic

membranes had hitherto revealed involvement of no more than half the total cytochrome *b*<sub>6</sub>. By use of a specific inhibitor, reoxidation of the cytochrome was slowed down, whereupon excitation with a second flash successfully demonstrated reduction of an additional *b* component now thought to be cytochrome *b*<sub>L</sub>, with a faster reoxidation rate (Fig. 6, right). These findings support the theoretical model developed by Nobel Laureate Peter Mitchell in which two *b* cytochromes lie on opposite sides of the lipid bilayer. Some of the free energy available when plastoquinol is oxidized by cytochrome *f* would be conserved by the reduction of cytochrome *b*<sub>L</sub>; subsequent electron transfer to cytochrome *b*<sub>H</sub> provides spatial separation of charge. This potential is the driving force responsible for ATP synthesis; it lies at the heart of the mechanism by which photosynthesis yields cellular energy for plant growth.

Blue-green algae (cyanobacteria), which commonly occur in marine and fresh waters, are

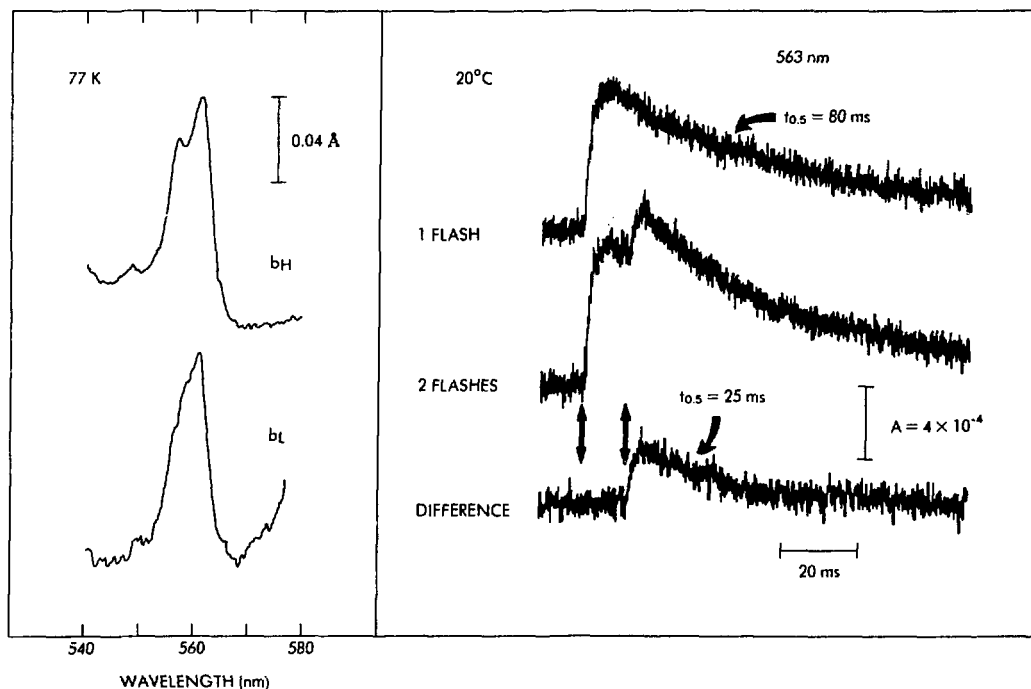


Figure 6. Resolution of cytochrome *b*<sub>6</sub> into distinct cytochromes. Left panel: resolution by spectroscopy at 77 K of isolated cytochrome *b*<sub>6</sub>-*f* complex. Right panel: resolution by relaxation kinetics following reduction by single or double flashes applied to native thylakoid membranes.

being studied by H. William Siegelman and his colleagues. The algae collect solar energy for photosynthesis by means of supramolecular arrays of colored phycobiliproteins called phycobilisomes. Light intensity and quality can regulate the composition and structure of these accessory pigments. Cells of *Microcystis aeruginosa*, a cosmopolitan blue-green alga, were grown at low and high light intensities (about one-twentieth and one-half of full summer sunlight). The content of phycocyanin (a component of the phycobiliproteins) in cells grown at high light intensity was about half that in cells grown at the low light intensity. Structural analyses of the phycobilisomes by analytical biochemical methods showed that those from cells grown at the high light intensity contained 6 molecules of phycocyanin per phycobilisome, while cells grown at low light intensity contained 12 molecules. The change in the cellular phycocyanin concentration with light intensity was paralleled by an alteration in the structure of the phycobilisomes. Similar changes in chlorophyll concentration with light intensity were also observed.

The fact that some cyanobacteria such as *M. aeruginosa* are capable of growing under light conditions which vary widely in intensity and spectral characteristics has also engaged the

interest of Myron C. Ledbetter and his group, who operate the Biology Department's electron microscope. The changes in the structure and shape of the accessory pigments, in response to light intensity, can be visualized readily by means of this instrument. When cells are grown in low light, the accessory pigments form larger phycobilisomes than when they are grown under high light. The photosynthetic pigments are associated with membranes which form broad flattened sacks known as thylakoids, with the phycobilisomes attached to the outer surface and chlorophyll molecules embedded within the membrane. Thylakoids in cells of *M. aeruginosa* grown under low light were arranged into rather closely packed parallel arrays, whilst in cells grown under high light intensity they were more irregular in outline and seldom parallel to one another (Fig. 7). These differences in thylakoid arrangement appear to be a response to differences in cell size and possibly to changes in the size of the phycobilisomes. Although the cells tend to be smaller when grown under low light, there is no apparent reduction in thylakoid membranes. This fact, and the fact that phycobilisomes become larger under low light, may produce tighter packing of all the organelles within such cells, forcing the thylakoids into parallel stacks.



Figure 7. Electron micrographs of *Microcystis aeruginosa* grown under high (left) and low (right) light intensities. Magnification  $\times 18,500$ .

Higher plants store substances that are endogenously produced and others that are acquired from their environment. Some of these accumulated substances are useful to humans while others are harmful. The former include minerals, vitamins, sugar, and pharmaceutically active molecules; the latter include toxins, heavy metals, residues from pesticides and herbicides, and hydrocarbons. Little is known regarding the mechanisms involved in cellular storage and sequestration of accumulated substances. The vacuole is a major compartment in this process, and a specific objective of George Wagner and his associates has been to understand the mechanisms which underlie the storage and sequestration of substances which are accumulated in plant vacuoles. They have shown that enzymes of phenyl propanoid and flavonoid metabolism are located in part of the endoplasmic reticulum. These enzymes are involved in the biosynthetic pathways common to the formation of lignin (the major constituent of wood, which makes up about 20% of the world's biomass), coumarins (containing many natural toxins and pharmaceutically active substances), and also flavonoids (natural pigments and toxins). To complete the picture, they are now investigating the mechanism of intracellular transport of the finished product of these pathways from the endoplasmic reticulum, through the cytosol, to their site of accumulation, the vacuole.

Vegetables are the main source of ingestion of certain toxic metals (including cadmium) for humans. But little is known about the mechanisms of toxic metal accumulation in plants or the nature of accumulated metals. Organo-Cd, -Zn, and -Ni complexes are being isolated from food plants and characterized, and their toxicities to experimental animals determined. In most studies of cadmium toxicity, experimental animals have been fed with inorganic metal salts in their drinking water or in their diet. The researchers found that cadmium occurs in plants as organo-cadmium complexes, which may have a different fate and perhaps a higher toxicity in animals than does inorganic cadmium. Methods have been developed for preparing extracts from plant leaves and from grain which contain cadmium and for characterizing the organo-cadmium complexes. By using radioisotopically labeled wheat grain, they will be

able to follow the metabolic route in mice of cadmium from grain which contains levels of the metal similar to those levels in agriculturally grown wheat.

Lloyd A. Shairer and his coworkers have continued their studies of mutagenesis with the higher plant *Tradescantia*. The very high sensitivity of the flower color gene in a hybrid clone 4430 makes *Tradescantia* eminently suitable for determining the mutagenic potential of ambient air pollution and background radiation. Exposure to complex mixtures of air pollutants, to smog, and to diesel engine emissions have enhanced mutagenic response in *Tradescantia* stamen hairs. In collaboration with Victor P. Bond (Medical Department) and Richard B. Setlow of Biology, detailed low-dose radiation experiments are being conducted to explore the mechanisms and cell kinetics involved in flower color mutation. The shapes of the dose-response curves for exposure to both chemicals and radiation show a distinct reduction in slope at low levels of the mutagen. Extrapolation of curves for effects at high doses would tend to underestimate the biological response at low doses — an observation most pertinent to health risk assessments (Fig. 8).

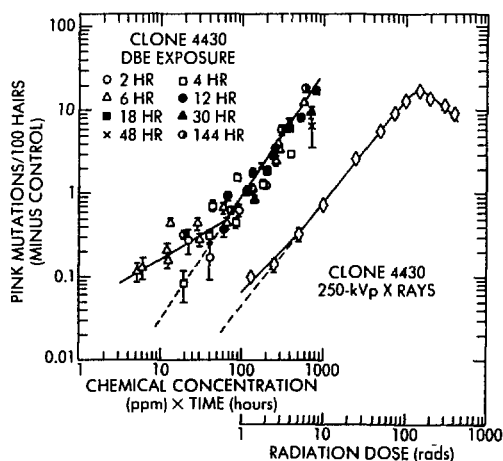


Figure 8. Mutation response induced by a chemical (ethylene dibromide) plotted against total dose. The standard x-ray curve is shown for comparison. Broken lines represent extrapolation from high-dose response curves.



## BIOLOGY DEPARTMENT

Richard B. Setlow, Chairman  
Geoffrey Hind, Deputy Chairman

### Molecular Genetics

- |   |   |
|---|---|
| <p><b>Carl W. Anderson</b><br/>Organization and expression of the adenovirus genome.</p> <p><b>John J. Dunn</b><br/>Synthesis, processing, and translation.</p> <p><b>Sanford A. Lacks</b><br/>Genetic transformation of bacteria: plasmid transfer and recombination; DNA restriction and methylation.</p> | <p><b>Jane K. Setlow</b><br/>Transformation, recombination, and repair in <i>H. influenzae</i> and its phages.</p> <p><b>Richard B. Setlow</b><br/>Damage to DNA by radiation and chemical carcinogens and its repair.</p> <p><b>F. William Studier</b><br/>Genetics and physiology of bacteriophage T7; gene expression, DNA metabolism, phage assembly.</p> |
|---|---|

### Biological Structure Determination

- |   |  |
|---|--|
| <p><b>Marshall Elzinga</b><br/>Muscle protein structure and function.</p> <p><b>Paul V.C. Hough</b><br/>Quantitative scanning transmission microscopy; interactions between RNA polymerases and defined genes.</p> <p><b>Anthony A. Kossiakoff</b><br/>Protein crystallography by neutron and x-ray diffraction.</p> <p><b>Alar C. McLaughlin</b><br/>High-resolution NMR studies of model and biological membrane systems.</p> <p><b>Benno P. Schoenborn</b><br/>Neutron diffraction of biological structures; ribosomes, membranes.</p> | <p><b>Elliott N. Shaw</b><br/>Structure and function of cellular and blood proteases; enzyme chemistry.</p> <p><b>John C. Sutherland</b><br/>Biological effects of UV; synchrotron radiation and spectroscopy.</p> <p><b>Joseph S. Wall</b><br/>High-resolution scanning transmission electron microscopy and heavy-atom staining of filamentous viruses.</p> <p><b>David S. Wise</b><br/>Small-angle x-ray and neutron scattering studies of biological receptor structure.</p> |
|---|--|

### Bioenergetics

- |  |   |
|--|---|
| <p><b>John Bennett</b><br/>Protein phosphorylation, thylakoid membranes, and phytochrome.</p> <p><b>Geoffrey Hind</b><br/>Mechanisms of energy conversion in photosynthesis.</p> | <p><b>John M. Olson</b><br/>Photosynthetic membranes.</p> |
|--|---|

### Plant Sciences

- |  |  |
|--|--|
| <p><b>Benjamin Burr; Frances A. Burr</b><br/>Higher plant molecular genetics.</p> <p><b>Myron C. Ledbetter</b><br/>Macromolecular studies by electron microscopy of DNA and other biomolecules.</p> <p><b>Lloyd A. Schairer</b><br/>Plant mutagenesis by physical and chemical agents.</p> <p><b>Daniela Sciaky</b><br/>Genetic engineering in plants.</p> <p><b>H. William Siegelman</b><br/>Plant biochemistry and physiology.</p> | <p><b>Harold H. Smith</b><br/>Use of cell and tissue culture in plant cell genetics.</p> <p><b>Jack Van't Hof</b><br/>Genetics and regulation of the plant cell division cycle.</p> <p><b>George J. Wagner</b><br/>Characterization of plant cell vacuoles; mechanisms of accumulation in plant cells.</p> |
|--|--|

# Applied Energy Science

Department of Energy and Environment  
Department of Nuclear Energy

107-108

# Life Sciences

Medical Department

Biology Department

---

# Department of Energy and Environment

---

## INTRODUCTION

The goals of the Department of Energy and Environment (DEE) are to generate a base of scientific, economic, and technical data on selected energy technologies and on the effects

of energy-related activities on the environment. These efforts are organized into four main areas: (1) Energy Sciences, (2) Environmental Sciences, (3) Energy Technology, and (4) The National Center for Analysis of Energy Systems.

---

## Energy Sciences

The Department's research in Energy Sciences comprises work in the chemical, materials, and process sciences fields. Chemistry studies include basic and applied research on synthetic photosynthetic compounds, kinetics and mechanisms of combustion reactions, metal hydrides, high temperature electrochemistry, cyclic separations, analytical methods, and related work. Materials research is being carried out on superconducting materials, hydrogen and other interstitials in metals, amorphous materials, properties of defects in materials, materials interfaces, and surface modifications. In process sciences chemical and physical methods and techniques are applied to the development of efficient and environmentally acceptable production processes and advanced materials.

### CHEMICAL SCIENCES DIVISION

#### Coulometric Titrations to Study Alloy Phases

Solid and liquid alloy phases have been studied between 700 and 900°C with the electrochemical technique of coulometric titration with

thin film electrodes. This method offers a very sensitive way to obtain the composition of the alloy phases present in a binary alloy, the thermodynamic properties of the alloys in the system, and the limits of stoichiometry of intermetallic compounds, as well as the type and degree of disorder of the compounds. Systems studied include Ca, Ba, Na, and K alloyed with Sn, Bi, Sb, and Au in the liquid and solid states.

Figures 1 and 2 show some results for Ca-Au alloys. In Fig. 1 the emf is plotted as a function of composition. Horizontal lines show two-phase regions, and vertical lines with a drop in potential show the existence of intermetallic compounds. In this case the following compounds were found:  $\text{CaAu}_5$ ,  $\text{Ca}_2\text{Au}_9$ ,  $\text{Ca}_2\text{Au}_7$ , and  $\text{CaAu}_2$ .

Figure 2 shows an enlargement of the results for  $\text{CaAu}_2$ . The experimental points are shown along with a theoretical curve; analysis indicates that the disorder present consists of Au interstitial atoms and Au vacancies. Analysis also yields the degree of disorder. Delta is the deviation from exact stoichiometry so that  $\text{CaAu}_2$  has a homogeneity range from  $\text{Ca}_{0.97}\text{Au}_2$  to  $\text{Ca}_{1.035}\text{Au}_2$ .

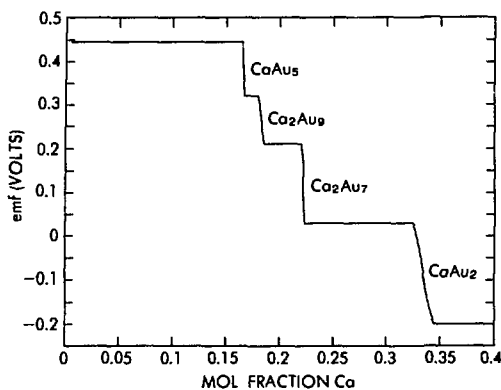


Figure 1. Electromotive force of various Ca-Au alloys, in the Ca-mole fraction range between 0.0 and 0.4, vs a liquid Ca-Sn alloy reference electrode. Horizontal lines show two-phase regions; vertical lines indicate existence of intermetallic compounds.

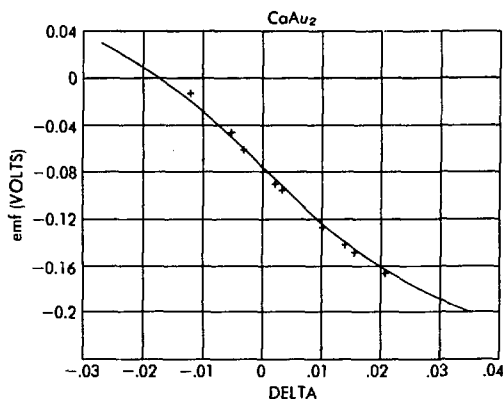


Figure 2. Variation of electromotive force of the intermetallic compound  $Ca_{1+\delta}Au_2$  around its stoichiometric point ( $\delta=0$ ), showing experimental points plotted against the theoretical curve.

### The [0.0]Ferrocenophane Cation

Dinuclear ferrocene derivatives are important for a variety of applications, e.g., conductivity in the solid state and the splitting of water. The proximity and potential interaction of the two iron atoms and the ability of these compounds to form mixed or average valence derivatives on oxidation to the monocations enhance their interest and utility. The [0.0]ferrocenophane cation has long been the subject of controversy.

Its average valence was alternatively interpreted as the result of an interaction through the cyclopentadienyl rings or as a direct interaction between the iron atoms. The structure of this cation (as a picrate with one-half of hydroquinone also in the lattice) was consequently determined by x-ray crystallography (Fig. 3), and the iron atoms were found to be  $0.34 \text{ \AA}$  closer than in the unoxidized species. This indicates that a direct interaction between the iron atoms does occur, but interaction between the rings is not excluded as a concurrent property.

The arrangement of the picrate and ferrocenophane moieties in the lattice resembles that of a charge transfer complex. Alternation of the two molecules in the stack explains the low conductivity that had been reported.

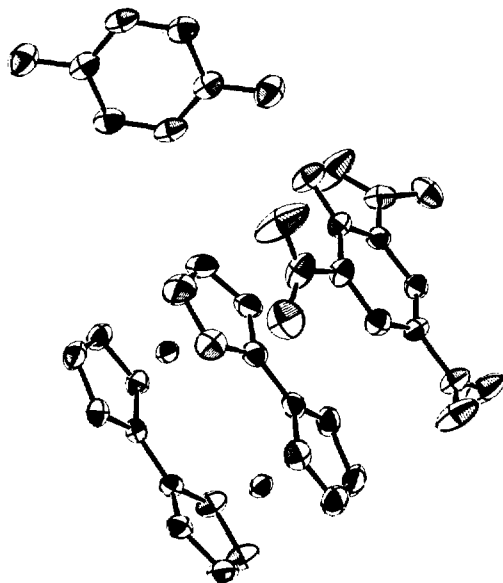


Figure 3. Diagram of [1.1]ferrocenophanium picrate hemihydroquinone. Hydrogen atoms are not shown.

## METALLURGY AND MATERIALS SCIENCE DIVISION

### Bronze-Processed $Nb_3Sn$ Superconducting Wires for Very High Magnetic Field Applications

A superconducting intermetallic compound,  $Nb_3Sn$ , has a high critical magnetic field which

makes it a suitable material for fabrication of high-field magnets. For a number of years fabrication methods and superconducting properties of multifilamentary  $\text{Nb}_3\text{Sn}$  wires have been investigated. These are now commercially produced for construction of magnetic fusion reactors and high energy particle accelerators. It has also been shown that the current-carrying capacity  $J_c$  of these wires at high magnetic fields ( $H > 12$  tesla) can be significantly improved by alloying the compound with elements such as Ti. Recently, the importance of this particular improvement in  $J_c$  has become very evident in the planned use of the superconducting wires for Magnetic Mirror Fusion Reactors. In a recent design of the reactor, it was shown that a pair of superconducting magnets producing 20 T and operating at 1.8 K are required, and these cannot be produced with the currently available  $\text{Nb}_3\text{Sn}$  conductors. The superconducting critical field  $H_{c2}$  at 4.2 K and critical current density  $J_c$  of the Ti-alloyed  $\text{Nb}_3\text{Sn}$  wires were measured at 1.8 K and 20 T for wires containing various amounts of Ti in the Nb core. As shown in Fig. 4, both the critical magnetic field  $H_{c2}$  (Fig. 4a) and the critical current density  $J_c$  (Fig. 4b) increased significantly with a small addition of Ti to  $\text{Nb}_3\text{Sn}$ . In particular, the critical current density of the wire can be improved by a factor 3 or more over that for the pure  $\text{Nb}_3\text{Sn}$  by an addition of 1 to 2 wt.% Ti in the starting materials. With this improvement, it is now possible to consider the construction of 20 T magnets for Magnetic Mirror Fusion Reactors. Although it was found that additions of other elements such as Ta can increase  $H_{c2}$  and  $J_c$  of  $\text{Nb}_3\text{Sn}$ , alloying Nb with Ti is most compatible with present commercial production of fine multifilamentary  $\text{Nb}_3\text{Sn}$  conductors. These wires are now being produced.

### The Effect of Alloying on Hydrogen Phase Equilibria in Niobium

The considerable interest in recent years in the properties of hydrogen when it is dissolved in the crystal lattice of metals or intermetallic compounds is due in part to the possible application of metals as storage media for hydrogen as a fuel and to the often disastrous effects of hydrogen on the mechanical properties of

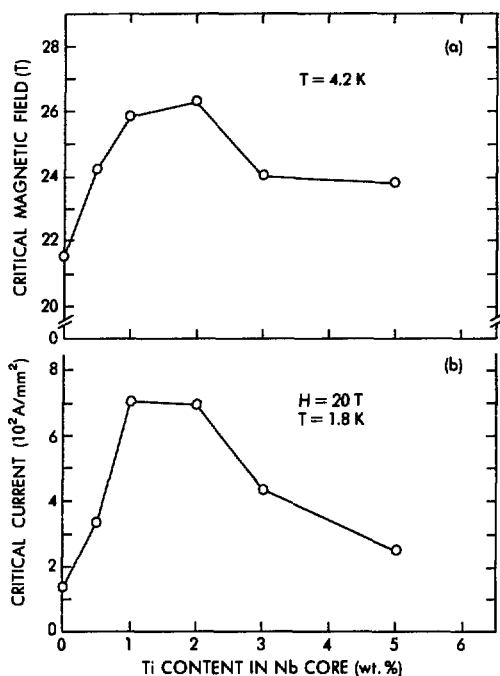


Figure 4. (a) Superconducting critical magnetic field  $H_{c2}$  and (b) critical current density  $J_c$  of  $\text{Nb}_3\text{Sn}$  wires as a function of Ti content of the Nb core.

metals. The hydrogen-niobium system is the prototypical hydrogen-metal system. More is known about this hydrogen-metal combination than any other. This system has been used as a model to investigate hydrogen-metal behavior ranging from hydrogen embrittlement to statistical mechanics. The distortion of the niobium lattice by the dissolved hydrogen atoms gives rise to an attractive interaction between them. This attraction can cause the condensation from the "lattice gas" ( $\alpha$  phase) of hydrogen atoms in niobium to either a disordered "lattice liquid" ( $\alpha'$  phase) or an ordered "lattice solid" ( $\beta$  phase). The equilibria between the  $\alpha$ ,  $\alpha'$ , and  $\beta$  phases shown in Fig. 5 resemble those of ordinary gases, liquids, and solids. The precipitation of the condensed  $\alpha'$  or  $\beta$  phases from the more dilute lattice gas can cause severe damage to the niobium lattice by cracking or plastic deformation. Some investigators have suggested that the formation of such phases at the tips of cracks in niobium is a mechanism of hydrogen embrittlement. It has been found that

replacing some of the niobium atoms by vanadium (which is completely miscible with niobium) substantially lowers the temperature at which such condensation occurs, as shown in Fig. 5. At vanadium contents near equiatomic, the precipitation is completely suppressed, apparently because of a combination of the change in the elastic properties of the metal lattice due to the substitution of vanadium atoms for some niobium atoms and the trapping of hydrogen atoms by vanadium atoms or clusters of atoms. Collaborative experiments between members of DEE and the Physics Department utilizing the inelastic scattering of neutrons revealed that the type of interstitial lattice site occupied by hydrogen changes from tetrahedral near niobium atoms to octahedral near vanadium atoms. Also, studies of internal friction caused by motion of hydrogen atoms within the metal lattice showed that the symmetry of the lattice distortion around the hydrogen atoms changes from cubic for pure niobium to tetragonal for equiatomic Nb-V alloys. Such symmetry changes alter the strength of the interaction between hydrogen atoms and crystal lattice defects, and thus the mechanical properties of the metal.

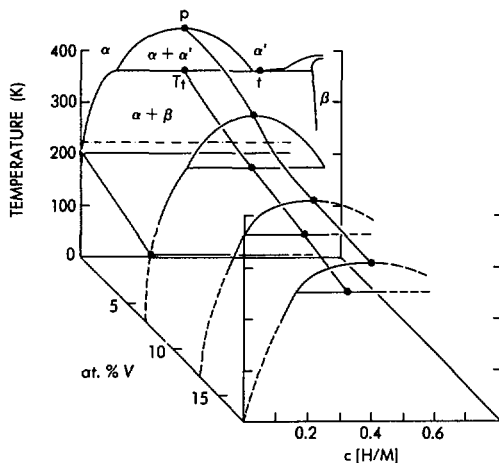


Figure 5. The addition of vanadium, a substitutional solute, into the lattice of niobium depresses the temperature of the critical point  $p$  of the equilibrium between the hydrogen lattice gas ( $\alpha$  phase) and hydrogen lattice liquid ( $\alpha'$  phase), as well as depressing the temperature  $T_l$  of the lattice gas-lattice liquid-lattice solid ( $\beta$  phase) triple point  $t$ .

### Impurity Effects in Amorphous Materials

Hydrogenated amorphous silicon (a-Si:H) is potentially useful for a variety of energy-related applications including photovoltaic devices, hydrogen production, and selective light-absorbing coatings. It is the prototype for a whole class of amorphous materials with a wide range of exploitable properties, such as extreme hardness and resistance to high temperatures and corrosion. Thin films of these materials are prepared by the Amorphous Materials Group by glow-discharge deposition, and a number of different techniques are used to study both the process of deposition and the properties of the resulting material. Solar cells with >6% conversion efficiencies have been fabricated by this group.

The starting material used in the deposition of amorphous silicon is the gas silane ( $\text{SiH}_4$ ). The purity of commercial silane in many cylinders obtained from several different manufacturers was analyzed, and the mass spectrum of silane from a rather impure cylinder shown in Fig. 6 illustrates the presence of different impurities. In general, the impurities can be divided into two categories: those containing chlorine and those containing oxygen.

The electrical conductivities of films prepared from these cylinders were found to depend on the amount of chlorine. In Fig. 7 the position of the Fermi level below the conduction band of undoped amorphous silicon films is plotted against the total concentration of chlorine-containing species in the silane used for their

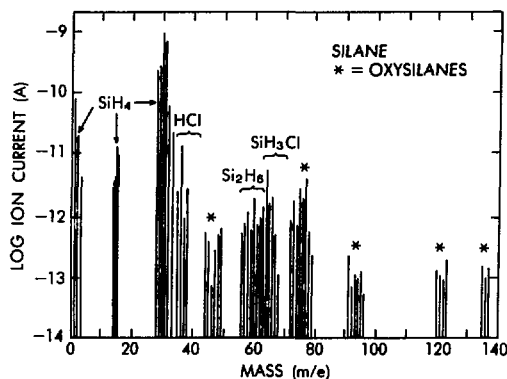


Figure 6. Mass spectrometric analysis of an impure silane cylinder, showing the presence of chlorosilanes and oxysilanes.

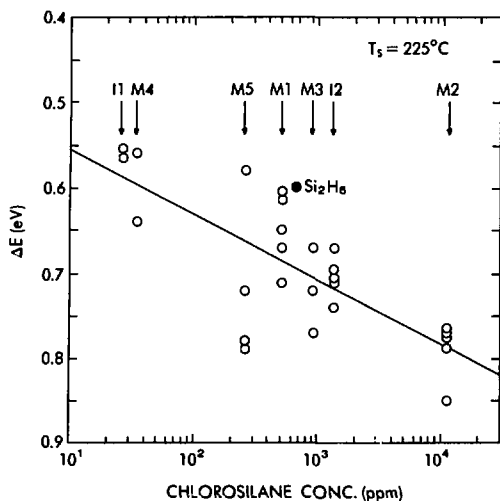


Figure 7. Fermi level position in a series of films prepared from different cylinders of silane, as a function of chlorosilane impurity concentration. Cylinder identification markings are shown.

deposition. Since the position of the Fermi level is a crucial factor affecting the performance of semiconducting devices, this study has identified an important source of variability in the electronic properties of amorphous silicon. Reproducibility of devices will require better removal of the chlorine from the starting silane in the future.

## PROCESS SCIENCES DIVISION

### Flash Pyrolysis of Coal and Biomass

The rapid or flash pyrolysis of a subbituminous coal has been performed in the presence of the nonreactive gases helium and nitrogen and the reactive gases hydrogen, methane, and carbon monoxide. The flash pyrolysis was conducted in a downdraft entrained-flow tubular reactor at temperatures ranging from 825 to 1000°C, pressures from 138 to 6900 kPa, and residence times of the coal particles between 0.5 and 8 sec. The fraction converted to gaseous and liquid products is in the order  $H_2 > CH_4 > He > CO > N_2 > Ar$ . A correlation appears to exist between the yields of product and the heat-up

rate of the coal particles. The flash pyrolysis in methane was characterized by a significantly high yield of ethylene, reaching 10.5% at 825°C and 345 kPa. This is approximately two times higher than with inert helium gas under similar conditions.

The flash pyrolysis of biomass (Douglas fir wood) with methane at 1000°C, 345 kPa, and 1-sec residence time produced a wood-carbon conversion to 22% ethylene, 12% benzene, and 48% carbon monoxide. These yields appear to be of value for an economically competitive process for the production of fuels and chemical feedstocks from wood.

### Geothermal Materials

Laboratory work, field tests, and economic studies are being carried out with polymers, elastomers, cements, polymer-concrete composites, and metallic alloys with the objective of developing materials that can withstand the corrosive effects of hot brine, that can be used for practical application of geothermal energy. A significant accomplishment was the development of a family of nitrogen-containing stainless steels. It was found that exceptionally high pitting resistance can be obtained at alloy contents much below those in conventional use today. Laboratory tests have shown that these alloys repassivate very rapidly in chloride-containing environments after the protective oxide film is broken by scratching.

### Polymer-Concrete Materials

The use of polymer-concrete materials technology developed at BNL for the repair of concrete structures is growing rapidly throughout the world. During the past year, it has been applied to numerous highway bridge decks and to the rapid repair of airport runways. The advantages of using these materials include reduced lifetime costs and energy conservation due to reduced transportation delay. A significant accomplishment is the development of a furfuryl alcohol-based polymer concrete as a water-compatible rapid-setting material for U.S. Air Force runways. A demonstration test of this material in repairing a simulated bomb crater has met Air Force specifications for military aircraft.



## Environmental Sciences

Research relating to the environment and to the impacts of energy operations is organized within four divisions: Atmospheric Sciences, Environmental Chemistry, Oceanographic Sciences, and Terrestrial and Aquatic Ecology.

### ATMOSPHERIC SCIENCES DIVISION

A varied program of basic and applied research is being conducted to study the transport, diffusion, and removal of atmospheric pollutants related to energy production and use, and their effects on air and precipitation quality. Research activities include mathematical modeling, experimental studies in the field and laboratory, and data base management. Facilities utilized in the research include meteorological towers, instrumented research aircraft, a research vessel, remote atmospheric sensing devices, meteorological tracers, automatic data acquisition systems, and a range of scientific computing facilities with peripheral hardware and graphics equipment. With these tools, processes occurring in the lower atmosphere are studied and simulated on a wide range of spatial and temporal scales.

A major modeling effort is the development of a hybrid Lagrangian-Eulerian model that will simulate the transport, simple chemical reactions, and deposition of pollutants. The model uses the output of a regional-scale numerical weather model with a moving two-dimensional grid and incorporates the effects of wind shear and variable diffusion without having to solve the full three-dimensional equations.

Another modeling study is obtaining an estimate of hydrogen peroxide ( $H_2O_2$ ) concentrations over the eastern U.S. by considering the gas-phase processes which create and destroy  $H_2O_2$ , an oxidizing agent involved in the formation of acidic precipitation.

Continued study of the chemistry of short-period precipitation samples is leading to an improved understanding of the relationships between meteorological processes and precipitation chemistry. A recent study has shown, for instance, that snow removes nitrate from the atmosphere much more efficiently than rain (Fig. 8).

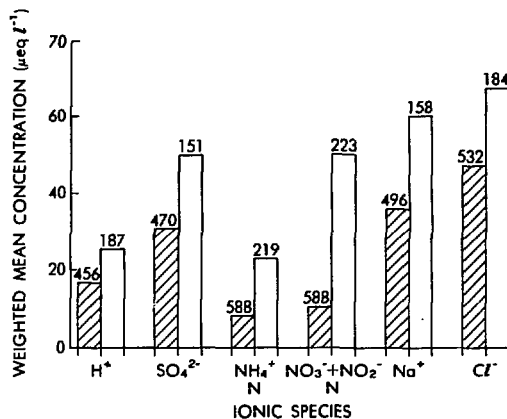


Figure 8. Weighted mean concentrations of six ionic species in all winter rain (hatched) and snow (open) hours, with number of cases indicated.

Recent studies are designed to investigate the role of clouds in the acidic precipitation process. Samples of cloudwater and rainwater are collected, using BNL's research aircraft, for real-time and laboratory chemical analysis, and concentrations of pollutants and precursors are measured around and within the cloud. Using these measurements, an understanding of those chemical reactions and cloud physics processes leading to acidification of precipitation is being obtained.

### ENVIRONMENTAL CHEMISTRY DIVISION

Research is directed toward the development and implementation of techniques to determine the concentrations of environmental pollutants arising from energy production, and the study of the interactions among them. Activities include development of measurement methodology, theoretical and laboratory studies of the reactions and properties of these substances, and field experiments.

#### Theoretical Studies

A rigorous extension of the classical theory of homogeneous nucleation to include a preexisting aerosol has been used to compute the vapor

supersaturation required to produce homogeneous nucleation for a range of equilibrium vapor pressures and aerosol surface area densities. While the aerosol corrections to classical nucleation theory are unimportant for the nucleation of high vapor pressure species, at low vapor pressures they play a major role resulting in large differences in critical supersaturation, depending upon aerosol surface area, for a given equilibrium vapor pressure.

The thermodynamics of the  $\text{H}_2\text{O}-\text{HNO}_3$  system was considered on the basis of new  $\text{HNO}_3$  partial pressure measurements. A set of thermodynamically consistent values for the nitric acid activity coefficients was first derived from water activity data using the Gibbs-Duhem equation. The Henry's Law constant was then computed from each  $\text{HNO}_3$  partial pressure measurement, including high concentration data available in the literature. A statistical evaluation of all computed values yields an average of  $(0.358 \pm 0.025) \times 10^{-6}$  for the Henry's Law constant.

### Measurement Methodology

Two new detection techniques are being developed for trace gas analysis based on the photothermal effect following light absorption. The resulting index of refraction change, which is proportional to the trace species absorption and concentration, is measured interferometrically. The first technique uses a conventional Fabry-Perot interferometer to monitor the refractive index change induced by light absorption. The second technique is a new Phase Fluctuation Optical Heterodyne (PFLOH) detection scheme whereby spectral detection is extended to the visible and ultraviolet regions. A "visible" PFLOH is currently employed for the kinetic study of surface adsorption and has been shown to be promising and sensitive for in situ measurements. In addition, a novel detection technique for a single particle is currently being employed for studying single-particle absorption spectroscopy.

A new gas chromatographic column for analyzing perfluorocarbon tracers provided improved resolution to allow determination of tracers at concentrations as low as 0.3 f/l (femto =  $10^{-15}$ ). This system will allow new tracers to be used, for example, in long-range multiple-source emission studies, while signifi-

cantly reducing the cost of the tracer. Passive samplers for collecting perfluorocarbon tracers, in studies of atmospheric air transport and building infiltration, were improved to reduce fabrication costs, increasing sampling rates 16-fold.

A new synthesis of peroxyacetyl nitrate (PAN), an important trace organic component in the atmosphere, has simplified the preparation of relatively pure samples of gas-phase PAN. With this new PAN synthesis, interference-free IR spectra of PAN can be obtained, which allows the precise measurement of PAN infrared bond strengths, which were previously unavailable. The decomposition of PAN in the absence of NO or  $\text{NO}_2$  has been studied by FT-IR spectroscopy at several temperatures and initial PAN pressures. The decomposition is measured to be first order, and PAN decomposes into predominantly methyl nitrate and  $\text{CO}_2$ , with approximately 10 to 15% of nitromethane being formed as a side product.

Optimum conditions under which a strain of *Pseudomonas aeruginosa* grows in the presence of high concentrations of thorium and uranium have been established. Under these conditions, the microorganism discriminates between thorium and uranium and produces, during its growth, new chelating agents for thorium and uranium. Preliminary studies show that these chelating agents are new natural products and differ for the two metals.

### Field Studies

In a field program carried out in Charleston, SC, the chemical composition of the liquid water and the interstitial trace gases and aerosols in liquid water stratiform clouds were measured. Interstitial trace gases and aerosols were generally found at levels consistent with their chemical and physical properties. Insoluble gases were generally present at levels comparable to those found under clear air conditions; soluble gases were never detected in clouds. The acidity of cloudwater was found to be at a level that suggests the importance of in-cloud transformation processes. Preliminary measurements suggest that an important oxidant may be  $\text{H}_2\text{O}_2$ , which has been found at levels sufficient to rapidly transform significant amounts of  $\text{SO}_2$  to  $\text{H}_2\text{SO}_4$ . In addition to the Charleston study, cloud composition measurements have

been made in the Northeast. Analysis of the data indicates that cloudwater cannot obtain its acidity by simple dissolution of ambient aerosol and nitric acid. Significant in-cloud conversion of an acid precursor (such as  $\text{SO}_2$ ) must be invoked to account for the composition of the samples.

Three Brookhaven continuous tracer analyzers were used in aircraft and at ground level for determination of parameters governing transport and dispersion from off-shore locations (~10 km) to the adjacent shoreline. Several thousand plume profiles were measured, demonstrating the utility of these analyzers. For the first time, a passive tracer sampling technique was successfully deployed in a short-range (12 km) transport and dispersion experiment. The same techniques were then employed in an 800-km tracer experiment involving transport and dispersion across the Appalachian mountains.

## OCEANOGRAPHIC SCIENCES DIVISION

The ability of continental shelves to absorb by-product materials released by energy-related activities of coastal communities depends upon the residence time of these by-products, controlled by the rate of their removal by marine ecosystem sinks. The production, transport, and fate of particles on the coastal shelf are poorly understood, when compared to the much better-known transport processes of dissolved substances resulting from the mixing and movement of the open ocean. The residence time of primary marine particles, phytoplankton, drifting with the currents in the coastal ocean is a balance of their growth from uptake of plant nutrients and other dissolved chemicals, and of their loss, both by sinking to the sediments and by consumption within the coastal food web leading to man. The ultimate repository of the biogenic coastal particles and their associated energy by-products is believed to be the sediments of the upper slope at depths of 200 to 2000 m, just seaward of the continental shelf. The Shelf Edge Exchange Processes (SEEP) program is a multidisciplinary study of the rate at which particles, and their associated energy by-products, are removed from the coastal ocean, transported to the upper slope, and processed

within these sediments. It is being carried out in cooperation with the other DOE-funded oceanographic institutions in the Northeast—Woods Hole Oceanographic Institution, Lamont-Doherty Geological Observatory, and Yale University. SEEP-I plans have been completed to make measurements of the physics, biology, and geochemistry at the edge of the continental shelf, where man-induced perturbations are minimal. The experimental plan includes field observations to be made by in situ instrumentation as well as a surface buoy, ships, aircraft, and satellites (Fig. 9).

On the basis of studies showing the absence of grazing by biological populations, and of studies on carbon and nitrogen content of sediment samples from the continental shelf and continental slope areas around the world, it has been hypothesized that organic matter produced in the ocean on the coastal shelf is exported from the shelf and ultimately deposited in the region beyond the shelf edge. The analysis of more than 36 sediment cores from the upper slope of the Mid-Atlantic Bight found  $^{14}\text{C}$  from atmospheric atom bomb testing in sufficient quantities to show that deposition was occurring over this region with rates of accumulation of 0.2 to 0.3 cm/yr. Additional evidence from  $^{12}\text{C}/^{13}\text{C}$  ratios, lignin content, amorphous silica, calcium carbonate, and clay mineralogy also supported the hypothesis that organic-rich material is exported from the continental shelf. This appears to be a mechanism for the transfer of  $\text{CO}_2$  from the upper ocean and of energy-related pollutants associated with phytoplankton from the coastal zone to the continental margin.

## TERRESTRIAL AND AQUATIC ECOLOGY DIVISION

### Sensitivity of Eastern U.S. Fresh Waters to Acidification

Work continued on building the data base of selected water quality data that had been established to identify fresh waters sensitive to acidification and to document long-term trends in water chemistry at particular sites throughout the U.S. The Acidification Chemistry Information Database (ACID) consists of  $1.75 \times 10^5$  water quality measurements on  $5.75 \times 10^5$  dates

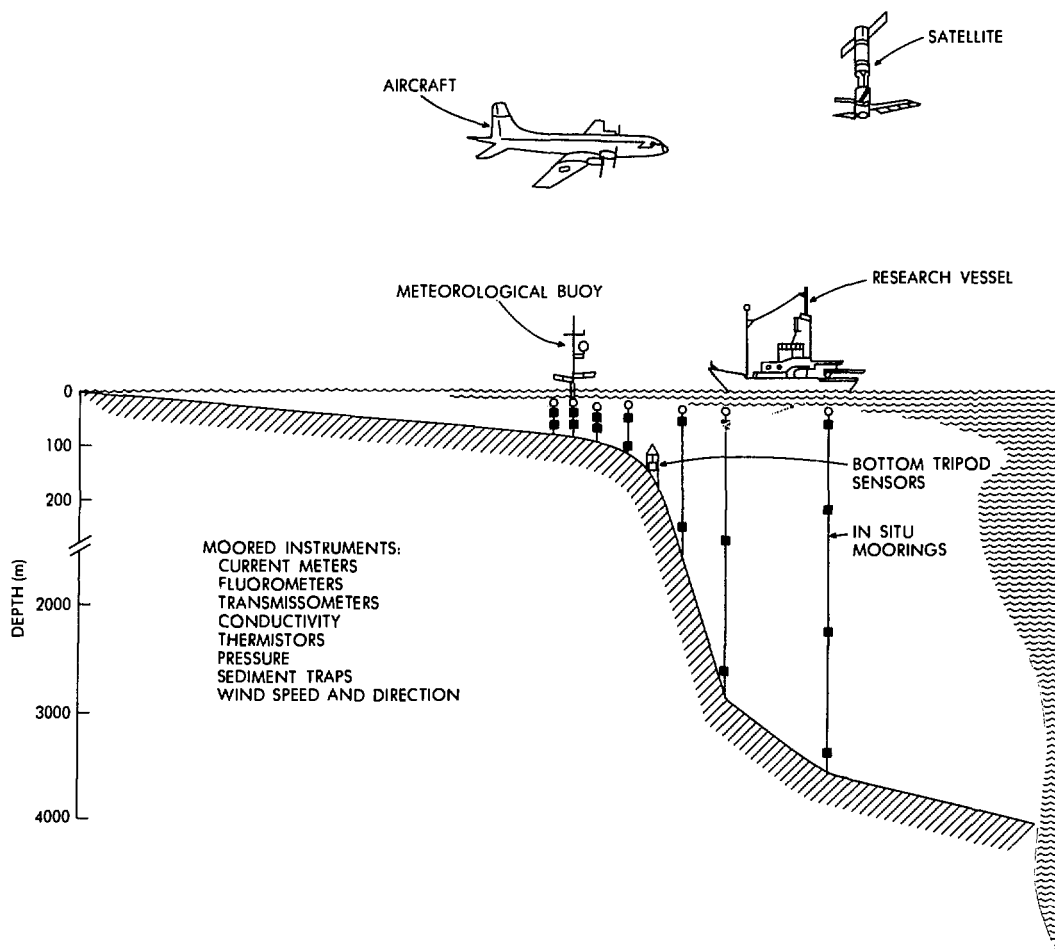


Figure 9. Diagram of the deployment of instrumentation for the SEEP Experiment.

from  $4.15 \times 10^4$  water sampling stations. Most of these data cover the 27 eastern states and come from the EPA STORET system, which emphasizes downstream sites. However, 157 sources of data not included in STORET have contributed information on sites which, for the most part, are located toward headwaters. Trend analyses found several hundred stations to have significantly decreasing alkalinity concentrations. However, the analysis of trends is not yet verified and their possible causes have not been evaluated.

### Effects of Lake Acidification on Biological Processes

The experiments on the decomposition of leaf litter in Adirondack Mountain lakes as a function of lake acidity are now in their third year. Of the five leaf species being exposed, two (red maple and sugar maple) have decomposed sufficiently that the difference in decay rates between lakes can be easily demonstrated indicating the inhibiting effect of acidity upon the microbial action.

## Energy Technology

---

Energy Technology programs are concerned with the development of advanced energy systems and components. These are technologies that offer significant improvement in energy conversion and storage, the utilization of sources that are abundant or renewable, and significant improvements in their environmental characteristics. Concepts that advance the state of the art beyond current or contemplated standards are of primary interest. These activities are organized within four divisions: Materials Chemistry and Energy Conversion, Architectural and Building Systems, Solar and Renewables, and Fossil.

### MATERIALS CHEMISTRY AND ENERGY CONVERSION DIVISION

Work in this Division encompasses the topics of electrochemistry, surface science, batteries, and fuel cells, with major emphasis on chemical/hydrogen energy storage systems.

A High Resolution Electron Energy Loss Spectrometer has been constructed which is being used to study the nature of chemical reactions on metal surfaces. The first in situ measurements using X-ray Absorption Fine Structure (EXAFS) were made on an operating fuel cell and showed structural changes of the catalyst surface as a function of cell voltage.

A range of physical and chemical means to control zinc morphology in battery systems continues to be explored and efforts continue to gain a basic understanding of mechanisms responsible for the positive and negative electrode effects observed.

Strontium-doped lanthanum has been established as a good cathodic material on high temperature zirconia-base fuel cell electrolytes, with work now under way to preserve the high catalytic activity in the anodic potential region.

The feasibility of a low temperature ( $\sim 90^\circ\text{C}$ ) alkaline fuel cell, which will oxidize carbon monoxide or  $\text{CO}/\text{H}_2$  mixtures and is likely to be tolerant of sulfur impurities in gaseous fuel feeds, was successfully demonstrated.

Static feedwater electrolysis developments have clearly shown that sea water can be electrolyzed without pretreatment in single-cell and

multicell engineering-scale hardware. Anode depolarization investigations show the potential of using coal/biomass in the electrolytic production of hydrogen at 1 V (vs 1.7 V for best current technology), with attendant energy savings and production of valuable organic by-products.

Work on  $\text{H}_2\text{SO}_4/\text{H}_2\text{O}$  industrial chemical heat pumps has culminated in the completion of detailed performance mapping of a 150,000-Btu/hr system, while markets have been identified in the pulp and paper and food processing industries.

### ARCHITECTURAL AND BUILDING SYSTEMS DIVISION

#### Energy-Conserving Architecture

Work was started on a project to evaluate a class of residential structures described as "super-insulated." By using above-normal levels of insulation and taking steps to achieve very low air infiltration, heating needs are met on all but the coldest days by heat from occupants, lighting, and appliances. Special problems must be dealt with, however, such as maintaining acceptable air quality. The effort includes a survey of the concept, instrumenting and monitoring the heating season thermal performance of a representative superinsulated house in Vermont (Fig. 10), and cooperation in field evaluation of houses which have been developed by the Small Homes Council of the University of Illinois, where the superinsulated home concept originated.

### FOSSIL DIVISION

Coal utilization and coal conversion continue to be of primary interest in 1982. Utilization efforts deal with improving the characteristics of coal as a fuel for direct combustion application, and with reducing the problem of the increased ash levels which result when oil-fired equipment is refitted for coal firing. Coal preparation, which includes cleaning and size reduction, represents another approach to improving coal utilization. Coal conversion presents a route to the production of liquid fuels from coal, and the work of the Division has been concerned with the production of jet and diesel fuel.



Figure 10. The Blouin Superinsulated House in South Royalton, VT, currently being monitored by Brookhaven.

### Catalysts for Coal Conversion

A highly flexible slurry reactor system (Fig. 11) has been designed and constructed which

facilitates long-term catalyst evaluation under a wide variety of conditions. Built around a one-liter Continuous Stirred Tank Reactor (CSTR), the system may be operated between ambient temperature and  $340^{\circ}\text{C}$ , and between ambient pressure and 13 800 kPa (2000 psi). The modular design allows for replacement of the CSTR with other reactor configurations, such as a bubble column. The system features precise temperature, flowrate, and pressure control. Precise monitoring of inlet and outlet flowrates is possible, with compositional variations followed by means of a simple and versatile gas chromatographic subsystem. Although designed to evaluate catalysts for the Fischer-Tropsch reaction, the system may be used for testing a wide variety of other types of catalysts. This system will also allow better assessment of chemical and engineering attributes of the slurry concept in catalysts.

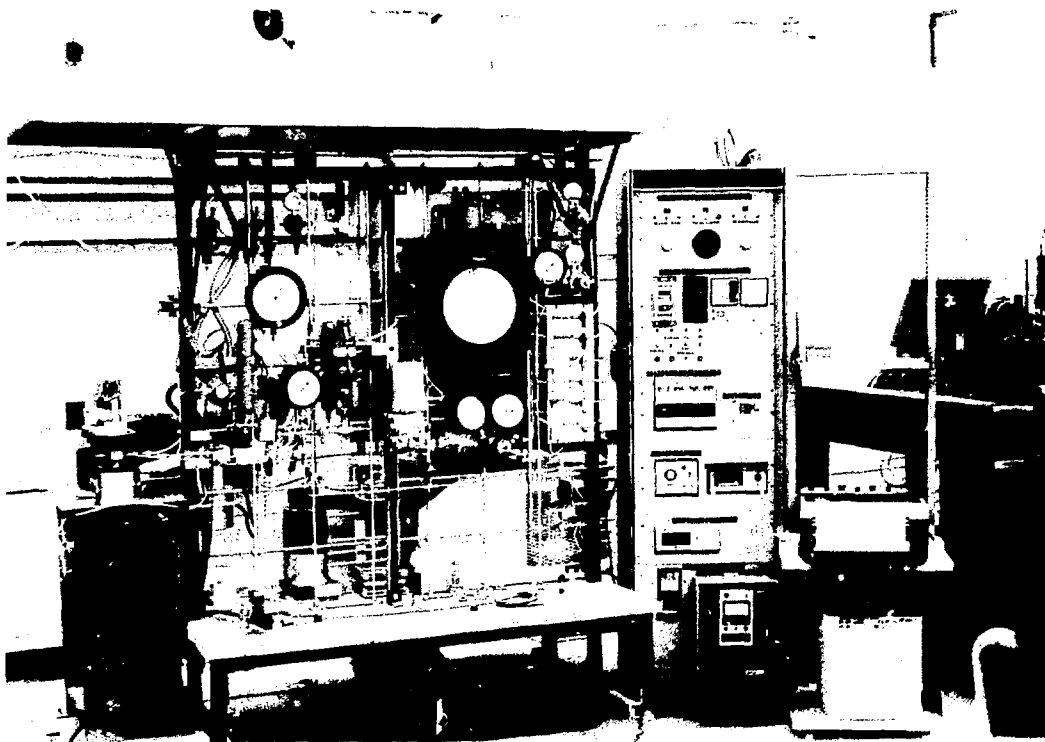


Figure 11. Slurry reactor system developed for the study of Fischer-Tropsch and other types of catalysts.

## SOLAR AND RENEWABLES DIVISION

### Low-Cost Solar Flat Plate Collector Development

The solar-energy collector program at BNL has been guided by strict cost goals, considered necessary to stimulate a large-scale solar industry, in the interest of reducing the use of fossil fuels. This development has matured beyond the proof-of-concept stage, with the creation of lightweight and durable solar panels now ready for limited field testing. The collectors can potentially meet the cost goal of \$53.81/m<sup>2</sup> (\$5/ft<sup>2</sup>) installed, with mass production techniques and advanced material development within current industrial capability. The low cost of these collectors is due to the design,

which permits the use of very thin materials in their construction. This is accomplished through the use of laminate technology, high-performance polymer films, monocoque construction, and nonpressurized liquid operation. The most advanced subcomponent in the design is a laminate absorber/heat exchanger made with a polymer-surfaced metal foil formed into a liquid-tight envelope. In operation, water or other fluid is pumped to the top of the envelope and permitted to flow down between the internal polymer surfaces of the laminate. The polymer film in the laminate functions as a corrosion barrier. Advantages of the new collector concept are very high thermal performance for application in northern climates and modular packaging for rapid installation of large-area arrays.

## National Center for Analysis of Energy Systems

---

The National Center for Analysis of Energy Systems emphasizes interdisciplinary studies of energy policy and planning at the regional, national, and international levels, which include the technological, economic, social, and environmental aspects of energy systems. The Center is currently organized into three divisions: Energy and Economic Analysis, Biomedical and Environmental Assessment, and Technology and Data. This organization reflects the recent demands for energy-systems analysis, and the need to maintain close contact between the activities of the Center and other energy-related program areas in the Department. Planning for future reorganization is carried out on a continuing basis in order to sustain these objectives, and the plans are implemented at appropriate intervals. Development of planning frameworks, analytical models, data bases, and assessment methods provides the foundation for the energy studies.

### ENERGY AND ECONOMIC ANALYSIS DIVISION

#### Assessment of Acid Deposition Impacts

NCAES has developed an important role in conjunction with the Federal Interagency Task

Force on Acid Precipitation. Under DOE sponsorship in conjunction with Oak Ridge, Argonne, and Pacific Northwest National Laboratories, an assessment framework was drafted, leading to newly defined program goals. The four laboratories are named in the legislation establishing the Task Force, and are referred to as the National Laboratories Consortium. From this beginning, a major coordination role has been assigned to BNL, to ensure that these assessment goals are met, beginning in 1985. In addition, various assessment and methodology development tasks are being performed to assist the overall national effort.

#### Assessing Aquifer Impacts From Diverse Surveillance Data

A new project was begun for the EPA Robert S. Kerr Environmental Research Laboratory to demonstrate how to assemble and use data from a wide variety of agencies to assess effects on groundwater of various human activities. Of particular interest are those areas dependent on "sole source aquifers," that is, areas where the populace is totally dependent upon aquifers for drinking water. In this project Long Island is used as a demonstration area, and interfaces are established with many of the agencies col-

lecting data pertinent to groundwater. To collect and assess such data, extensive procedures are required, as well as the application of statistics, computer graphics, and numerical models. Both the existing state of an aquifer system and potential future states under alternative land-use decisions will be evaluated.

### **Water and Energy in the Northeast U.S.**

Two studies were completed to compare the energy production sector with other sectors vis-à-vis water availability and use in the Northeastern U.S. In the first, relationships between water resources and energy development were studied in 11 New England and Mid-Atlantic states. Hydrological conditions for 19 Northeastern river basins were examined to estimate their existing and potentially developable safe yields. Also examined were technical, institutional, and legal aspects of supply development related to new reservoirs, use of groundwaters, recycling and reuse of water, and interbasin transfers. Demands for water by the energy sector were placed into the context of demands by the industrial, agricultural, and residential sectors. A scenario of projected demands in the year 2000 was developed to illuminate important planning and policy issues which will face all Northeastern water users. Safe yield was the hydrological parameter chosen to delimit existing and potential water supplies.

Building upon the previous study, the second project estimated present and future possibilities for water conservation, recycling, and reuse (CR&R) in New England and the Middle Atlantic states. Telephone interviews and questionnaires sent to trade associations, public utility commissions, and federal, state, and other agencies were used to supplement information gathered in the literature. Water intake and consumptive demands in 1980 were calculated for industrial, electric utility, agricultural, and residential sectors. Corresponding information for the year 2000 was estimated using data from utilities, public utility commissions, and the U.S. Bureau of Economic Affairs.

Most industrial sectors were found to be aware of the need for CR&R. Generally, the greatest use of water within each category is for cooling and condensing. Industrial water was found to be more easily recycled than waste water. A revised scenario of water use in the year 2000

was developed to account for potential CR&R. It was estimated that amounts of water withdrawn and consumed could potentially be reduced to comparable 1980 levels. This is particularly significant because no major water supply projects will have been started or completed in this region during the period 1965-2000. Nevertheless, several major industrial states should expect to experience periods of significant water shortage, even with maximum CR&R.

### **Land-Use and Demographic Change Around Operating Nuclear Stations**

An analysis of population and land-use change occurring in the vicinity of 49 operating nuclear power station site areas discovered that local area population increased 64% compared to a 26% national increase during 1960-1980. To determine the reasons for the faster rate of growth, a questionnaire was directed at local area planners and officials (93% response rate). Frequently mentioned factors were a major highway (40%), high-quality municipal infrastructure (39%), proximity to an urban area (39%), recreation facilities (29%), and low taxes (25%). While land-use controls were found in the vast majority of local areas, growth was still encouraged by 63% of local governments and 44% of utilities. Over 70% of the respondents anticipated the ensuing growth and only 10% felt that land-use controls were inadequate for the present time. However, the concern over nuclear safety and area growth has caused 21% of respondents to indicate that they plan to introduce new land-use techniques in the foreseeable future.

### **Water Issues Associated With Enhanced Oil Recovery (EOR)**

A study of water quantity and quality requirements for each EOR process was completed for the DOE Bartlesville Energy Technology Center. Of particular interest were estimates of reductions in water use by reuse and recycling, because water used for EOR production is lost for all other uses. This is a source of potential problems throughout the U.S., particularly in Midwest areas where irrigated agriculture represents the greatest competition for scarce water resources. The project resulted in a handbook useful to those groups interested in the application of a particular EOR process in



an area where conflicts over water use might arise. The handbook demonstrates the data and calculations necessary to estimate water requirements for EOR, and lists state agencies with jurisdiction over such water usage.

#### **Studies of Residential Wood Burning**

A series of studies of residential wood combustion has been completed. The work began with development of an algorithm for the distribution of wood usage for space heating. The results suggest that the entire country uses firewood in much the same way. The density of use (cords per square mile) depends on heating degree-days and population density. These statistics were then used to estimate the resulting air pollution impacts, which were largely found to be modest by regulatory standards. However, since several trace compounds in wood smoke may be carcinogenic, it was suggested that air pollution monitoring for these substances be stepped up. Finally, an economic analysis of price-share data for various fuels was conducted, in order to estimate future usage of firewood as a function of future relative prices for competing fuels. If wood prices remain low (and the proportion of wood cut free does not change significantly), wood usage by the year 2000 could substantially increase to around 3 quads from the present (1977-79) 0.8-quad level.

#### **IEA Energy Technology Systems Analysis Project**

NCAES has represented the United States in a 17-nation project that performs systems analysis to assist the International Energy Agency in establishing its energy R&D priorities. In 1982, an improved version of MARKAL, the model developed by the project to represent national energy systems, was released, together with an updated volume of the characterizations of technologies to be evaluated in the national model runs. In workshops at BNL and Dublin, national results using the updated data and revised scenario assumptions were presented and evaluated. These are being incorporated into the multinational report to be released in 1983.

#### **Energy Information Administration Model Development**

The Energy Data and Model Analysis Program, formerly known as the Mid-Range Energy

Forecasting System Extensions Program, has developed, refined, and implemented models used by the Energy Information Administration (EIA). The activities and accomplishments of the program during 1982 include: the development and implementation of a market adjustment algorithm in the Mid-Range Energy Markets Model; the design and implementation of a mini-macro economic model for linkage with the Intermediate Future Forecasting System (IFFS); the design and implementation of the computerized linkages between two macro economic models (9DGEM and the mini-macro), IFFS, and the EIA demand models to allow for energy economy interactions; design and implementation of a new commercial energy demand model; design and implementation of a new simplified industrial energy demand minor fuels model; estimation of the manufacturing production function equations (from Fraumeni-Jorgenson) from 1958-1979 data; modification of the electric utility, gas, and coal modules in IFFS; analysis of new auto, bus, truck, and airplane fuel consumption data and use of these to reformulate and re-estimate the transportation energy demand modules.

#### **Policy Analyses**

Several projects were completed for the DOE Office of Environmental Assessments in areas related to coastal zone management and amendments to both Clean Water and Safe Drinking Water Acts. Widespread cutbacks in the federal budget have affected federal, state, and local coastal zone management programs. This project, conducted together with the Lawrence Berkeley Laboratory, investigated possible effects of these budgetary cuts on the operation and coordination of coastal programs, particularly as they relate to energy development. Because issues of national policy interest and security are intimately intertwined in all coastal energy development, it was suggested that DOE, to fulfill its own statutory requirements, must assume a greater interest and a more active role in coastal energy issues, particularly those involving conflicts between energy development and environmental protection.

A study was completed of the effects of the environmental review process created by Section 404 of the Clean Water Act on coal-port dredging designed to increase U.S. coal exports.

It was found that Section 404 reviews generally have not constrained the deepening of coal ports and the development of U.S. coal exports and are not likely to do so. The time required for dredging projects will be substantially shortened only if the Congressional review process is overhauled and the question of who will pay for dredging is resolved by Congress. This latter question is now the major obstacle to new dredging proposals.

#### **TECHNOLOGY AND DATA DIVISION**

A major effort has been made to develop a model that simulates the attributes and configuration of district heating systems, which distribute hot water for space heat and domestic hot water needs. Since 40% of Denmark's residential sector is served by district heating, a Danish contractor was engaged to supply a data base appropriate for use in the Brookhaven model. These data provide detailed costs for materials and labor for various pipe sizes and system demands, and are being incorporated for use in the model. A district heating technical handbook is being written for the International District Heating Association.

#### **BIOMEDICAL AND ENVIRONMENTAL ASSESSMENT DIVISION**

The Biomedical and Environmental Assessment Division (BEAD) received international

recognition through its designation by the World Health Organization (WHO) and the United Nations Environmental Programme as a Collaborating Center for the Assessment of Health and Environmental Effects of Energy Systems. In addition to participating in joint programs assessing health and environmental aspects of energy systems with the two international organizations, BEAD will represent WHO at meetings on energy and health at the United Nations in New York.

After more than two years of preliminary efforts, a joint DOE-EPA-National Institute for Occupational Safety and Health (NIOSH) project to study health effects on workers at the Kosovo coal-gasification plant in Yugoslavia is making headway. A delegation from Yugoslavia spent a week at BNL reviewing progress and plans. Approximately 400 men who have worked at the plant for 10 years are being compared with a similar group of surface coal miners. The work will help predict potential health effects from future U.S. synfuels plants. The Medical Department and the Industrial Hygiene Group of S&EP are also taking part in the project.

Parallel to the Kosovo study, an epidemiological study of U.S. coke-oven workers is being conducted in collaboration with the University of Pittsburgh Graduate School of Public Health. This is being coordinated with clinical studies planned for the BNL Medical Department.

## DEPARTMENT OF ENERGY AND ENVIRONMENT

**B. Manowitz, Chairman**

**A. Goland, Associate Chairman for Energy Sciences Programs**

**T. O'Hare, Associate Chairman for Energy Technology Programs**

**W. Tucker, Assistant to the Chairman**

### ENERGY SCIENCES

#### Chemical Sciences Division

**D. Metz, Division Head**

G. Armen  
K. Barkigia  
J. Bookless  
H. Cheng  
J. Egan  
J. Fajer  
S. Feldberg

E. Fujita  
I. Fujita  
T. Gangwer  
B. Gordon  
L. Hanson  
R. Heus  
F. Hill

M. Hillman  
T. Horning  
J. Johnson  
D. Keil  
R. Klemm  
J. Michael  
F. Nesbitt

A. Newman  
F. Reidinger  
J. Reilly  
N. Singletary  
T. Skotheim  
J. Sutherland

#### Metallurgy & Materials Science Division

**M. Suenaga, Division Head**

J. Bethin  
J. Billelo  
J. Chow  
R. Corderman  
A. Delahoy  
M. Garber

V. Ghosh  
R. Griffith  
S. Heald  
M. Hirsch  
S. Hwang  
O. Kammerer

F. Kampas  
C. Klamut  
T. Luhman  
T. Metzger  
A. Muller  
M. Pick

G. Rajesewaran  
R. Sabatini  
C. Snead  
P. Vanier  
D. Welch

#### Process Sciences Division

**M. Steinberg, Division Head**

N. Carciello  
P. Fallon  
J. Fontana  
F. Kainz

L. Kukacka  
P. McGauley  
P. Pruzansky

W. Reams  
D. Sethi  
T. Sugama

M. Sundaram  
R. Webster  
H. Yoo

### ENVIRONMENTAL SCIENCES

#### Atmospheric Sciences Division

**P. Michael, Division Head**

C. Benkovitz  
R. Brown  
V. Evans

J. Hayes  
M. Hjelmfelt  
L. Kleinman

M. Leach  
A. Levin  
A. Patrinos

G. Raynor  
S. SethuRaman  
J. Tichler

#### Environmental Chemistry Division

**L. Newman, Division Head**

P. Daum  
R. Dietz  
C. Dodge  
R. Doering  
R. Fajer  
E. Ferreri  
D. Fluckiger  
J. Forrest

J. Gaffney  
R. Goodrich  
T. Kelly  
M. Kinsley  
P. Klotz  
D. Leahy  
J. Lee  
Y. Lee

S. Levine  
H. Lin  
M. Lin  
W. Marlow  
R. McGraw  
H. Munkelwitz  
M. Phillips  
E. Premuzic

S. Schwartz  
G. Senum  
D. Spandau  
I. Tang  
R. Tanner  
R. Wilson

**Terrestrial and Aquatic Ecology Division****G. Hendrey, Division Head**

Y. Chen  
H. Conway  
A. Francis

N. Gmur  
C. Hoogendyk  
E. Landry

K. Lewin  
H. Quinby

M. Thomas  
J. Vaughn

**Oceanographic Sciences Division****J. Walsh, Division Head**

W. Behrens  
D. Dieterle  
P. Falkowski  
T. Hopkins

P. Lane  
T. Malone  
S. Oakley  
G. Rowe

S. Smith  
A. Swoboda  
J. Vidal  
K. Von Bock

T. Whitedge  
R. Wilke  
C. Wirick  
K. Wyman

**ENERGY TECHNOLOGY****Materials Chemistry & Energy Conversion Division****F. Salzano, Division Head**

M. Bonner  
E. Findl  
C. Fredrickson  
E. Gannon

E. Grohse  
H. Isaacs  
A. Jackson  
C. Linkous

J. McBreen  
A. Mezzina  
W. O'Grady  
H. Olender

S. Srinivasan  
G. Strickland  
C. Yang

**Architectural & Building Systems Division****R. Isler, Division Head**

G. Dennehy  
H. Ghaffari

W. Graves  
R. Hoppe

R. Jones  
R. Krajewski

R. McDonald  
L. Woodworth

**Solar & Renewables Division****J. Andrews, Division Head**

M. Catan  
P. LeDoux

P. Metz  
W. Wilhelm

**Fossil Division****C. Waide, Division Head**

A. Beaufre  
C. Bock  
T. Butcher

J. Chua  
R. Goldberg  
C. Krishna

P. Marnell  
R. Sapienza  
J. Saunders

W. Slegeir  
J. Wegryzn

**NATIONAL CENTER FOR ANALYSIS OF ENERGY SYSTEMS****Energy & Economic Analysis Division****F. Lipfert, Division Head**

G. Anandalingam  
E. Balzer  
J. Benneche  
K. Carr  
E. Cherniavsky  
G. Goldstein  
P. Groncki  
D. Hill  
S. Howe

D. Jhirad  
E. Kaplan  
A. Kydes  
J. Lee  
R. Malone  
W. Marcuse  
L. McCoy  
P. Meier  
W. Metz

M. Minasi  
V. Mubayi  
J. Munson  
P. Patil  
B. Pierce  
D. Pilati  
S. Rogers  
B. Royce  
J. Schaedler

M. Schnader  
T. Sills  
T. Teichmann  
K. Tingley  
M. Toscano  
K. Van Valkenburg  
S. Wade

**Biomedical & Environmental Assessment Division**  
**L. Hamilton, Division Head**

J. Barancik  
S. Bozzo  
E. Coveney  
A. Crowther

H. Fisher  
F. Galdos  
C. Kramer  
W. Medeiros

S. Morris  
P. Moskowitz  
J. Nagy  
K. Novak

M. Rowe  
W. Sevian  
J. Smith  
H. Thode

**Technology & Data Division**  
**M. Beller, Division Head**

N. Bhagat  
R. Bright  
J. D'Acerno  
K. Fendler

V. Fthenakis  
A. Hermelee  
J. Lamontagne

R. Leigh  
J. Martorella  
R. Newcombe

A. Queirolo  
A. Reisman  
W. Rutter

# Department of Nuclear Energy

## INTRODUCTION

The Department of Nuclear Energy is involved in programs primarily related to fission and fusion reactor development. The Department is currently engaged in experimental and theoretical studies on the safety of fission reactors and on the development of fusion reactors, development of improved methods for safeguarding

nuclear materials, nuclear waste management, and compilation and evaluation of nuclear data required for users throughout the world. Approximately two thirds of the funding for these programs is received from the Nuclear Regulatory Commission (NRC) and the remainder from the Department of Energy (DOE) and other sources, such as the Electric Power Research Institute.

## Nuclear Safety

Nuclear safety programs at BNL, sponsored by the Nuclear Regulatory Commission, consist of research to improve the understanding of how various types of reactors will function under hypothetical accident conditions. The work involves research activities for LWRs, HTGRs, and LMFBRs, and includes the running of computer codes for accident analysis and the provision of technical support to NRC for reactor regulation.

### PROBABILISTIC RISK ASSESSMENT

In the aftermath of the TMI-2 accident, several investigative groups recommended probabilistic risk assessment as an adjunct to safety review. In response, the National Reliability Evaluation Program (NREP) was initiated. BNL has performed an options study for implementing the National Reliability Evaluation Program. This includes descriptions of the options relevant to the end uses of the NREP studies and how they are related to safety benefits. A discussion of the resources required and possible schedules for implementation of such are also included.

BNL also developed a standard methodology to be used in the National Reliability Evaluation Program, along with a manual for auditing the results.

At the request of the Nuclear Regulatory Commission, the Philadelphia Electric Company has performed a probabilistic risk assessment of the Limerick Generating Station. BNL reviewed this Probabilistic Risk Assessment (PRA) to assess its accuracy and completeness.

A PRA study of a BWR/6 standard plant with a reference Mark III containment has been submitted by the General Electric Company. BNL is evaluating this GESSAR-II PRA to compare the risk posed by the GESSAR-II design with that of the reference BWR plant in the WASH-1400 study, and the proposed NRC Safety Goals.

BNL is performing studies of the effects of inverter failures, multiple failures of redundant components and/or systems, steam generator rupture, and loss of main feedwater for the Washington Public Power Supply System Units 1 and 4.

BNL is studying the unavailability of nuclear power plant (NPP) hydraulic systems having 1, 2, or 3 trains, taking into account functional requirements, testability, automatic initiation, and monitoring and control. Ideal fluid systems that satisfy the functional requirements and have the lowest unavailabilities will be identified.

## SEVERE ACCIDENT ANALYSIS

The containment building failure mode and consequence analyses for the Zion-Indian Point facilities rely heavily on the MARCH/CORRAL/CRAC system of codes. BNL is evaluating these codes and has made several modeling and calculational improvements to the MARCH code.

Since the TMI-2 accident, the subject of hydrogen generation and release into the containment has received increased attention from the NRC, especially for lower design pressure containment buildings where, under some circumstances, hydrogen burning could threaten containment integrity. BNL has reviewed a number of questions bearing on this problem.

## HUMAN ERROR RATE DATA ANALYSIS

The importance of human error to safe and efficient production of electric power by nuclear plants has grown in recent years, with operation, test, and maintenance being identified as areas of potential reduction of risk. BNL develops and applies human performance data to quantify nuclear power plant safety.

In FY 1982, the identification, analysis, and categorization of over 400 implicit human errors were obtained from a study of over 6000 Licensee Event Reports (LERs). These have provided a human error data base many times greater than that provided by the LERs "cause code" or the LER Data Summaries. Also, the multiple sequential failure model has undergone a series of preliminary validation checks. An initial appraisal of performance-shaping factors and quantified expert judgment in evaluation of human reliability has been performed. A feasibility study on the improvement in human error data identification, storage, and retrieval has been completed, as has a report on the Operator Action Tree/Time Reliability Correlation model.

## ENGINEERING ANALYSIS

The ability of nuclear power plants to shut down safely during a fire was questioned after the fire at the Browns Ferry Nuclear Plant. In 1981 a fire protection rule (Appendix R of 10 CFR 50) provided criteria for the protection of

systems required for safe shutdown, and BNL was given the task of evaluating for the NRC the licensee submittals for the operating nuclear power plants. These evaluations have been identifying areas of plants requiring alternative safe shutdown capability. The systems needed for hot shutdown and subsequent cold shutdown have been reviewed to determine compliance with requirements.

In operating (licensed) plants, it has been determined that containment purge and vent valves have not been designed to close under accident-induced internal pressure. The NRC has imposed on plants the requirement to demonstrate the ability of these valves to close in an accident. BNL has been evaluating for the NRC the licensee submittals for both near-term operating license (NTOL) and licensed NPPs.

## RELIABILITY MODELING

Programs have been under way to develop time-dependent unavailability models and to use such models within the licensing framework.

Three systems have been analyzed, viz., a PWR Emergency Feedwater System, a BWR Automatic Depressurization System, and a BWR High Pressure Coolant Injection System. The analysis includes system description, fault tree quantification, unavailability calculation, and error propagation. In each case, emphasis is placed on those features specific to time-dependent unavailability analysis which make the method more suitable than traditional methods for analyzing aspects of reliability associated with these standby safety systems.

Programs are under way to develop guidelines for establishing limiting conditions for operations (LCOs). The overall methodology, closely akin to the time-dependent unavailability approach described above, is expected to develop recommendations for time periods of both scheduled and unscheduled downtimes. The method has been applied for determining the LCOs for an emergency feedwater system of a plant, studied under the Interim Reliability Evaluation Program.

## SYSTEMS IMPORTANT TO SAFETY

The NRC action plan developed after the TMI-2 accident indicated that several systems

important to safety were not designed, fabricated, or maintained at a level appropriate to their safety importance. BNL has initiated a program to develop criteria and methodologies for use in classifying, and designing requirements for, systems important to safety.

### SEISMIC RISK SENSITIVITY

A program has been under way to (1) determine the seismic sensitivity of safety system components, (2) perform cost/benefit analysis of seismic qualification of equipment, and (3) develop guidelines and criteria for seismic and dynamic qualification. A probabilistic methodology for identifying seismic risk-sensitive systems, or portions thereof, has been used in this study. The approach taken augments an existing BNL-developed sensitivity analysis, which is based on the WASH-1400 study, by accounting for fragility with state-of-the-art probabilistic models, and by including the requisite seismic data in recently published reactor safety studies. By parametrically adjusting the seismic-related variables (seismicity, component fragility) and ascertaining their effects on overall plant risk, core-melt frequency, accident sequence probability, etc., one can identify these seismically risk-sensitive systems and equipment.

### FIRE PROTECTION RESEARCH

The Laboratory has been providing NRC with technical summaries of national and international fire protection research programs useful in formulating nuclear reactor plant fire protection programs and guidelines. In considering some of the fire protection issues that have arisen over the past several years, it is necessary to be aware of ongoing fire research programs such as (1) electrical cable flammability and damageability under varying thermal environments; (2) fire hazard assessment of cable trays; (3) flame retardant coating, fire barrier (and shield), and fiber insulation; (4) flame spread rates and enclosure fire growth rates; (5) aerosol detector response and siting criteria; and (6) fire-plume dynamics and smoke spread.

Recent efforts have provided the NRC staff with a rationale with which to review exemption requests from licensees.

Prior efforts have provided the staff with a summary of fire science phenomenology conducted through the National Bureau of Standards Ad Hoc Mathematical Modeling Committee.

The background and experience acquired from these earlier efforts will be useful in assessing the value/impact of NRC-sponsored fire protection research and review.

### CLINCH RIVER BREEDER REACTOR LICENSING REVIEW

Licensing activities for the Clinch River Breeder Reactor (CRBR), which were suspended in 1977, have been resumed. At the time of the suspension, BNL was heavily involved in the NRC review of CRBR and many issues were left unresolved. BNL is again providing assistance to the NRC in its review of the calculated results of sodium leaks and postulated core-melt accidents.

The accident analysis in support of CRBR licensing has resulted in a comparison of CRBR design basis accident (DBA) events with those of foreign plants. The key findings are: (a) It is harder to distinguish between the DBA and beyond-DBA events in foreign plants, and (b) the scram functions used in the CRBR are not as diversified as those in the SNR-300 prototype reactor, under construction in Kalkar, W. Germany.

The SNR-300 plant has two important additional scram functions for which there are no counterparts in the CRBR: (1) the delayed neutron detector signal, and (2) low feedwater temperature. The first acts to arrest fuel failure propagation. The second primarily provides protection for the steam generator. CRBR relies on alarms and manual scram.

The safety review concerns the proposed heat transport system and the accident analyses of the Applicant. The major findings of this review include:

(1) The CRBR heat removal subsystems have a high degree of redundancy, but the diversity depends on the Direct Heat Removal System (DHRS) which must be modified to satisfy the NRC's single failure criterion.

(2) Pre-operational test programs must test not only the emergency DHRS, but also novel components of decay heat removal systems



under all anticipated accident conditions (including natural circulation).

(3) The analysis of reactivity events does not yet recognize the importance of power tilting in the new heterogeneous core.

(4) The proposed inspections, leak detection, and material surveillance will have a strong effect on the consequences of design basis events.

### CORE SAFETY AND PLANT TRANSIENT ANALYSIS

Because of concern over accidents in which the vessel of a pressurized water reactor may be subjected to pressurized thermal shock, an evaluation was made of the accumulated pressure vessel fluence. This has shown that substantial fluence reduction may be achieved by low-leakage fuel management in which the core peripheral power is reduced, and by replacement of core peripheral assemblies by non-fuel-bearing assemblies.

Other analyses treated effects of fuel rod bowing on core performance, determination of three-dimensional core power distributions during severe transients with interaction between fuel and cladding, and reactor control problems.

As part of maintaining a complete system of nuclear and thermal-hydraulic codes for nuclear reactors, nuclear cross-section data sets for pressurized and for boiling water reactors are being produced, and are being benchmarked against reactor measurements.

Analysis has been made of transients in a boiling water reactor initiated by loss of the feedwater. Various assumptions were made as to whether relief valves, emergency core cooling, and automatic depressurization systems function properly. An audit was made of analyses by reactor manufacturers. The effectiveness of safety systems and emergency operating procedures was analyzed.

### CONTAINMENT SYSTEM INTEGRITY

Boiling water reactors are provided with large pools of water to condense steam released during a loss-of-coolant accident or actuation of a safety valve. This would prevent excessive pressure buildup inside the containment. The BNL staff continues to advise the Nuclear Reg-

ulatory Commission on the technical merits of the methods proposed by the reactor manufacturer and the reactor owners and operators for predicting the hydrodynamic loads on the pool walls and on structures located in and above the pools. As part of this activity BNL reviews foreign test programs and advises NRC on the impact of these data on domestic reactors.

### PLANT ANALYZER DEVELOPMENT

The plant analyzer will give NRC and the nuclear power plant operators accurate and realistic on-line plant transient simulations at speeds much faster than real-time. This is the first plant analyzer to combine advanced mathematical modeling with modern special-purpose peripheral processors designed for high-speed systems simulation.

The plant analyzer will reduce sharply the cost and time of safety analyses. The plant analyzer will also support plant management by monitoring plant performance, diagnosing instrumentation and component failures, and predicting well in advance the outcome of contemplated operator actions.

The AD10 of Applied Dynamics International at Ann Arbor, Michigan, is the selected special-purpose processor. It is being programmed through a PDP-11/34 host computer.

The AD10 has sufficient computing capacity to simulate the nuclear steam supply system with its controls for a BWR power plant. It has sufficient accuracy and dynamic range, with its 16-bit arithmetic, to simulate design base transients and small-break loss-of-coolant accidents. It can simulate transients ten times faster than real time. It is 110 times faster than the large mainframe general-purpose computer, CDC-7600, executing the same simulation. These conclusions have been reached by comparing computed results from the AD10 and the CDC-7600, using the same basic models for nonequilibrium, nonhomogeneous, two-phase coolant flow and simulating the same transients.

The model is being improved to include major BWR plant subsystems and their controls, and to interface with multicolor graphic display systems. Future plans are to simulate PWR systems and to interface the plant analyzer with training simulators and plant computers.

## SYSTEM-WIDE TRANSIENT CODE FOR LMFBRs

The analysis of a variety of off-normal and accident conditions is essential in any reactor safety evaluation. Some examples of transient conditions of an LMFBR are withdrawal of control rods, pump seizure in a heat transport loop, decay heat removal via natural circulation, and a major rupture of a sodium-carrying pipe.

The Super System Code (SSC) Development, Validation, and Application Project at BNL is funded by the Division of Accident Evaluation, NRC. Work is progressing on three versions of the SSC series of codes: (1) SSC-L, which simulates the thermohydraulic response of loop-type LMFBRs, (2) SSC-P for pool-type LMFBRs, and (3) SSC-S for shutdown (i.e., long term) transients of the "L" and "P" versions.

The SSC-L effort provides direct support to licensing for the Clinch River Breeder Reactor Plant (CRBRP). Applications include (1) assessment of natural circulation capability, (2) assessment of long-term shutdown heat removal capability, and (3) analysis of the consequences of major breaks in the sodium piping. Future work will include analyses of operational transients, such as (1) reactivity insertions, (2) control system malfunctions, and (3) loss-of-heat-sink excursions.

Because of the current stress on providing support for the CRBRP licensing effort, only limited work is being done on the SSC-P version to keep it abreast of improvements made to the SSC base program library. Work on SSC-P will accelerate once the level of support required for CRBRP activities decreases.

Progress continues in several areas under SSC-S activities. Model development of aspects important for long-term transients includes (1) improved upper plenum representation, where a two-dimensional treatment is needed for many applications, (2) inclusion of interassembly heat transfer effects, and (3) special numerical techniques to reduce machine time for long simulations.

The principal validation is based on comparisons with data from a series of natural circulation tests conducted at the Fast Flux Test Facility. Results to date compare well with test data over a wide range of system operating conditions.

## BALANCE OF PLANT MODELING

Until recently, little attention was given to the complexity of subsystems and components past the primary side of the steam generator, in what is generically referred to as the balance of plant (BOP). The interaction and feedback of the BOP on the primary system are essential for assuring normal and long-term shutdown heat removal.

The Balance of Plant Modeling Program develops safety analysis tools for system simulation of nuclear power plants. It develops and validates models to represent and link together BOP components (e.g., steam generator components, feedwater heaters, turbine/generator, condensers) of the Clinch River Breeder Reactor, that at the same time are generic to all types of nuclear power plants.

This program provides an independent licensing tool by developing deterministic thermohydraulic models and an associated computer program not only for steady state, but also transient capability. The computer code MINET either can be used on a stand-alone basis or, with a minimum of modification, can be adapted to other system analysis codes. MINET will be very fast-running (at a minimum, faster-than-real-time on a CDC-7600).

The first version of MINET is operational. It has been successfully interfaced with SSC (Super System Code). It provides a representation of the steam generation system and BOP components. SSC/MINET is now being used by NRC in its continuing licensing activities for the CRBRP. Adequate representations of the steam generator and BOP are important for analyzing the long-term consequences of natural circulation and removal of shutdown heat through normal circuits.

## LWR CODE DEVELOPMENT, ASSESSMENT AND APPLICATION

This program includes improvement of the RAMONA-3B code for calculating boiling water reactor transients. In addition, the TRAC and RELAP5 code packages are studied and assessed.

RAMONA-3B contains many improvements to the RAMONA-III code which was developed by Scandpower A/S and later purchased by

BNL for the NRC. The code can now be used to analyze a wide range of abnormal BWR transients such as the control rod drop accident, anticipated transients with or without partial scram, loss of feedwater, recirculation pump trip, turbine trip with or without bypass, etc. A number of modifications are now being made to further expand the code's capabilities. RAMONA-3B will become a useful and versatile tool for analyzing BWR transients, where direct coupling between neutron kinetics and thermal hydraulics is essential.

The independent assessment of the latest versions of TRAC and RELAP5 codes has continued with the simulation of separate effects tests to identify the strengths and weaknesses of these codes in predicting thermohydraulic phenomena that would be important under accident or transient conditions. Specific areas where these codes need improvement have been identified and, in some cases, BNL has suggested improved models.

In the code application area, BNL is beginning to apply the TRAC codes in PWR and BWR large-break LOCA calculations. These will be used to determine the margin of safety in the present licensing calculations and to suggest revisions to Appendix K of 10 CFR 50. Analysis has begun of the Anticipated Transients Without Scram (ATWS) for BWR/4 using the TRAC-BD1 and RAMONA-3B codes. BNL is also participating in a program of Pressurized Thermal Shock (PTS) studies of the Oconee-1, Calvert Cliffs, and Robinson-2 plants.

#### **THERMAL-HYDRAULIC REACTOR SAFETY EXPERIMENTS**

The objective of this program is to develop and experimentally evaluate models of thermal-hydraulic phenomena relevant to reactor safety. Thermal-hydraulic experiments and modeling relevant to two aspects of containment loading are being conducted, viz., core-concrete interactions leading to penetration of the containment basemat, and containment pressurization by thermal interaction between core debris and water.

LWR accident analysis requires models of thermal interaction between fragmented core debris and cooling water. Two programs are under way to develop and evaluate models

which predict the quench characteristics of debris beds which may develop in either the reactor vessel (in-vessel) or the containment building (ex-vessel). The two programs address the phenomena of debris bed quenching with bottom-injection and with top-flooding of cooling water. The top-flood experimental program studies the heat transfer of packed beds of superheated core debris cooled by an overlying pool of water. Results thus far suggest that a debris bed quenches in two-stage frontal heat transfer. The rate of steam generation is limited by the rate of flow of cooling water to the dry region of the superheated bed of particles. The water flow rate is limited by countercurrent two-phase flow. It has been shown that a water cooling front initially propagates down the debris bed. The debris ahead of the front is uncooled during this stage. The reactor safety implication of this result is that core debris in contact with the concrete would be uncooled for some period of time and would thermally attack the concrete. The gases released upon concrete heating may further limit the coolability of the debris. The possibility of a melt attack on the concrete must also be considered in the containment accident sequence.

A program has recently been initiated on quench of in-vessel debris beds cooled by emergency cooling water introduced from below. An experimental apparatus has been designed and fabricated and is being assembled. A model has been developed to characterize the process.

In the event of a core meltdown in a PWR, where the core debris in the reactor cavity is not coolable, the debris would melt and attack the concrete basemat, both thermally and chemically. The ensuing core-concrete interaction could be a major contributor to containment loading by generation of gases from the concrete as well as aerosol generation from the bubbling melt. An experimental and analytical program is conducted on the core-concrete interaction stage of a degraded core accident in a LWR. The objective of the core-concrete interactions program is to develop analytical and semi-empirical models in support of the CORCON code under development at Sandia National Laboratory.

Core-concrete interactions would release large quantities of steam and CO<sub>2</sub> from the concrete, which would bubble up through the molten

debris and pressurize the containment building. Other chemical reactions would contribute quantities of CO and H<sub>2</sub> which are combustible. Understanding of a wide variety of two-phase phenomena is required for input into accident analysis codes, such as CORCON, for accurate calculation of degraded core accidents. One phenomenon being investigated is coupled mass and heat transfer at the interface between overlying strata of molten core oxides (UO<sub>2</sub>, ZrO<sub>2</sub>) and steel, driven by intense gas release from the concrete. These studies have indicated that the rate of upward heat transfer between molten layers may be several orders of magnitude greater than now modeled in codes. The reason is that bubbling induces liquids to entrain into the upper layer, enhancing heat transfer rates over the interface model in CORCON by as much as two orders of magnitude. Experiments and supporting analyses have been performed to model the onset and rate of bubbling-induced mass transfer between immiscible liquid layers, interfacial heat transfer, and liquid entrainment-dominated heat transfer. These models have been coded at BNL into CORCON and are available for the next formally released version of CORCON (MOD2). Code sensitivity studies point to the probability of early development of frozen crusts with significant impact on containment loading as well as release of volatile fission products to the containment.

Another program investigates the interaction of hot, molten core debris and an overlying layer of water during core-concrete interactions.

Experiments to investigate liquid-liquid film boiling use various liquid metals to simulate molten core debris and several boiling liquids. Wood's metal and bismuth have been used with saturated water and Freon. All experiments to date using Freon resulted in stable film boiling. In a second series of tests with bismuth and saturated water, however, vapor explosions were observed. Their occurrence appears to depend on initial liquid metal temperature, with some evidence of dependence on geometric scale. The implications of both for core-concrete interactions are being assessed.

## STRUCTURAL ANALYSIS

The Structural Analysis Division provides technical assistance to the NRC in the areas of

seismic design and analysis, soil-structure interaction, structural behavior, stress analysis, structural failure analysis, and structural reliability. The current programs include the following: Piping Benchmark Development, Confirmatory Piping Analysis, Structural Benchmark Development, Review of Dynamic Qualification of Safety-Related Electrical and Mechanical Equipment for both operating plants and plants undergoing license review, Confirmatory Review of the Dynamic Response of the Diablo Canyon Plant, Ultimate Capacity Evaluation of a Mark III Containment, Development of 3-D SSI Computer Code, and the Development of Probability Based Load Combinations for the Design of Nuclear Seismic Category I Structures and Reliability Analysis of Nuclear Power Plant Structures.

The Piping Benchmark Program which has been going on for several years has been extended to include use of the measured results from piping tests by other organizations.

A program entitled Confirmatory Piping Analysis has been undertaken to assist NRC in assessing the methods used by applicants to qualify nuclear power plant piping. Confirmatory evaluations were completed for two piping problems from the Diablo Canyon Unit 1 power plant, and evaluations for two additional piping problems from this plant are currently under way. Assistance is provided to NRC in review and evaluation of technical reports from the Independent Design and Verification Program for the Diablo Canyon Project.

Members of the Structural Division developed independent vertical floor response spectra based on a detailed 3-D model of Diablo Canyon. These evaluations were done for the 7.5M HOSGRI earthquake. The spectra were then used in evaluations of selected piping systems.

The Division was asked by NRC to extend the Diablo Canyon Plant Review by (1) developing independent horizontal floor response for the annulus structure based on a three-dimensional model, and (2) evaluating the seismic response of buried diesel oil tanks at the plant.

The ultimate capacity of a reinforced Mark III containment was evaluated using a detailed model of the concrete and steel, and a detailed review of the current methodology for reinforced concrete structural evaluations was made.

A probability-based reliability analysis of methodology for seismic Category I structures has been developed. An important feature of this methodology is the simultaneous use of finite element analysis and random vibration theory. With this method, it is possible to evaluate the safety of nuclear structures under various static and dynamic loads in terms of limit state probability. The method was applied to a realistic reinforced concrete containment subjected to dead and live loads, accidental internal pressures, and earthquake ground accelerations.

### CORROSION SCIENCE

DOE-sponsored research has revealed the role of surface films in crack initiation and propagation in an aggressive environment and further elucidated mechanisms of pitting corrosion. A unique vibrating reed electrochemical probe developed at Brookhaven was used. Testing has demonstrated that a high-nitrogen high-molybdenum stainless steel developed at BNL is extremely resistant to pitting corrosion in an aggressive high temperature geothermal brine. The effect of sulfur compounds in stress corrosion cracking (SCC) of the nickel base alloy, Inconel 600, was demonstrated and studied at length.

EPRI-sponsored testing during 1982 confirmed an in situ technique for relieving stress in Inconel steam generator tubing, to reduce the probability of primary-side SCC. The inter-

granular attack on steam generator tubes in the field was duplicated in the laboratory.

Research is under way for NRC on development of a predictive model for primary-side SCC of steam generator tubing and on developing a better understanding of the SCC of ferritic steel bolts that has occurred in steam generators. Failure analyses have been performed on a number of bolts from nuclear reactors and on specimens cut from the pressure vessels of the steam generators at Indian Point Unit 3. Laboratory tests have duplicated the phenomenon and given further insight into its mechanism.

### HIGH TEMPERATURE GAS-COOLED REACTOR SAFETY EVALUATION

Graphite-moderated reactors cooled by helium could satisfy a significant part of future nuclear power needs, and they promise unique environmental and safety advantages over other concepts. The NRC maintains a program of safety evaluation of such reactors.

The program provides support to the NRC in safety analysis of the High Temperature Gas-Cooled Reactor (HTGR) through determinations of the effects of impurities on structural properties of graphites used for core and core support structures, the transport of fission products during severe accidents, and analysis of the primary system under severe accident conditions. In addition, source terms are developed for accidents in a new evaluation of siting of HTGRs.

## Nuclear Waste Management

---

One part of the Department of Nuclear Energy is engaged in a large nuclear waste management program for the Nuclear Regulatory Commission. A separate part of the Department assists the Department of Energy and the Environmental Protection Agency in their programs of low-level waste management.

### HIGH-LEVEL NUCLEAR WASTE MANAGEMENT (NRC)

The Department of Energy is currently developing technology to solidify high-level radioac-

tive waste and emplace it in deep geologic formations of rock salt, basalt, and tuff. The BNL program sponsored by the NRC Office of Nuclear Material Safety and Safeguards has two parts. The first is a technical evaluation of the DOE waste package research and development, in which BNL considers waste glass leaching, container corrosion, and advantages of geologic packing material. In the second part of this program, laboratory testing is performed to quantify the local conditions which would control the corrosion of carbon steel containers in a basalt repository, and the rates of migration of

groundwater through bentonite clay packing which would be used in basalt.

In a separate program sponsored by the NRC Office of Nuclear Regulatory Research, corrosion of titanium alloy TiCode-12 exposed to high temperature brines typical of those in a salt repository is studied. Uniform corrosion rates have been evaluated. Hydrogen embrittlement effects have been identified. Embrittlement was shown to be associated with hydride formation at the tips of propagating cracks. Two new failure processes have been identified for TiCode-12 at 150°C: crevice attack and pitting in crevices. The two mechanisms are associated with oxygen depletion and reductions in pH in the crevices. Metallographic and theoretical studies confirm the proposed failure processes.

#### **LOW-LEVEL NUCLEAR WASTE MANAGEMENT (NRC)**

The Nuclear Waste Management Division provides technical assistance and experimental research for the NRC. The technical assistance program is subdivided into programs on fuel-cycle and non-fuel-cycle waste.

The major contributors to the source term for non-fuel-cycle waste are industries and institutions which produce, use, and test radiopharmaceuticals, sealed sources, and static eliminators. The staff has helped to characterize the waste generated by two major industrial contributors to this waste. The probable long-term stability of the waste packaged for permanent disposal by shallow land burial was assessed.

The experimental program includes leaching of low-level solid radioactive waste, the study of commercial low-level radioactive waste disposal sites, and the characterization of radioactive wastes generated in unusual circumstances such as at the Three Mile Island reactor.

Leaching and compressive strength of simulated waste forms typical of reactor waste were

studied. The effects of radiation on the physical and chemical properties of organic ion-exchange resins and corrosive by-products were studied.

The properties of ion-exchange media are modified by intense radiation. The effects of radiation dose rate, chemical loading, moisture content, and composition are studied.

#### **LWR DECONTAMINATION (NRC)**

It is believed that many LWRs will require chemical decontamination at intervals in order to reduce the radiation exposure of operating personnel during inspection, repairs, and maintenance.

BNL conducts two programs of research to evaluate the management of waste from LWR decontamination. A program sponsored by the Chemical and Engineering Branch of NRC studies techniques for converting decontamination wastes to more innocuous forms. These wastes would contain organic chelating complexing agents that are thought to enhance the migration of radionuclides. The processes being evaluated include incineration, chemical digestion, and wet air oxidation.

A companion program sponsored by the Division of Health, Siting, and Waste Management (NRC) evaluates the release of chelates or complexing agents from solidified decontamination wastes.

#### **NUCLEAR WASTE RESEARCH (DOE)**

The development of improved methods of immobilizing low-level radioactive waste has been conducted over the past three years. At present, a selection is being made of two or three solidification agents to bring to commercial demonstration.

Actual radioactive waste is obtained from commercial nuclear power plants for leach testing. This work supports lysimeter studies at other national laboratories.

## Nuclear Material Safeguards

---

### TECHNICAL SUPPORT ORGANIZATION

The Technical Support Organization (TSO) provides assistance to a number of federal agencies, particularly DOE, in both domestic and international safeguards.

Several internationally oriented studies have been done this year. Effective safeguards inspection of Gas Centrifuge Enrichment Plants by the International Atomic Energy Agency (IAEA) have been analyzed. This must be done with minimal risk of undesirable technology transfer. A study has been made of the effect of relative safeguardability of the various advanced isotope separation techniques. A broadly applicable safeguards effectiveness assessment methodology was developed. An independent assessment of the ACDA-developed Remote Continuous Verification (RECOVER) system was completed and a long-term project was started to prepare guidelines to aid countries in designing their nuclear materials control and accounting systems to facilitate the application of IAEA safeguards.

Domestic safeguards studies, sponsored by the DOE Office of Safeguards and Security, have emphasized the field implementation of developed safeguards technology. TSO partici-

pated in material control and accountability field exercises at two DOE facilities.

### INTERNATIONAL SAFEGUARDS PROJECT OFFICE

The Program of Technical Assistance to IAEA Safeguards (POTAS), under the technical management of the International Safeguards Project Office (ISPO), is in its seventh year. Since the program's inception in 1977, 250 tasks mutually agreed upon by the IAEA and the U.S. have been completed, and another 50 are under way. Fifteen cost-free experts are now stationed at IAEA Headquarters in Vienna. Twenty types of equipment have been developed for verification of nuclear material, and first-of-a-kind units have been transferred to the Agency. Many of these devices are now being used routinely by IAEA inspectors. Ninety man years of service by cost-free experts have helped to develop and establish procedures for inspections and evaluation of results.

Over the next five years the IAEA will spend more than \$20 million for new inspection equipment. The current U.S. support program emphasizes assistance to IAEA in procurement and effective use of this new technology.

## National Nuclear Data Center

---

The National Nuclear Data Center (NNDC) provides services to the entire low energy nuclear science community. The services include information on neutron physics, charged-particle reactions, nuclear structure, and decay data.

The IAEA Nuclear Data Section coordinates an international effort in nuclear structure and decay data (NSDD). A network of NSDD evaluation centers has been set up within the United States, and is called the U.S. Nuclear Data Network (USNDN). The USNDN is coordinated by the NNDC, which also serves as the United States representative to the international net-

work. The center contributes mass chain evaluations to the Nuclear Data Sheets.

Responsibility for the Nuclear Structure Reference Bibliographic File has been transferred from Oak Ridge National Laboratory to the NNDC. This file is used by the Center to produce the Recent Reference issue of the Nuclear Data Sheets (Academic Press).

The transfer of the Evaluated Nuclear Structure Data File (ENSDF) and the production responsibility for the Nuclear Data Sheets (NDS) to NNDC has been completed. Beginning with the June 1981 issue, monthly publication of the NDS was made by NNDC through Academic

Press, Inc. NNDC also provides support for the NSDD network and coordinates mass-chain evaluation.

The NNDC continues to produce about 12 issues of the Nuclear Data Sheets a year. Of

these, nine are devoted to nuclear structure evaluation and three to the Recent References.

Neutron Cross Section Volume I, Part B, Z61-100, is expected to be ready for publication in September 1983.

## Advanced Reactor Systems

Compact high-performance reactor designs for space power using HTGR-like nuclear fuel particles are being developed by the Department. The large surface area available with the small-diameter ( $\approx 500$  micron) particulate fuel allows very high power densities (MW/liter), small temperature differences between fuel and coolant ( $\approx 10$  K), high coolant outlet temperature (1500 to 3000 K, depending on design), and rapid reactor start-up ( $\approx 2$  to 3 seconds). Two reactor concepts are being developed: the fixed-bed reactor (FBR) (Fig. 1), where the fuel particles are packed into a thin annular bed between two porous cylindrical frits, and the rotating-bed reactor (RBR), where the fuel particles are held

inside a cold rotating (typically  $\approx 500$  rpm) porous cylindrical frit. The FBR can operate for long periods (month-to-years) in the closed-cycle He-cooled mode, or because of  $H_2$  storage limitations, for short periods (a few hours) in the open-cycle  $H_2$ -cooled mode. The RBR will operate only in the open-cycle  $H_2$ -cooled mode. Depending on cycle mode, maximum power capability for the FBR ranges from  $\approx 300$  to 1000 MW(th); maximum power for the RBR is  $\approx 5000$  MW(th). The FBR would be used with a turbine in either the closed- or open-cycle mode; the RBR could be used for direct thrust, or could produce electricity with MHD or turbo-generators. Experiments on particle beds relating to the FBR and RBR are being carried out.

System studies coupling both tokamak and mirror fusion reactors to high temperature electrolyzers to produce hydrogen and hydrogen-based synthetic fuels are under study. On the basis of current high temperature electrolysis technology ( $\approx 1100^\circ\text{C}$  operating temperature), overall efficiencies are in the range of 50 to 55% for conversion of fusion energy to hydrogen chemical energy, depending on process conditions. Cost of hydrogen produced ranges from 5 to 10 dollars per million Btu. Previous BNL experimental tests under simulated blanket conditions have shown that  $ZrO_2$  and  $Al_2O_3$  appear to be suitable materials for high temperature steam-cooled blankets for the extraction of high-grade heat ( $1100^\circ\text{C}$  or higher). Results of the studies indicate that the key technology development required for the consideration of fusion as a heat source for  $H_2$  production is a high temperature blanket.

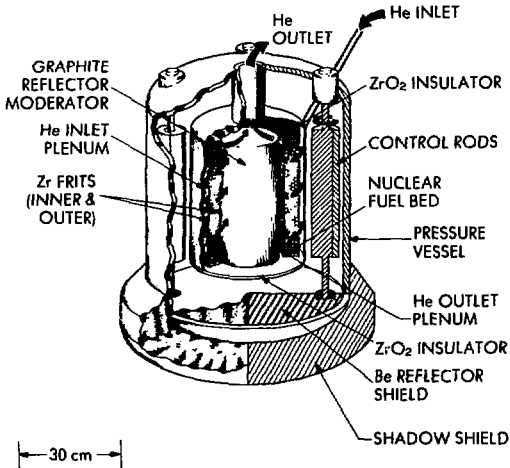


Figure 1. Fixed-bed reactor.



## DEPARTMENT OF NUCLEAR ENERGY

**H. J. C. Kouts, Chairman**  
**W. Y. Kato, Deputy Chairman**  
**A. J. Romano, Department Administrator**  
**A. J. Weiss, Administrative Technical Assistant**

### Nuclear Safety

**Reactor Safety Research Division**  
**R. J. Cerbone, Associate Chairman**

B. Baggoura	G. Greene	S. Lekach	Y. Sanborn
E. Cazzoli	J. Guppy	A. Mallen	G. Slovik
B. Chan	W. Horak	T. Nepsee	N. Tutu
H. Cheng	J. Jo	L. Neymotin	G. Van Tuyle
H. Connell	R. Kennett	U. Rohatgi	W. Wulff
T. Ginsberg	M. Khatib-Rahbar	P. Saha	C. Yuelys-Miksis

**Reactor Safety Licensing Assistance Division**  
**M. M. Levine, Associate Chairman**

A. Aronson	L. Eisenhart	P. Neogy
E. Auerbach	P. Kohut	J. Penoyar
J. Carew	J. Lehner	J. Ranlet
D. Cokinos	C. Lin	W. Shier
D. Diamond	M. Lu	M. Todosow
C. Economos	G. Maise	

### Engineering and Risk Assessment Division

**R. A. Bari, Associate Chairman**  
**R. E. Hall, Deputy Division Head**

A. Agrawal	T. Ginzberg	H. Ludewig	Y. Sun
E. Anavin	N. Hanan	E. MacDougall	J. Taylor
M. Azarm	R. Hodor	B. Miller	T. Teichmann
J. Boccio	S. Hsieh	J. O'Brien	H. Thomas
W. Bornstein	R. Jaung	I. Papazoglou	A. Tingle
G. Bozoki	S. Karimian	K. Perkins	K. Voska
N. Cho	R. Karol	W. Pratt	J. Yang
P. Farahzad	L. Lederman	C. Ruger	R. Youngblood
S. Fiarman	V. Lettieri	P. Samanta	W. Yu
A. Fresco	W. Luckas	K. Shiu	J. Zahra
R. Gasser			

### Structural Analysis Division

**M. Reich, Division Head**

R. Alforque	C. Constantino	A. Philippopoulos	D. Suwannakate
P. Bezler	J. Curreri	S. Sharma	P. Wang
P. Brown	R. Goldman	S. Shteyngart	Y. Wang
M. Chang	H. Hwang	M. Subudhi	

### HTGR Division

**C. A. Sastre, Division Head**

K. Araj	J. Heiser	B. Lee	A. Prince
J. Colman	C. Hsu	K. Lee	G. Ueberg
G. Fischer	P. Kroeger	C. Pescatore	

**Corrosion Science****J. R. Weeks**

C. Auerbach  
R. Bandy  
C. Czajkowski  
H. Isaacs

R. Newman  
Y. Sanborn  
K. Sieradzki  
L. Teutonico

D. van Rooyen  
J. Woodward

**Waste Management****Nuclear Waste Management Division (NRC)****D. G. Schweitzer, Associate Chairman****M. S. Davis, Deputy Division Head**

J. Adams  
T. Ahn  
J. Allentuck  
H. Arora  
R. Barletta  
B. Bowerman  
S. Chan

J. Clinton  
R. Davis  
R. Dayal  
D. Dougherty  
D. Eastwood  
E. Gause  
H. Jain

R. Kempf  
D. MacKenzie  
L. Milian  
S. Panno  
P. Piciulo  
R. Pietrzak  
J. Shao

C. Shea  
B. Siskind  
J. Smalley  
P. Soo  
K. Swyler  
E. Veakis

**Nuclear Waste Research (DOE/EPA)****V.L. Sailor, P. Colombo**

E. Franz

M. Fuhrmann  
P. Kemeny

P. Kalb  
S. Levins

**National Nuclear Data Center****S. Pearlstein, Division Head**

B. Barton  
M. Bhat  
T. Burrows  
M. Divadeenam

C. Dunford  
N. Holden  
R. Kinsey  
W. Kropp

B. Magurno  
V. McLane  
S. Mughabghab  
L. Peker

S. Ramavataram  
P. Rose  
E. Schmidt  
J. Tuli

**Nuclear Materials Safeguards****Technical Support Organization Division****J. H. Cusack, Division Head****E. V. Weinstock, Deputy Division Head**

A. Bieber  
J. Cadwell  
A. Fainberg  
L. Fishbone

D. Gordon  
W. Higinbotham  
J. Indusi  
W. Kane

B. Keisch  
J. Lemley  
J. Sanborn  
S. Suda

M. Zucker

**International Safeguards Project Office Division****L. Green, Division Head****A. J. Waligura, Deputy Division Head**

B. Booman

J. Skalyo

L. Solem

**Advanced Reactor Systems****J. R. Powell**

T. Botts  
J. Fillo

P. Grand  
F. Horn  
O. Lazareth

H. Takahashi  
J. Usher

# Support Activities

Applied Mathematics Department  
Instrumentation Division  
Reactor Division  
Safety and Environmental  
Protection Division

# Applied Mathematics Department

## INTRODUCTION

The Applied Mathematics Department is responsible for carrying out research in the mathematical sciences and for providing extensive scientific computation services to all the Laboratory programs. The research program consists of two major activities: investigations in analytic and numerical methods, and research in statistical methods. Among the services provided are consultation and professional assistance in the application of computational, statistical, and mathematical techniques; the operation of the Central Scientific Computing Facility; the support of distributed computing equipment throughout the Laboratory; and the planning and development of future data processing facilities and tools.

## ANALYTIC AND NUMERICAL METHODS

The work in analytical and numerical techniques is concerned with investigation and development of computational methods for problems in a variety of scientific and engineering fields. The goal is to develop methods which are both reliable and efficient. Much of the current emphasis is on the need for improved methods for solving problems in three dimensions. Many of the existing methods were developed in ad hoc engineering contexts and are of unknown reliability. Although the applications are in quite diverse fields, many of the techniques and tools, such as fast Fourier transforms, iterative matrix solvers, relaxation methods, adaptive procedures, etc., are common to these fields. Currently, effort is being concentrated in four areas. Tools for the study of nonlinear dynamical systems are being developed with a special emphasis on multiphase fluid flow. In the solution of partial differential equations in unbounded domains, work is in progress on improv-

ing the approximate treatment of wave propagation and on implementation of faster finite element procedures for solving elliptic boundary value problems. Improved methods for electromagnetic field computation are being developed. Applications include both magnetostatic fields and eddy current problems. In image reconstruction, development of algorithms for the full three-dimensional case is being pursued with emphasis on nuclear magnetic resonance (NMR) imaging.

## Fluid Flow and Nonlinear Dynamical Systems

The flow of more than one fluid often leads to interpenetration of the fluids, such as raindrops in air or air bubbles in the ocean near breaking waves. A number of multifluid differential equations have been developed, and a few are used intensively in engineering applications such as reactor safety, internal combustion engines, and fluidized particle beds. The most popular multifluid equations are not hyperbolic, and hence not well posed as initial value problems. Since solutions cannot be shown to depend continuously on data, there is no classical approximation theory to verify that any one model is close to another, let alone to a real flow. Confidence in multifluid models could be enhanced if their stability properties were better understood.

An example of a two-fluid instability may be observed when an air-water mixture circulates rapidly through an L-shaped chamber. Depending on the incoming mass flow rate, pulsations of outflow may occur. Figure 1 shows, across the top row, plots of outlet mass flow versus time from a numerical simulation of this instability. Reading from left to right, the inlet flow rate has been slightly increased for each plot. The oscillation is first periodic, then periodic with doubled period, then quadrupled, and finally chaotic. The spectra in the next row confirm the period doubling route to chaos. Finally, the

third row in the figure shows portraits of period doublings in a different context, a simple dynamical system discovered by E. N. Lorenz. This and other behavior typical of simple nonlinear differential equations can be studied with an interactive computer graphics program under development, which also produces animated 16-mm films via an off-line micrographics device. Other dynamical systems which can be studied in this way range from chemical kinetics equations to ecological predator-prey equations to almost any kind of nonlinear driven oscillator.

### Solution of Partial Differential Equations in Unbounded Domains

These equations arise in many physical situations such as fluid flow around an object, acoustic and electromagnetic wave propagation, and magnetostatic field computation.

An iterative solution of the non-self-adjoint system of equations arising from application of the finite element method to Helmholtz-type equations in unbounded domains was developed. The iterative method was incorporated in a previously developed code based on the finite element method with local radiation boundary conditions. The method was tested on a variety

of problems, including variable coefficients, complicated geometries, and discontinuities across an interface. Specific problems treated include scattering from a small aperture resonator, two models of a laser-plasma interaction, and a model of the interaction of an electromagnetic wave with a periodic interface. In all cases, the method was accurate and efficient, even for reasonably large frequencies. Various high-frequency phenomena (such as shadow effects) show up qualitatively in the intermediate-frequency range under consideration.

### Numerical Methods for Electromagnetic Problems

Progress in many areas of energy-related research, including the design of particle accelerators, magnetic fusion, and the development of free-electron lasers, requires the construction of magnets which push the state of the art in terms of strength and quality of field. The understanding of eddy current effects is also important. The basic electromagnetic equations describing the field due to an assembly of current-carrying conductors and ferromagnetic elements are well known, but methods for solving them for realistic three-dimensional magnets are neither reliable nor well understood. Both

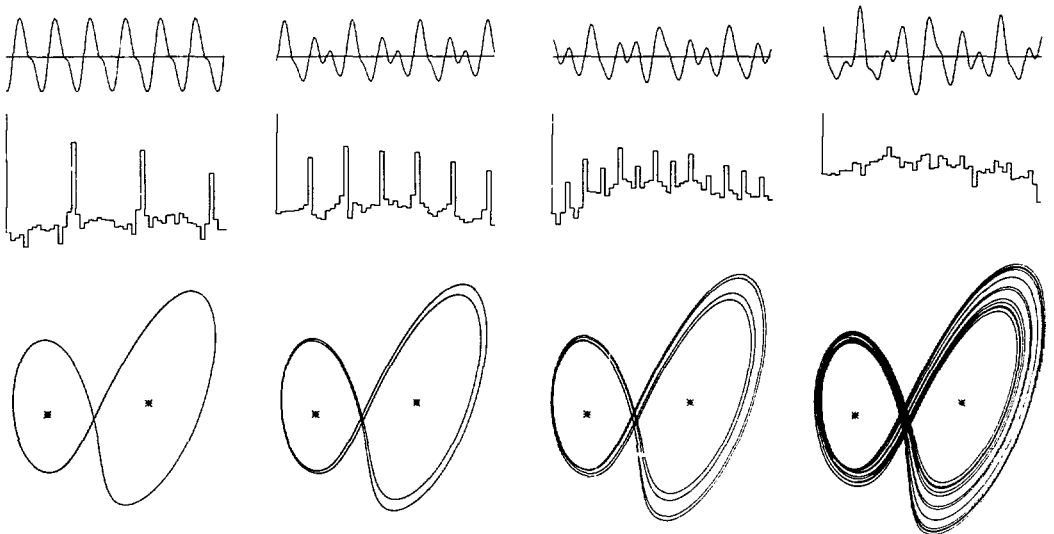


Figure 1. Period doublings lead to chaos. Top row: Flow rate vs time from a two-phase flow. Middle row: Corresponding spectra. Bottom row: Views of 3 D phase space trajectories of the Lorenz system.

differential and integral equation methods involving a variety of approaches to discretization of the problem need study to understand their potential accuracy. More serious, however, is the fact that an adequately fine-grained discretization in most existing methods leads to prohibitive computational times for numerical solution.

A new method for magnetostatic field computation was developed. Although existing algorithms seem adequate for predicting the qualitative behavior of complex magnet systems, the algorithms fail to give good quantitative agreement in complicated three-dimensional calculations. One reason for this seems to be that many methods are not well conditioned in low-field calculations. Some results obtained with the new method were analytically derived, which suggests that it will give quasi-optimal convergence even in low-field problems. The new method is similar to a scalar potential-boundary integral formulation, and its computational complexity is no greater than the methods now used.

A new numerical method for approximating the steady-state harmonic eddy current problem in flat plates was formulated and analyzed. The continuous model for this eddy current problem was formulated by Moon et al. as an integral-differential boundary value problem. Attempts with standard discretization methods showed little success because of the singular and nonlocal nature of the integral equation part. The new approach is based on iterative methods with the discrete Fourier transform and leads to a matrix problem which can be solved with computational effort proportional to the number of unknowns in the discretization. Quasi-optimal convergence estimates were also proven.

### Image Reconstruction

A number of techniques are used in attempting to solve the widely varying scientific and engineering problems associated with image reconstruction, the best known of which is medical tomography. In each of these problems, the quantities measured in practice differ from the idealized mathematical projections because of noise, resolution, and other effects. Even more important is the fact that in realistic situations only a discrete subset of the possible projections can be observed. The choice of subset can signif-

icantly affect the resolution of the resulting reconstruction and the magnitude of the numerical task involved. Research in this area entails both the search for optimal design of the observation procedure and the development and implementation of efficient numerical algorithms to achieve the mathematical reconstruction. For example, efficient, fully three-dimensional algorithms are needed for use in NMR imaging.

While attempting to achieve a better understanding of the existing nuclear magnetic resonance imaging strategies and their interrelationships, it was discovered that an important subclass of these strategies can be described and investigated in a unified way by associating each strategy with a certain type of "trajectory" in spatial frequency space. This subclass encompasses all those techniques in which the data are obtained by observing the free-induction decay following a broad-band pulse, in the presence of a spatially uniform but possibly time-dependent magnetic field gradient; it includes projection reconstruction as well as such other well-known techniques as Fourier zeugmatography and echo-planar imaging.

### STATISTICAL METHODS

This task is concerned with the mathematics underlying the process of confrontation between measurement or observation on the one hand, and a theory, model, or expectation on the other. It involves questions of experimental design as well as those of data analysis and estimation. The mathematical tools to implement objectives in design or analysis do not depend directly on the field of application, and a considerable portion of the work carried out lies in the general area of statistical inference. At the same time, particular fields may raise statistical questions with a specialized focus. The primary emphasis is on the development of innovative methodologies for analysis of data sets which are restricted, incomplete, or complex in other ways. It is characteristic of such problems that the observations to be analyzed are on subjects which are valuable, irreplaceable, and not easily reproducible. This is true especially in biostatistics but also in weapons tests, nuclear reactors, large-scale engineering structures, and other systems of importance in energy research. To obtain reliable results from the limited data sets asso-

ciated with such exotic systems more sophisticated analysis is required than can be obtained with conventional statistics, as well as extensive computation, both in the implementation of these more sophisticated methods and in their development through simulation and Monte Carlo methods.

### **Survival, Risk, and Reliability Analysis**

Survival data arise whenever one is studying such events as death, failure of machine parts, or recurrence of disease, which are time dependent and which may or may not have occurred for all subjects in the experiment. Thus, some of the data are referred to as "censored" in that only partial lifetimes are observed. Their analysis raises many mathematical problems, including difficult questions on estimating the survival curve, the mean survival time, conditional survival time given that an experimental subject survived to a given threshold, etc. Despite much recent activity, the statistical methodology for this type of data is in its infancy compared with methodology for uncensored data. Such methodology is extremely important in studying the effects of any treatment, procedure, or external factors on lifetimes of humans, animals, or machinery. Techniques for comparing different subgroups using this methodology are also in need of much work.

Reliability analysis and risk assessment are closely related to survival analysis, in that they deal with the potential failure of a device, structure, or living organism. Risk assessment typically involves the assessment of exposure levels of a certain substance which leads to a specified level or risk to subjects at hazard. Reliability analysis usually is concerned with understanding the expected failure rates of engineering components or structures. The problem of reliability of structures subjected to abnormal, violent motions, such as earthquakes, is not well understood and has much in common with the low-dose extrapolation problem. The objective in this case, however, is to develop design rules to reduce vulnerability to risks which are unavoidable, rather than avoidance rules for human beings whose design cannot be altered.

Over the past year, the techniques of survival reliability and risk analysis have been used in a large variety of applications. Progress was made

on an accelerated lifetime model which enables study of the log lifetime as it depends on covariants when censoring is present. Techniques were developed for the study of toxicity data in dose response and time-to-tumor models. Safety questions relating to the safety relief valve arrangement in nuclear power plants were studied. A procedure for modeling random violent motions (like those produced by earthquakes) was implemented and applied to nuclear reactor data.

A method was developed (and the actual calculation was made) to relate expected reliability to the specification of warranty requirements. It was applied to components for the vacuum system of the planned BNL Colliding Beam Accelerator. This seems to be the first published piece of work regarding such relations between reliability and warranty.

### **Empirical Bayes Methods and Statistical Inference**

Empirical Bayes methods, which originated in the work of Robbins starting in 1950, form a blend of the two classical and seemingly conflicting frequentist and subjective theories of probability. The frequentist approach bases statistical inference on the operating characteristics or procedures where the unknown parameters are regarded as arbitrary constants. The Bayesian endows these parameters with a more or less arbitrary prior distribution, and considers only the posterior distribution of the unknown parameters given the observed data. Neither method has gained general acceptance, since each is based on an arbitrary element, significance level, or prior distribution. The Empirical Bayesian postulates that, when many subjects are observed, it is possible to estimate those characteristics of the unknown but true population distribution of the parameters that will determine the optimal statistical decision function. The possibilities for application in statistics are enormous and include, for example, better estimates or predictions of outcome from subsets of a population. A particular example might be the prediction of future error rates for nuclear power plant operators based on past records or tests. While the general principles of the method and its importance are well understood, practical implementations for real-

istic classes of population need to be developed and tested.

A variety of problems relating to Empirical Bayes estimation was considered, including the problem of estimating several variances from a number of observations drawn from each of several members of a family of normal distributions. A formulation of the general Empirical Bayes estimates for this problem was given with a procedure for expressing the result as a density estimation problem. The relation between Empirical Bayes estimation and a variety of prediction problems, which deal with the expected future performance of individuals on the basis of past observation, was clarified.

Large sample properties for generalized maximum likelihood estimation (GMLE) were derived. The conditions required are analogous to the conditions for maximum likelihood estimation so that the GMLE method can serve as a unifying principle in the field of nonparametric estimation just as the maximum likelihood does for parametric problems.

### **Sequential Decisions and Adaptive Methods**

Sequential experiment design involves specifying the way in which the course of action at any time is determined on the basis of observations to date. It is particularly important when the experiment is intrinsically undesirable because of cost, time, risk, or ethical considerations. An important example is the design and analysis of clinical trials in which two or more therapies are compared on human subjects. The objective of some experiments is simply to achieve a high probability of selecting the best therapy when the difference in effect is appreciable. In others the aim is to minimize the total number of patients out of a large but finite patient population who will receive the inferior treatment rather than to achieve some arbitrarily prescribed error probability. It is clear that there are many similar non-health-related problems. For example, the set of all present and future nuclear power plants form a finite "patient" horizon. Economic, rather than ethical, considerations dictate the objective of minimizing the number of plants built according to the poorer of a number of alternative strategies which are being evaluated as the plants are being built.

A systematic treatment of the so-called "multi-armed bandit" problem of selecting the best of a number of treatments has been developed for the binomial and nomial cases. The procedure is adaptive and sequential and is designed to minimize the "regret," which characterizes the cost associated with cases for which an inferior treatment is selected. A solution which is valid for the nonterminating case, as well as for the case with finite horizons, has been obtained. This solution is proved to be asymptotically optimal.

A sequential adaptive procedure was developed for assigning successive observations to a number of different populations in such a way as to minimize the expected error in estimating a linear combination of the population means. Its motivation was the problem of Monte Carlo numerical quadrature by adaptive stratification, where even after the stratification is complete the allocation of the remaining function evaluations was to be determined. In connection with the same problem, an algorithm was developed to decide whether or not to accept a potential stratification.

### **COMPUTING SERVICES**

The Department continues to devote most of its resources to the Central Scientific Computing Facility (CSCF). As currently constituted, the CSCF represents a still-powerful and unique research tool. It is made available to all Brookhaven research programs and to outside collaborators and government agencies under special arrangements. Users interact with the facility through an extensive data communications system. The facility's major computers are two Control Data 6600s, one Cyber 76, and a Digital Equipment Corporation VAX 11/780. A recent addition, DEC PDP 11/44, incorporates the popular UNIX operating system.

Service has been significantly improved by the recent procurement of a large mass storage system, which provides a long-needed expansion of the amount of on-line data storage available to users. Further, it provides file storage management capability through a control processor, which is in fact an IBM compatible computer. Perhaps most important, it provides a network capability through a product called



MASSNET, which will eventually allow access from a variety of computers at the site.

The Lab-wide computer networking environment consists of a hierarchy of three interconnected network segments, each with its own complementary set of characteristics. The previously mentioned MASSNET serves as the high-speed local area file transfer network. A somewhat lower-speed more versatile network segment suitable for longer distances is DECNET, which is based upon a product of Digital Equipment Corporation. The ARPANET segment is Brookhaven's connection to an international network developed some years ago for the U.S. Department of Defense Advanced Research Projects Agency. The three segments are interconnected through computers which are termed gateway processors. The development of this networking capability and its successor products (which are expected to be less expensive, simpler, and more versatile) are the chief activities on the Department's planning and development agenda.

Another development attracting considerable attention, including that of at least one commercial firm interested in production, is PUMA, a collaborative effort between AMD engineers and staff at New York University's Courant Institute of Mathematical Sciences. The PUMA project was undertaken to merge the advantages of modern electronics and design tech-

niques with a familiar long-established product which has been in operation for many years at BNL, the CDC 6600 computer. The result is a computer which is essentially compatible with the 6600, but far smaller, more energy efficient, expandable, reliable, and replicable at a small fraction of the cost. PUMA has demonstrated its compatibility by running many of the same programs and even the same operating systems as the 6600.

In recognition of the trend toward distributed computing on smaller decentralized computers, the role of the Department as a center of expertise may soon overshadow its function as an operator of equipment. These personnel-related computer services include consultation on numerical methods, statistics, and computer science; computer procurement guidance; hardware and software maintenance, including support of extensive libraries of program products and applications packages; conducting of classes on various topics; and long-term applications programming and digital engineering services. Through such services, staff members have participated in the development of the AGS polarized proton facility, nuclear reactor safety analyses, data bases for the Industrial Medicine Clinic, and similar activities. This emphasis on provision of personnel rather than on computing machine cycles alone is expected to increase in the years ahead.

## APPLIED MATHEMATICS

**R.F. Peierls**, Department Chairman

**A.M. Peskin**, Deputy Chairman

**R.B. Marr**, Associate Chairman for Research

**S.S. Rideout**, Administrator

**G.H. Campbell, S. Heller.** Computer Science: Distributed computing and computer networking.

**J.E. Denes, K. Fuchel, A. Harris, C. Pittenger.** Computer Service: Central Scientific Computing Facility, distributed systems. Hardware and software services.

**C.I. Goldstein, H.B. Stewart, J. Pasciak, R.B. Marr.** Analytical and Numerical Methods: Solution in unbounded domains, magnetic field computations, multifluid flow, image reconstruction.

**C.S. Kao, H.E. Robbins, W. Tsai, J. Van Ryzin.** Statistics: Survival and risk analysis, Empirical Bayes methods, clinical trials, reliability.

**Y. Shimamoto.** Combinatorial Methods.

# Instrumentation Division

The Instrumentation Division engages in research and development on recognized problems in scientific instrumentation important to the long-term goals of the Laboratory and the Department of Energy. The Division provides consultation services to other departments of the Laboratory in the areas of instrument specification and selection, and also designs and constructs some of the instruments required in their research. These instruments are typically of such advanced design that they are not commercially available. In addition, the Division provides services in electron microscopy, vacuum technology, printed circuit board fabrication, scientific instrument repair, and computer maintenance.

Members of the Division also collaborate in experiments at BNL and at other laboratories when they can contribute significantly to the advance of scientific research with new devices, methods, and techniques developed at BNL. The principal areas of research activity are the detection of nuclear particles and radiation with semiconductor, gaseous, and liquid detectors, processing of signals from detectors, low-noise and other special electronic circuits, systems for acquiring data from and control of scientific experiments, and application of nuclear and atomic techniques in elemental analysis and other fields. Some of the more important recent results are described.

## RADIATION DETECTION AND SIGNAL PROCESSING

### Basic Studies

In these studies, various basic questions in detector development are investigated, such as ionization statistics, charge collection, avalanche development, electrode geometry, signal formation, space charge effects at high counting rates, properties of detection media (gases, liquids, and their mixtures), and position-sensing methods.

Our studies of signal formation in detectors, signal processing, position sensing, and electronic noise have been the basis for the development of new position readout methods and their introduction to high energy physics experiments, and for the development of better x-ray and neutron detectors. Most of our work on signal processing is oriented toward solving detection problems of "difficult" detectors where unique properties are required: high resolution for particle position or energy, very high or extremely low counting rates, uniformity of detection efficiency, particle identification, etc. In developing new detector concepts and designs, we find that a joint study of detector physics and signal processing is most productive.

The emphasis in our work is on the following devices and problems:

1. X-ray detectors for synchrotron radiation.
2. Thermal (and "cold") neutron detectors.
3. Low energy electron detectors (for experiments with UV synchrotron radiation).
4. Silicon strip detectors.
5. Solid state drift detectors for high resolution in the micrometer range.
6. Gaseous vertex detectors: studies of the position resolution limits.
7. High rate drift chambers.
8. Readout methods and detector electrode configuration for high position and energy resolution for high accuracy calorimeters in high energy particle experiments.
9. Signal processing and readout methods for rare-event experiments (proton decay, solar neutrinos, neutrino mass measurements).

### Position-Sensitive X-ray Detectors

We have developed a class of high-resolution position-sensitive single-photon-counting x-ray detectors for use at the NSLS and elsewhere. Our goal was to develop a relatively simple detector design which would provide a high position accuracy and operation at moderately high counting rates of a few times  $10^5$  photons

per second. The design is based on multiwire gas proportional chamber principles with position readout from the charge induced on the cathode by an avalanche at the anode. The induced-charge (cathode) readout utilizes a delay line as a position-sensing medium. The concept of this class of detectors is that the detector dimensions can be chosen or linearly scaled, within certain limits, accompanied by any necessary changes in gases, pressures, windows, etc., while the position readout remains the same. This type of detector is one of many needed for molecular and crystal structure research using synchrotron radiation. Because of their high position resolution (1 to 2 parts per thousand of the detector length), they are of particular interest for low-angle scattering studies in biology and solid state physics. Their capacity for moderately high counting rates makes them suitable for dynamic studies of structures changing in time.

A number of detectors for diverse applications in the x-ray energy range of 2 to 20 keV were recently constructed using the delay line readout system. The main achievements of this effort are a more complete understanding of readout optimization, and the underlying ionization and gas physics, and better position accuracy and resolution than reported elsewhere. Position resolution  $\text{FWHM}/l \sim 1$  to  $2 \times 10^{-3}$ , for detector lengths  $l = 60$  to  $180$  mm, has been achieved at counting rates of  $\sim 2 \times 10^5 \text{ sec}^{-1}$ , with the best absolute resolution of  $\sim 60 \mu\text{m}$  (FWHM) for 5- to 8-keV x rays.

These same properties — high precision resolution at high counting rates — make such detectors suitable for plasma diagnostics in fusion research. They can be used in conjunction with x-ray crystal spectrometers for plasma temperature determination by measuring Doppler broadening of x-ray lines emitted by impurities excited by the hot plasma. A detector for such application, e.g., at the Tokamak of the Princeton Plasma Physics Laboratory, is shown without its enclosure in Fig. 1. The detector has a sensitive area of  $18 \times 10 \text{ cm}^2$ , a thin beryllium window, and evaporated aluminum cathodes on a quartz substrate to avoid high energy fluorescence, and uses a Xe + CO<sub>2</sub> gas mixture. Fuller exploitation of synchrotron radiation in dynamic studies of biological structures requires development of detectors for very high counting

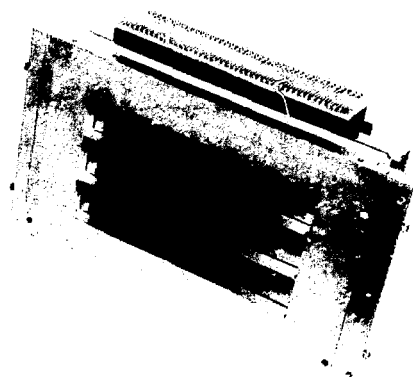


Figure 1. Detector with a sensitive area of  $18 \times 10 \text{ cm}^2$ , a thin beryllium window, evaporated aluminum cathodes on a quartz substrate, mixture of Xe and CO<sub>2</sub> gas.

rates, in the range of  $10^7$  to  $10^8 \text{ photons sec}^{-1}$ . These detectors should allow sampling of x-ray diffraction patterns in time intervals as short as one millisecond. We have developed such a detector based on a number ( $\sim 100$ ) of semi-independent anode cells arranged in a linear array. Its properties at high counting rates are now under investigation.

### Two-Dimensional Thermal Neutron Detectors

Two-dimensional position-sensitive detectors are being increasingly used in neutron diffraction experiments to determine molecular and crystal structures in biology, solid state physics, and polymer chemistry. Position-sensitive detectors for neutrons in the wavelength range of  $1.2 \text{ \AA}$  ( $\sim 60 \text{ meV}$ , i.e., "thermal" neutrons) to about  $8 \text{ \AA}$  ( $\sim 1.2 \text{ meV}$ , i.e., "cold" neutrons) require a high detection efficiency for neutrons and a low efficiency for background  $\gamma$  rays, high uniformity of efficiency, good position resolution at counting rates of up to approximately  $10^5 \text{ sec}^{-1}$ , high position accuracy, little scattering in the entrance window, and stable maintenance-free operation over long periods of time.

Our neutron detectors are gas proportional detectors based on the ionization produced by the charged particles from the reaction  ${}^3\text{He} + n \rightarrow {}^3\text{H} + p + 0.764 \text{ MeV}$ . The energetic reaction

products (proton, 573 keV, and triton, 191 keV) are emitted isotropically in opposite directions. We measure the centroid of the ionization produced. Because of the large difference in energy and range of the proton and the triton, the ionization centroid is displaced from the interaction point. The position resolution limit is thus determined by (besides the electronic noise in the position readout) the stopping power of the gas for the charged particles. A study of gases has resulted in  $^3\text{He}-\text{C}_3\text{H}_8$  mixtures with stopping powers which can improve the resolution to the 1-mm region. A new  $18 \times 18\text{-cm}^2$  detector based on these advances is in operation at the HFBR. A position resolution of 1.3 mm (FWHM) and an absolute position accuracy of 1 part in  $10^3$  are routinely achieved. The chamber operates at a pressure of 6 atm with a  $^3\text{He}-\text{C}_3\text{H}_8$  gas mixture. A centroid finding method by convolution is employed for the position readout. This performance is achieved at a low gas gain ( $\sim 30$ ), which results in good energy resolution. This is important for well-defined separation of neutrons from background  $\gamma$  rays. The position resolution reaches the limit determined by the range of the proton-triton pair.

A  $50 \times 50\text{-cm}^2$  detector, based on the extension of these ideas, has been built. The electrodes in this detector consist of two wire grid planes for position readout of induced charges, centered between the anode and each cathode. The readout grids are oriented, one parallel (grid Y) and one orthogonal (grid X) to the anode wires (Fig. 2).

Flat window pressure vessels for large detectors are not practical at 6 to 10 atm. Therefore, a

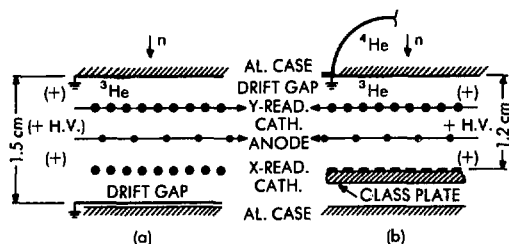


Figure 2. Electrode configurations. (a)  $18 \times 18\text{-cm}^2$ -type detectors; (b)  $50 \times 50\text{-cm}^2$  detector with pressure-containing dome. Arrows indicate the direction of anode and Y-readout wires; circles indicate relative spacing of wires.

double chamber with a strong, thin spherical dome window on one side has been developed. An intermediate flat window separates the inactive hemispherical volume from the active flat chamber and also serves as the front cathode. The inactive chamber is filled with  $^4\text{He}$ , which is transparent to neutrons, to the same pressure as the neutron-sensitive  $^3\text{He}$  mixture in the active chamber. A view of this arrangement for the large-area neutron detector is shown in Fig. 3. The position readout cathode, with its fine segments "printed" on a glass plate, can be seen attached to the inside of the heavy rear enclosure plate.

### High Rate Drift Chambers for High Energy Particles

High rate drift chambers are required in experiments where particle momentum analysis has to be performed at high event rates with good spatial resolution. The detectors can accommodate counting rates over  $10^7$  per second, even when the particle flux is concentrated over a fraction of the detector area. The resolution of about  $140 \mu\text{m}$  (rms) is limited in part by the time digitizing electronics. At such high rates, the operating conditions, low gas amplification, electrode geometry, choice of gas and its purity, and outgassing of components are of increasing importance for the performance and life of the detector (Fig. 4). These detectors were developed and constructed in collaboration with the Hypernuclear Spectrometer Group in the Physics Department.



Figure 3. Principal components of a  $50 \times 50\text{-cm}^2$  detector (left-to-right): pressure-containing dome, window-front cathode, and base plate.

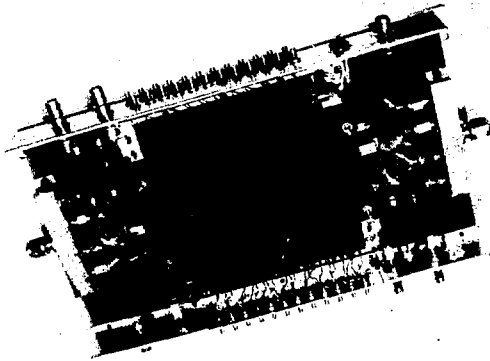


Figure 4. Double-layer high rate drift chamber with internal amplifiers close to each anode wire.

### Silicon Position-Sensitive Detectors

Further studies have been carried out on silicon detectors with segmented electrodes that yield high resolution position information for high energy particle detection. Position resolution below  $10\ \mu\text{m}$  is possible for minimum ionizing particles using an array of detectors having one-dimensional strip electrodes with a pitch as small as  $\approx 25\ \mu\text{m}$ . Devices have been fabricated by conventional silicon junction detector methods with the addition of simple lithography technology long available in the microcircuitry field. To fully understand the limitations and potentialities of these devices, it is necessary to understand the details of charge collection in this detector geometry. The proton microbeam at the 3 MV Research Van de Graaff Accelerator has been a useful probe for this purpose.

Highly collimated 2.5-MeV proton beams with a  $60\text{-}\mu\text{m}$  range in silicon and a lateral spread of  $20\ \mu\text{m}$  have been injected into each side of a "strip" detector (Fig. 5) having groups of six segmented strip electrodes of 200, 100, and  $40\ \mu\text{m}$ -pitch. The detector was moved across the external proton beam in increments as small as  $10\ \mu\text{m}$ . The charge collected (the detector response) by two adjacent electrodes was monitored simultaneously with a two-dimensional data collection system. In Fig. 6, we see the pulses from the proton energy loss at each adjacent strip ("A" and "B") displayed along the x and y axes with the number of events on the z axis. Events in which some collected charge

appears on each electrode lie in the x-y plane. Purely single electrode events are not well displayed, but would appear *only* on the x or y axis.

In Fig. 6(a), protons are incident on the planar face opposite the strip electrode, and spectra are taken at  $20\text{-}\mu\text{m}$  steps between  $100\ \mu\text{m}$ -pitch electrodes. The detector was not quite fully depleted, which allowed some time for charge to diffuse between the two collecting electrodes. Thus, we see a uniform distribution of shared events between the two electrodes and a capability of sensing particle position  $\leq 10\ \mu\text{m}$ . However, this is not a stable condition in which to operate the detector.

Figure 6(b) shows the more realistic condition observed for protons incident on the strip electrode side. Again, spectra are taken at  $20\text{-}\mu\text{m}$  incremental steps between  $100\ \mu\text{m}$ -pitch electrodes. Only in the very nearly central position between both electrodes is charge shared between electrodes. In all other positions, it is collected principally by the nearest electrode. The position sensitivity is thus determined in this condition principally by the pitch of the electrodes and not by charge diffusion for the detector thickness ( $300\ \mu\text{m}$ ). Diffusion effects can be discerned, however, and further measurements place an upper limit of  $\approx 20\ \mu\text{m}$  for lateral diffusion, in agreement with calculations. More finely segmented strip detectors would therefore

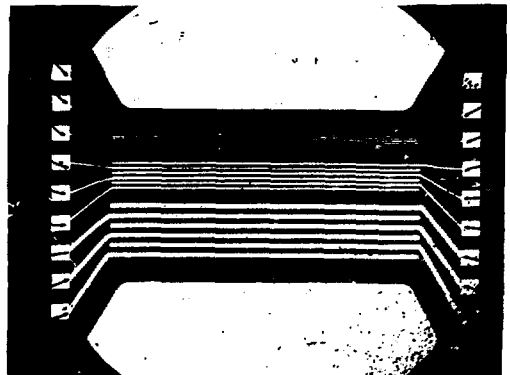


Figure 5. A silicon "strip" detector with a test pattern of three segments of six strips having pitches of 40, 100, and  $200\ \mu\text{m}$ , respectively. Wire bonding to external circuitry is evident from the "land" at the end of each strip.

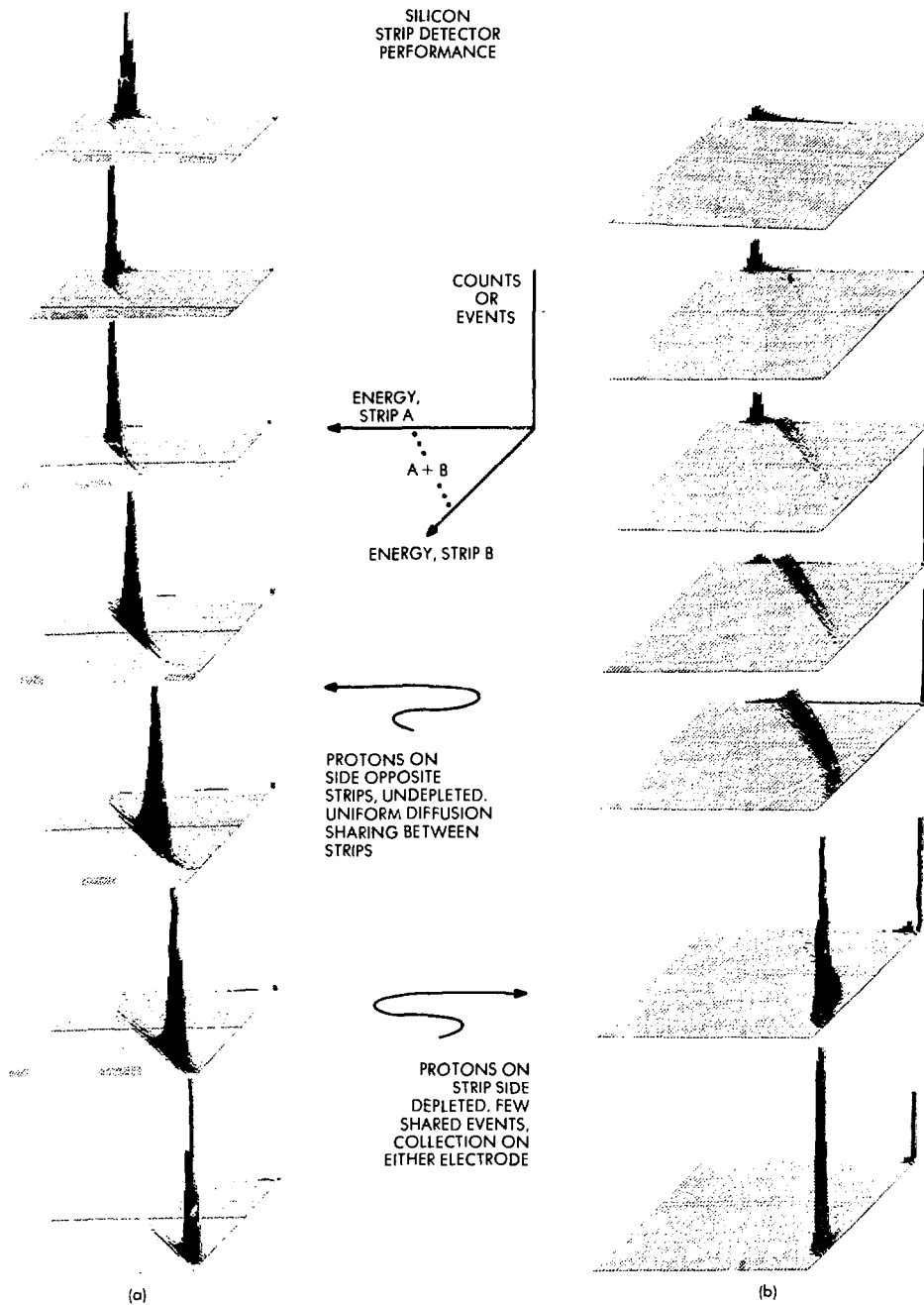


Figure 6. Graphs of electronic pulses from proton energy loss at each adjacent strip ("A" and "B") of detector displayed along the x and y axes with the number of events on the z axis. Graphs (a) and (b) correspond to protons incident on the undepleted side opposite the strips and the depleted strip side, respectively.

provide better spatial resolution (to perhaps a few micrometers). To achieve this requires further developments in the technology of device production and signal processing.

### Low-Noise Microcircuit Technology

The most demanding detectors for use in high energy physics, research with synchrotron radiation, and other areas require low-noise amplifiers which are an integral part of the detector. Commercially available amplifiers fabricated in monolithic and hybrid technologies have generally an order of magnitude higher noise than the existing limit of discrete devices (field-effect or bipolar transistors). We have made considerable progress in introducing hybrid circuit technology for low-noise amplifiers (Fig. 7), using state-of-the-art discrete devices. Two types of amplifiers have been successfully developed for use with high counting rate drift chambers, time projection chambers, x-ray detectors, and silicon strip detectors. One is a charge-sensitive feedback amplifier with a field effect transistor at the input. The other is a very fast amplifier with a bipolar transistor in common base configuration. The direction of this work is to develop the capability for fabrication of development prototypes and small quantities (~100 units), and to provide a standard of performance for industry. Several hundred of these amplifiers have been fabricated for new detector development at BNL, FNAL, SLAC, MIT, and other laboratories. The latest of our amplifiers use alumina substrates, thick film resistors, chip capacitors, and transistors in a miniature package (known as SOT 23). The new techniques and components provide the small size essential for new detectors.

## DATA ACQUISITION AND EXPERIMENT CONTROL

### Control, Monitoring, and Data Handling at the Inhalation Toxicology Facility

Operation of an inhalation toxicology facility requires the ability to perform well-controlled reproducible experiments with large numbers of animals. To satisfy these requirements, a distributed computer system was developed and installed which is used for monitoring and/or

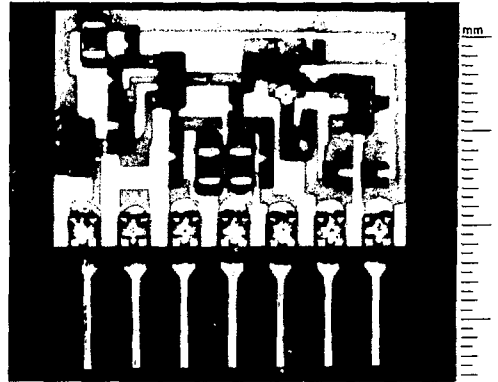


Figure 7. The latest low-noise charge-sensitive amplifier used in high energy particle detectors and in x-ray detectors. The hybrid technology used in fabrication of low-noise amplifiers at BNL employs state-of-the-art discrete devices.

controlling a number of animal exposure chambers, barrier-room exposure integrity, automated animal weighing, alarm signals, and data management. The computer system consists of approximately 30 LSI-11 microcomputers which are distributed into six clusters throughout the facility. The distributed computer system has at least 250,000 words of random-access semiconductor memory, through which high-speed intracluster communication between the microcomputers takes place. Communication between the clusters is accomplished by using a coaxial cable and frequency-modulated serial data transmission at 1 MHz. The clusters are located as close to the data source as is feasible to allow for short and uncomplicated connection of the sensors. Alphanumeric raster-scan monitors with keyboards are distributed throughout the facility to display up-to-date information and facilitate very rapid communication between the experimenter and the system. Figure 8 shows a typical monitor image displaying the status of two active inhalation chambers. The image is maintained for 15 seconds and then the status of the next chamber group is displayed.

Access to the system is hierarchical through unique identification numbers, with operational modifications and data editing limited to supervisory personnel. The system maintains a complete and continuous record of user access, data

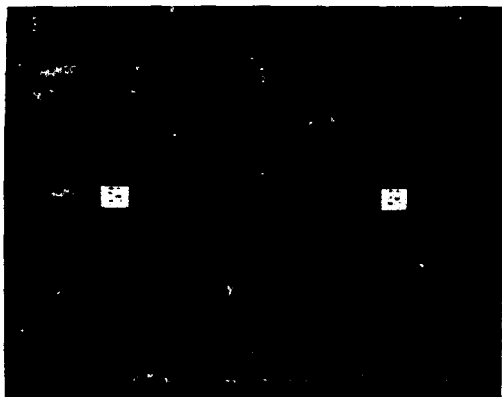


Figure 8. Typical alphanumeric monitor displaying the status of two exposure chambers: present use, top and bottom temperatures, static air pressure, air flow rate through chambers, and relative humidity.

entry, measured parameters, and alarm conditions. Graphic and documented records are generated automatically or upon request.

#### Motor Control Unit for Use at the NSLS

A motor control subsystem to be used in several experiments at the National Synchrotron Light Source has been developed. Six subsystem units have been constructed and one of these units has been placed into operation at the Light Source.

The motor controller subsystem occupies a position between an experiment control computer system and a set of stepping motors (up to 15) and their associated position encoders. The driving computer issues positioning commands to the control unit via a standard RS-232-C serial communication line operated in full duplex mode. The commands are coded as ASCII character strings and hence are easily generated and interpreted by a standard ASCII character terminal.

At the "other side" of the motor control unit, two streams of stepping pulses are generated. The streams correspond to clockwise and counterclockwise motor motion. The control unit accepts limit switch and home position switch information from a set of switches associated with each motor axis. Each axis may have its current position read out by one of several types

of position encoders — absolute, incremental, or a pseudo encoder which simply counts motor pulses.

A package of FORTRAN-callable software routines has been written to aid users in driving the motor control unit. The package may be used for any Digital Equipment Corporation computer system which utilizes FORTRAN programs executing under the RSX-11M operating system.

## ANALYTICAL TECHNIQUES

### Analysis of Electron Diffraction Intensity Profiles Using a Photodiode Array Detection System

Electron diffraction intensity profiles have been used extensively in studies of polycrystalline (Fig. 9a) and amorphous thin films. Previous methods used to probe intensity profiles, such as mechanical scanning with densitometers, are slow, and the intensities must still be converted from analog to digital form for quantitative analysis. We have designed and constructed an electron diffractometer, based on a silicon photodiode array, that overcomes these disadvantages. The compact instrument (Fig. 9b) acquires the data in a form immediately accessible by microcomputer.

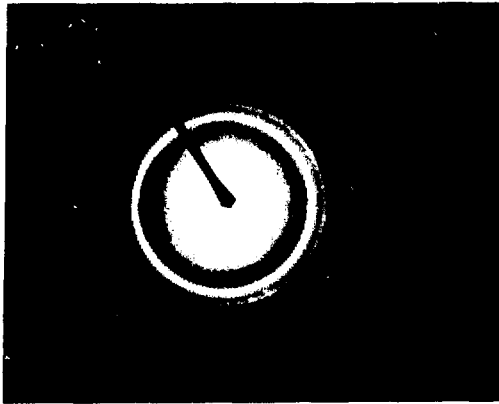
Major components include a RETICON 1024 element photodiode array for the detector, an Analog Devices MAS-1202 analog-digital converter, and a Digital Equipment Corporation LSI-11/2 microcomputer. When the detector is electronically scanned, the photocurrent from each diode is amplified and then converted to a binary number. Data from low-intensity images can be summed repeatedly and averaged until an acceptable signal-to-noise ratio is achieved. High intensity images permit the detector to be operated at higher frequencies. At a clock frequency of 50 kHz, and an analog-to-digital conversion time of 1.5  $\mu$ sec, as many as 50 spectra per second (each with 1024 channels) can be entered into memory, enabling the study of many rapidly varying phenomena.

Diffraction spectra intensities are displayed in histogram fashion as shown in Fig. 9c. Although the background from inelastic scattering is rapidly changing near the center of the

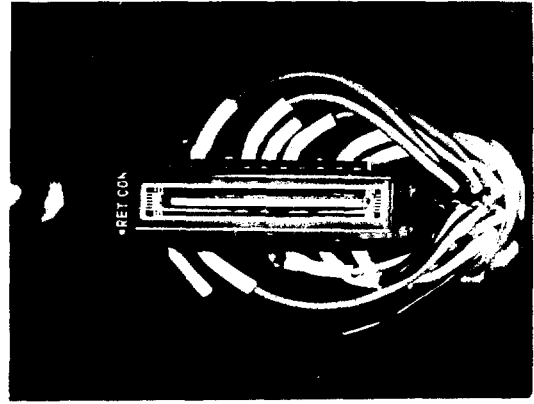


pattern, the spectra exhibit signal-to-noise ratios large enough so that many of the methods used for background subtraction in energy-dispersive x-ray analysis can be adopted to determine diffraction peak intensities and centroid positions.

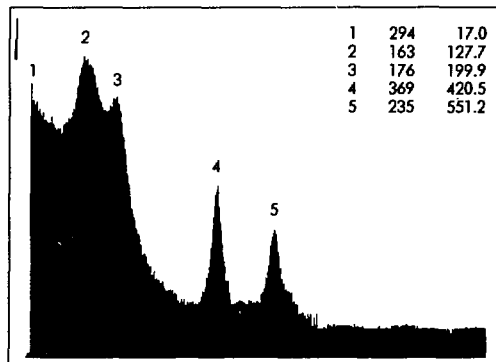
This instrument is now being used to analyze reflection electron diffraction patterns from ion-implanted stainless steel, *in situ* studies of the nucleation and growth of metallic films, and grain-boundary orientation problems in polycrystalline materials.



(a)



(b)



(c)

Figure 9. (a) Diffraction pattern from polycrystalline gold film. (b) RETICON photodiode array mounted on copper pedestal used for cooling. Wiring harness connects detector to all electronic components external to the detector chamber. (c) Diffraction intensity profile from polycrystalline gold film. Peak intensity and position are printed in upper right-hand corner of display. Total computation time is approximately 10 seconds.

**INSTRUMENTATION DIVISION****V. Radeka, Head**

- D.G. Dimmler** Control and data acquisition system architectures, microprocessor applications, and design automation
- R.P. Di Nardo** Electrical and optical coatings, detector fabrication, and specialized materials processing
- J. Fischer** Physics of radiation and particle detectors, applications of detectors in physics, chemistry, and biology
- E. Gatti\*** Visiting Senior Scientist: signal processing and noise in physical measurements; detectors and electronics
- M.A. Kelley** Data acquisition and experiment control systems software
- H.W. Kraner** Nuclear analytic techniques and semiconductor technology
- D.W. Potter** Laboratory instrumentation, Radio Communications Officer
- V. Radeka** Signal processing and noise in physical measurements; detectors and electronics
- S. Rankowitz** Systems, electronics, and design automation
- L.C. Rogers** Signal processing electronics and low background counting systems
- G.F. Sintchak** Pulse-height analyzers, computer-based instrumentation, biomedical electronics, rf system design
- G.C. Smith** Physics of and electronics for advanced ionization detectors; applications of such detectors to particle physics, solid state physics, and biology
- D. Stephani** Development of microcircuit technology for low-noise amplifiers
- F.W. Stubblefield** Multiprocessor operating systems, high-speed data acquisition electronics and computer interfaces, medical electronics for flow microfluorometry
- J.B. Warren** Analytical electron microscopy, including SEM, EDX, microdiffraction, and computer simulation of crystal defect images
- B.J. Panessa-Warren** Guest Associate Scientist, Department of Anatomical Sciences, SUNY, Stony Brook, NY

---

\*Polytechnic Institute of Milan, Milan, Italy.

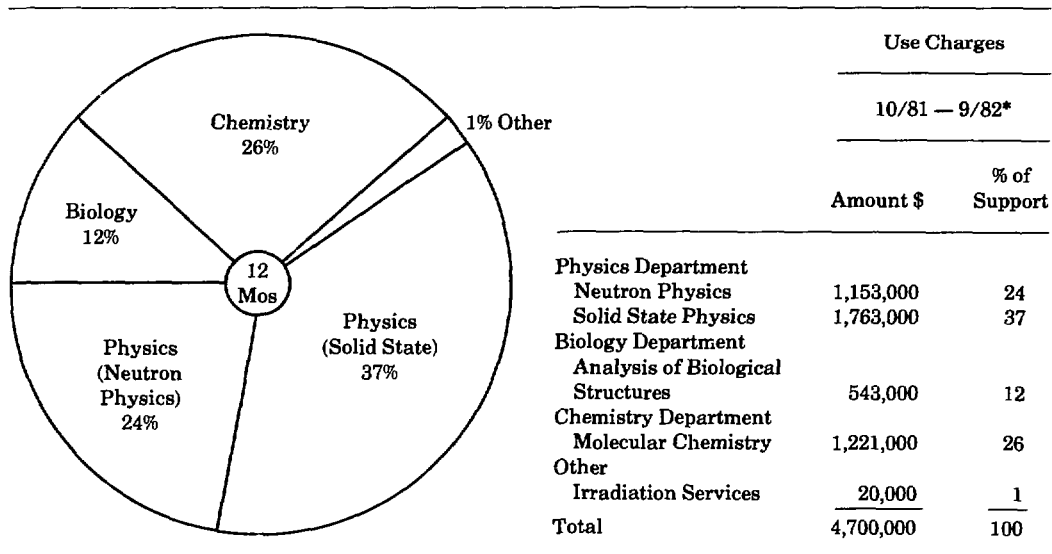
# Reactor Division

The Reactor Division operates two facilities which provide intense sources of neutrons for use in the fields of biology, chemistry, medicine, and physics. The High Flux Beam Reactor (HFBR) is one of the world's foremost facilities for the production of intense external neutron beams and for irradiation of samples in internal thimbles in extremely high neutron flux. The Brookhaven Medical Research Reactor (BMRR) is a versatile and flexible tool for providing

external neutron beams of variable intensity and for irradiating specimens in internal thimbles.

During this reporting period, the HFBR produced 10,879 megawatt-days of integrated thermal energy. Neutrons were available during 91.9% of the scheduled operating time, corresponding to a total of 483 hours of nonscheduled outage time. The BMRR was run upon demand and produced a total of 331 megawatt-

Table I  
Distribution of Support of HFBR Operations  
From Scientific Programs



\*Beginning with FY 83, funding for the operation of the HFBR is provided from a single program, the Office of Energy Research, Division of Materials Sciences.

hours of energy. The distribution of programmatic support among the various scientific disciplines is presented in Table I. The number of service irradiations performed at both reactors is given for each BNL Department in Table II.

A milestone was reached in the operation of the HFBR in September 1982 when the reactor power was increased from 40 to 60 MW. This change required the installation of larger heat exchangers and fuel more heavily loaded with  $^{235}\text{U}$ , and was carried out only after an extensive safety review by BNL and the DOE, which took over two years to complete. Operation at the new higher power level provides a 50% increase in the neutron flux available. This not only reduces the time required for experimenters to obtain their data, but also makes it possible to carry out a wider range of experiments than ever before.

Table II  
Reactor Service Irradiations

Organization	HFBR	BMRR
Chemistry Department	151	0
Department of Energy and Environment	3	0
Department of Nuclear Energy	0	2
Medical Department	44	92
Physics Department	1	1
Reactor Division	12	3
Safety and Environmental Protection Division	0	7
Outside Organizations	21	69
<b>Total</b>	<b>232</b>	<b>174</b>

## REACTOR DIVISION

G.C. Kinne, Division Manager  
D.C. Rorer, Deputy Division Manager\*

### High Flux Beam Reactor Operations

M. Brooks, Group Leader  
D. Oldham, Asst. Group Leader  
R. Bergoffen, Reactor Supervisor

#### Reactor Instrument Group

D.G. Pitcher, Group Leader

#### Reactor Maintenance Group

M. Zukas, Group Leader

#### Research Coordination Group

D.C. Rorer, Group Leader\*

#### Water Chemistry

S. Protter, Group Leader

#### Reactor Technical Assistance

P. Tichler, Chemical Engineer

### Quality Assurance Office

J. Detweiler, Coordinator\*

### Medical Research Reactor Operations

J. Detweiler, Supervisor\*

### Training & Procedures Office

L. Junker, Group Leader

### Source & Special Nuclear Materials Group

P. Colsmann, Group Leader  
K. Dahms, Engineer

### DOE Standards Group

W. Brynda, Group Leader

\*More than one position.

# Safety and Environmental Protection Division

## INTRODUCTION

The Safety and Environmental Protection Division provides technical and professional services in areas of health and safety. It also carries out basic and applied research in these areas. Its health and safety services include professional consultation, guidance, and review of safety aspects of new facilities or programs; sampling, analysis, and evaluation of potentially hazardous operations already in existence; development of safety guides; waste management; and training in industrial safety, cardiopulmonary resuscitation, respirator use, health physics, industrial hygiene, fork truck and crane safety, and emergency response. The Division's fire rescue and police groups play key roles in ensuring that the Laboratory can cope effectively with local emergencies.

The Division is responsible for several research programs relating to the evaluation of potential health and safety hazards of energy sources or by-products. Among these programs are two directed at evaluation of the past and anticipated future ionizing radiation dose equivalents to residents of the Marshall Islands; studies of basic quantities in radiological physics and their relationship to biological effects of ionizing radiation and other agents having carcinogenic or mutagenic potential; assessment of hazards and development of protection guidelines for chemical and physical hazards; genetic effects of energy-related agents, e.g., strong magnetic fields and ionizing radiation; surveillance of Long Island's aquifer; and job and task analysis of health physics technicians at nuclear power plants. The Division also provides practical field training and research experience for graduate students in radiological and environmental sciences.

Division professionals actively participate in work of the National Committee on Radiation Protection and Measurements, the Interna-

tional Committee on Radiation Protection, and many scientific and professional organizations.

## MARSHALL ISLANDS STUDIES

Radiological monitoring of people exposed to fallout from the weapons testing program in the Pacific was performed at Enewetak and Rongelap Atolls. A follow-up study of persons who inhabited Bikini Atoll was also performed. The above exposures, predominantly  $^{137}\text{Cs}$  and  $^{90}\text{Sr}$ , were from low-level contamination of the three atolls.

During a field trip in January 1982, body burdens were measured and bioassay samples were collected from individuals residing at Enewetak Atoll. Body burdens of  $^{137}\text{Cs}$  in adult males, although well below recommended limits, were above the female body burdens by an order of magnitude. Food from an experimental garden at Engebi Island which contained several acres of coconut and breadfruit trees was the source of  $^{137}\text{Cs}$  in the adult males, who traveled to Engebi often. The experimental garden was part of another Department of Energy program.

During a field trip in August 1982, internal personnel monitoring was performed at Rongelap Atoll, Kili Island, and Majuro Atoll. At Rongelap, the adult average body burden of  $^{137}\text{Cs}$  was 20% above that of the previous year. Obtaining food from the more contaminated but uninhabited islands of the atoll may have been a reason body burdens were elevated. Follow-up of the former Bikini Atoll residents took place at Kili Island and Majuro Atoll. A comparison population with characteristics similar to the study population participated in the internal personnel monitoring program at Majuro. Recent body-burden measurements for  $^{137}\text{Cs}$  in the adult study populations are indicated on Fig. 1.

The accidental acute exposures on March 1 and 3, 1954, at Rongelap and Utirik Atolls were

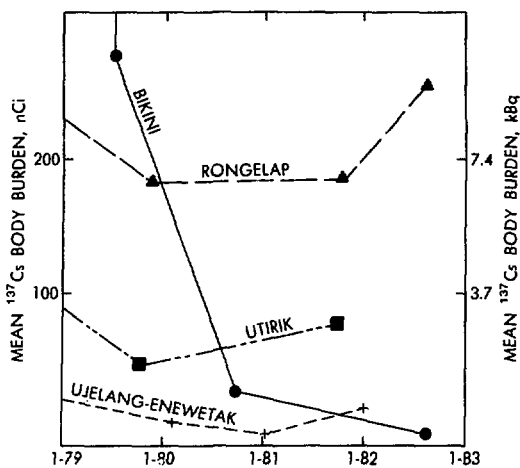


Figure 1. Adult  $^{137}\text{Cs}$  body-burden history for the Marshallese people.

reevaluated in view of the fact that incidence of thyroid adenoma indicated a critical difference relative to that reported for other radiation-exposed groups. Reanalysis of thyroid absorbed dose was based on comprehensive fallout models in conjunction with dietary and living pattern data suitable to the time of acute exposure. On the basis of tentative results, thyroid dose appears to have been underestimated in earlier studies by factors varying from 2 to 10 for the Rongelap people exposed in March 1954. Thyroid nodule incidence will be evaluated in terms of new estimates for thyroid absorbed dose for both atoll populations.

Several methods for measuring extremely low levels of plutonium were advanced. Procedures for solvent extraction of plutonium were developed based on the properties of Marshallese excreta samples and on methods developed at other laboratories. An electron-rejecting alpha liquid scintillation spectrometer based on plans developed at Oak Ridge National Laboratory was built. The spectrometer and radiochemical separation technique are now suitable for detection of plutonium at the 1.0-femtoCurie ( $3.7 \times 10^{-5}$  becquerels) level.

Fission track methods outlined in the literature for sensitive detection of  $^{239}\text{Pu}$  were advanced. Techniques for slide and sample assembly, plutonium deposition, and lighting for

track detection were also studied. A detection limit of 0.03 fCi or less appears achievable and may allow 100-ml aliquots of urine to be analyzed more quickly and inexpensively than by other less sensitive methods.

## TOXIC MATERIAL ADVISORY PROGRAM

The Toxic Material Advisory Program continues to provide the basic foundation for the development of interim exposure guidelines and work practices, and for supplying consultation in the functional areas of toxicology, physiology, biological monitoring, workplace sampling, health assessment methodologies, risk assessment, and hazard analysis. These activities are carried out by Brookhaven's Center for Assessment of Chemical and Physical Hazards (CACPH).

Fiscal year 1982 accomplishments included: revised Toxic Material Advisory reports on 2-mercaptoethanol and acetylacetone, toxic material summary reports on diethylhexylsebacate, and biological effect summaries on chrysene, pyrene, and acridine. An extensive literature review was performed on benzo(a)pyrene (BaP).

CACPH efforts to assist in the development of a draft internal generic standard for DOE's Office of Operational Safety, Operational Safety Health and Environment Division, have been directed toward the evaluation of the need for a uniform policy and the development of generic guidelines. To achieve these objectives, CACPH developed a questionnaire and a form designed to obtain information on specific chemicals in use, quantity, number of employees potentially exposed, existence of internal guidelines for handling carcinogens, and other features deemed important for inclusion in a DOE generic standard. The questionnaire and form were sent to all DOE contractors and returned to CACPH. The results of this survey indicated that, within the DOE community, the compounds that should be treated as regulated carcinogens are those chemicals currently regulated by OSHA as carcinogens and those listed in Appendix A of the American Conference of Governmental Industrial Hygienists "Threshold Limit Values for Chemical Substances."

Approximately 76% of respondents preferred both criteria. A lower percentage preferred the "List of Carcinogens" generated by EPA's Carcinogen Assessment Group and those proposed in OSHA's Candidate List of Potential Carcinogens, respectively 21% and 18%. Approximately 32% of the respondents preferred criteria different from the four suggested.

In September, a workshop on addressing the problem areas associated with developing carcinogen guidelines was held at BNL. Participants included highly qualified scientists from ORNL, BNL, DOE, NRC, State of California, NYU Environmental Law Institute, EPA's Carcinogen Assessment Committee, MIT's Center for Policy Alternatives, Environ, and Harvard's Energy and Environmental Policy Center. The proceedings are undergoing editing. Information gained from the workshop will be incorporated in the next draft of the generic policy.

CACPH prepared and submitted an Implementation Plan for the Hazardous Materials Control Program at Laramie Energy Technology Center (LETC). The purpose of this program was to provide the LETC manager and employees with guidance in the selection, control, use, handling, storage, and disposal of hazardous chemicals, including carcinogens. The program included major requirements in DOE Order 5480.1, Chapter X, for maintaining an effective industrial hygiene program. The program also provided a project-specific safety and health analysis, health surveillance, and environmental monitoring plan for LETC workers and workplaces. The implementation plan has been reviewed by LETC and no modifications of the plan have been requested.

CACPH continues to provide liaison and technical support to the Joint U.S./Yugoslavia Health Effect Study at the Kosovo Coal Gasification Plant.

#### **ASSESSING DIVERSE GROUNDWATER SURVEILLANCE DATA**

Groundwater investigations on Long Island, where the aquifer system has been designated as a "sole source aquifer," have been approached with different goals in mind. The

methodology used to assess detrimental effects on water supplies, contamination due to landfills, spills, or agricultural activities, or concerns of citizens who solely use groundwater has varied. The analysis of data in assessment of the total impact on the aquifer in both the temporal and spatial scale has been inadequate. To facilitate assessment, BNL is developing a methodology that will

1. create a data base management system,
2. generate a quality assurance and statistical sieve,
3. evaluate the data in terms of geohydrological principles, and
4. study impacts from land use, both historical and future.

This study is being sponsored by the EPA Groundwater Research Branch, Robert S. Kerr Laboratory, Ada, Oklahoma, and is being done at BNL as a joint effort with the Department of Energy and Environment. The end product will be a handbook which will present a methodology that local agencies can use to assess impacts on their "sole source aquifer."

#### **RADIOLOGICAL PHYSICS**

Precise and accurate determination of two fundamental dosimetric quantities, W-value (average energy to form an ion pair) and stopping power for heavy ions in various gases, have indicated dependence of W-values on energy as well as atomic number of incident ions. These dependences are investigated to determine the basic physical mechanisms of interaction of ionizing radiation with matter. New concepts in radiation protection are also being developed. In the studies, fluence rather than dose is emphasized as the conceptually correct parameter which should be correlated with biological effects, especially at the low doses of concern in radiation protection. A hit-size weighting theory has been developed to explain and predict radiobiological effects at low doses and dose rates. Basic assumptions of this theory are (1) a minimum amount of energy transfer or minimum hit-size must take place in a critical volume of a cell for an all-or-none (quantal) response, and (2) at some large hit-size the probability of inducing a quantal effect reaches unity. This probability function is termed the hit-size weighting function and has

been evaluated for one particular biological end point, namely, pink mutations in *Tradescantia*. In this case, the threshold event size was about 0.4 keV/ $\mu\text{m}$ , and the event size at which the probability reaches unity was about 75 keV/ $\mu\text{m}$ .

## DOE RADIOLOGICAL ASSISTANCE PLAN

The Safety and Environmental Protection Division furnished support for Region I of the Radiological Assistance Plan (RAP). The purpose of the RAP is to give advice and assistance during radiological incidents to the 11 northeastern states and the District of Columbia, as well as to organizations and private individuals. Under RAP, health physicists, together with appropriate medical and safety professionals and support personnel, have been organized into a RAP Response Team. They supply emergency advice and assistance to minimize loss of property, to cope with radiological hazards, and to protect the public health and safety.

Specifically, RAP provides:

1. technical support in response to requests from state agencies or others within DOE Region I for radiological assistance;

2. collection, calibration, and maintenance of monitoring instruments and equipment necessary to facilitate this support;

3. liaison with state and local emergency planning and response groups;

4. training and information exchanges within our region;

5. collaboration with Federal Emergency Management Agency and participation in utility reactor emergency drills; and

6. liaison with other federal emergency response groups.

During 1982, the basic response capability was maintained. This included testing and calibration of some 50 conventional survey instruments, 15 specialized survey instruments, and 2 multichannel analyzers with their associated detectors.

Calls for assistance were received for 20 non-reactor incidents. All were handled by telephone and reporting or referral to state agencies. Two unusual events and two power reactor site emergencies occurred. During one, the steam tube rupture at the Robert A. Ginna Power Plant on January 25, 1982, full preparations short of an "on-the-scene" response were made. Calls were received and our availability was verified during seven emergency exercises at power reactors within DOE Region I.



**SAFETY AND ENVIRONMENTAL  
PROTECTION DIVISION**

**C.B. Meinhold, Division Head**  
**W.R. Casey, Deputy Division Head**  
**J.W. Baum, Research Coordinator**  
**R.W. Young, Security Officer**

<b>W.G. Adams</b>	Industrial Hygiene	<b>R.J. McWilliams</b>	Safety Engineering, Construction Safety
<b>J.C. Balsamo</b>	Instrumentation		
<b>J.W. Baum</b>	Radiological Physics, Health Risk Assessments	<b>R.F. Miltenberger</b>	Marshall Islands, Environmental Monitoring
<b>N.M. Bernhole</b>	Industrial Hygiene	<b>A.R. Moorthy</b>	Radiochemistry
<b>B.F. Brennan</b>	Laboratory Police	<b>S.V. Musolino</b>	Marshall Islands
<b>J.E. Brower</b>	Center for Assessment of Hazards	<b>J.R. Naidu</b>	Environmental Studies, Ecology
<b>L.E. Day</b>	Environmental Regulations	<b>S.G. Pearsall</b>	Safety Audit, Emergency Planning
<b>J.B. Deitz</b>	Fire Protection	<b>L.F. Phillips</b>	Personnel Dosimetry, Health Physics, Calibrations
<b>P.G. Edwards</b>	Hazardous Waste Management		
<b>N.J. Fallon</b>	Computer Science	<b>N.D. Rohrig</b>	Health Physics, Radiological Physics
<b>C.W. Flood</b>	Health Physics	<b>H. Schulman</b>	Safety Engineering, Pressure Systems
<b>P.J. Gollon</b>	Health Physics		
<b>M.G. Hauptmann</b>	Groundwater Studies	<b>J.J. Shonka</b>	Health Physics, Radiological Physics
<b>A.P. Hull</b>	Radiological Assistance Program	<b>B.D. Silverstein</b>	Industrial Hygiene
<b>S.L. Jackson</b>	Groundwater Studies	<b>J.R. Steimers</b>	Analytical Chemistry
<b>H.M. Kalbach</b>	Administration	<b>C.F. Swezey</b>	Personnel Monitoring
<b>P.G. Kale</b>	Mutagenesis	<b>M.N. Varma</b>	Dosimetry Research, Radiological Physics
<b>D.G. Keimig</b>	Epidemiology		
<b>S.D. Keimig</b>	Industrial Hygiene	<b>G.N. Wall</b>	Electrical Safety, Safety Engineering
<b>A.V. Kuehner</b>	Computer Science, Radiological Physics	<b>J.A. Weynand</b>	Computer Security
<b>E.T. Lessard</b>	Marshall Islands, Internal Dosimetry	<b>O. White, Jr.</b>	Industrial Hygiene
<b>F.J. Marotta</b>	Training	<b>R.W. Young</b>	Safety Engineering, Security and Plant Protection
<b>I.R. Marshall</b>	Radiological Physics		

# General and Administrative

# General and Administrative

## PERSONNEL DIVISION

### Statistics

Compared to the 9.8% decline in employment in 1981, total employment at the Laboratory remained virtually stable in 1982 (Table I). A relatively small layoff during the year was offset by hiring in selected areas.

The regular scientific staff declined by 4.9% from 1981 to 1982 (Table II). The 1982 Summer Program (Table III) saw an increase of 22 in staff and a decrease of 16 students as compared to 1981. Table IV, showing guest and collaborator appointments, reports data pertinent to the National Synchrotron Light Source Department separately for the first time. The number of consultant contracts remained static (Table V).

Table I  
Employment Statistics

	Dec. 31, 1982	Dec. 31, 1981	Dec. 31, 1980
Scientific Staff <sup>a</sup>	713	734	779
Scientific Professional Staff	456	453	515
Nonscientific Staff <sup>b</sup>	2114	2108	2359
<b>Total</b>	<b>3283</b>	<b>3295</b>	<b>3653</b>

### Turnover Data

	1982		1981		1980	
	Number	Annual Rate (%)	Number	Annual Rate (%)	Number	Annual Rate (%)
<b>Accessions</b>						
Scientific Staff <sup>a</sup>	79	11	69	9	111	15
Scientific Professional Staff	41	9	25	5	87	16
Nonscientific Staff <sup>b</sup>	109	5	103	5	210	10
<b>Total</b>	<b>229</b>	<b>7</b>	<b>197</b>	<b>6</b>	<b>408</b>	<b>12</b>
<b>Separations</b>						
Scientific Staff <sup>a</sup>	100	14	102	14	98	13
Scientific Professional Staff	58	13	92	18	86	15
Nonscientific Staff <sup>b</sup>	157	7	338	15	201	9
<b>Total</b>	<b>315</b>	<b>10</b>	<b>532</b>	<b>15</b>	<b>385</b>	<b>11</b>
<b>Net Accessions</b>						
Scientific Staff <sup>a</sup>	-21	-3	-33	-5	13	2
Scientific Professional Staff	-17	-4	-67	-14	1	
Nonscientific Staff <sup>b</sup>	-48	-2	-235	-10	9	
<b>Total</b>	<b>-86</b>	<b>-3</b>	<b>-335</b>	<b>-10</b>	<b>23</b>	<b>1</b>

<sup>a</sup> Includes Research Associates and Visitors.

<sup>b</sup> Figures do not include temporary summer nonstudent employees. Temporary student employees are included in Table III.

**Table II**  
Scientific Staff and Students on December 31

	Regular Staff			Salaried Visitors		
	1982	1981	1980	1982	1981	1980
<b>By Appointment Category</b>						
<b>Staff</b>						
Senior Scientist	120	120	127	2	0	2
Scientist	321	334	308	8	6	15
Associate Scientist	116	131	142	3	4	9
Assistant Scientist	46	49	77	8	6	3
Senior Research Associate	0	0	0	2	5	9
Research Associate	0	0	0	44	44	52
<b>Students</b>						
Junior Research Associate	0	0	0	4	3	8
Research Assistant	0	0	0	0	0	0
<b>Total</b>	<b>603</b>	<b>634</b>	<b>654</b>	<b>71</b>	<b>68</b>	<b>98</b>
<b>By Academic Degree</b>						
Ph.D. or M.D.	506	531	538	64	64	85
Master	38	41	47	5	4	11
Bachelor	54	57	64	2	0	2
No Degree	5	5	5	0	0	0

**Table III**  
Summer Program 1982

Department	Staff	Students <sup>a</sup>	Salaried	Unsalaries	Institutions
Accelerator	5	8	3	10	8
Applied Mathematics	4 <sup>b</sup>	1	2	4	4
Biology	14	9	2	21	14
Chemistry	5	6	3	8	6
Director's Office	0	3	0	3	2
Energy and Environment	18	34	15	37	41
Instrumentation	3	0	3	0	3
Medical	5	16	1	20	13
National Synchrotron					
Light Source	16	6	3	19	17
Nuclear Energy	10	10	9	12	15
Physics	85	14	32	67	66
Reactor	0	0	0	0	0
Safety and Environmental Protection	0	14	0	14	8
<b>Total</b>	<b>165</b>	<b>121</b>	<b>73</b>	<b>215</b>	

<sup>a</sup> Includes 78 participants in Summer Student Program.

<sup>b</sup> Includes one individual with combination of salaried and unsalaried appointments.

Table IV

Scientific Guest and Collaborator Appointments (Unsalariated) in Effect on December 31, 1982	
Accelerator	26
Applied Mathematics	2
Biology	85
Chemistry	131
Energy and Environment	79
Instrumentation	2
Medical	259
National Synchrotron Light Source	38
Nuclear Energy	18
Physics	669
Reactor	5
Safety and Environmental Protection	10
<b>Total</b>	<b>1324<sup>a</sup></b>

<sup>a</sup> Represents 305 institutions, including 95 outside the United States.

Table V  
Consultant Services

1982 Fiscal Year	
Total Contracts in Effect	276
No. of Consultants Used	156

Table VI  
Minority and Female Employees

Category	12/31/82		12/31/81	
	Total	%	Total	%
Minority	481	14.7	480	14.6
Black	258	7.9	254	7.7
Hispanic	70	2.1	79	2.4
American Indian/ Alaskan Native	8	0.2	7	0.2
Asian/Pacific Islander	145	4.4	140	4.2
Female	730	22.2	724	22.0
<b>Total</b>	<b>3283</b>		<b>3295</b>	

### New Program

An Employee Suggestion System was developed to be introduced early in 1983. Under its provisions, any regular employee who has an idea for improving a specific operation, process, method, or practice at the Laboratory is invited to put this idea in writing and submit it as a

suggestion. Ideas may be of either tangible or intangible benefit. If approved for implementation, a suggestion could earn the employee a cash award up to \$10,000. The purposes of this system are to provide a vehicle for recognizing employee initiative in increasing productivity and to effect cost savings for the Laboratory.

### Training and Development Programs

A continuation of the Resources Management Training Program, whose objective is to give supervisors the skills to establish a mechanism for implementing cost-saving ideas and improving productivity, was attended by 60 supervisors and managers. Scientific and engineering supervisors participated in two Project Management Courses in 1982. These workshops address the skills and techniques required of successful project management from the planning stages including budgeting through completion.

### AFFIRMATIVE ACTION

Employment statistics for minorities and women as of the end of 1981 and 1982 are presented in Table VI. Minority employees increased 0.2% and women by 0.8% during this period.

Three black students participated in the Graduate Engineering Minorities Program (GEM) during the summer of 1982.

### ADMINISTRATION

During the calendar year 1982, the following events took place: On January 1, Deputy Director Dr. Nicholas P. Samios was appointed Acting Director of Brookhaven National Laboratory. Dr. Samios replaced Dr. George Vineyard who served as Director for nine years.

Kenneth W. Ryan was appointed Manager of the Technical Information Division January 7.

On February 3, it was announced that Dr. John P. McTague had accepted the position of head of the National Synchrotron Light Source Division. Dr. Arie van Steenbergren agreed to serve as deputy division head.

On February 24, Dr. Martin Blume, Associate Director for Low Energy Physics and Chemistry, received the 1981 E. O. Lawrence Award in Physics.

On March 1, Dr. Veljko Radeka agreed to continue as head of the Instrumentation Division through December 31, 1986.

In March, Dr. Warren Winsche, Deputy Director, was elected to the National Academy of Engineering.

Dr. Nicholas P. Samios was elected to the National Academy of Sciences, along with Dr. Raymond Davis Jr., senior scientist, on April 27.

Acting Director Dr. Nicholas P. Samios was appointed Director of Brookhaven on May 1.

On July 1, Michael Guacci was named Manager of the Supply and Materiel Division.

On October 11, Dr. William Marcuse was named head of the newly established Office of Research and Technology Application.

On October 11, Earl M. Blanton was named Manager of the Affirmative Action Office, replacing Harvey J. Thomas.

The dedication of the National Synchrotron Light Source was held on November 22. Two days later the National Synchrotron Light Source Division became a Department of the Laboratory.

## SERVICE ORGANIZATIONS

### Division of Contracts and Procurement

During Calendar Year 1982, the Division of Contracts and Procurement (DCP) processed over 27,000 transactions, totaling more than \$72,000,000. Negotiation efforts by DCP resulted in savings in excess of \$4,800,000, primarily in the High Energy Physics Program.

DCP started Phase I implementation (actual purchase information) of the Integrated Purchasing and Accounts Payable System.

Representatives of DCP attended the second annual Long Island Minority Business Procurement Conference to acquaint representatives of minority business firms with DCP's operations at BNL, and also to encourage the DCP Minority Business Program.

DCP formulated a 31-week training program covering all aspects of procurement for its professional staff, consisting of films produced by NASA and/or Harbridge House. The programs were made available to the various departments and divisions.

### Fiscal Division

Continually seeking ways to expand services to the Laboratory employees, the Fiscal Division, in conjunction with the Director's Office, successfully completed negotiations with the Teachers Federal Credit Union for an on-site office. Employee reaction has been very positive, with approximately 18% of the employees participating at this time.

Through close collaboration with the Personnel Division, employees were offered the opportunity for greater flexibility in the management of their tax-sheltered annuities. The new option provides for investment in a number of annuities offering a wide range of investment objectives and the advantage of transferring accumulations from one fund to another.

For the first time, BNL went out on a competitive bid for the management and operation of the on-site banking facility. Twenty-eight commercial banks operating in Suffolk County were solicited. Barclays Bank of New York was the successful bidder and continued to operate the on-site bank.

### Plant Engineering

The first major nonprogrammatic budget line item since 1966 was approved in 1982. The \$12 million project will materially improve the operating efficiency of the Central Steam Facility, extend the underground steam system, and improve and expand the Laboratory water system.

Significant gains toward installation of a comprehensive maintenance management system were accomplished during the year, specifically in the areas of material control and documentation. Material control for contributed technical services was improved by having all bill-of-material requests prepared by the Maintenance Management Center (MMC) estimators, and staged by the Supply and Materiel Division prior to the scheduled start of work. Establishment of a central telephone number for receiving maintenance calls and the use of a "Limited Work Request" form provide the means of documenting work-load and establishing a realistic maintenance backlog. Documentation of preventive maintenance continues to expand through the use of the Automated Equipment Maintenance System (AEMS).

To prevent energy usage from attaining premium demand rates, a site demand recording and pre-alarming instrument was installed in the AGS control room alerting operators to effect a load shedding procedure. This system was designed and installed to operate when the Laboratory is being fed from either the preferred or alternate LILCO feeders.

The billing process for distribution of electrical power usage to the scientific departments was improved by the development of a software package for use at the CSCF. The same package has also been used to create a data file storage and retrieval system to aid in report generation and may be applied to other utilities for accurate energy monitoring of buildings and facilities.

### **Photography and Graphic Arts**

Progress toward consolidation of all P&GA functions under one roof was made in 1982 by transferring the color darkroom facilities from a remote building into the newly renovated areas of the Photography and Graphic Arts Division Building.

The platemaking operation within printing has become automated with the installation of an Encomatic Plate Processor. This has provided efficiencies of operation which have helped compensate for a reduction in staff.

Word Processing Optical Character Recognition (OCR) scanning capabilities have been greatly enhanced with the purchase of a new scanner having the capability of reading up to eight different typefaces. This will enable most Laboratory typewriters to be used for input to our centralized word processing section.

### **Supply and Materiel**

Property management policies and procedures were reviewed during the year. The Laboratory has initiated a Bar Code Tagging System designed to reduce the manual effort expended by Laboratory personnel in conducting the biannual physical inventory of property. In addition to the retagging, members of the Supply and Materiel Division will be performing a wall-to-wall inventory of the entire site.

Work on the Integrated Inventory, Procurement, and Accounts Payable System is continuing. The Inventory Control and Stores Withdrawals Module is being tested and should be fully installed and operational by June 1983.

These modules will allow the user community to access material availability, place orders directly, and issue back order requests. The system will automatically generate a stock picking list at the appropriate stocking location which then becomes the packing list and shipping labels.

Excess Procurement has continued to develop additional sources of supply for excess combustible products available through the Department of Defense Disposal activities. Products for the Alternate Liquid Fuel Program for use in the Central Steam Plant are being acquired from as far away as California, resulting in reduced energy costs for the Laboratory.

### **Technical Information Division**

The Technical Information Division (TID) showed considerable progress toward its goals in a Laboratory environment of high demand for publications and information services, coupled with some fiscal constraints. TID became more responsive to the present and future needs of BNL scientific and technical staff by undergoing a reorganization, by formalizing and restructuring job descriptions and personnel assignments, and by reclassifying a number of personnel. An audit of TID by DOE technical information experts was successfully conducted with no major problems or weaknesses found.

A number of physical and operational changes were successfully implemented in TID, primarily in the Research Library. Approximately 20,000 bound periodical volumes, or about one-half the total holdings, were boxed and temporarily stored in a warehouse for several months, and then reshelfed in an annex which had previously been a theatre. This move relieved severe overcrowding in the Research Library periodicals areas and provided some short-term growth space to handle annual increases in periodical holdings. Shelving installed in conjunction with a new reference center provided relief in the abstracts and indexes area. Shifting of books into the area vacated by relocating serials into the annex solved a number of problems faced by library users and provided a much more "user-friendly" atmosphere for access to all materials.

To further the automation efforts in the library, a large-scale cataloging conversion project was planned and executed. As a result, over

35,000 unique cataloging records with individual BNL library or collections holdings information were added to the OCLC database. The project, which brings the total number of records up to over 40,000, was completed on schedule and had a database "hit" rate of well over 90%, with a very low error rate. This augmented database lays the groundwork for developing and implementing, or for purchasing automated systems which will provide on-line access to local library catalogs and circulation files, and which will enhance user access to materials.

### Management Information Systems Division

The Management Information Systems Division has been engaged in a large-scale software development program throughout the year. MIS Division operates one IBM and three Hewlett-Packard computers in support of Laboratory administrative activities. Over two hundred terminals and remote printers access the MIS network performing data entry, inquiry, reporting, and development tasks.

The primary thrust of the MIS development effort has been directed toward the phased implementation of the Integrated Inventory, Purchasing, Accounts Payable System (IPAP), researching software packages to support a Job Cost Accounting and Reporting System and the transfer of various administrative systems from the IBM-360 to the Hewlett-Packard HP-3000 computers. The goal of the IPAP system is to integrate the laboratory-wide functions of materials and service requisitioning, purchasing, stores inventory control, and accounts payable. The creation of a database of purchase history and stores utilization will enable the Laboratory to provide needed goods and services expeditiously and economically, in support of research goals.

The IBM-360 to HP-3000 Conversion project will enable the Laboratory to retire obsolete computing equipment that is both costly and difficult to maintain. As a result of this effort, MIS Division will be able to offer an internal solution to hardware backup, by operating three compatible Hewlett-Packard computers, with one normally dedicated to separate and distinct administrative functions. The Laboratory will thereby be assured of continuity of operations.

### Energy Management

Energy conservation has been BNL policy since the post-embargo days of 1973. The Laboratory's long-range goal is to reduce energy consumption in buildings and facilities more than 20% by fiscal year 1985, as compared with FY 1975. Toward this goal, Plant Engineering's Energy Management and Design and Construction Groups continued to search for, develop, and implement energy retrofit projects that will reduce the Laboratory's consumption of electric power and petroleum fuels. At the end of 1982, BNL had achieved a 15.3% reduction as compared with 1975. To date, BNL's Energy Management Program has received \$8.0 million funding for implementation of energy retrofit projects at the Laboratory. This funding is provided by the Department of Energy In-House Energy Management Retrofit Program. When these funded projects are complete, it is expected that the Laboratory will save 560 billion Btu of source energy annually, the equivalent of 3.8 million gallons of imported oil or enough energy to heat about 3700 homes for a year. This energy reduction represents 17% of the total energy used in FY 1975, the DOE base year. The Laboratory received an additional \$3.7 million funding in FY 1983 to implement eight new energy projects. These projects will conserve an additional 117 billion Btu of source energy per year. Six major project proposals were submitted for DOE funding in FY 1984 with a total estimated construction cost of \$2.5 million. When implemented, these projects will conserve 165 billion Btu. These measures will save the Laboratory over \$1.2 million per year, in a period when budget cutting is a way of life.

In 1982, the engineering firm of Pope, Evans, and Robbins prepared for BNL a feasibility study and conceptual design report for cogenerating electric power and steam on site. Cogeneration offers economies of operation due to the simultaneous generation of electric and thermal energy. This project was submitted for FY 1985 funding for \$21 million and is expected to save 546 billion Btu of source energy per year.

Energy conservation projects presently under construction and projects completed during calendar year 1982 are:

a) Insulation of piping, valves, and fittings in steam manholes throughout the site.



b) Adding vestibules on heavily used entrances.

c) Adding storm-type windows to single-pane windows.

d) Replacement of wooden overhead truck doors with insulated metal doors and weather-stripping.

e) Installation of an economizer on Boiler No. 5 at the central steam plant, reducing fuel bills by \$175,000.

f) Equipment modifications, new burners, controls, and boiler-burner management system, at the central steam plant to permit maximum utilization of alternate liquid fuels.

g) Night setback and equipment turn-off in 9 buildings.

h) Equipment modifications to 4 major refrigeration systems (i.e., steam absorption and centrifugal water chillers) to reduce energy input per ton output.

i) Adding or increasing the amount of wall and roof insulation in 3 buildings throughout the site. Adding exterior foam insulation to 7 trailers, and 3 masonry buildings.

j) Relamping selected buildings with high efficiency, low energy usage fluorescent and high pressure sodium fixtures.

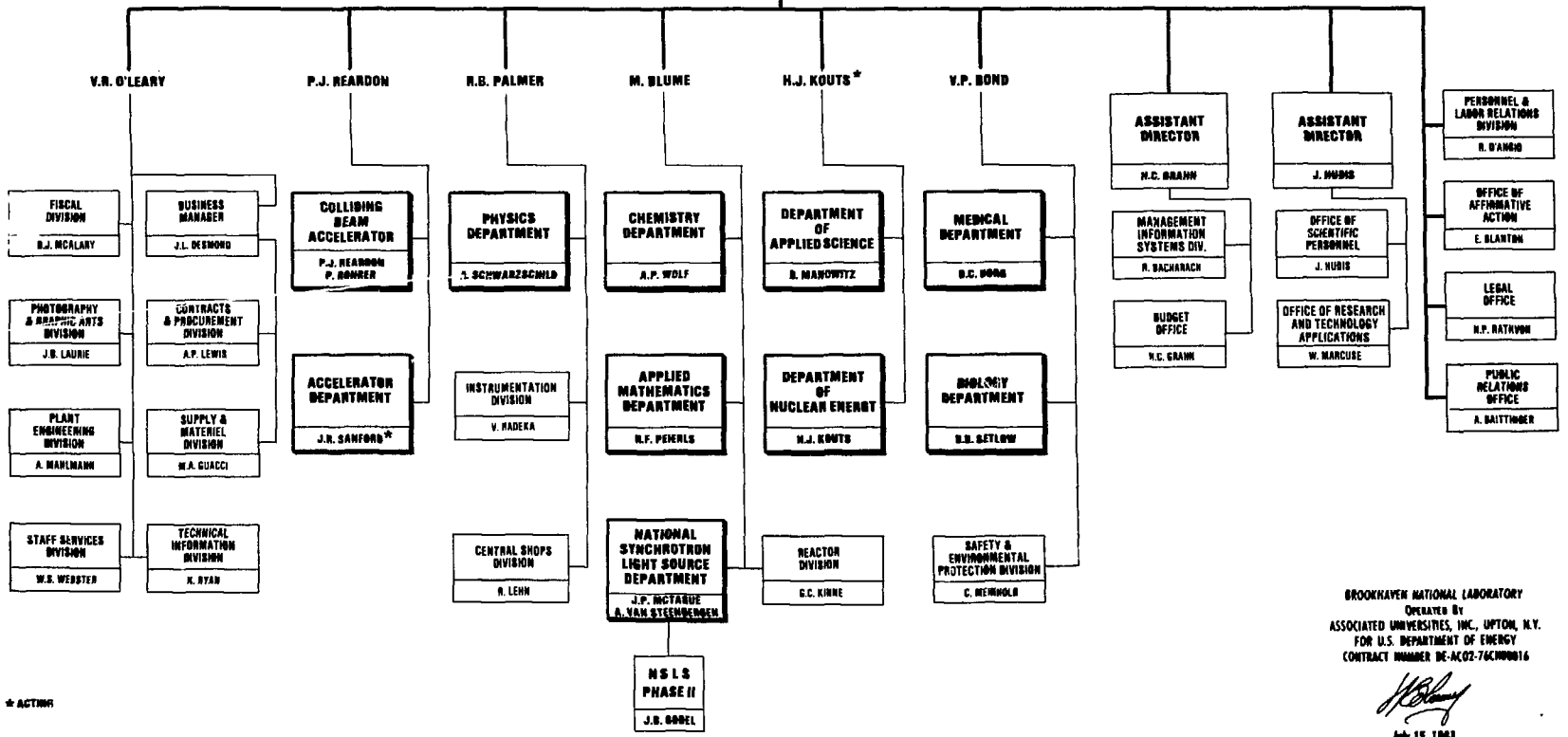
k) Installation of stack dampers on all small local heating units.



# BROOKHAVEN NATIONAL LABORATORY

**DIRECTOR**  
H.P. SAMIOS

ASSOCIATE DIRECTOR - Low Energy Physics & Chemistry M. BLUME  
 ASSOCIATE DIRECTOR - Life Sciences & Safety V.P. BOND  
 ASSOCIATE DIRECTOR - Applied Research H.J. KOUTS\*  
 ASSOCIATE DIRECTOR - Administration V.R. O'LEARY  
 ASSOCIATE DIRECTOR - High Energy Physics Research R.B. PALMER  
 ASSOCIATE DIRECTOR - High Energy Facilities P.J. REARDON



\* ACTING

BROOKHAVEN NATIONAL LABORATORY  
 OPERATED BY  
 ASSOCIATED UNIVERSITIES, INC., UPTON, N.Y.  
 FOR U.S. DEPARTMENT OF ENERGY  
 CONTRACT NUMBER DE-AC02-76BN0016

*H.P. Samios*  
 July 15, 1983